

THE UNIVERSITY OF ASTON IN BIRMINGHAM

THE PROPERTIES OF MICROBIAL AGGREGATES AND THEIR

BEHAVIOUR IN TOWER FERMENTERS

by

ALAN JAMES , B.Sc.

Being a thesis submitted in support of an application for
the Degree of Doctor of Philosophy

THESIS
577-15831
JAM
4 dec 73 167677

OCTOBER 1973

Summary

This research has been concerned with the physical characteristics of microbial aggregates and their liquid suspensions; most of the experimental work being carried out with Aspergillus Niger and various flocculent yeasts. The aim, where possible, has been to quantify the structure and behaviour of microbial aggregates and broths such that their properties may be predicted in various situations. To simplify the presentation, each topic has been examined in a separate chapter, and attempts have been made to illustrate the interaction of the topics and how the information may be used to obtain a better understanding of fermenter operation, especially tower systems.

The variability of aggregate structures has made precise quantitative work difficult. Comparison with the behaviour of conventional materials has been hindered by the difficulty of estimating the liquid content of individual cells and cell aggregates. However, fluidisation and sedimentation studies indicated that for microbial suspensions the voidage to the power "n" equalled the ratio of settling/fluidising velocity to aggregate terminal velocity. The value of "n" varied over a considerable range of 5 to 40, and was controlled by morphology, environmental conditions and stratification effects. These values of "n" were much greater than for conventional materials. Microbial suspension viscosities were found to be Bingham plastic at low concentrations and Pseudoplastic at high concentrations. Mycelial suspensions were found to have very high viscosities due to the interaction of mycelial networks.

Mathematical models of microbial aggregates are proposed which provide insight into structural and physical property variations. The strong influence of suspension concentration forms the basis of predictions of biomass yields and tower fermenter performance.

The research has been concerned with the physical characteristics
 of suspensions and their liquid suspensions; most of the
 work being carried out with *Spermatophytes* and various
 other plants. The aim, where possible, has been to quantify the
 behavior of individual aggregates and broths such that their
 behavior can be predicted in various situations. To simplify the
 treatment of topics has been examined in a separate chapter, and
 the main body of the thesis is devoted to the interaction of the topics and how
 this may be used to obtain a better understanding of former
 relationships.

The variability of aggregate structures has been studied
 without work difficult. Comparison with the behavior of conventional
 suspensions has been hindered by the difficulty of estimating the liquid
 state of individual cells and cells in aggregates. However, fluidization
 studies have indicated that for microbial suspensions the
 value of μ "settling" velocity, the value of μ varied over a considerable
 range, and was controlled by morphology, environmental
 conditions, and the interaction of these factors. These values of μ were much greater
 than conventional materials. Microbial suspension viscosities were
 also higher than those at low concentrations and pseudoplastic at
 high concentrations. Special suspensions were found to have very high
 viscosities.

The interaction of the interaction of physical and chemical properties
 of individual cells and physical properties are proposed which
 may be used to predict the behavior of suspensions. The
 interaction of suspension concentration forms the basis of predictions
 of behavior and for further performance.

This thesis is dedicated to the Count of St. Germain, the
 greatest of all alchemists, "who knows everything, and who never
 dies." (Voltaire)

List of Contents

<u>Section</u>	<u>Contents</u>	<u>Page</u>
Chapter 1	Of Microbes, Men and Research	1
1.1	The uses of fermentation	1
1.2	Single cell protein	1
1.3	The tower fermenter	3
1.4	The objectives of the research	7
Chapter 2	A description of microorganisms used in the tower fermenter	10
2.1	Introduction	10
2.2	The moulds	11
2.2.1	<u>Aspergillus Niger</u>	14
2.3	The Yeasts	20
2.3.1	Yeast flocculence	24
2.4	Activated Sludge	25
2.5	Final comments	26
Chapter 3	The determination of microbial physical properties	29
3.1	Introduction	29
3.2	Literature Survey	29
3.3	Experimental programme and procedure	34
3.3.1	Dry mycelial densities	34
3.3.2	Wet to Dry weight ratios	34
3.3.3	Pellet and floc diameters	35
3.3.4	Pellet densities	35
3.3.5	Preparation of microbial samples	36
3.4	Results and Analysis	38
3.4.1	The density of dry mycelium	38
3.4.2	Wet to Dry weight ratios	39
3.4.3	Pellet and floc dimensions	42
3.4.4	Pellet density determinations	45

3.4.5	Yeast floc densities	51
Chapter 4	Mathematical Models of microbial structures	54
4.1	Introduction	54
4.2	Fungal pellet Model	56
4.3	Microbial floc Model	64
4.4	Microbially coated solids	67
Chapter 5	Fluidisation and Sedimentation phenomena	70
5.1	Introduction	70
5.2	Literature Survey	70
5.2.1	A single particle in an infinite medium	70
5.2.2	A single porous particle	73
5.2.3	The effect of polymers on drag forces	75
5.2.4	Non-biological, multiparticle systems	79
5.2.4.1	Theoretical concepts	79
5.2.4.2	Experimental Investigations	88
5.2.5	Biological, multiparticle systems	98
5.3	Experimental equipment and techniques	104
5.3.1	Equipment	104
5.3.2	Experimental materials and methods	113
5.3.2.1	Materials	113
5.3.2.2	Experimental methods	115
5.4	Experimental results and analysis	121
5.4.1	A summary of relevant equations	121
5.4.2	Ballotini results	123
5.4.3	Diakon results	130
5.4.4	Mustard Seed results	142
5.4.5	Kaolin results	161
5.4.6	<u>Aspergillus Niger results</u>	164
5.4.7	Yeast results	170

5.4.8	Activated sludge results	179
5.5	Summary of fluidisation/Sedimentation work	181
Chapter 6	The viscosities of microbial suspensions	183
6.1	Introduction	183
6.2	Literature Survey	183
6.2.1	Measurement of microbial viscosities	184
6.3	Experimental methods	186
6.3.1	<u>A.Niger</u> Tests	187
6.3.2	Yeast Tests	187
6.4	Results and Analysis	188
6.4.1	<u>A.Niger</u> Results	188
6.4.1.1	Variation of apparent viscosity with morphology and biomass concentration	188
6.4.1.2	Rheological characteristics of <u>A.Niger</u>	192
6.4.1.3	Variation of apparent viscosity during fermentation	193
6.4.1.4	Fluidised bed viscosities	197
6.4.2	Yeast Results	197
6.4.2.1	Dry material concentration vs. apparent viscosity	199
6.4.2.2	Relative viscosity vs. volume fraction of solids	199
6.4.2.3	Rheological properties	200
6.4.2.4	The effect of pH on viscosity	200
6.5	Conclusions	200
Chapter 7	The design and operation of tower fermenters	203
7.1	Introduction	203
7.2	The prescence of the gas phase	203
7.2.1	Literature review of gas-liquid fluidisation	203
7.2.2	Qualitative observations on low-density solids	207
7.2.3	The behaviour and effects of the gas phase on fermentation	208
7.3	The effect of a fermenting liquid on a fluidised bed of microorganisms	210

175	Survey of Fluidisation/Sedimentation work
181	Viscosities of microbial suspensions
183	Fluidisation
183	Temperature survey
183	Measurement of microbial viscosities
184	Experimental methods
186	Batch tests
187	Flow tests
187	Static and dynamic
188	Batch results
188	Relation of apparent viscosity with morphology
188	Cellular concentration
192	Biological characteristics of <i>A. niger</i>
193	Relation of apparent viscosity during fermentation
197	Unfluidised bed viscosities
197	Unit formulae
199	Apparent concentration vs. apparent viscosity
199	Relative viscosity vs. volume fraction of solids
200	Biological properties
200	Effect of pH on viscosity
200	Conclusions
203	Design and operation of tower fermenters
203	Introduction
203	Relevance of the gas phase
203	Continuous transfer of gas-liquid fluidisation
207	Qualitative observations on low-density solids
208	Behaviour and effects of the gas phase on fermentation
210	Effect of a fermenting liquid on a fluidised bed of microorganisms

7.4	A mathematical model of a fermentation in a tower	214
7.5	Operational characteristics of a tower fermenter	217
7.5.1	The prediction of biomass yield	217
	Appendix A. Fluidisation / Sedimentation Results	222
	Nomenclature	237
	Bibliography	240
		38
		39
		40
		40
		42
		43
		44
		48
		58
		63
		65
		67
		68
		69
		114
		123
		123
		125
		126
		135
		136
		144
		152

List of Tables

Number	Description	Page
2.1	Fungal Classification	10
3.2.1	Microbial densities (Aiba et alia,1964)	30
3.2.2	Microbial dimensions (Sterbacek,1972)	33
3.2.3	Microbial densities (Sterbacek,1972)	33
3.4.1	Dry Yeast densities	38
3.4.2	<u>A.Niger</u> dry mycelial densities	39
3.4.3	<u>A.Niger</u> mycelial composition	40
3.4.4	<u>A.Niger</u> wet mycelial densities	40
3.4.5	Centrifuged wet weights for yeasts	42
3.4.6	<u>A.Niger</u> pellet dimensions (uniform pellets)	43
3.4.7	<u>A.Niger</u> pellet dimensions (non-uniform pellets)	44
3.4.8	<u>A.Niger</u> pellet densities	48
4.1	Pellet Model describing morphology	58
4.2	Pellet structures predicted from Model	63
4.3	Floc properties predicted from Floc Model ($E=0.4$)	65
4.4	Floc properties predicted from Floc Model ($E=0.2$)	67
5.2.2	Pigment properties (Henszelmann et alia,1967)	92
5.2.1	Summary of investigations into non-flocculent, non-biological fluidisation/sedimentation	93
5.3.1	Sieve analysis of dry mustard seeds	114
5.4.1	Ballotini terminal velocities	123
5.4.2	Wall-effect correction for ballotini	123
5.4.3	Minimum fluidisation velocities for ballotini	125
5.4.4	Richardson-Mielke analysis for 0.3cm ballotini	126
5.4.5	Hydrodynamic Models	135
5.4.6	Friction factors for diakon	136
5.4.7	Richardson-Mielke analysis for uncoated,uniform seeds	148
5.4.8	Physical properties of uncoated,multisized seeds	152

Description

Richardson-Mielke analysis for coated, uniform seeds (Alba et alia, 1967)

Richardson-Mielke analysis for coated, uniform seeds (Sterbacel, 1972)

Richardson-Mielke analysis for coated, uniform seeds (Sterbacel, 1972)

Richardson-Mielke analysis for coated, uniform seeds

Richardson-Mielke analysis for coated, uniform seeds

Richardson-Mielke analysis for coated, uniform seeds

Richardson-Mielke analysis for coated, uniform seeds

Richardson-Mielke analysis for coated, uniform seeds

Richardson-Mielke analysis for coated, uniform seeds

Richardson-Mielke analysis for coated, uniform seeds

Richardson-Mielke analysis for coated, uniform seeds

Richardson-Mielke analysis for coated, uniform seeds

Richardson-Mielke analysis for coated, uniform seeds

Richardson-Mielke analysis for coated, uniform seeds (B.O.S.)

Richardson-Mielke analysis for coated, uniform seeds (B.O.S.)

Richardson-Mielke analysis for coated, uniform seeds (B.O.S.)

Richardson-Mielke analysis for coated, uniform seeds (B.O.S.)

Richardson-Mielke analysis for coated, uniform seeds

Richardson-Mielke analysis for coated, uniform seeds

Richardson-Mielke analysis for coated, uniform seeds

Richardson-Mielke analysis for coated, uniform seeds

Richardson-Mielke analysis for coated, uniform seeds

Richardson-Mielke analysis for coated, uniform seeds

Richardson-Mielke analysis for coated, uniform seeds

Richardson-Mielke analysis for coated, uniform seeds

Richardson-Mielke analysis for coated, uniform seeds

Richardson-Mielke analysis for coated, uniform seeds

5.4.9	Pressure drop for coated/uncoated, uniform seeds	153/154
5.4.10	Richardson-Mielke analysis for coated, uniform seeds	154
5.4.11	Kaolin sedimentation analysis	161
5.4.12	Description of yeast strains in fluidisation / sedimentation tests	171
5.4.14	Richardson-Mielke analysis for CFCC 34	174
5.4.13	Yeast fluidisation/sedimentation analysis	176
5.4.15	Activated sludge hydrodynamics	179
6.1	Rheological constants for <u>A.Niger</u> (Bongenaar et al.)	186
6.2	Viscometer data	186/187
6.3	Variation of <u>A.Niger</u> suspension apparent viscosity with concentration and morphology	188
6.4	<u>A.Niger</u> apparent viscosity and volume fractions	191
6.5	Suspension viscosity theories	192
6.6	<u>A.Niger</u> rheology and morphology	193
6.7	Time variations in apparent viscosity during <u>A.Niger</u> fermentation	193
6.8	Fluidised bed viscosity for <u>A.Niger</u>	197
6.9	Viscosity results for a physically-limited yeast	199
7.1	The effect of <u>A.Niger</u> on gas-liquid behaviour	208
7.2	Biomass yields at $U = 0.1$ cm/s for <u>A.Niger</u>	218
5.1	Fluidisation factors for uniform seeds	72
5.2	Porous sphere Model (Guthrie & Fan, 1970)	72
5.3	Polymeric drag reduction in pipes (Liu et alia, 1972)	70
5.4	Polymeric drag increase for spherical particles (Liu et al, 1971)	70
5.5	Pressure drop in fluidised beds	63
5.6	Batch settling	63
5.7	Richardson-Mielke analysis	69
5.8	Motion in a liquid fluidised bed (Liu et alia, 1967)	67

List of Figures

Number	Description	Page
1.1	The APV tower fermenter	4
1.2	Scheme of the thesis	9
2.1	Some features of moulds	13
2.2	A Yeast cell	21
2.3	The budding process	21
3.1	<u>A.Niger</u> dry mycelial density profiles	41
3.2	<u>A.Niger</u> diameter ratios	41
3.3	<u>A.Niger</u> pellet densities	49
3.4	Pellet total liquid content	50
3.5	Pellet composition	50
3.6	CFCC 8 floc voidages	52
3.7	CFCC 8 terminal velocities	52
4.1	Floc simulations	55
4.2	Predicted floc voidages	57
4.3	Fungal pellet Model	57
4.4	Pellet Model for 38h. pellets	60
4.5	Pellet Model for 16h. pellets	61
4.6	Pellet Model for 22h. pellets	62
4.7	Floc Models	66
5.1	Friction factors for spheres	72
5.2	Porous sphere Model (Sutherland & Tan,1970)	72
5.3	Polymeric drag reduction in pipes (Zakin et alia,1972)	78
5.4	Polymeric drag increase for spheres(James et al ,1971)	78
5.5	Pressure drop in fluidised beds	83
5.6	Batch settling	83
5.7	Richardson-Mielke analysis	89
5.8	Motion in a liquid fluidised bed (Lawson et alia,1967)	97

5.9	Activated sludge settling (Aiba et alia ,1971)	97
5.10	The 3" Column	105
5.11	The two-dimensional bed	107
5.12	The 3.2cm. column and accessories	111
5.13	Ballotini fluidisation	124
5.14	Friction factor vs. Blake No.	128
5.15	0.065 cm. diakon fluidised in 3" column	132
5.16	0.055cm. diakon fluidised in 3"column	133
5.17	0.055cm. diakon fluidised in two-dimensional bed	134
5.18	Pressure drop across 0.055cm. diakon in two-dimensional bed	137
5.19	0.055cm. diakon ,settling curves in two-dimensional bed	140
5.20	0.055cm. diakon sedimentation analysis	141
5.21	Uncoated,uniform seeds settling in two-dimensional bed	145
5.22	Uncoated,uniform seeds fluidisation/sedimentation	146
5.23	Regression Programme	150
5.24	Uncoated,multisized seeds fluidised in 3" column	151
5.25	Pressure drop across bed of fluidised seeds	155
5.26	Coated,uuniform seeds,analysis of two-dimensional bed results,using the theoretical U_t	156
5.27	As above ,but using the experimental U_t	157
5.28	Coated,multisized seeds fluidised in 3" column	160
5.29a,b	Kaolin sedimentation	163
5.30	<u>A.Niger</u> fluidisation/sedimentation analysis	165
5.31	Pellet sedimentation curves	168
5.32	Yeast fluidisation in 3.2 cm column	177
5.33	CFCC 34 fluidisation analysis	178
5.34	Activated sludge settling	180

6.1a	The Ferranti Viscometer	189
6.1b	The effect of <u>A.Niger</u> morphology on viscosity	190
6.2	Viscosity vs. volume fraction solids for <u>A.Niger</u>	194
6.3	Rheology of <u>A.Niger</u> suspensions	195
6.4	<u>A.Niger</u> viscosity vs. time into fermentation	196
6.5	Fluidised bed viscosities for <u>A.Niger</u>	196
6.6	Yeast concentration vs. viscosity	198
6.7	Theoretical comparison of yeast suspension viscosities	198
6.8	Rheology of yeast suspensions	202
6.9	Effect of pH on viscosity of CFCC 83 suspensions	202
7.1	Three phase systems	206
7.2	Wake structures	206
7.3	Gas holdup in batch <u>A.Niger</u> fermentation	209
7.4	Surface tension and viscosity variations	209
7.5	Biomass predictions for batch <u>A.Niger</u> production	219
7.6	Biomass predictions for continuous <u>A.Niger</u> production	220
5.1		22
5.2		23
5.3		24
5.4		25
5.5		26

List of Plates

Number	Description	Page
2.1	<u>Aspergillus Niger</u> hyphae	12
2.2	Apical branching	12
2.3	"Hairy" pellet	17
2.4	"Hairy" pellet	17
2.5	"Furry" pellet	18
2.6	Autolysed pellet	18
2.7a,b	Czapek pellets	19
2.8	<u>S.Carlsbergensis</u> cells	22
2.9	Yeast flocs	22
2.10	Yeast floc	27
2.11	Activated Sludge	27
2.12	Activated Sludge	28
3.1	1½ litre tower fermenter	37
4.1	Yeast coating 0.2 cm. Ballotini	69
5.1	Uncoated and coated Mustard Seed	77
5.2	The 3" diameter column	108
5.3	The Two-Dimensional Bed	108
5.4	The 3.2 cm. column	112
5.5	Yeast fluidised in the 3.2 cm. column	112

Page	Description
12	Introduction
13	Materials and Methods
14	Results
15	Discussion
16	Conclusions
17	Acknowledgements
18	Literature Cited
19	Appendix
20	Index
21	Summary
22	References
23	Notes
24	Tables
25	Figures
26	Plates
27	Photomicrographs
28	Chemical Analysis
29	Physical Properties
30	Biological Data
31	Statistical Analysis
32	Concluding Remarks
33	Final Comments
34	References
35	Notes
36	Tables
37	Figures
38	Plates
39	Photomicrographs
40	Chemical Analysis
41	Physical Properties
42	Biological Data
43	Statistical Analysis
44	Concluding Remarks
45	Final Comments
46	References
47	Notes
48	Tables
49	Figures
50	Plates
51	Photomicrographs
52	Chemical Analysis
53	Physical Properties
54	Biological Data
55	Statistical Analysis
56	Concluding Remarks
57	Final Comments
58	References
59	Notes
60	Tables
61	Figures
62	Plates
63	Photomicrographs
64	Chemical Analysis
65	Physical Properties
66	Biological Data
67	Statistical Analysis
68	Concluding Remarks
69	Final Comments
70	References
71	Notes
72	Tables
73	Figures
74	Plates
75	Photomicrographs
76	Chemical Analysis
77	Physical Properties
78	Biological Data
79	Statistical Analysis
80	Concluding Remarks
81	Final Comments
82	References
83	Notes
84	Tables
85	Figures
86	Plates
87	Photomicrographs
88	Chemical Analysis
89	Physical Properties
90	Biological Data
91	Statistical Analysis
92	Concluding Remarks
93	Final Comments
94	References
95	Notes
96	Tables
97	Figures
98	Plates
99	Photomicrographs
100	Chemical Analysis
101	Physical Properties
102	Biological Data
103	Statistical Analysis
104	Concluding Remarks
105	Final Comments
106	References
107	Notes
108	Tables
109	Figures
110	Plates
111	Photomicrographs
112	Chemical Analysis
113	Physical Properties
114	Biological Data
115	Statistical Analysis
116	Concluding Remarks
117	Final Comments
118	References
119	Notes
120	Tables
121	Figures
122	Plates
123	Photomicrographs
124	Chemical Analysis
125	Physical Properties
126	Biological Data
127	Statistical Analysis
128	Concluding Remarks
129	Final Comments
130	References
131	Notes
132	Tables
133	Figures
134	Plates
135	Photomicrographs
136	Chemical Analysis
137	Physical Properties
138	Biological Data
139	Statistical Analysis
140	Concluding Remarks
141	Final Comments
142	References
143	Notes
144	Tables
145	Figures
146	Plates
147	Photomicrographs
148	Chemical Analysis
149	Physical Properties
150	Biological Data
151	Statistical Analysis
152	Concluding Remarks
153	Final Comments
154	References
155	Notes
156	Tables
157	Figures
158	Plates
159	Photomicrographs
160	Chemical Analysis
161	Physical Properties
162	Biological Data
163	Statistical Analysis
164	Concluding Remarks
165	Final Comments
166	References
167	Notes
168	Tables
169	Figures
170	Plates
171	Photomicrographs
172	Chemical Analysis
173	Physical Properties
174	Biological Data
175	Statistical Analysis
176	Concluding Remarks
177	Final Comments
178	References
179	Notes
180	Tables
181	Figures
182	Plates
183	Photomicrographs
184	Chemical Analysis
185	Physical Properties
186	Biological Data
187	Statistical Analysis
188	Concluding Remarks
189	Final Comments
190	References
191	Notes
192	Tables
193	Figures
194	Plates
195	Photomicrographs
196	Chemical Analysis
197	Physical Properties
198	Biological Data
199	Statistical Analysis
200	Concluding Remarks
201	Final Comments
202	References
203	Notes
204	Tables
205	Figures
206	Plates
207	Photomicrographs
208	Chemical Analysis
209	Physical Properties
210	Biological Data
211	Statistical Analysis
212	Concluding Remarks
213	Final Comments
214	References
215	Notes
216	Tables
217	Figures
218	Plates
219	Photomicrographs
220	Chemical Analysis
221	Physical Properties
222	Biological Data
223	Statistical Analysis
224	Concluding Remarks
225	Final Comments
226	References
227	Notes
228	Tables
229	Figures
230	Plates
231	Photomicrographs
232	Chemical Analysis
233	Physical Properties
234	Biological Data
235	Statistical Analysis
236	Concluding Remarks
237	Final Comments
238	References
239	Notes
240	Tables
241	Figures
242	Plates
243	Photomicrographs
244	Chemical Analysis
245	Physical Properties
246	Biological Data
247	Statistical Analysis
248	Concluding Remarks
249	Final Comments
250	References
251	Notes
252	Tables
253	Figures
254	Plates
255	Photomicrographs
256	Chemical Analysis
257	Physical Properties
258	Biological Data
259	Statistical Analysis
260	Concluding Remarks
261	Final Comments
262	References
263	Notes
264	Tables
265	Figures
266	Plates
267	Photomicrographs
268	Chemical Analysis
269	Physical Properties
270	Biological Data
271	Statistical Analysis
272	Concluding Remarks
273	Final Comments
274	References
275	Notes
276	Tables
277	Figures
278	Plates
279	Photomicrographs
280	Chemical Analysis
281	Physical Properties
282	Biological Data
283	Statistical Analysis
284	Concluding Remarks
285	Final Comments
286	References
287	Notes
288	Tables
289	Figures
290	Plates
291	Photomicrographs
292	Chemical Analysis
293	Physical Properties
294	Biological Data
295	Statistical Analysis
296	Concluding Remarks
297	Final Comments
298	References
299	Notes
300	Tables
301	Figures
302	Plates
303	Photomicrographs
304	Chemical Analysis
305	Physical Properties
306	Biological Data
307	Statistical Analysis
308	Concluding Remarks
309	Final Comments
310	References
311	Notes
312	Tables
313	Figures
314	Plates
315	Photomicrographs
316	Chemical Analysis
317	Physical Properties
318	Biological Data
319	Statistical Analysis
320	Concluding Remarks
321	Final Comments
322	References
323	Notes
324	Tables
325	Figures
326	Plates
327	Photomicrographs
328	Chemical Analysis
329	Physical Properties
330	Biological Data
331	Statistical Analysis
332	Concluding Remarks
333	Final Comments
334	References
335	Notes
336	Tables
337	Figures
338	Plates
339	Photomicrographs
340	Chemical Analysis
341	Physical Properties
342	Biological Data
343	Statistical Analysis
344	Concluding Remarks
345	Final Comments
346	References
347	Notes
348	Tables
349	Figures
350	Plates
351	Photomicrographs
352	Chemical Analysis
353	Physical Properties
354	Biological Data
355	Statistical Analysis
356	Concluding Remarks
357	Final Comments
358	References
359	Notes
360	Tables
361	Figures
362	Plates
363	Photomicrographs
364	Chemical Analysis
365	Physical Properties
366	Biological Data
367	Statistical Analysis
368	Concluding Remarks
369	Final Comments
370	References
371	Notes
372	Tables
373	Figures
374	Plates
375	Photomicrographs
376	Chemical Analysis
377	Physical Properties
378	Biological Data
379	Statistical Analysis
380	Concluding Remarks
381	Final Comments
382	References
383	Notes
384	Tables
385	Figures
386	Plates
387	Photomicrographs
388	Chemical Analysis
389	Physical Properties
390	Biological Data
391	Statistical Analysis
392	Concluding Remarks
393	Final Comments
394	References
395	Notes
396	Tables
397	Figures
398	Plates
399	Photomicrographs
400	Chemical Analysis
401	Physical Properties
402	Biological Data
403	Statistical Analysis
404	Concluding Remarks
405	Final Comments
406	References
407	Notes
408	Tables
409	Figures
410	Plates
411	Photomicrographs
412	Chemical Analysis
413	Physical Properties
414	Biological Data
415	Statistical Analysis
416	Concluding Remarks
417	Final Comments
418	References
419	Notes
420	Tables
421	Figures
422	Plates
423	Photomicrographs
424	Chemical Analysis
425	Physical Properties
426	Biological Data
427	Statistical Analysis
428	Concluding Remarks
429	Final Comments
430	References
431	Notes
432	Tables
433	Figures
434	Plates
435	Photomicrographs
436	Chemical Analysis
437	Physical Properties
438	Biological Data
439	Statistical Analysis
440	Concluding Remarks
441	Final Comments
442	References
443	Notes
444	Tables
445	Figures
446	Plates
447	Photomicrographs
448	Chemical Analysis
449	Physical Properties
450	Biological Data
451	Statistical Analysis
452	Concluding Remarks
453	Final Comments
454	References
455	Notes
456	Tables
457	Figures
458	Plates
459	Photomicrographs
460	Chemical Analysis
461	Physical Properties
462	Biological Data
463	Statistical Analysis
464	Concluding Remarks
465	Final Comments
466	References
467	Notes
468	Tables
469	Figures
470	Plates
471	Photomicrographs
472	Chemical Analysis
473	Physical Properties
474	Biological Data
475	Statistical Analysis
476	Concluding Remarks
477	Final Comments
478	References
479	Notes
480	Tables
481	Figures
482	Plates
483	Photomicrographs
484	Chemical Analysis
485	Physical Properties
486	Biological Data
487	Statistical Analysis
488	Concluding Remarks
489	Final Comments
490	References
491	Notes
492	Tables
493	Figures
494	Plates
495	Photomicrographs
496	Chemical Analysis
497	Physical Properties
498	Biological Data
499	Statistical Analysis
500	Concluding Remarks

Acknowledgements

The Author is indebted to the following,

1. The University of Aston in Birmingham, for financial assistance in the form of a Research Studentship.
2. Professor G.V. Jeffreys and all the Staff of the Chemical Engineering Department, for technical assistance and the use of facilities.
3. Dr. E.L. Smith, for his friendly and very valuable supervision of this research project.
4. Dr. G.G. Morris, for assistance in growing A. Niger pellets and discussions on their morphology.
5. Mr. M. Figgett, for his discussions on the Tower Fermenter model.
6. The Research Students of the Biological Sciences Tower Fermentation Group, for their assistance with microbiological aspects of the work.

CHAPTER 1

OF MICROBES , MAN AND RESEARCH1.1 The Use of Fermentation

Microorganisms have played an important role in shaping the history of civilisation. In addition to their disease-inducing qualities, microorganisms have been exploited by man ,often unwittingly, for many centuries. Within the last fifty years man has found an increasing use for microorganisms and their ability to perform complex chemical syntheses or decompositions. The production of some industrial organic chemicals such as citric, lactic and gluconic acids still involves microbes. However, the use of microbes in the production of edible materials has been, still is and probably will be , a most important one; although the use of them in waste treatment is rapidly rivaling the food uses. Yeasts are used for brewing, winemaking and baking and as a food supplement. Bacteria are used in vinegar production and together with filamentous fungi in cheese & yogurt manufacture. Whilst these uses will continue many see them as an answer to a potentially disastrous situation i.e. over-population and its resulting food shortages.

1.2 Single Cell Protein

The rapid growth in the population of this planet has only recently received the publicity and attention it merits, despite the gloomy predictions of Malthus over 200 years ago. In many respects this sudden interest has been detrimental to the cause, e.g. to quote the American President's Science Advisory Committee (1967) " ..the large amount of published and oratory material has caused the subject to be obscured by rhetorical overkill .." The author is not qualified, nor is it his intention, to contribute further to this overkill. However, this topic is associated with the *raison d'être* for this thesis and as such deserves some

discussion.

Yeasts and mushrooms have been eaten for many years, but it is only recently that the concept of using the protein in microorganisms as a food has been considered seriously. Bacteria consist of 80 % protein and yeasts of 53 % protein and as such are protein-rich when compared to some traditional food sources. The U.N. Economic & Social Council(1967) stated " If microorganisms can be processed to yield products which will be safe, nutritious, acceptable and within the economic resources of the developing countries, then they could supply a large part of the protein requirements in these areas.....producing and utilising, on a large scale, protein from single cells offers the best hope for major new protein supplies independent of agricultural land use. "

Microbial protein or "single cell protein "(SCP) as it has become known would serve as a supplement to the diet of both humans and animals. There are many papers relating to this subject. Two recent and fine reviews are by Snyder (1970) and Mateles &Tannenbaum (1968). The main attraction of SCP is its rapid production , which may be illustrated by the following figures,

Basis; one day's growth;	
1000 lb. cow produces	1 lb. protein
..... soybeans	80
..... yeast	112,000.....

The recommended quantity of SCP supplement is 15g. per day for humans. However, continuous consumption of such material may not be desirable as the build-up of certain metabolites, e.g. uric acid, may occur.

The use of fungi may not be so easy due to,

- i. the poor palatability of mycelia
- ii. the large quantities of water required in production,
(19 gals, per pound of mycelia)

and iii. that mainly mesophiles appear to be edible, which could be a problem in tropical areas.

Despite the many difficulties several industrial concerns have been actively pursuing research into SCP production, since the rewards for success are considerable. For example, British Petroleum Co. have grown yeast on gas-oil fractions (Laine, 1972) and intend to build a large production unit in Sardinia; Rank Hovis McDougall, Ltd. have developed a multipurpose mycelial food base from a *Fusarium* species; and Tate & Lyle, Ltd. have pursued a similar path using *Aspergillus Niger*. Clearly, the concept of SCP is taken very seriously and once the biochemical and nutritional problems associated with organism selection and growth are solved, the most important consideration is that of production cost. This must be minimised if SCP is to be of use in the developing countries. The fermentation stage will influence production costs considerably and choice, design and operation of the fermenter require a better understanding of the physical behaviour of fermentation broths and of microbial structures within broths.

1.3 The Tower Fermenter

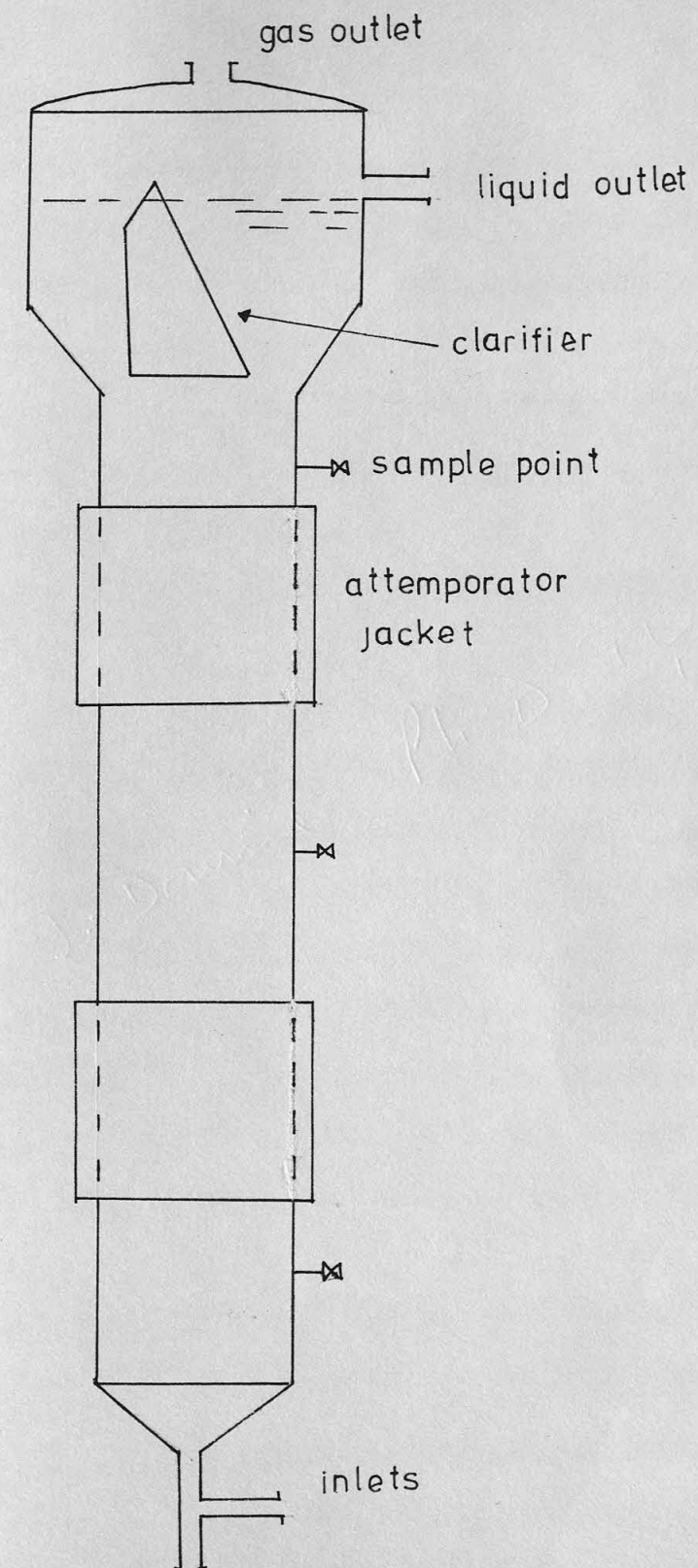
Minimising the cost of SCP or any other fermentation product depends on:

- i. Having low power requirements for mixing, pumping, etc.
- ii. Having a large reactor volume per unit floor area.
- iii. Having a fermenter of low capital cost which is easily and cheaply maintained.
- iv. Minimising labour costs, e.g. a continuous system.
- v. Producing as much microorganism per reactor volume as can be.

The tower fermenter has been developed with these points in mind, and for some processes may rival the more conventional stirred tank system.

The simplest form of tower system is shown in Fig. 1.1. The microbial population is contained within a tubular, vertical vessel. Sterile air may be introduced at the base of the tower.

FIG 1.1 TOWER FERMENTER (A.P.V.)



This provides oxygen for the microorganisms and also serves to agitate the suspension. In continuous operation nutrient liquid is introduced into the base of the tower: this may cause the microbes to be fluidised and possibly be removed in the overflow stream. The tower behaves as a plug-flow reactor in anaerobic operation and as a well mixed reactor when air is introduced.

Maximum microbial growth occurs in well mixed systems, whereas maximum metabolite production occurs in plug-flow systems (Stevens, 1966). The tower fermenter can be operated to fulfill these dual requirements. Plug-flow operation may be achieved by

- i. using perforated plates to compartmentalise the system,
- ii. placing baffles and a shaft fitted with agitators along the length of the tower, or

iii. using natural means, such as particle stratification, within an empty tube.

Methods i. & ii. are of most interest in the case of aerobic processes. The work in this thesis has been concerned with the latter method.

However, a brief description of the others will follow.

Kitai et alia (1969, 1970) tested a perforated plate column using Escherichia coli and noted that a critical plate hole diameter/column diameter was required to produce a multistage system with no intermixing between plates. The column was operated co-currently with respect to the gas and liquid. They also noted that the cell populations decreased with distance from the base and attributed this to residence time distribution.

However, Prokop et alia (1969) concluded that this was due to sedimentation. They used an eight compartment column growing Saccharomyces

Cerevisiae and their results showed a considerable deviation from the desired eight tanks-in-series model. Two, four and eight compartment towers were mathematically modelled by Erickson et alia (1972). An analysis of the steady state growth of cells accounting for backflow

and sedimentation was attempted. The model predicted that a wide range of operating conditions could be used.

A fermenter containing paddles attached to a central shaft was described by Falch & Gaden (1969,1970). They grew E.Coli in a four compartment column. In contrast to the sieve-plate type, this was operated counter-currently, which led to difficulties in controlling the gas and liquid flowrates. The system was modelled mathematically and a comparison of the observed and the predicted values were made, (this mainly concerned the liquid residence time distributions). The oxygen transfer rate and the gas hold-up were found to be influenced by the agitator speed. Means et alia (1962) have used a horizontal paddle type column for the production of filamentous fungi.

The "open" type of tower fermenter, shown in Fig.1.1, was originally developed by the APV Co., Sussex, for beer production. Initial investigations with beer producing towers was reported by Kloppe et alia (1965), who found that wort flowrate had little effect on the rate of decrease of wort gravity (which is a convenient measure of sugar concentration) with residence time. In a later paper, Ault et alia (1969) attributed the rapid fall in gravity to the initial fermentation of glucose and fructose. They also measured changes in sugar concentration at different wort flowrates and at different positions in the tower.

Royston (1966) has described in some detail the characteristics of the APV tower. The expansion section (see Fig. 1.1) is fitted to encourage yeast retention and to reduce foaming. The mean yeast concentration is initially about 250 g/l. with a residence variation of between 2 to 8 h., depending on wort gravity, yeast strain and degree of attenuation. The position in the tower at which the concentration of yeast approaches a maximum level depends on the liquid flowrate. The behaviour of the yeast can be related to i. the phenomenon of hindered settling, ii. the effect of the fermentation on the flocculence and iii. the effect of the gas bubbles on the floc motion. The residence time of

the yeast was roughly fifty times that of the liquid.

The complete APV continuous brewing process was described by Shore & Royston (1968). They concluded that the maximum theoretical rate of fermentation was obtained when the yeast concentration was 50% by vol. This was based on the assumption that the rate of ethanol production was first order with respect to yeast concentration.

Greenshields & Smith (1971) have described the work performed at Aston University on batch yeast and mould growth, together with the continuous, small-scale production of ethanol and vinegar. Yeasts were classified as;

- i. Non-flocculent, i.e. yeasts not attaining concentrations greater than 30 g/l. (on a wet cell wt. basis).
- ii. physically-limited, flocculent, i.e. yeasts attaining concentrations up to about 300 g/l., and
- iii. fermentation-limited, ^{flocculent} i.e. yeasts attaining concentrations upto 400 g/l. and forming such large flocs that washout did not occur.

The basic engineering problems associated with the design and operation of tower systems were also mentioned. These include rate processes, diffusion, reaction kinetics, fluidisation and sedimentation. Their approach was to assume the applicability of equations and ideas arising from studies of conventional solid / fluid systems.

1.4 The Objectives of This Research

The interest in tower systems at Aston University began in the Biological Sciences Department with the industrially related research supervised by Dr. R.N. Greenshields. Collaboration with the Chemical Engineering Department and Dr. E.L. Smith led to certain tower engineering problems being investigated.

An extensive study of gas-liquid systems was first made by Downie (1972). The need to study the behaviour of solid-liquid systems was also recognised at an early stage, and this led to the formulation

of objectives for the author's research. The main aim has been to attempt to physically characterise microbial aggregates and then to use this information to examine fluidisation / sedimentation effects and broth viscosities. A better understanding of the structure and properties of microbial aggregates was viewed as imperative considering the lack of fundamental information in the literature. The trend towards continuous fermentation requires knowledge of microbial hydrodynamics, which again was lacking. This information was necessary for the prediction of mass-transfer rates, reaction rates, biomass yields, operational flowrates and fermenter geometry. The subject proved diverse and encompassed many different topics. Where possible microbial systems have been compared to more conventional ones. The whole subject has been divided into distinct, but related chapters for clarity. The author has attempted in the next five chapters to present a logical buildup of ideas and information on the following topics,

- i. A qualitative description of microbial morphology.
- ii. The physical properties of microbial aggregates.
- iii. Mathematical models of microbial aggregates
- iv. The fluidisation / sedimentation of microbial aggregates, together with information on more conventional materials.
- v. The viscosity of microbial suspensions.

In the final chapter it is hoped to show how this information may be used to achieve a better understanding of tower fermenter operation and design. A schematic representation of this thesis plan is shown in Fig. 1.2.

The yeast was roughly fifty times that of the liquid. The complete APV continuous brewing process was described by Shore & Royston (1968). They concluded that the maximum theoretical rate of fermentation was obtained when the yeast concentration was 50% by vol. This was based on the assumption that the rate of ethanol production was first order with respect to yeast concentration.

Greenhalgh & Smith (1971) have described the work performed at Aston University on batch yeast and mould growth, together with the continuous, small-scale production of ethanol and vinegar. Yeasts were classified as:

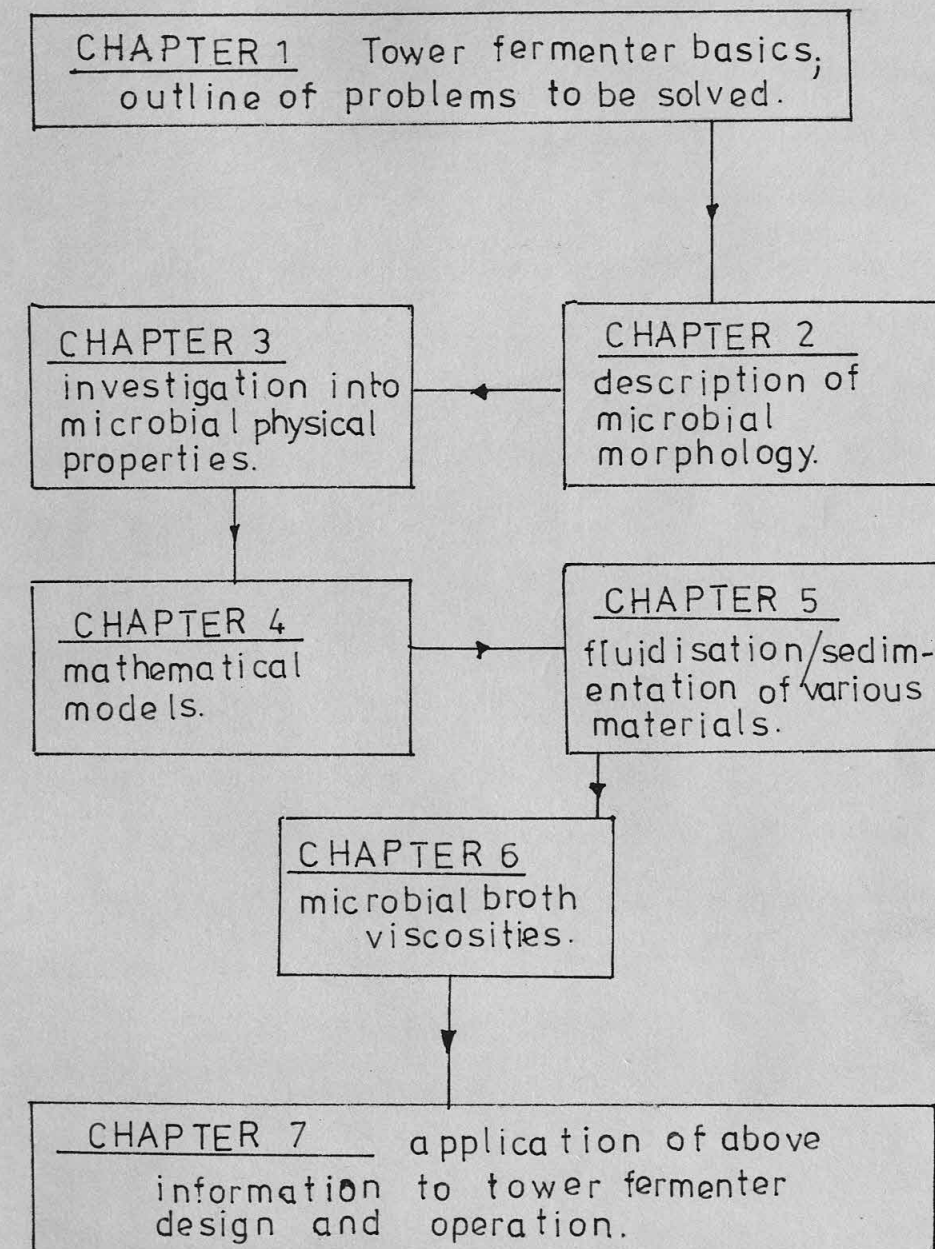
- i. Non-flocculent, i.e. yeasts not attaining concentrations greater than 30 g/l. (on a wet cell wt. basis).
 - ii. Physically-limited, flocculent, i.e. yeasts attaining concentrations up to about 300 g/l. and
 - iii. Fermentation-limited, i.e. yeasts attaining concentrations up to 400 g/l. and forming such large flocs that without did not occur.
- The basic engineering problems associated with the design and operation of tower systems were also mentioned. These include rate processes, diffusion, reaction kinetics, fluidisation and sedimentation. Their approach was to assume the applicability of equations and ideas arising from studies of conventional solid / fluid systems.

1.4 The Objectives of This Research

The interest in tower systems at Aston University began in the Biological Sciences Department with the industrially related research supervised by Dr. R.M. Greenhalgh. Collaboration with the Chemical Engineering Department and Dr. E.L. Smith led to certain tower engineering problems being investigated.

An extensive study of gas-liquid systems was first made by Downie (1972). The need to study the behaviour of solid-liquid systems was also recognised at an early stage, and this led to the formation

FIG.12 SCHEME FOR THESIS



of objectives for the author's research. The main aim has been to attempt to physically characterise microbial aggregates and then to use this information to examine fluidisation / sedimentation effects and broth viscosities. A better understanding of the structure and properties of microbial aggregates was viewed as imperative considering the lack of fundamental information in the literature. The trend towards continuous fermentation requires knowledge of microbial hydrodynamics, which again was lacking. This information was necessary for the prediction of mass-transfer rates, reaction rates, biomass yields, operational flow rates and fermenter geometry. The subject proved diverse and encompassed many different topics. Where possible microbial systems have been compared to more conventional ones. The whole subject has been divided into distinct but related chapters for clarity. The author has attempted in the next five chapters to present a logical buildup of ideas and information on the following topics:

- i. A qualitative description of microbial morphology.
- ii. The physical properties of microbial aggregates.
- iii. Mathematical models of microbial aggregates.
- iv. The fluidisation / sedimentation of microbial aggregates, together with information on more conventional materials.
- v. The viscosity of microbial suspensions.

In the final chapter it is hoped to show how this information may be used to achieve a better understanding of tower fermenter operation and design. A schematic representation of this thesis plan is shown in Fig. 1.2.

CHAPTER 2

A DESCRIPTION OF MICROORGANISMS USED IN THE TOWER FERMENTER

2.1 Introduction

It is the microorganisms which constitute the most important phase in a fermenter, for without them the fermenter is not a fermenter. This basic truth has sometimes been ignored by engineers who tend to view fermenters with the same eye as any other chemical reactor.

The bulk of this thesis is concerned with a few important commercial microorganisms, with how they behave macroscopically in liquid suspensions and with their physical properties and structure. These characteristics are governed at a microscopic level by the cell behaviour of each microbial species. Hence, in this Chapter a general outline of the mycology of the relevant organisms will be attempted. The author does not claim to be a microbiologist and for more detailed information the reader is advised to consult the many excellent texts, such as Pelczar & Reid (1972), Carpenter (1967) and Doudoroff et alia (1970).

At present the types of organism most frequently used in the tower fermenter are the fungi. A basic classification, with some species, is given below.

True Fungi (Eumycophyta)			
I:Phycomycetes	II:Ascomycetes	III:Basidiomycetes	IV:Fungi Imperfecti
Mucor, Rhizopus (non-septate mycelium) Pythium, (septate)	Yeasts, Aspergillus.	Mushrooms, Smuts, Rusts	lacking sexual spores Aspergillus, Penicillium.

Table 2.1 Fungal Classification

2.2 The Moulds

These are distinguished from other fungi by the presence of filamentous fruiting bodies. The body of a mould is composed of mycelium, which is an aggregation of threadlike filaments called hyphae, which anchor the mould and secure nutrients. Some Aspergillus niger hyphae are shown in Plate 2.1. These hyphae are septate (i.e. have cross walls within the strand). Non-septate hyphae also occur in some species. The hyphae may be "fertile"(reproduction role) or "vegetative"(food-gathering role).

Septate hyphae may grow either by division of the cell at the end of the thread (apical growth), or by cell division within the main bulk (intercalary growth). Branching of the hyphae may occur at the end (apical, see Plate 2.2) or in the main thread (lateral). The kinetics of hyphal growth have been studied by Trinci (1970).

Reproduction of moulds may occur through division, (budding), but does so mainly through spore formation. Sexual spores are produced by perfect fungi, but in stable species propagation occurs through asexual spore production, which is characteristic of Fungi Imperfecti. Several types of asexual spore may be produced including conidia and sporangiospores. Conidia may be produced singly or in chains at the end of a fertile hyphae called a conidiophore. Conidia are attached to a special cell, the Sterigma, on the conidiophore. These configurations often characterise the species and examples are shown in Fig. 2.1. The sporangiospores are produced in a special type of fertile hyphae, the sporangium or sac. Sporulation is a complex subject and special reference should be made to Galbraith and Smith (1966) who studied A. niger sporulation in submerged culture.

Moulds are notably hardy organisms: they can grow in conditions of low moisture, high osmotic pressure, high temperature and over a wide pH range (2 to 9). Many of these conditions would inhibit yeasts or bacteria

CHAPTER 2

A DESCRIPTION OF MICROORGANISMS USED IN THE TOWER FERMENTER

2.1 Introduction

It is the microorganisms which constitute the most important phase in a fermenter, for without them the fermenter is not a fermenter. This basic truth has sometimes been ignored by engineers who tend to view fermenters with the same eye as any other chemical reactor.

The bulk of this thesis is concerned with a few important commercial microorganisms, with how they behave macroscopically in liquid suspensions and with their physical properties and structures. These characteristics are governed at a microscopic level by the cell behaviour of each microbial species. Hence, in this Chapter a general outline of the mycology of the relevant organisms will be attempted. The author does not claim to be a microbiologist and for more detailed information the reader is advised to consult the many excellent texts, such as Pelczar & Reid (1972), Carpenter (1967) and Doudoroff et alia (1970). At present the types of organism most frequently used in the tower fermenter are the fungi. A basic classification, with some species, is given below.

True Fungi (Eumycophyta)			
I: Phycomycetes	II: Ascomycetes	III: Basidiomycetes	IV: Fungi imperfecti
Mucor, Rhizopus (non-septate mycelium) Pythium, (septate)	Yeasts, Aspergillus,	Mushrooms, Smuts, Rusts	Lacking sexual spores, Aspergillus, Penicillium

Table 2.1 Fungal Classification

These are distinguished from other fungi by the presence of filamentous fruiting bodies. The body of a mould is composed of mycelium, which is an aggregation of threadlike filaments called hyphae, which anchor the mould and secure nutrients. Some *Aspergillus niger* hyphae are shown in Plate 2.1. These hyphae are septate (i.e., have cross walls within the strand). Non-septate hyphae also occur in some species. The hyphae may be "fertile" (reproduction role) or "vegetative" (food-gathering role).

Septate hyphae may grow either by division of the cell at the end of the strand (apical growth), or by cell division within the main bulk (intercalary growth). Branching of the hyphae may occur at the end (apical, see Plate 2.2) or in the main strand (lateral). The kinetics of hyphal growth have been studied by Trinci (1970).

Reproduction of moulds may occur through division, budding, but does so mainly through spore formation. Sexual spores are produced by perfect fungi, but in stable species propagation occurs through asexual spore production, which is characteristic of fungi imperfecti. Several types of asexual spores may be produced including conidia and sporangiospores. Conidia may be produced singly or in chains at the end of a fertile hyphae called a conidiophore. Conidia are attached to a special cell, the sterigma, on the conidiophore. These configurations often characterize the species and examples are shown in Fig. 2.1. The sporangiospores are produced in a special type of fertile hyphae, the sporangium or asc. Sporulation is a complex subject and special reference should be made to Calbreath and Smith (1969) who studied *A. niger*.

Sporulation in submerged culture. Moulds are notably hardy organisms: they can grow in conditions of low moisture, high osmotic pressure, high temperature and over a wide pH range (2 to 9). Many of these conditions would inhibit yeasts or bacteria.

PLATE 2.1 ASPERGILLUS NIGER HYPHAE (x 745)

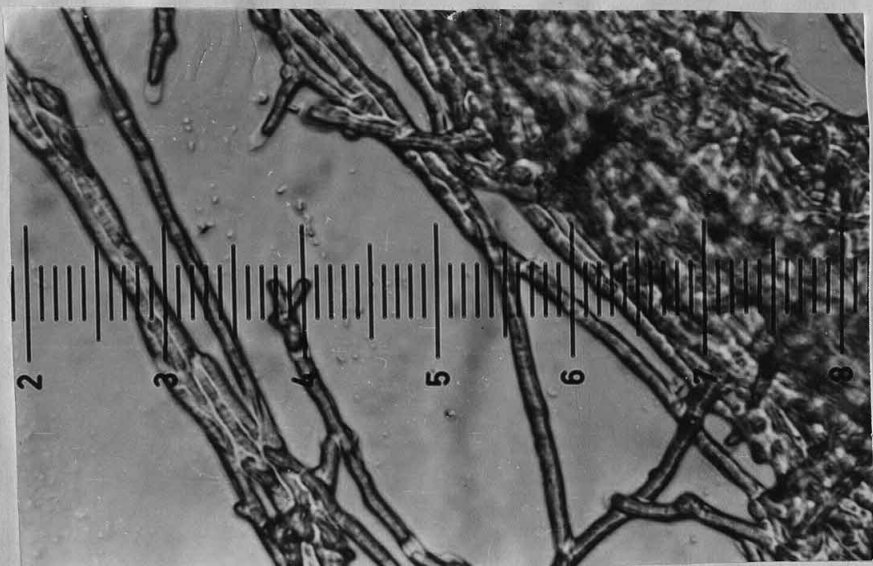


PLATE 2.2 APICAL BRANCHING (x 1060)

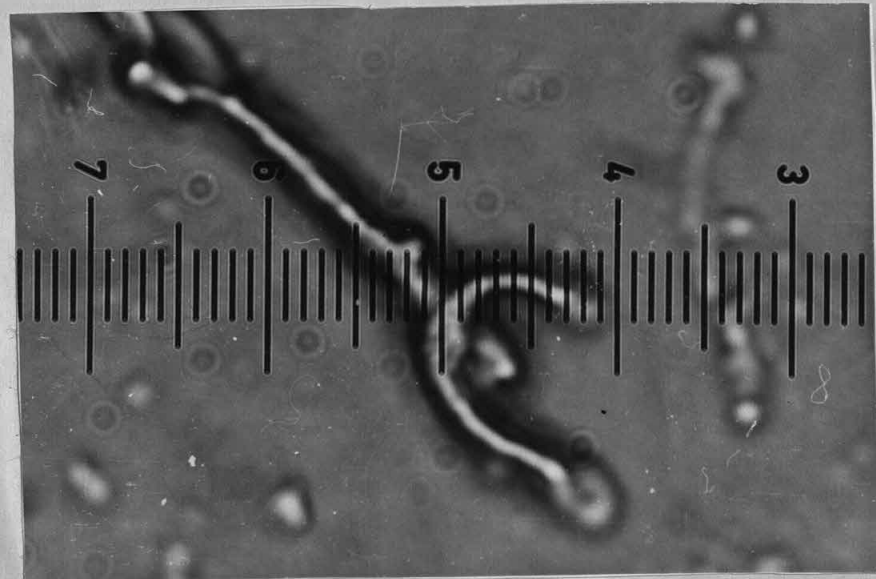
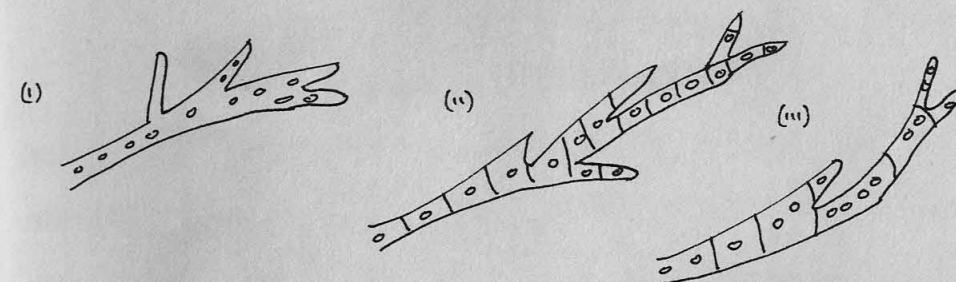
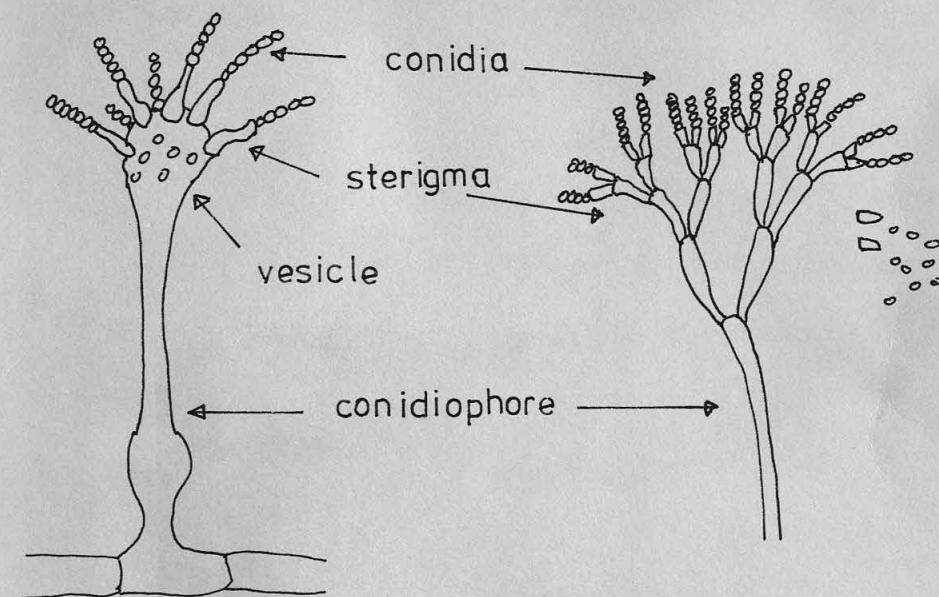


FIG. 21 FEATURES OF MOULDS



Types of hyphae: (i) nonseptate
(ii) septate - uninucleate cells
(iii) multi



Aspergillus

Penicillium

The moisture available for growth may be expressed as water activity,

a_w = vapour pressure of solution / vapour pressure of solvent.

Each mould has an optimum a_w for growth and germination, e.g.

<u>Species</u>	<u>Optimum a_w</u>
Aspergillus	0.980
Rhizopus	0.995
Penicillium	0.994

An $a_w < 0.62$ would inhibit mould growth. The temperature range for mould survival is large. Mostly, they are mesophilic (22 to 30°C), although some thermophilic species may grow at 62°C. Moulds are aerobic and require abundant supplies of oxygen for growth. They can utilise most carbohydrates as food sources. Some common types of mould and their occurrence are listed below.

<u>Species</u>	<u>Aspects</u>
Rhizopus Nigricans	causes mouldy bread, white mould.
Mucor Mucedo	a grey fruit mould.
Aspergillus Niger	Gluconic, Citric acid production
A. Glaucus	causes leather spoilage, green mould.
A. Fumigatus	pathogenic, pulmonary disease
Penicillium Chrysogenum	Penicillin antibiotic
or Notatum	
P. Camemberti	cheese mould.

2.2.1 Aspergillus Niger

This species has been used extensively in the author's work. The strain was obtained from Tate & Lyle, Ltd. and was designated M1. The growth of this organism in submerged culture leads to two basic forms depending on the local shear conditions. A filamentous mycelium is produced in stirred tanks (high shear) and a pellet form is produced in shake flasks and tower fermenters. The pellet form was the one examined in this study.

An early investigation into the production of fungal pellets was made by Burkholder & Sinnott (1945). They examined the morphology of 150 species grown in shake flasks. They consistently observed the pellet form as opposed to surface mat cultures found on stationary media. Various pellet morphologies were observed, e.g. smooth, hairy, or ragged forms, depending on the species. They ascribed the formation of pellets to the multi-directional exposure to nutrients produced in a lightly agitated media. Yanagita (1963) reported similar results and conclusions.

Steel et alia (1954, 1955) examined the morphology of *A. Niger* grown in tower fermenters. The aim of the investigation was to maximise the yield of citric acid from beet molasses using this organism. They found that the quantity of acid produced was directly proportional to the size of the inoculum, as was pellet development. The effects of different media on morphology were also examined.

The Tower Fermentation Group at Aston University has made detailed studies of *A. Niger* grown in towers. The author, when working with *A. Niger* suspensions, worked in collaboration with Morris (1972) and the description of pellet morphology which follows is a result of these investigations.

The medium used extensively was based on beet molasses, and it was found to give good growth. The size of the pellets varied depending on the initial spore concentration. If the spores were well-dispersed initially with Tween-80 surfactant, then the colony size distribution was small compared to a poorly-dispersed suspension. The full sequence of development achieved with molasses medium is described below.

1. Spore aggregate

The spores in solution aggregate together into small clusters which contain varying numbers of spores (in a well-dispersed suspension an average of 50 spores / aggregate is common). About 12 h. after inoculation these spores begin to germinate, and for M1 one hypha per spore

The moisture available for growth may be expressed as water activity, a_w = vapour pressure of solution / vapour pressure of solvent. Each would have an optimum a_w for growth and germination, e.g.

Species	Optimum a_w
<i>Aspergillus</i>	0.980
<i>Botrytis</i>	0.995
<i>Penicillium</i>	0.994

An $a_w < 0.62$ would inhibit mould growth. The temperature range for mould survival is large. Mostly, they are mesophilic (22 to 30°C), although some thermophilic species may grow at 62°C. Moulds are aerobic and require abundant supplies of oxygen for growth. They can utilise most carbohydrates as food sources. Some common types of mould and their occurrence are listed below.

Species	Aspects
<i>Rhizopus nigricans</i>	causes mouldy bread, white mould.
<i>Mucor mucedo</i>	a grey fruit mould.
<i>Aspergillus Niger</i>	Gluconic, citric acid production
<i>A. Glaucus</i>	causes leather rot, green mould.
<i>A. Fumigatus</i>	pathogenic, pulmonary disease
<i>Penicillium Chrysogenum</i>	Penicillin antibiotic
<i>or Botrytis</i>	
<i>F. Complanatus</i>	cheese mould.

2.2.1 *Aspergillus Niger*

This species has been used extensively in the author's work. The strain was obtained from Tate & Lyle, Ltd. and was designated M1. The growth of this organism in submerged culture leads to two basic forms depending on the local shear conditions. A filamentous mycelium is produced in stirred tanks (high shear) and a pellet form is produced in shake flasks and tower fermenters. The pellet form was the one examined in this study.

develops. These hyphae grow and begin to branch such that a loose structure

develops.

ii. "Hairy" Pellet

These are loose hyphal structures that develop by continuous branching and hyphal intertwining into more compact structures. These may exist from 2 to 3 cm. into the fermentation. The various degrees of

"hairiness" are illustrated in Plates 2.3, 2.4.

iii. "Furry" Pellet

Eventually, the centre of the pellet fills out such that a compact structure with a short protrusion of hyphae is obtained. This state may exist up to 300. Fermentation and is illustrated in Plate 2.5. Pellets grown in a poorer medium, such as Czapek, remain in this state perpetually (see Plate 2.7) and do not develop into the smooth type.

iv. "Smooth" Pellet

A pellet morphology may be reached where the pellet consists of a compact and apparently solid ball of mycelium, with a few hyphae protruding for a short distance from the core. The exact mechanism which produces this state is not clear. The lack of development of surface hyphae may be caused by strand breakage when the hyphae reach a certain size.

A. Niger hyphae, in particular, are brittle (Tateno, 1971), and when poorly supported by surrounding hyphae may be broken by the local shear forces. Alternatively, the lack of nutrient in solution at this stage in the fermentation may lead to excessive branching of hyphae in the main core of the pellet, thus giving a more uniform appearance to the pellet.

v. Autolysed Pellet

The formation of the strong mycelial shell in smooth pellets causes the diffusion of nutrients into the centre to be very slow. This leads, eventually, to the breakdown of the centre and a cavity forms. This cavity may be considerable. Pellets of some age have been observed to have only a fine mycelial shell, the inside being filled with liquid. Such pellets may be inflated and deflated easily using a hypodermic needle.

PLATE 2.3 "HAIRY" PELLETS (x 400)

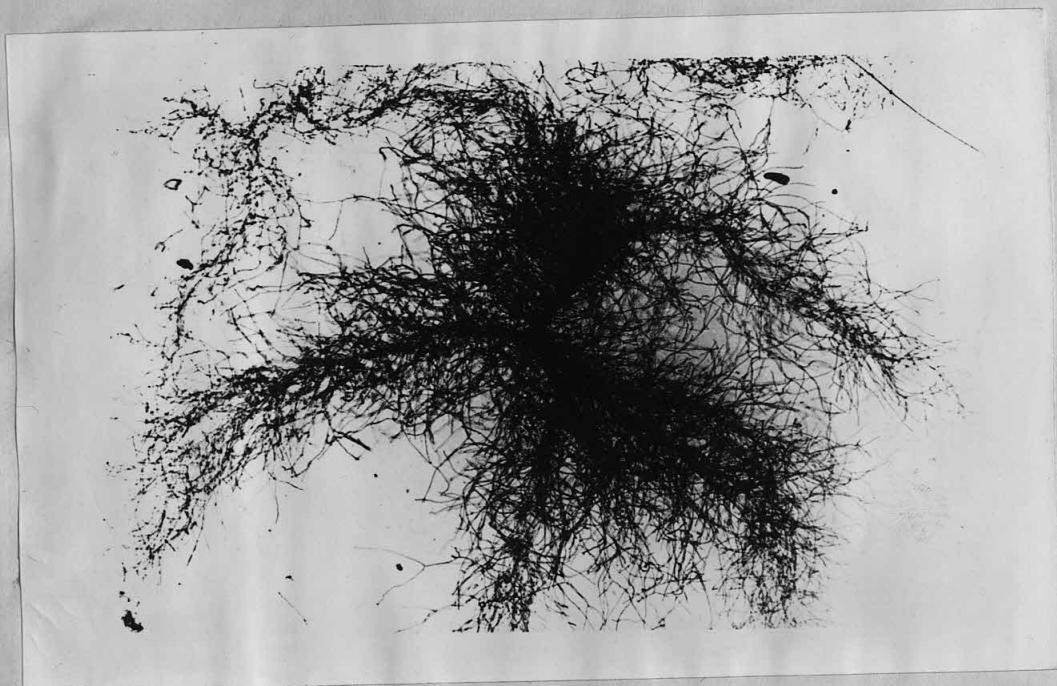
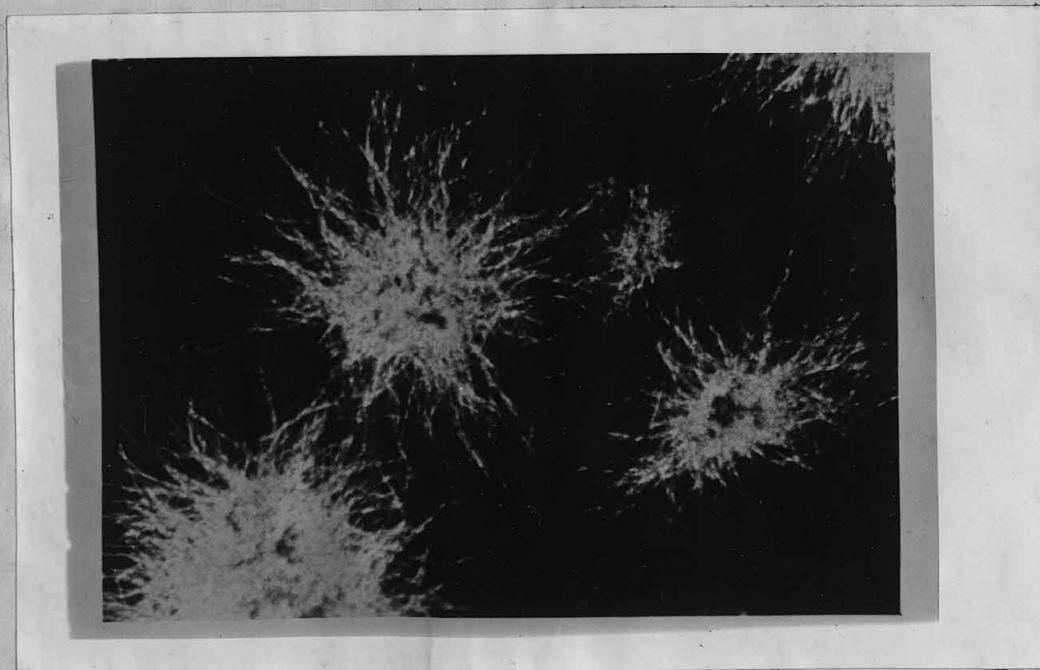
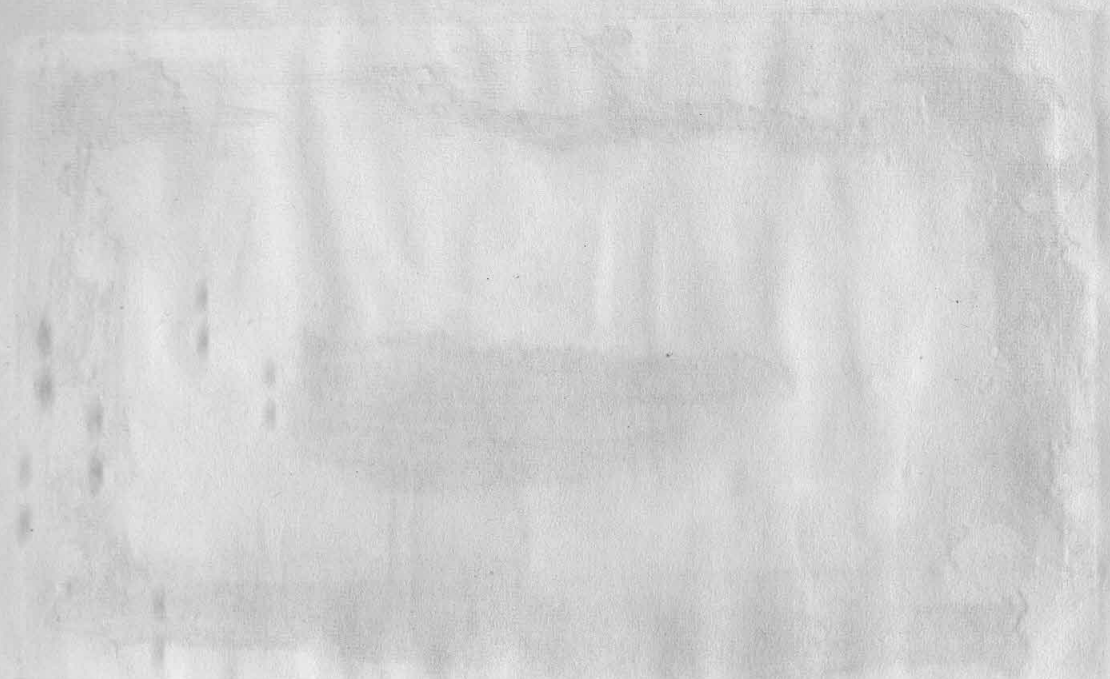


PLATE 2.4 "HAIRY" PELLETS (x 80)



(100 x) "FURRY" PELLETS (x 130)



(100 x) "FURRY" PELLETS (x 130)



PLATE 2.5 "FURRY" PELLETS (x 130)

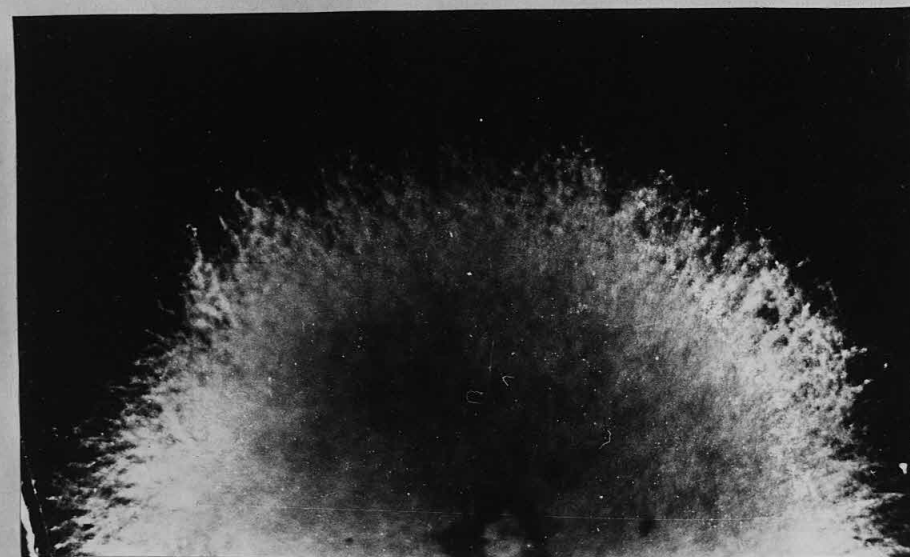


PLATE 2.6 AUTOLYSED PELLETS (x 2)

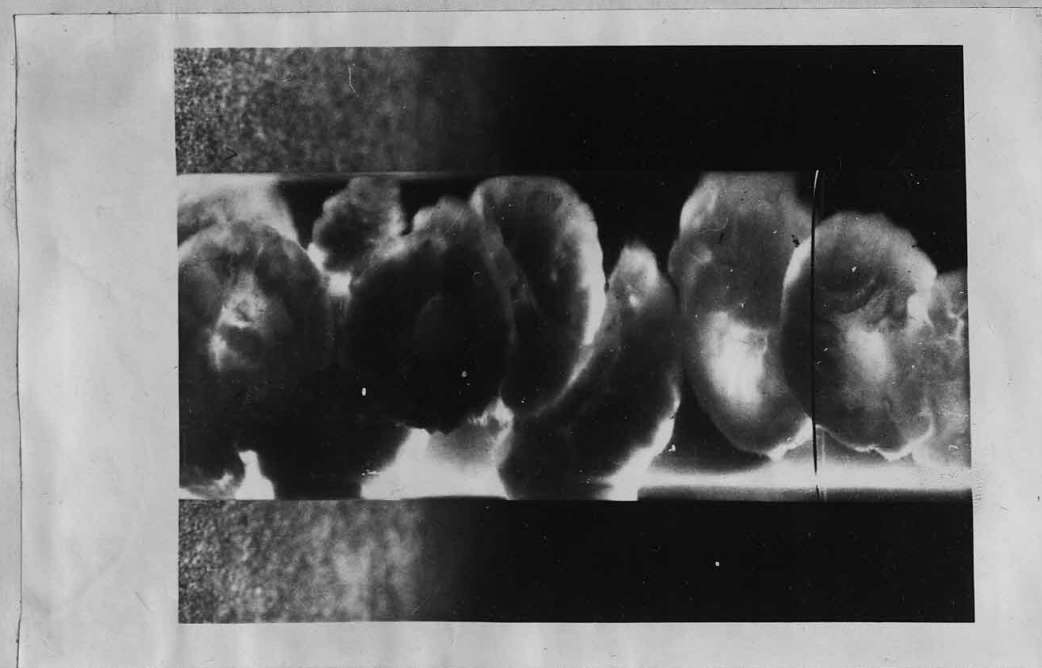
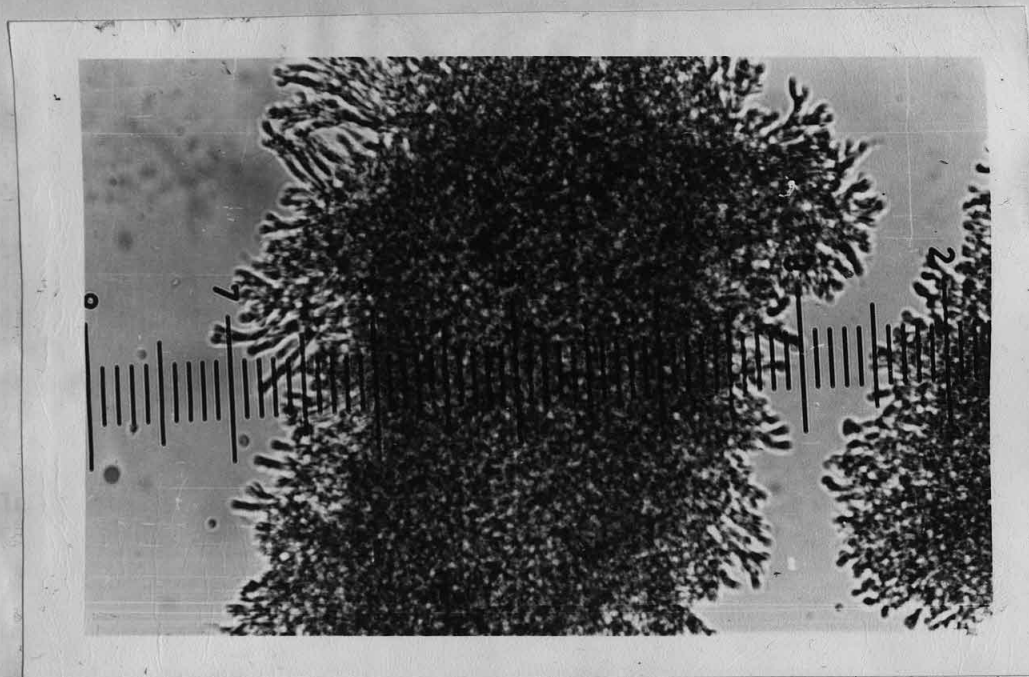


PLATE 2.7 CZAPEK PELLETS (x267)

(a)



(b)



and syringe. Some sectioned autolysed pellets are shown in Plate 2.6.

The formation of pellets is probably due to both biochemical and physical factors. Pellet morphology may certainly be altered by changing the available nutrients. However, the basic reason for the development of pellets must be due to the presence of shear forces in the liquid medium. In stationary liquids the spores float to the surface and develop there to produce a filamentous mass. When this surface is being continually disturbed the spores are forced to exist in the bulk of the agitated liquid. Thus, it is the agitation which leads to spore formation by forcing the spores into isolated clusters within the liquid. It may also be possible that the shear forces in the liquid shape the pellet by causing the hyphae to grow in certain directions. There may be a relationship between the size of eddies in the agitated liquid and the size and shape of pellets produced. In the author's opinion pellet morphology is a complex subject controlled by a complex interaction between liquid shear forces and nutrient supply.

2.3 Yeasts

The term "yeast" encompasses a very large group of unicellular fungi. Yeasts have played an important role in the nutrition of mankind for many centuries. Whilst this study has only dealt with a few species of the large *Saccharomyces* family, certain general characteristics apply to most yeasts. A schematic diagram of a yeast cell is shown in Fig.2.2, and a group of *Saccharomyces Carlsbergensis* cells are shown in Plate 2.8. Cell size can be from 1 to 5 microns in width and 5 to 30 microns length. Cell shape varies between ellipsoidal, cylindrical and spherical. The basic cell components are as follows.

i. Cell wall

The thickness varies with age, but averages $1/7$ of the cell diameter. It is composed of the polysaccharides, glucan and mannan. The walls of *S. Cerevisiae* contain about 7% protein, which is probably enzyme.

PLATE 2.8 S.CARLSBERGENSIS CELLS (x2670)

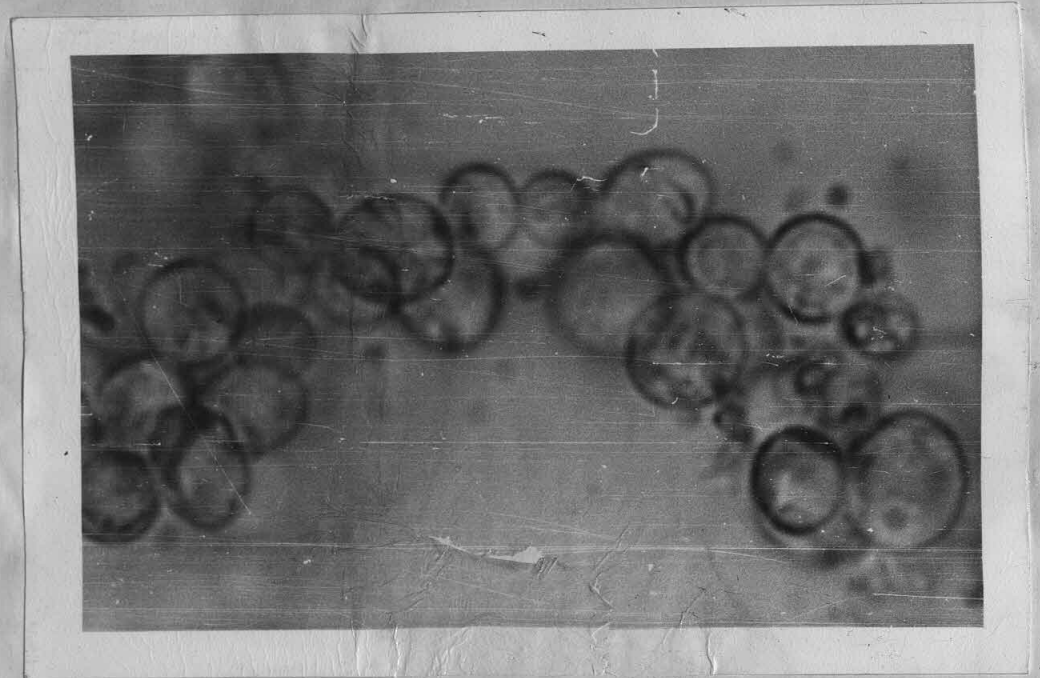
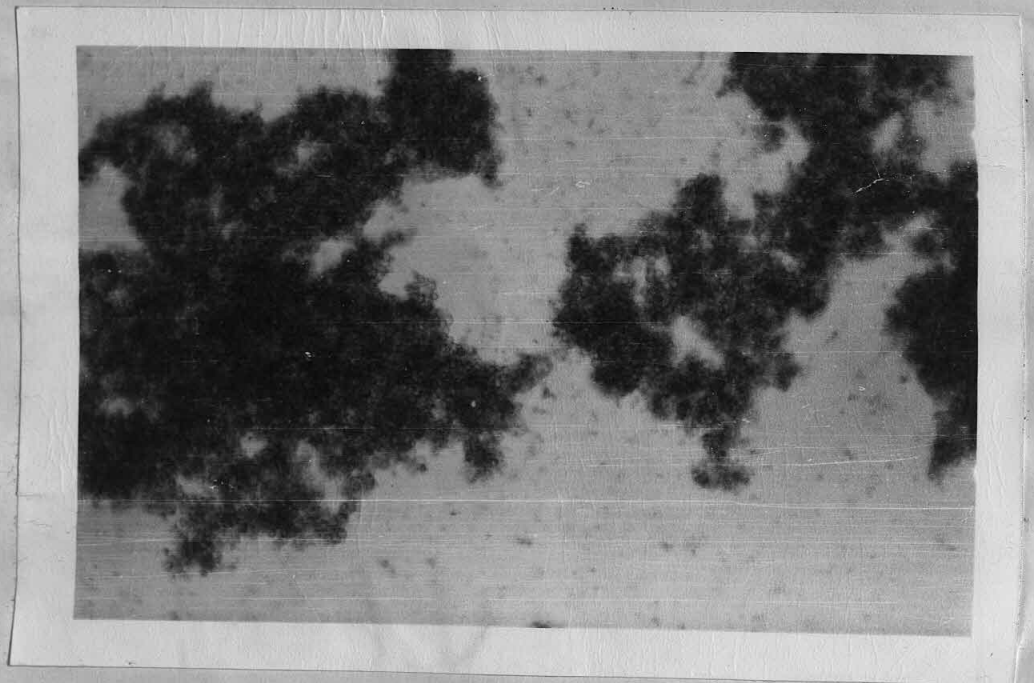


PLATE 2.9 YEAST FLOCS (x267)



Various other constituents are present such as chitin and lipid.

ii. Cytoplasmic membrane

This is an osmotic barrier of 80 angstroms thickness composed of protein and lipid.

iii. Nucleus

Some confusion exists as to exact role, although it generally controls metabolic and reproductive functions.

iv. Mitochondria

These contain respiratory enzymes in a membrane structure and control the energy production for the cell.

v. Vacuoles

These are transparent droplets in the cytoplasmic fluid of the cell. They contain "volutin", an RNA/ polyphosphate mixture important in reproduction.

Yeasts require plenty of available moisture, unlike moulds.

Expressed as water activity, a_w ,

For brewing yeasts, $a_w = 0.94$ and for baking yeasts $a_w = 0.905$.

Osmophilic yeasts may grow in syrup, with $a_w = 0.65$.

The normal growth temperature range is 0 to 47°C with 20 to 30°C the optimum for most species. They prefer acidic media with a pH \approx 3.7 :this inhibits most bacterial activity.

The assimilation of sugars (e.g. glucose) may occur anaerobically (fermentation) or aerobically (respiration). Anaerobic utilisation leads to alcoholic fermentation:



This occurs via the Enden-Meyerhof pathway. In aerobic respiration, atmospheric oxygen is used and glucose breaks down to $CO_2 + H_2O$, yielding energy for the cell. The Krebs cycle is the main path for this.

Yeasts may reproduce by sporulation, budding or fission.

Many yeasts use the asexual budding process (shown in Fig.2.3).

A mature cell may produce 24 generations of daughter cells during its lifetime. A recent paper on yeast budding is that by Sentandreu et alia (1969). Reproduction using spores may occur in some species (often in conjunction with budding). S.Cerevisiae produces four spores contained in an ascus. Each spore has only half the Chromosome requirement; hence, two fuse together to form a complete cell. Until conditions are right for sporulation this cell continues to reproduce by budding.

Examples of some yeasts and their uses are ,

<u>S.Cerevisiae</u>	Beer and bread making
<u>S.Carlsbergensis</u>	Lager making
<u>S.Ellipsoideus</u>	Wine making
<u>S.Sake</u>	Rice-wine making

Some yeasts are classified as "false" yeasts. They may cause spoilage or be pathogenic. Examples are ;

Torula , Mycoderma , Candida , Cryptococcus neoformans .

2.3.1 Flocculence in yeasts

For the successful operation of certain processes in tower fermenters the microorganisms must not be washed out readily. Flocculence, by increasing the size of aggregates, helps the organisms to settle against the substrate flow. Many species of yeast do flocculate readily, the degree of flocculence being controlled by genetic mechanisms, pH, temperature and the electrolyte in the solution.

The ways in which yeast cells join together has been examined by Mill (1964,1966). His work showed that,

- glucose should be present if flocculence is to occur,
- calcium induces flocculation by forming salt-bridges between cells by linking with carboxyl groups,
- decreasing the dielectric constant of the medium using organic solvents causes non-flocculent cells to aggregate, and
- phosphorylation of cell wall mannan to produce mannose-6-phosphate is often found in flocculent yeasts.

However, several other factors have been suggested as contributing to flocculence. These include electrical charge (Geys, 1922), pH (Schoenfeld, 1918) and sugar concentration (Burns, 1937). The most important mechanisms are probably chemical bonding at the cell wall as mentioned by Mill and Lyons & Hough (1970) and electrical charge and genetics as discussed by Gilliland (1951). Deflocculation may be induced by the presence of other organisms in the culture (Malkow, 1934).

Biologists generally measure flocculence using the settled volume vs. time relationships: the tests proposed by Burns (1937) and Thorne (1952) are most commonly used. These merely provide a number for describing flocculent behaviour in a semi-qualitative manner. Some typical flocs are shown in Plates 2.9 & 2.10.

The effect of flocculence on the hydrodynamic behaviour of aggregates and the effect of physical changes on flocculence will be discussed in Chapter 5.

2.4 Activated Sludge

This conglomerate material plays an important role in biological engineering. Such sludge is of variable composition and so detailed descriptions can only apply to one particular type of sludge. Flocculent bacteria are often found in them and the factors influencing flocculence in these were discussed by McGregor and Finn (1969) and Ganser & Wang (1972). Generally, they found that flocculence was affected by the

- following:
- | | |
|-------------------|------------------------------|
| i. temperature | ii. ionic environment |
| iii. age of cells | iv. genetic effects |
| v. surface shear | vi. presence of biopolymers. |

McGregor & Finn used E. coli in which they induced flocculation using chemical additives. The release of polysaccharides, protein and nucleic acids could be induced in bacterial cells by shear forces and temperature increase. The presence of these biopolymers on the cell surface greatly affected the aggregation. Small animals such as rotifers, protozoa and nematodes may also be found. The sludge used for the work described in this

thesis is shown in plates 2.11 & 2.12.

2.5 Final comments

The description of the types of microorganism used in the author's work has been deliberately brief since it was meant to serve as an introduction to later sections of the thesis. In the next chapter, some of the physical properties of these organisms are discussed and in Chapter 4 some mathematical models of these aggregates are presented.

However, several other factors have been suggested as contributing to flocculence. These include electrical charge (Gey, 1922), pH (Schonfeld, 1918) and sugar concentration (Barnes, 1937). The most important mechanisms are probably physical bonding at the cell wall as mentioned by Hill and Lyons & Hough (1970) and electrical charge and genetics as discussed by Gilliland (1951). Flocculation may be induced by the presence of other organisms in the culture (Malkow, 1934). Biologists generally measure flocculence using the settled volume vs. time relationships; the tests proposed by Barnes (1937) and Thorne (1952) are most commonly used. These merely provide a number for describing flocculent behavior in a semi-quantitative manner. Some typical flocs are shown in plates 2.9 & 2.10.

The effect of flocculence on the hydrodynamic behavior of aggregates and the effect of physical changes on flocculence will be discussed in Chapter 5.

2.4 Activated Sludge

This conglomerate material plays an important role in biological engineering. Such sludge is of variable composition and so detailed descriptions can only apply to one particular type of sludge. Flocculent bacteria are often found in them and the factors influencing flocculence in these were discussed by McGregor and Finn (1969) and Gassner & Wang (1972). Generally, they found that flocculence was affected by the following:

- i. temperature
- ii. ionic environment
- iii. age of cells
- iv. genetic effects
- v. surface shear
- vi. presence of diatoms.

McGregor & Finn used *E. coli* in which they induced flocculation using chemical additives. The release of polysaccharides, protein and nucleic acids could be induced in bacterial cells by shear forces and temperature increase. The presence of these diatoms on the cell surface greatly affected the aggregation. Small animals such as rotifers, protozoa and nematodes may also be found. The sludge used for the work described in this

PLATE 2.10 YEAST FLOC (x 1060)

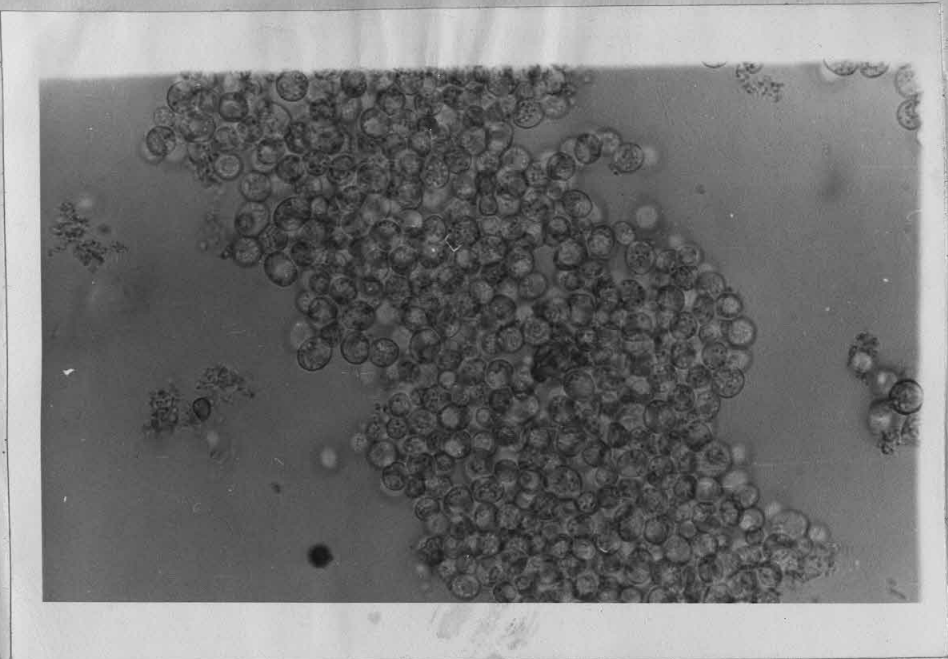


PLATE 2.11 ACTIVATED SLUDGE (x 292)

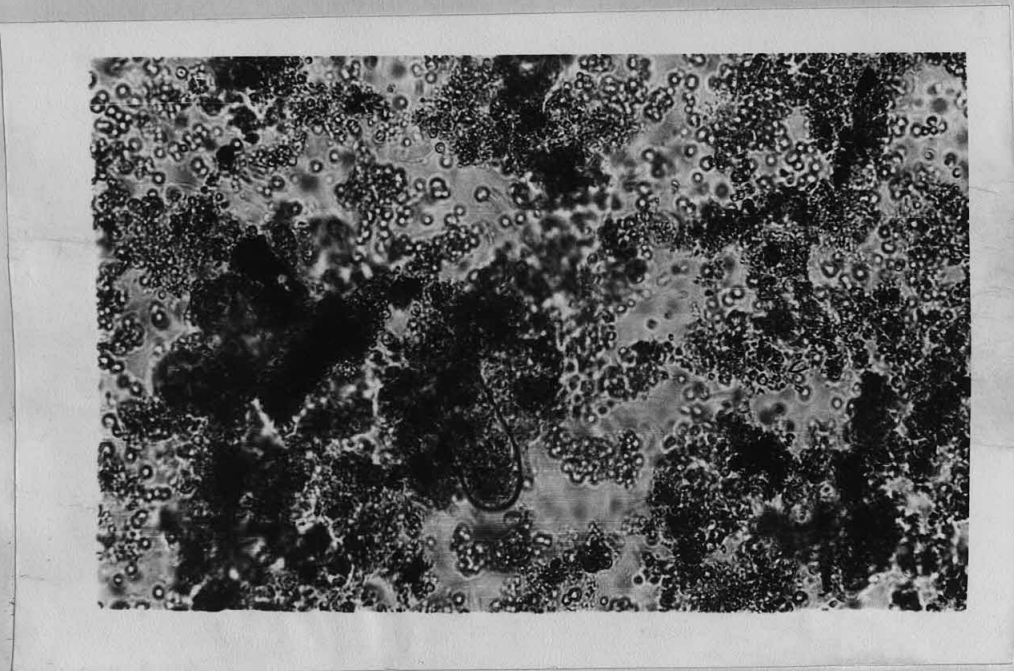
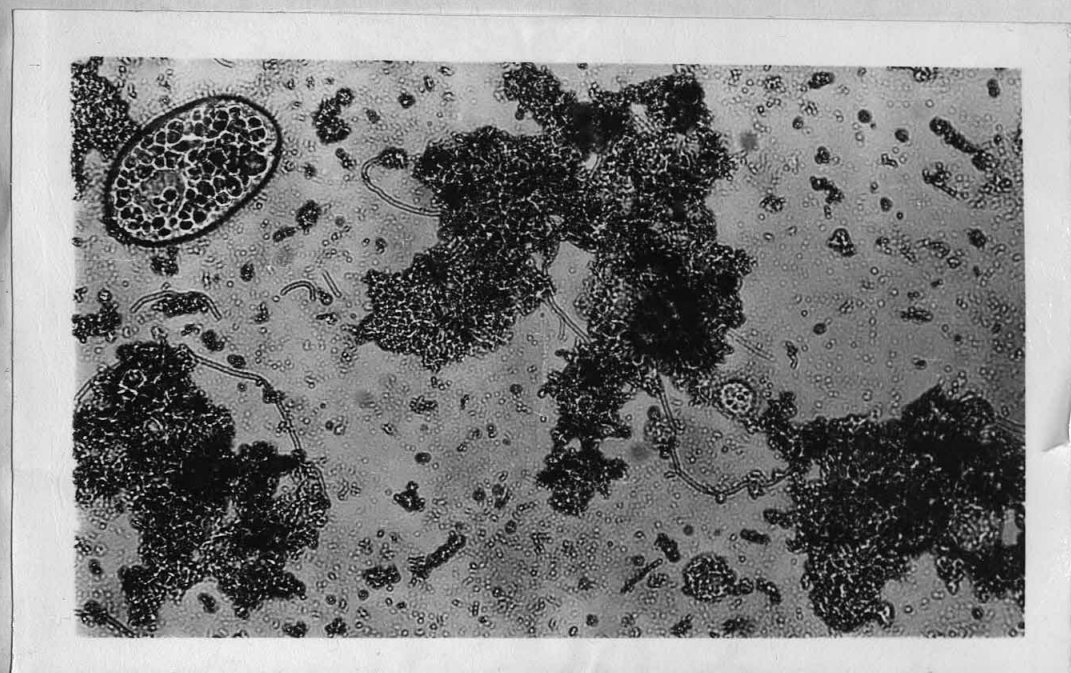


PLATE 2.12 ACTIVATED SLUDGE FAUNA (x292)



THE DETERMINATION OF MICROBIAL PHYSICAL PROPERTIES

3.1 Introduction

An analysis of the behaviour of microbial suspensions requires a knowledge of cell or floc size, cell or floc liquid content and cell or floc densities. These properties were determined for yeasts and for Aspergillus Niger prior to further investigations. The results are used extensively in subsequent chapters.

3.2 Literature Survey

To the author's knowledge only one paper, that by Sterbacek (1972), deals exclusively with the physical properties of microorganisms. However, several workers have published papers in which some physical property data ^{are} given.

The main technique for the determination of cell or floc density and diameter has been sedimentation. This technique has been used in this thesis for the determination of A. Niger pellet densities. It is a simple method in which the measurements may be made with good accuracy. The use of this method assumes that the cell or floc obeys the laws of classical theory, although this may not be true due to the nature of the floc-liquid interface and its frictional properties. Consequently, the values of microbial physical properties obtained by this method must be regarded with caution.

Aiba et alia (1962, 1964) have obtained some data for yeast and other organisms. Initially, they performed a statistical analysis of S. Cerevisiae cell diameters measured under a microscope. This revealed that the cell size averaged 6.2 microns (minor axis) by 6.9 microns (major axis). The cell density was determined by measuring the density and volume fraction of a suspension of cells.

This method gave a cell density of 1.073 g/cm^3 for cells suspended in a phosphate buffer (s.g. = 1.004 g/cm^3). It is probable that the density of a microbial cell depends on the density of the liquid surrounding it. Hence, absolute densities for microbial cells cannot be found; all densities should be quoted relative to a reference fluid, say water at 20°C .

In their 1964 paper they report the determination of microbial densities (ρ_y) by a different technique. The density of a cell suspension (ρ_c) in phosphate buffer (ρ_m) was measured with a 5 cm^3 pycnometer. Then the volume fraction of cells was determined by the volume fraction (c) occupied by the sediment obtained after prolonged gravity settling or centrifugation. Previously the value of c had been obtained by counting the number of cells. The value of ρ_y was found using

$$\rho_y = (\rho_c - (1-c)\rho_m)/c \dots\dots\dots 3.2-1$$

The technique assumed no interstitial fluid in the sediment & was thus less accurate than their original concept. They obtained the following results.

Organism	$\rho_y, \text{g/cm}^3$	c determination
<u>S. Cerevisiae</u>	1.09	700g for 10 mins.
<u>Serratia Marcescens</u>	1.03	10 g for 15
<u>Streptomyces Griseus</u>	1.003	settling for 72 h.
Activated Sludge	1.01324 ..

Table 3.2-1

Microbial densities as determined by Aiba et alia (1964)

From settling tests they calculated equivalent cell diameters & compared them with the measured values. The agreement was generally good.

Haddad & Lindegren (1953) determined the density of yeast cells from terminal velocity measurements. Single cells were allowed to settle in a 1% dextrose solution inside a Hemacytometer. The rate of fall was measured photographically & by using Stokes Law, ^{they} obtained $\rho_y = 1.087 \pm 0.026 \text{ g/cm}^3$ which was similar to that obtained by Aiba et alia.

Several workers have used the sedimentation method to evaluate the properties of non-biological flocs. Using aluminium flocs Tambo et alia (1967) reported that for $200 < d < 2000$ microns the floc particle volume fraction, $(1-e) = 0.003 / (\rho_s - 1) d^{1.3 \sim 1.45}$ 3.2-2 where e = floc voidage & ρ_s = solid density.

This gave $(1-e) = 0.05 \sim 0.1$ for $d = 180 \mu$ & $\rho_s = 2 \text{ g/cm}^3$.

Thomas (1963) used a variety of materials, such as kaolin & for his flocculated systems $(1-e) \div 0.13$ for $d = 180 \mu$

Aiba et alia (1971) used turbidimetry to determine floc cell volume fraction for the organism Chlorella Vulgaris. By relating the turbidity of non-flocculant & flocculant systems to the cell & floc diameters they found,

$$\text{Floc cell volume fraction, } (1-e) = \left(\frac{d}{d_p} \right)^{-0.733} \text{ 3.2-3}$$

where d = floc diameter, d_p = cell diameter.
(It should be noted that e represents the volume fraction of immobile liquid within the floc. This does not include the fraction of liquid within the cells.) Their results revealed that for values $d/d_p > 20$ the immobile liquid volume fractions were very large (between 0.9 & 0.95)

Schroepfer et alia (1955) estimated the density of activated sludge flocs using terminal velocity measurements. They used Stokes Law even though the Reynolds No. was up to 200.

A number of workers have studied the structure of microbial pellets. These have usually originated from investigations into oxygen diffusion within pellets. Yano et alia (1961) investigated the structure of A. Niger pellets grown in shake flasks. The pellet diameter was measured microscopically & then the pellet was heated to dryness to obtain the weight of dry mycelium. From this they obtained the relationship $\rho_{y'} = 0.03 d^{-0.82} \text{ g/cm}^3$ 3.2-4 where $\rho_{y'}$ = wt. of dry mycelium / unit pellet volume
 d = pellet diameter in mm.

The accuracy of this is difficult to ascertain as these workers do not give adequate details of the method used to estimate the pellet diameter.

This method gave a cell density of 1.073 g/cm^3 for cells suspended in a phosphate buffer (e.g. 1.004 g/cm^3). It is probable that the density of a microbial cell depends on the density of the liquid surrounding it. Hence, absolute densities for microbial cells cannot be found; all densities should be quoted relative to a reference fluid, say water at 20°C .

In their 1964 paper they report the determination of microbial densities (ρ_y) by a different technique. The density of a cell suspension (ρ_c) in phosphate buffer (ρ_m) was measured with a 5 cm³ pycnometer. Then the volume fraction of cells was determined by the volume fraction (e) occupied by the sediment obtained after prolonged gravity settling or centrifugation. Previously the value of e had been obtained by counting the number of cells. The value of ρ_y was found using $\rho_y = (\rho_c - (1-e)\rho_m) / e$ 3.2-1

The technique assumed no interstitial fluid in the sediment & was thus less accurate than their original concept. They obtained the following results.

Organism	$\rho_y \text{ g/cm}^3$	e determination
<u>S. cerevisiae</u>	1.02	100g for 10 mins.
<u>Serratia Marcescens</u>	1.03	10 g for 15
<u>Streptomyces Griseus</u>	1.003	settling for 72 h.
Activated Sludge	1.013 24 ..

Table 3.2-1

Microbial densities as determined by Aiba et alia (1964)

From settling tests they calculated equivalent cell diameters & compared them with the measured values. The agreement was generally good.

Hadad & Lindgren (1953) determined the density of yeast cells

from terminal velocity measurements. Single cells were allowed to settle in a 1% dextrose solution inside a Hemacytometer. The rate of fall was measured photographically & by using Stokes law obtained

$\rho_y = 1.087 \pm 0.026 \text{ g/cm}^3$ which was similar to that obtained by Aiba et alia.

These results will be discussed later (see section 3.4-4).

Using the same approach Yosida et alia (1967) investigated Lenticus Edodes pellets. They quote ρ_y' values for two types of pellet

For " low density " pellets $\rho_y' = 0.15 \text{ g/cm}^3$

... " high density " pellets $0.25 \dots$

The pellets used were less than 0.02 cm. diameter. Their oxygen diffusion measurements indicated that for pellets greater than 0.02 cm. diameter the pellet centre does not receive oxygen. Hence, for pellets of greater diameter the centre may be autolysed. They found that their calculated oxygen diffusion rates, based on Michaelis-Menten respiration rates, were much lower than observed. This was ascribed to bulk liquid flow through the pellet, although they have no direct evidence of this. The discrepancy could arise from the inapplicability of the equations used in their model.

Thorne (1954) measured the liquid content of yeast cells using wet & dry wt. values. His average value for the filtered wet wt./dry wt. was 4.5.

Mueller et alia (1967) reviewed floc sizing techniques & present data obtained photographically for the size of activated sludge flocs. In a previous paper (1966) they measured the densities of activated sludge flocs by balancing the floc density against that of an electrolyte solution. By additionally measuring the dry material density they were able to estimate the liquid content of the floc. The values of dry matter density ranged from 1.29 to 1.65 g/cm³. A floc density of 1.09 g/cm³ was found & thus the liquid contents ranged from 63% to 90%. Measurement of the liquid trapped in a sediment presents many difficulties. Several workers have attempted to use tracer which is not absorbed into the cells. One of the more successful attempts was made by Wetherell et alia (1962) who used polyvinyl pyrrolidone tracer. The concentration of tracer in a floc sediment was measured to give an indication of the interstitial liquid.

Sterbacek (1972) presents physical data for S. Cerevisiae,

Candida Lipolytica & A. Niger. Firstly, he determined the living cell size distribution for two strains of S.Cerevisiae & C. Lipolytica.

The results were

Organism	Length, μ	Diameter, μ
<u>S.Cerevisiae</u> (ex Kolin Distillery, Czechoslovakia)	5.65	4.42
<u>S.Cerevisiae</u> (ex Hopkin & Williams, England)	5.53	3.94
<u>C.Lipolytica</u>	4.74	3.01

Table 3.2-2 Microbial dimensions from Sterbacek (1972)

Secondly, he measured dry mycelium density (ρ_s) using a density bottle method. The values obtained are the average for the organisms. The effect of fermentation time was not explored.

Organism	Dry mycelial density g/cm. ³
<u>S.Cerevisiae</u>	1.342
<u>C.Lipolytica</u>	1.247
<u>A.Niger</u>	1.323

Table 3.2-3 Mycelial densities from Sterbacek (1972)

Finally, the viscosities of suspensions of S.Cerevisiae & C.Lipolytica were measured using a concentric cylinder & a falling sphere viscometer. The temperature range was from 15 to 35°C and the concentration range from 0.25 to 15% dry wt. (w/v). His results agreed with those of Aiba et alia (1962) and may be summarised by

$$\ln \mu_s = A + B.C_m + D/t \quad \dots\dots\dots 3.2-5$$

where μ_s = suspension viscosity, cp.

C_m = dry wt. concentration, w/v %

t = temperature, °C

The values obtained for the constants were

	A	B	D
<u>S.Cerevisiae</u>	-0.796	0.166	9.159
<u>C.Lipolytica</u>	-0.885	0.168	15.12

The yeast suspensions appeared to be Newtonian in behaviour.

Taguchi (1971) investigated the shear stresses required to disrupt mycelia. This was to ascertain the power requirements of stirred tank fermenters, containing mycelial suspensions. The tensile strength of mycelium was determined using a pendulum strength tester. This showed that A. Niger mycelium was one of the strongest with a tensile strength of 0.278 kg./cm.² Thus, the mycelium would only disrupt after prolonged and weakening impacts.

3.3 Experimental programme and Procedure

The literature review shows that the physical data for microbial systems ^{are} ~~is~~ limited. Comprehensive information for given strains and on the time dependency of physical properties has not yet been produced. It was therefore decided to investigate fully the following physical properties for A. Niger and various yeast strains.

- Dry mycelial density
- Wet/dry wt. ratios
- Floc/pellet size and structure
- Pellet densities

3.3-1 Dry mycelial density, ρ_s

Mycelial or cellular material was dried in an oven to constant weight. A known weight was then placed in a specific gravity bottle & the volume of mycelium determined by water displacement. Care was taken to ensure that all air bubbles attached to the sample were removed and that the sample did not contain any medium liquid.

3.3-2 Wet /dry wt. ratios

These fall into two categories, the first being the ratio for filtered material and the second for centrifuged material. In the former case, the material was filtered under vacuum and then after measuring the weight of the cake, the sample was dried to constant wt. This procedure gave an indication of the amount of liquid in the cell.

A convenient, but less reliable, measure of the amount of

material within a suspension was provided by the centrifuged wet wt. In this method the suspension was centrifuged first, the liquid decanted and then the sludge wt. obtained. The sludge was then dried to constant weight. Ideally, by using the centrifuged wet wt. / dry wt. ratio the amount of liquid within a floc may be estimated. Also, the centrifuged wt. should give an estimate of the effective weight of flocs in suspension. However, the floc structure breaks down under high gravity fields. This leads to variable interstitial liquid content in the sediment. The centrifuged wet wt. cannot therefore be used reliably as it stands.

3.3-3 Pellet and floc diameters

Pellets are integral units whose size and structure change due to mycelial growth. Floc units are not integral in that a floc tends to be a transient structure where the particles are continually being removed and replaced. Thus, an average structure for a floc is the best that can be achieved.

From the microbial descriptions given earlier it can be seen that two characteristic diameters may be measured in a pellet. These are

- Outside diameter, d_o , or the full pellet diameter.
- Inside diameter, d_i , representing the size of the compact hyphal centre; a difficult value to assess.

The measurements were made microscopically with the pellet suspended in the liquid. For a given time during a fermentation the average of about twenty values of d_o/d_i was used to characterise pellet size.

For flocs only a visual estimation was made with the flocs in suspension as their size altered when removed from the suspension.

3.3-4 Pellet densities

A hydrodynamic pellet density was obtained by measuring the terminal velocity of pellets in water. The pellet diameter was measured microscopically and then the pellet was placed in a 1000 cm.³ cylinder of 6cm. diameter containing water at a known temperature.

The pellet was allowed to fall until it reached its terminal velocity, which was then accurately measured. They fell without spinning or deformation, and care was taken to avoid thermal convection currents.

Classical hydrodynamic theory was assumed to apply to the pellet. This involved an evaluation of the Schiller-Naumann equation, applicable for $2 < Re_t < 500$, which covered the range of Reynolds Nos. used.

$$(\rho_p - \rho_m) = 18 \mu U_t (1 + 0.15 Re_t^{0.687}) / d_o^2 g \dots\dots 3.3-1$$

where U_t = terminal velocity, cm./s. Re_t = particle Reynolds No. = $U_t d_o \rho_m / \mu$

Thus, ρ_p values could be found for pellets of known d_o & d_o/d_i

values. Use of this method assumed that all liquid within the volume described by the outside diameter remained immobilised. This may be a reasonable assumption in the light of the calculations made by Sutherland & Tan (1970) for the flow through a porous sphere, which is discussed in more detail in the later chapter (5).

The accuracy of the density obtained in this way has been questioned in the literature survey. It is, however, a convenient and useful density measurement, which gives an indication of the small density difference between the pellets and the bulk liquid phase.

3.3-5 Preparation of microbial samples

(a) Yeasts

The yeasts used in these tests were obtained from plate cultures collected in the Biological Sciences Fermentation Research Group at the University. They are designated by a CFCC prefix which represents "Continuous Fermentation Culture Collection".

The yeasts were grown in a 150 g/l. malt extract medium, supplied by Edme, Ltd., Essex. A 1½ l. tower fermenter was used which could be autoclaved as a complete unit. The fermenter is shown in Plate 3.1. Air supplied from an Austen air pump was passed through a cotton wool filter and a sterilisable paper filter unit. The yeasts were harvested after about 3 days' growth. The suspension was centrifuged and the sediment

It was allowed to fall until it reached its terminal velocity, then accurately measured. They fell without spinning or tumbling, and care was taken to avoid thermal convection currents.

Classical hydrodynamic theory was assumed to apply to the pellet. It gave an evaluation of the Schiller-Numann equation, applicable to Re_p values covered the range of Reynolds Nos. used.

$$\left(\frac{C_D}{Re_p^2} \right) = 18 \mu_f (1 + 0.15 Re_p^{0.687}) \quad (3.3-1)$$

μ_f = terminal velocity, cm./s. Re_p = particle Reynolds No. = $\frac{U_p d_p}{\nu}$ ν = kinematic viscosity of fluid, cm.²/s. C_D values could be found for pellets of known d_p and U_p .

Use of this method assumed that all liquid within the volume des. by the outside diameter remained immobilized. This may be a reasonable assumption in the light of the calculations made by Sutherland (1970) for the flow through a porous sphere, which is discussed in detail in the next chapter (5).

The accuracy of the density obtained in this way has been questioned by some workers. It is, however, a convenient and useful density measurement, which gives an indication of the small density difference between the pellets and the bulk liquid phase.

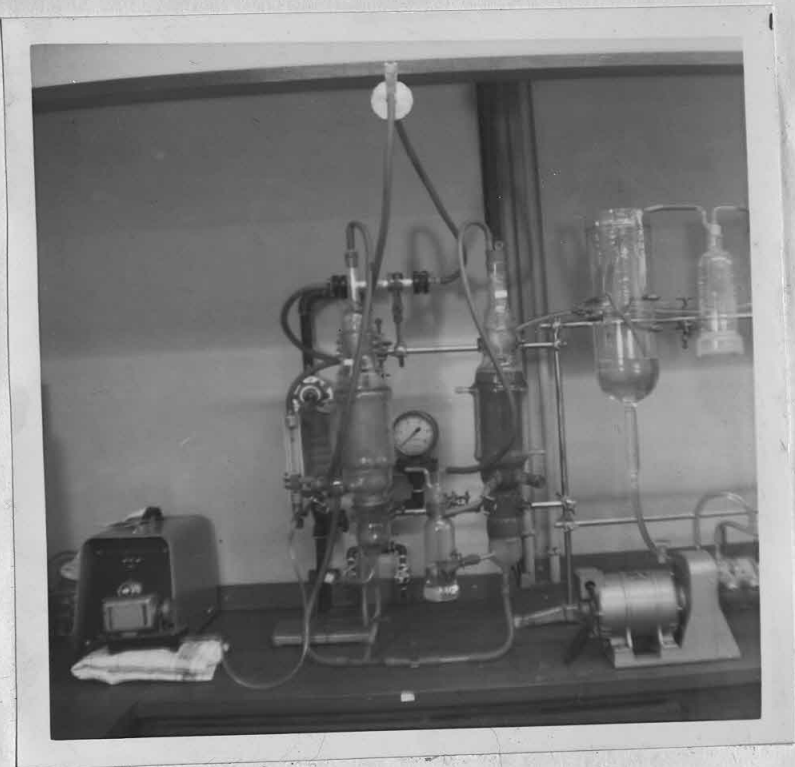
Preparation of microbial samples

(a) Yeasts

The yeasts used in these tests were obtained from plate cultures in the Biological Sciences Fermentation Research Group at the University of Cambridge. They are designated by a GFCO prefix which represents the "Fermentation Culture Collection".

The yeasts were grown in a 150 g/l. malt extract medium, supplied by the Biological Sciences Fermentation Research Group. A 1.5 l. tower fermenter was used which could be operated as a complete unit. The fermenter is shown in Plate 3.1. Sterilized air was passed through a cotton wool filter and an air pump was passed through a cotton wool filter. The yeasts were harvested by centrifugation. The suspension was centrifuged and the sediment washed with water. The suspension was centrifuged and the sediment washed with water.

PLATE 3.1 1½ LITRE FERMENTER UNIT



washed twice in water and recentrifuged to remove the attached medium.

(b) A.Niger

A strain of A.Niger was obtained from Tate & Lyle Ltd. and was designated M1. Much additional microbiological and biochemical work has been performed with this strain by Tate & Lyle research workers. The A.Niger was grown in the pellet form on molasses based medium in 50l. tower fermenters with the help of Dr. G.Morris(1972). Samples were taken at given time intervals and were washed with water to remove any attached medium.

3.4 Results and Analysis

3.4-1 The density of dry mycelium, ρ_s

These results will be presented for yeasts and A.Niger separately.

Measurements for various strains of yeasts were taken for 72 h. samples.

Measurements on A.Niger were taken at various intervals during the growth cycle. The results are shown below. for yeasts.

Yeast strain	Dry mycelial density	Average value of ρ_s
CFCC83 <u>S.Carlsbergensis</u>	1.26 g/cm. ³ 1.34 1.33 1.32	1.32 g/cm. ³
CFCC 8 <u>S.Cerevisiae</u>	1.29 1.32	1.305
CFCC 34 <u>S.Cerevisiae</u>	1.33 1.33	1.33

Table 3.4-1 Dry yeast densities

For yeast an average value of $\rho_s = 1.32 \text{ g/cm.}^3$ was taken. This may be compared to Sterbacek's value of $\rho_s = 1.34 \text{ g/cm.}^3$.

The variation of ρ_s with fermentation time for A.Niger, M1 can be seen in Fig. 3.1. Sterbacek's value of $\rho_s = 1.323 \text{ g/cm.}^3$ for his

A.Niger strain compared with the 23 h. value in this work. The decrease in A.Niger mycelial density with time suggests that the composition of the mycelium was varying. It can be seen that the density drops rapidly between 20 -25 h. growth, which corresponds with the onset of organic acid production by the mycelium.

Table 3.4-2 A.Niger dry mycelial densities

Mycelial age ,h.	Dry mycelial density, g/cm. ³
14	1.39
16	1.38
19	1.37
22	1.37
24	1.265
28	1.28
29	1.27
30	1.24
38	1.24

3.4-2 Wet /Dry weight ratios

(a) A.Niger

The filtration method was used to determine the wet/dry wt. ratio for the mycelium. It was probable that some interstitial liquid remained in the cake. As the structure of the filtered mycelium may be compared to a cellular foam then a value of 10% by wt. of interstitial liquid was assumed. Using the corrected wt. of mycelium the volume fraction of liquid inside the cells may be found as follows;

$$\begin{aligned} \text{"Corrected" wt. of filtered mycelium/ Dry wt. of mycelium} &= M \\ \text{Dry wt. of mycelium/ (Dry mycelial wt. + mycelial liquid wt.)} &= 1/M \\ \therefore X = \text{wt. fraction of liquid} &= \frac{M-1}{M} \quad \dots\dots 3.4-1 \end{aligned}$$

$$\begin{aligned} \text{Using the dry mycelial density, } \rho_s, \text{ the volume fraction of liquid, Y,} \\ \text{can be calculated. Let mycelial liquid wt. = W, then volume of dry} \\ \text{mycelium} &= W / (M-1) \rho_s \\ \therefore \text{Volume fraction of mycelium} &= W / (M-1) \rho_s * 1 / ((W / (M-1) \rho_s) + W / \rho) \dots\dots 3.4-2^a \end{aligned}$$

$$\text{or } Y = 1 - 1 / (1 + (M-1) \rho_s / \rho) \dots\dots\dots 3.4-2$$

Table 3.4-3 A.Niger mycelium composition

Mycelial age ,h.	Actual wet wt.,g.	"Corrected" wt,g.	dry wt. g	X	Y
16	0.249	0.224	0.08	0.65	0.71
19	0.8	0.73	0.246	0.66	0.73
22	1.25	1.125	0.40	0.65	0.71
25	2.29	2.06	0.66	0.68	0.73
29	2.81	2.53	0.71	0.72	0.76

The values of mycelium density, ρ_y , may now be calculated using the equation $\rho_y = \rho Y + \rho_s (1-Y)$ 3.4-3 where $\rho = 1 \text{ g/cm.}^3$

Table 3.4-4 A.Niger mycelial densities

Mycelial age ,h.	$\rho_s, \text{g/cm.}^3$	$\rho_y, \text{g/cm.}^3$
16	1.385	1.110
19	1.375	1.102
22	1.34	1.098
25	1.28	1.076
29	1.255	1.060

The difficulty of centrifuging A.Niger to a firm sediment leads to the use of the dry weight in characterising suspensions. The relationship between this value and the effective pellet wt, in suspension will be discussed in section 3.4-4 .

(b) Yeast

A similar approach to that adopted for A.Niger was used to determine the liquid content of yeast cells. Tests performed on CFCC 83 resulted in an average value for the ratio filtered wet wt. /dry wt. of 4.48. This may be compared to the value quoted by Thorne (1954) of 4.5 As previously, assuming 10 % by weight of interstitial fluid in the cake then the corrected cell wt./ dry wt. = $M = 4.05$

$$\therefore X = 0.75 \text{ and from eqn. 3.4-2 , } Y = 0.8 \text{ for } \rho_s = 1.32 \text{ g /cm.}^3$$

A.Niger strain compared with the S3 h. value in this work. The decrease in A.Niger mycelial density with time suggests that the composition of the mycelium was varying. It can be seen that the density drops rapidly between 20-25 h. growth, which corresponds with the onset of organic acid production by the mycelium.

Table 3.4-2 A.Niger dry mycelial densities

Mycelial age ,h.	Dry mycelial density, g/cm. 3
14	1.32
16	1.38
19	1.37
22	1.37
24	1.26
28	1.28
29	1.27
30	1.24
38	1.24

Table 3.4-2 Wet / Dry weight ratios

(a) A.Niger

The filtration method used to determine the wet/dry wt. ratio for the mycelium. It was probable that some interstitial liquid remained in the cake. As the structure of the filtered mycelium may be compared to a cellular form then a value of 10% by wt. of interstitial liquid was assumed. Using the corrected wt. of mycelium the volume fraction of liquid inside the cells may be found as follows:

$$\text{"Corrected" wt. of filtered mycelium / dry wt. of mycelium} = M$$

$$\text{Dry wt. of mycelium} / (\text{dry mycelial wt.} + \text{mycelial liquid wt.}) = 1/M$$

$$X = \text{wt. fraction of liquid} = M-1 \dots\dots\dots 3.4-1$$

Using the dry mycelial density, ρ_s , the volume fraction of liquid, Y, can be calculated. Let mycelial liquid wt. = W, then volume of dry

$$\text{mycelium} = W / (M-1) \text{ g}$$

$$\text{Volume fraction of mycelium} = W / (W + (M-1)W) = 1 / M \dots\dots\dots 3.4-2$$

DENSITY OF DRY MYCELIUM (g/cm³)

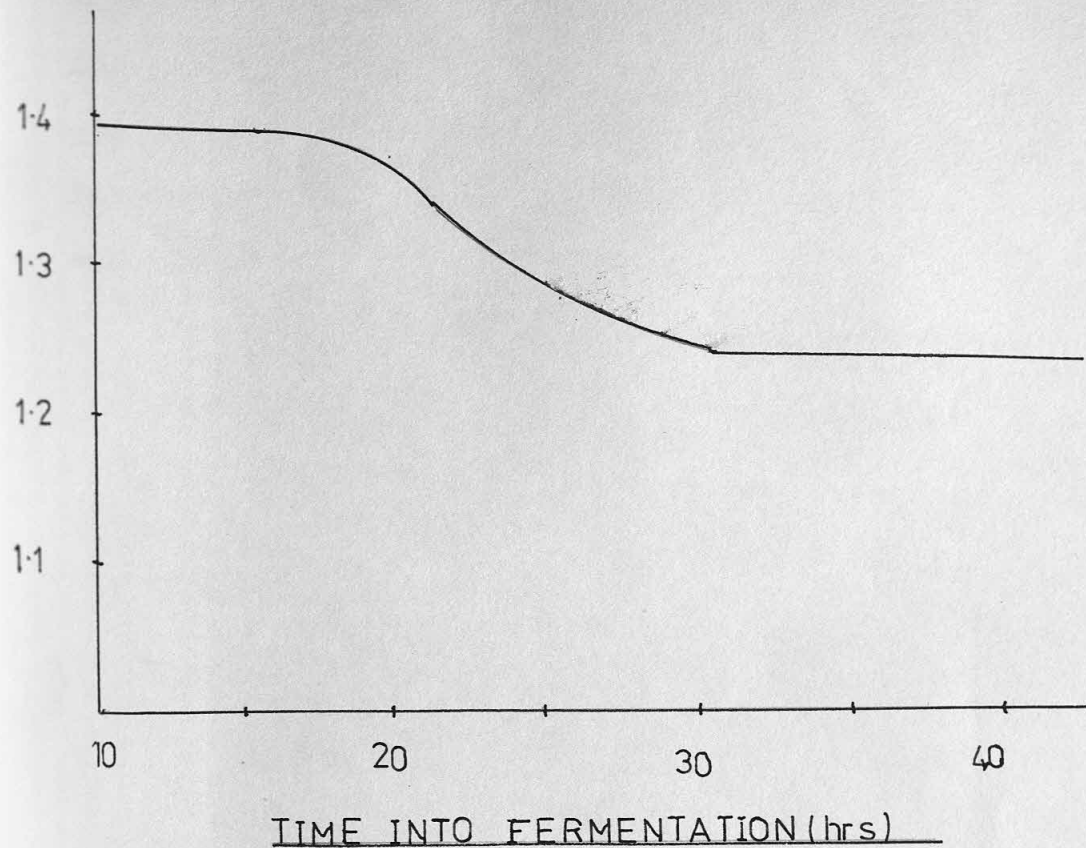


FIG31: A. NIGER DENSITY PROFILE

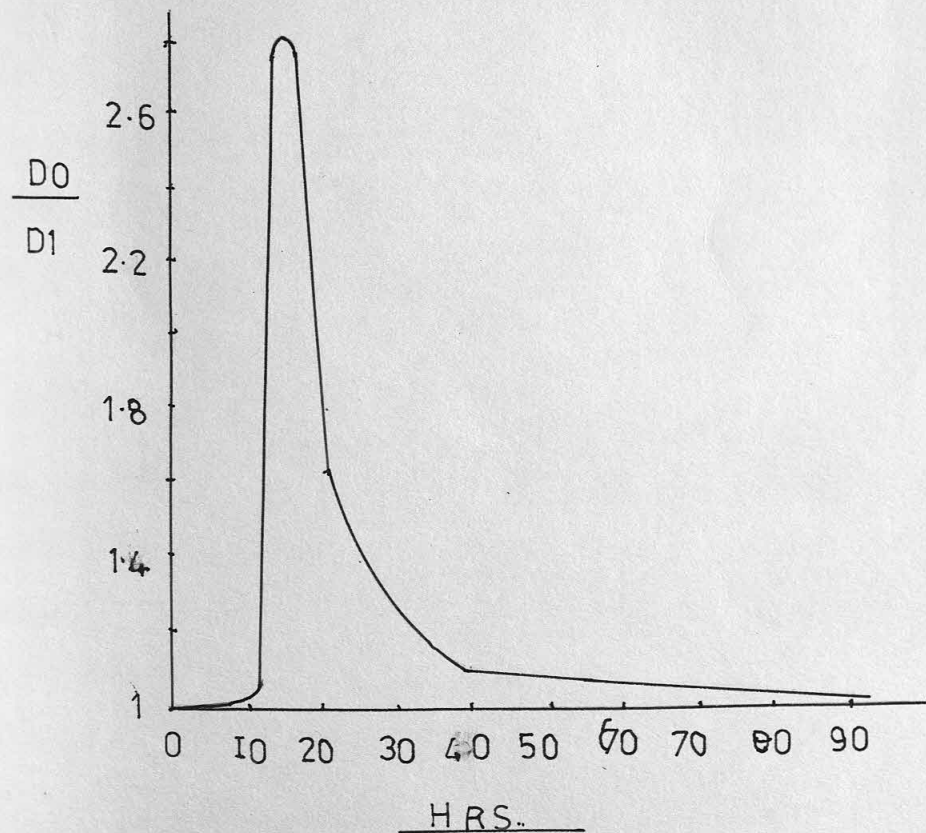


FIG32 A. NIGER DIAMETER RATIOS

Table 3.4-3 A. niger mycelium composition

Time, hr.	Actual wet wt., g.	"Corrected" wt., g.	Dry wt., g.	X	Y
10	0.249	0.224	0.08	0.65	0.71
15	0.8	0.73	0.256	0.66	0.73
20	1.25	1.125	0.40	0.65	0.71
25	2.20	2.05	0.66	0.68	0.73
30	2.81	2.53	0.71	0.72	0.76

The values of mycelium density, ρ_y , may now be calculated using

$$\rho_y = \rho_a + \rho_a (1 - Y) \quad 3.4-3$$

Table 3.4-4 A. niger mycelial densities

Time, hr.	ρ_a , g/cm ³	ρ_y , g/cm ³
10	1.385	1.110
15	1.375	1.102
20	1.34	1.098
25	1.28	1.076
30	1.255	1.060

The efficiency of centrifuging A. niger to a firm sediment

is to the use of the dry weight in characterizing suspensions. The

relationship between this value and the effective pellet wt. in suspension

is discussed in section 3.4-4.

(b) Yeast

A similar approach to that adopted for A. niger was used to

determine the liquid content of yeast cells. Tests performed on CTC 83

yielded an average value for the ratio filtered wet wt. / dry wt.

of 4.5. This may be compared to the value quoted by Thorne (1954) of 4.5

assuming 10% by weight of interstitial fluid in the cake

corrected cell wt. = 4.05

$\rho_y = 1.28$ g/cm³ for $\rho_a = 1.38$ g/cm³, $Y = 0.8$ from eqn. 3.4-3

Therefore, cell density = $0.8 \times 1 + 0.2 \times 1.32 = 1.064 \text{ g/cm}^3$. (Using Sterbacek's value of $\rho_s = 1.34 \text{ g/cm}^3$ then cell density = 1.069 g/cm^3 .)

Aiba (1962) quoted cell density = 1.073 g/cm^3 . An average value of 1.07 g/cm^3 was therefore taken. Use was also made of the centrifuged wet wt. Typical data, based on the average centrifuged wt. / dry wt. ratio for each strain was,

Table 3.4-5 Centrifuged wet weights for yeasts

Yeast strain	Centrifuged wet wt.	Cell wt.	Cell wt.
	Dry wt.	Dry wt.	Centrifuged wt.
CFCC 8	4.5	4.05	0.9
CFCC 34	5.9	4.05	0.69
CFCC 3	5.5	4.05	0.74
CFCC 83	5.4	4.05	0.75

(c) Activated Sludge

This material was essentially different in character to the yeasts and filamentous fungi which consisted of a single organism. Within a typical sludge are to be found bacterial flocs, protozoa, nematodes and unclassified material. Filtered dry wt. ratios averaged 12.5 for this material. Consequently, about 94% by volume of the sludge is liquid. This was probably due to the higher liquid contents of the individual organisms compared to fungal cells.

3.4-3 Pellet and Floc dimensions

(a) A.Niger

A mould pellet is an integral unit that can be handled, washed and tested without any apparent change in shape. Consequently, pellet dimensions may be easily measured and have significance. The sample results shown below apply to a culture where the spores had been well distributed by using a surfactant, Tween 80. This led to uniform spore aggregates. The inoculum used was $\approx 10^4$ spores / cm^3 . (see Table 3.4-6).

The results shown in Table 3.4-7 were for a spore culture in which the initial clumps were of unequal size due to the absence of Tween 80. The spore inoculum was $\approx 10^5$ spores / cm^3 .

Table 3.4-6 A.Niger pellet dimensions (uniform size aggregates)

Fermentation time, h.	d_o , cm.	d_i , cm.	d_o/d_i
14	0.128	0.048	2.67
	0.152	0.08	1.92
	0.132	0.028	4.7
18	0.112	0.052	2.16
	0.132	0.076	1.74
	0.144	0.08	1.8
	0.124	0.072	1.72
	0.12	0.064	1.88
19	0.252	0.14	1.8
	0.18	0.10	1.8
	0.22	0.12	1.83
	0.21	0.104	2.0
29	0.20	0.112	1.83
24	0.248	0.18	1.38
	0.292	0.212	1.38
	0.308	0.224	1.38
	0.32	0.236	1.36
28	0.324	0.252	1.28
	0.34	0.272	1.25
	0.325	0.26	1.25
	0.332	0.267	1.24
	0.36	0.276	1.30
38	0.20	0.14	1.42
	0.204	0.144	1.42
	0.18	0.124	1.45
90	0.28	0.24	1.16
	0.28	0.192	1.46
	0.20	0.152	1.31
	0.268	0.22	1.22
	0.232	0.196	1.29
	0.4	0.33	1.20
	0.4	0.33	1.20
	0.5	0.43	1.15

Table 3.4-5 Centrifuged wet weights for yeasts

Yeast strain	Centrifuged wet wt., dry wt.	Cell wt., dry wt.	Centrifuged wt., dry wt.
OTCC 8	4.5	4.05	4.5
OTCC 34	5.9	4.05	5.9
OTCC 3	5.5	4.05	5.5
OTCC 83	5.4	4.05	5.4

(c) Activated Sludge

This material was essentially different in character to the yeasts and filamentous fungi which constituted of a single organism. Within a typical sludge are to be found bacterial flocs, protozoa, nematodes, and unclassified material. Filtered dry wt. ratios averaged 12.5 for this material. Consequently, about 8% by volume of the sludge is liquid. This was probably due to the higher liquid contents of the individual

organisms compared to fungal cells.

3.4-3 Pellet and floc dimensions

(a) A.Niger

Latent pellet is an integral unit that can be handled, washed and tested without any apparent change in shape. Consequently, pellet dimensions may be easily measured and have significance. The sample results shown below apply to a culture where the spores had been well distributed by using a surfactant, Tween 80. This led to uniform spore aggregates. The inoculum used was 10^5 spores / cm³ (see Table 3.4-6). The results shown in Table 3.4-7 were for a spore culture in

which the initial clumps were of unequal size due to the absence of

Tween 80. The spore inoculum was 10^5 spores / cm³.

Table 3.4-7 A.Niger pellet dimensions (non-uniform spore clumps)

Fermentation time, h.	d_o , cm.	d_i , cm.	d_o/d_i
13	0.237	0.187	1.27
	0.088	0.06	1.47
	0.225	0.20	1.12
	0.08	0.064	1.25
16	0.212	0.177	1.20
	0.124	0.072	1.72
	0.160	0.132	1.21
	0.096	0.06	1.6
22	0.36	0.272	1.32
	0.216	0.148	1.46
	0.249	0.157	1.59
29	0.416	0.394	1.06
	0.252	0.247	1.12
	0.356	0.326	1.09
	0.20	0.163	1.22

These results are shown graphically in Fig. 3-2. The rapid increase and then decrease of the d_o/d_i ratio between 12 and 18h. after inoculation may be explained by the morphological development outlined previously in Chapter 2. The onset of germination after 12 to 14h. leads to a rapid increase in the d_o/d_i ratio as the hyphae develop and grow radially. This trend continues until about 16 h. when the ratio attains a maximum. The centre of the pellet then fills out more rapidly than the outer hyphae can grow, so the d_o/d_i ratio falls. Eventually, the ratio attains a low value; indeed for smooth (often autolysed) pellets the ratio is for all practical purposes equal to unity. The ratios quoted for such pellets (i.e. 90 h. pellets) are greater than unity because fine, well spaced hyphae still protrude.

(b) Yeast

Yeast flocs do not individually retain a constant size. A single floc constantly fluctuates in size and structure, as other particles coalesce and break away. However, the yeasts used in the tests each had

a characteristic floc size which was estimated visually.

Yeast strain	Type	Approx. floc size, cm.
CFCC 8	Flocculent, fermentation	0.3
	limited.	
CFCC 34	0.6
CFCC 3	Flocculent, physically,	0.2
	limited.	
CFCC 83	0.15

3.4-4 Pellet density determinations

As was stated in the literature survey, a number of workers have used terminal velocity measurement to estimate aggregate densities. The assumptions underlying this method are open to question. Nevertheless, for the estimation of the density of a mould pellet this is the only method that may be readily applied.

When using this method, the density difference between the pellet and the liquid was calculated from the terminal velocity using the Schiller - Naumann eqn. (3.3-1). The value of ρ_p so obtained was then related to the d_o/d_i ratio. Sample results for uniformly sized pellets are shown in Table 3.4-8 and Fig. 3-3. These results indicate the magnitude of the parameter involved. It could be seen that the calculated densities were very close to, and hence very dependent on, the liquid density. This indicated that the pellet contained a very large amount of liquid, both within the cells and immobilised within the pellet structure. The volume fraction of total water within the pellet, A, may be calculated from the relationship $A = (\rho_s - \rho_p) / (\rho_s - \rho_m) \dots 3.4-4$. Values of A are also listed in Table 3.4-8 and plotted in Fig. 3-4.

The volume fraction of liquid within the pellet was clearly very high and for most pellet sizes was approximately 99%. It was then possible to estimate the composition of a pellet. Since by definition,

$$\text{Volume fraction of total liquid} = A$$

$$\text{Volume fraction of dry mycelium} = (1-A)$$

Table 3.4-7 A. Niger pellet dimensions (non-uniform spore clumps)

Fermentation time, h.	d_o , cm.	d_i , cm.	d_o/d_i
13	0.237	0.187	1.27
	0.088	0.06	1.47
	0.225	0.20	1.12
	0.08	0.064	1.25
16	0.212	0.177	1.20
	0.124	0.072	1.72
	0.160	0.132	1.21
	0.096	0.06	1.6
22	0.216	0.272	1.32
	0.249	0.148	1.68
	0.249	0.124	1.99
29	0.416	0.394	1.06
	0.222	0.247	1.12
	0.326	0.326	1.00
	0.20	0.163	1.22

These results are shown graphically in Fig. 3-2. The rapid increase and then decrease of the d_o/d_i ratio between 12 and 16 h. after inoculation may be explained by the morphological development outlined previously in Chapter 2. The onset of germination after 12 to 14 h. leads to a rapid increase in the d_o/d_i ratio as the hyphae develop and grow radially. This trend continues until about 16 h. when the ratio attains a maximum. The centre of the pellet then fills out more rapidly than the outer hyphae can grow, so the d_o/d_i ratio falls. Eventually, the ratio attains a low value; indeed for smooth (often autohyal) pellets the ratio is for all practical purposes equal to unity. The ratios quoted for each pellet (i.e. 90 h. pellets) are greater than unity because fine, well spaced hyphae still protrude.

(b) Yeast

Yeast flocs do not individually retain a constant size. Although floc constantly fluctuates in size and structure, as other particles coalesce and break away. However, the yeasts used in the tests each had

and volume of mycelial liquid = Y
 then the volume fraction of liquid in the mycelium = $Y(1-A)/(1-Y)$..3.4-5
 For A= 0.99 and Y=0.73, then the pellet composition by volume was
 approximately Dry mycelium =1%
 Liquid in the mycelium = 2.7%
 Immobile liquid =96.3%

The figures revealed that the apparently solid pellets were largely liquid. In the case of autolysed pellets the immobilised water was initially considered to exist inside the shell of the pellet. Taking a value of $\rho_y = 1.055 \text{ g/cm}^3$ and $\rho_m = 0.996 \text{ g/cm}^3$ then if Z= the volume fraction of the central cavity;

$$\rho_p = Z*0.996 + (1-Z) *1.055 \dots\dots\dots 3.4-6$$

 Hence, by substituting the measured densities of autolysed pellets shown in Table 3.4-8 the value of Z was found to be 0.91. However, microscopic examination of the pellets revealed that the true value of Z was 0.5 to 0.8. Therefore, some of the immobilised liquid must have been located within the very fine hyphal coating.

Now taking $d_o/d_i = 1.2$, then the volume of the coating was $\pi d_i^3 (1.2^3 - 1)/6$. Thus, for a pellet of density= 1.0015 g/cm^3 then

$$(1.2^3 d_i^3 \pi/6) * 1.0015 = 0.996 * 0.73 \pi d_i^3/6 + F * \pi d_i^3/6 \dots\dots 3.4-7$$

 where F is an average density for the material forming the central cavity and the mycelial shell. Hence , $F = 1.01 \text{ g/cm}^3$ and thus,
 $0.996 * Z + (1-Z) * 1.055 = 1.01 \dots\dots Z = 0.76$

This answer was in better agreement with microscopic examination and shows that a few hyphae on the outside of the pellet can immobilise a large amount of liquid. For autolysed pellets therefore,

Volume fraction of internal cavity = 0.76
outer liquid = 0.15
mycelial shell = 0.09
 Yosida et alia (1967) stated that for pellets less than 0.02 cm. diameter; "low density " pellets have $0.15 \text{ g dry mycelium /cm}^3$ and

aspherical pellets whose size was estimated visually.

Approx. size, cm.	Type	Yeast strain
0.3	Flocculent, fermentation limited.	CPCC 8
0.6	CPCC 34
0.8	Flocculent, physically limited.	CPCC 3
0.15	CPCC 83

3.4-4 Pellet density determinations

As was stated in the literature survey, a number of workers have used terminal velocity measurement to estimate aggregate densities. The assumptions underlying this method are open to question. Nevertheless, for the estimation of the density of a mould pellet this is the only method that may be readily applied.
 When using this method, the density difference between the pellet and the liquid was calculated from the terminal velocity using the Schiller - Naumann eqn. (3.3-1). The value of ρ_p so obtained was then related to the d_o/d_i ratio. Sample results for uniformly sized pellets are shown in Table 3.4-8 and Fig. 3-3. These results indicate the magnitude of the parameter involved. It could be seen that the calculated densities were very close to, and hence very dependent on, the liquid density. This indicated that the pellet contained a very large amount of liquid, both within the cells and immobilised within the pellet structure. The volume fraction of total water within the pellet, A, may be calculated from the relationship $A = (\rho_p - \rho_m) / (\rho_p - \rho_y)$ 3.4-4
 Values of A are also listed in Table 3.4-8 and plotted in Fig. 3-4.
 The volume fraction of liquid within the pellet was clearly very high and for most pellet sizes was approximately 99%. It was then possible to estimate the composition of a pellet. Since by definition,
 Volume fraction of total liquid = A
 Volume fraction of dry mycelium = (1-A)

"high density" pellets have 0.25 g. dry mycelium /cm.³ Hence, the dry mycelial density was = 1.38 g/cm.³ and the volume of dry mycelium/unit pellet volume = 0.15/1.38 = 0.109 or 0.25/1.38 = 0.181.

This led to immobile liquid volume fractions for the "low" and "high" density types of 0.891 and 0.819 respectively. Unfortunately, pellets of this size were not tested in the author's work using the terminal velocity technique. Yosida et alia volume fraction values yielded pellet densities of 1.04 & 1.07 g/cm.³ respectively. Whilst these are much higher than the values shown in Table 3.4-8 they fitted into the overall pattern of pellet density vs. diameter.

Yano et alia (1961) also determined the dry wt. of mycelium / cm.³ of pellet, for pellets less than 0.1 cm. diameter. Their pellets were approximately 15h. old and were grown in shake flasks. This suggested that the pellets were of the same morphology as those used in this work. Since the pellets varied in size it is likely that they developed from poorly dispersed spore cultures.

By definition, the volume fraction of total liquid = A and so the dry wt. of mycelium /unit pellet volume = (1-A) * ρ_s . Some sample values are shown in Table 3.4-8. Yano et alia's correlation of Dry mycelial wt./unit volume = 0.027 d₀^{-0.82} is shown in comparison with the present results in Fig. 3-5. The agreement was satisfactory. Note the two types of pellet systems, viz. those grown in well dispersed or poorly dispersed spore cultures. It should also be mentioned that Yano et alia's data was mainly for pellets less than 0.1 cm. diameter, whereas most of the present results were for pellets greater than 0.1 cm.

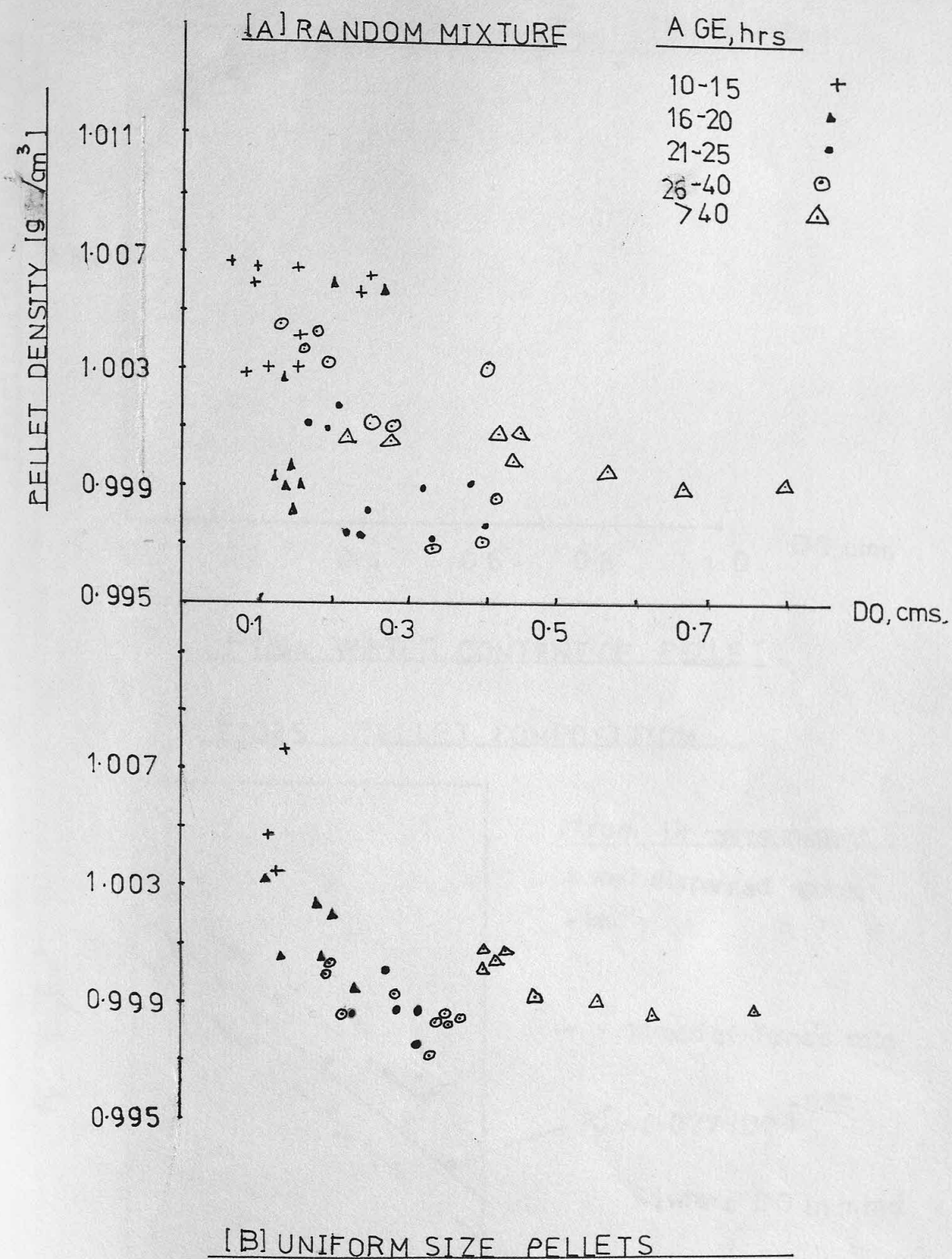
From Yano's data for dry wt. of mycelium/unit pellet volume, pellet density values may be calculated in the following manner.

Let dry mycelial wt. /unit volume = 0.02 g/cm.³
hence, volume of dry mycelium/unit volume = 0.02/ ρ_s = (1-A); and
 $\rho_p = (1-A)\rho_s + A\rho$ assuming $\rho_s = 1.3$ g/cm.³, then $\rho_p = 1.0$ g/cm.³
Similar calculations revealed that the pellet densities

Table 3.4-8 Pellet densities for *Molasses grown A. Niger*

Pellet age, h.	d_o , cm.	d_o/d_i	U_t , cm/s	Re_t	$T^\circ C$	ρ_m , g/cm. ³	μ , cp.	$\rho_p - \rho_m$	ρ_p , g/cm. ³	ρ_s , g/cm. ³	A	$(1-A) \cdot \rho_s$, g/cm. ³
14	0.128 0.152	2.67 1.92	0.572 0.893	8.93 16.55	29.1	0.9959	0.817	0.00877 0.01176	1.0047 1.0077	1.39	0.977 0.971	0.032 0.040
19	0.204 0.208 0.220	1.83 2.0 1.83	0.606 0.610 0.820	14.98 15.37 21.86	28.8	0.9960	0.822	0.00431 0.00421 0.00575	1.0003 1.0002 1.0018	1.375	0.989 0.985	0.029 0.034
24	0.248 0.292 0.320	1.38 ... 1.36	0.526 0.795 0.666	15.71 27.96 25.67	28.5	0.9961	0.827	0.00260 0.00351 0.00236	0.9987 0.9996 0.9985	1.295	0.991 0.988 0.991	0.0117 0.0156 0.0117
28	0.394 0.325 0.332	1.16 1.25 1.24	0.820 0.657 0.418	39.34 25.72 16.86	29.0	0.9960	0.818	0.00227 0.00226 0.00117	0.9982 0.9984 0.9972	1.260	0.991 0.994	0.0114 0.007
38	0.30 0.204	1.54 ... 1.42	0.820 0.426 0.552	29.8 10.6 13.6	28.9	0.820	0.00349 0.00270 0.00380	0.9994 0.9987 0.9998	1.24	0.984 0.998 0.984	0.0198 0.0149 0.0198
90	0.50 0.443 0.40	1.15 1.16 1.20	1.62 1.70 1.54	100 93 76	29.4	0.9959	0.810	0.00437 0.00562	1.0002 1.0015	0.932=Z 0.907...

FIG. 33A. NIGER PELLET DENSITIES



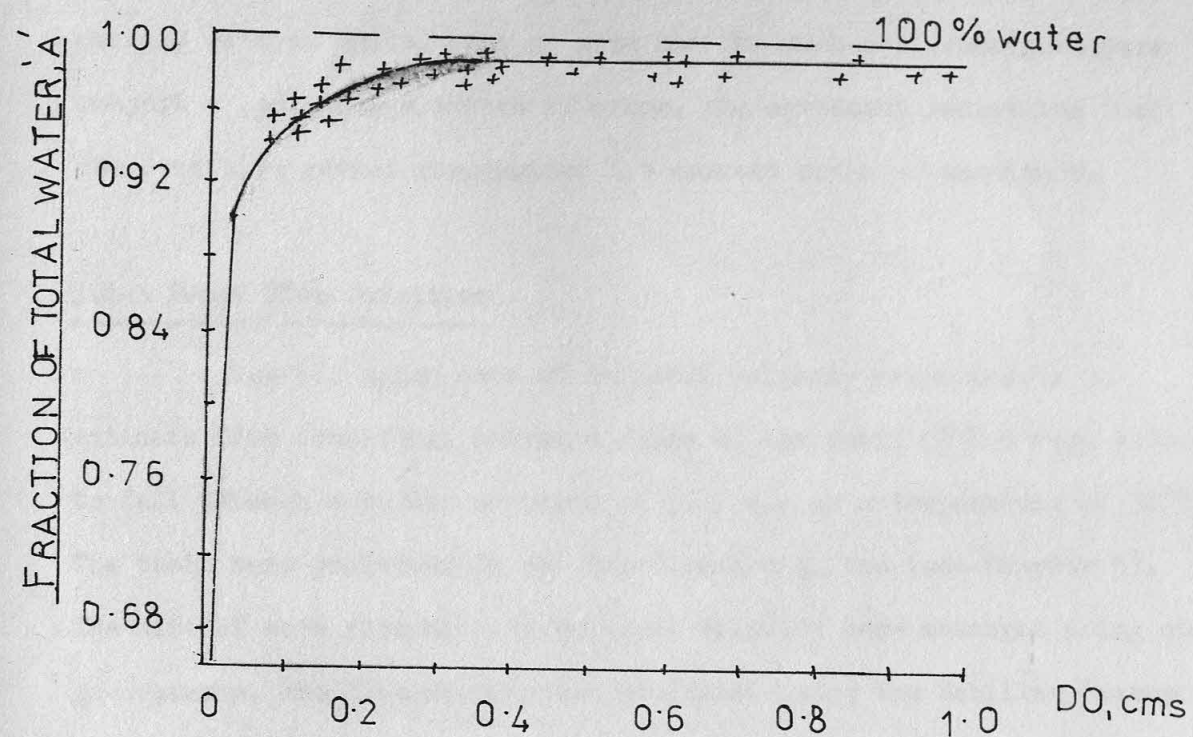
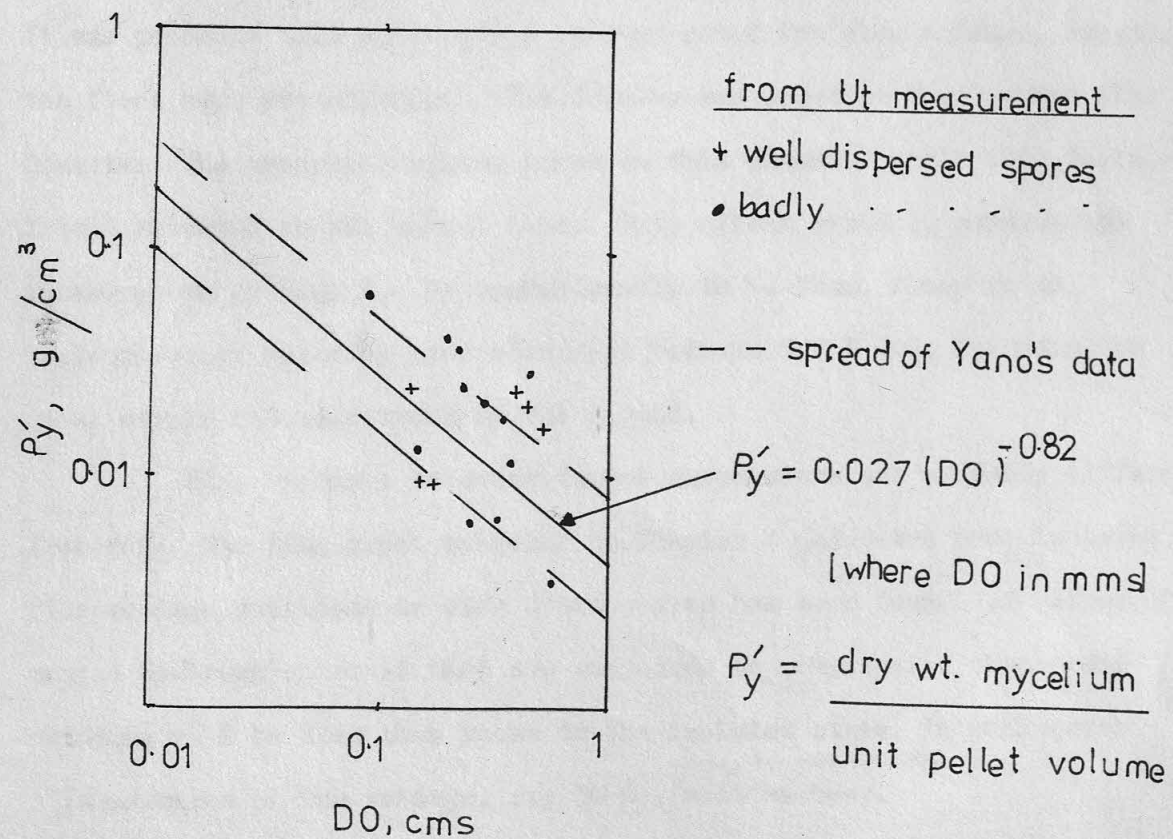


FIG34 WATER CONTENT OF PELLET

FIG35 PELLET COMPOSITION



predicted from Yano et alia's data were in agreement with those calculated in this work based on terminal velocity values. Variations of 150% in dry wt./unit volume values produced only 0.7% variation in density values. Whilst Yano et alia and the author's techniques were subject to possible elements of error, the agreement indicated that the densities quoted represented the correct order of magnitude.

3.4-5 Yeast Floc Densities

Use was again made of terminal velocity measurements to estimate floc densities. Isolated flocs of the yeast CFCC 8 were allowed to fall through a buffer solution of pH = 4.8 at a temperature of 30°C. The tests were performed in the Two-dimensional bed (see Chapter 5). The size of each floc and its terminal velocity were measured using cine-photography. The floc density was evaluated using the Schiller-Naumann equation as before.

The terminal velocity was not proportional to d^2 as might be expected and an evaluation of the floc voidage, based on the density, revealed that large flocs had higher voidages than small ones (see Fig.3.6). It was probable that this method overestimated the floc voidage, because the flocs were not spherical. The density was based on the largest floc diameter. The spherical volume based on this diameter would thus include liquid external to the actual floc. This effect probably reduces the values shown in Fig. 3.6 by approximately 10 %. Thus, flocs in an isolated state probably have a voidage between 0.7 & 0.8, depending on size, strain and conditions in the liquid.

Floc voidages in concentrated suspensions are probably different from this. The floc model proposed in Chapter 4 indicates that isolated floc voidage decreases as size decreases, as has been found. If flocs are caused to break-up or if they are subjected to compression then their voidages will be less than those in the isolated state. In such cases a lower value of the voidage, say 50 %, ^{may be appropriate} ~~must be used~~.

predicted from Yano et alia's data were in agreement with those calculated in this work based on terminal velocity values. Variations of 150% in dry wt./unit volume values produced only 0.5% variation in density values. Whilst Yano et alia and the author's techniques were subject to possible elements of error, the agreement indicated that the densities quoted represented the correct order of magnitude.

3.4-5 Yeast Floc Densities

Use was again made of terminal velocity measurements to estimate floc densities. Isolated flocs of the yeast CFCC 8 were allowed to fall through a buffer solution of $\text{pH} = 4.8$ at a temperature of 30.0°C . The tests were performed in the two-dimensional bed (see Chapter 2). The size of each floc and its terminal velocity were measured using cine-photography. The floc density was evaluated using the Schiller-Numann equation as before.

The terminal velocity was not proportional to d^2 as might be expected and an evaluation of the floc voidage, based on the density, revealed that large flocs had higher voidages than small ones (see Fig. 3.6). It was probable that this method overestimated the floc voidage, because the flocs were not spherical. The density was based on the largest floc diameter. The spherical volume based on this diameter would thus include liquid external to the actual floc. This effect probably reduces the values shown in Fig. 3.6 by approximately 10%. Thus, flocs in an isolated state probably have a voidage between 0.7 & 0.8, depending on size, strain and conditions in the liquid.

Floc voidages in concentrated suspensions are probably different from this. The floc model proposed in Chapter 4 indicates that isolated floc voidage decreases as size decreases, as has been found. If flocs are caused to break-up or if they are subjected to compression then their voidages will be less than those in the isolated state. In such cases a lower value of the voidage, say 50%, must be used.

FIG. 3.6 FLOC VOIDAGES FOR CFCC 8 ($T=30^\circ\text{C}$; $\text{pH}=4.7$)

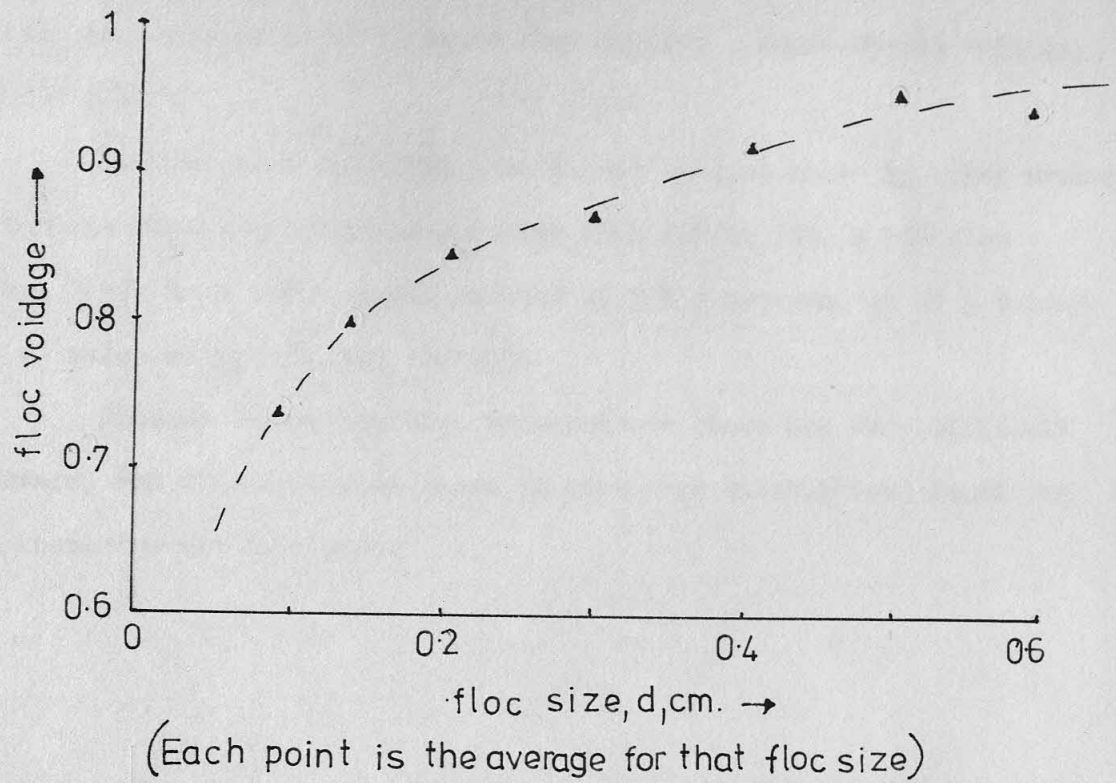
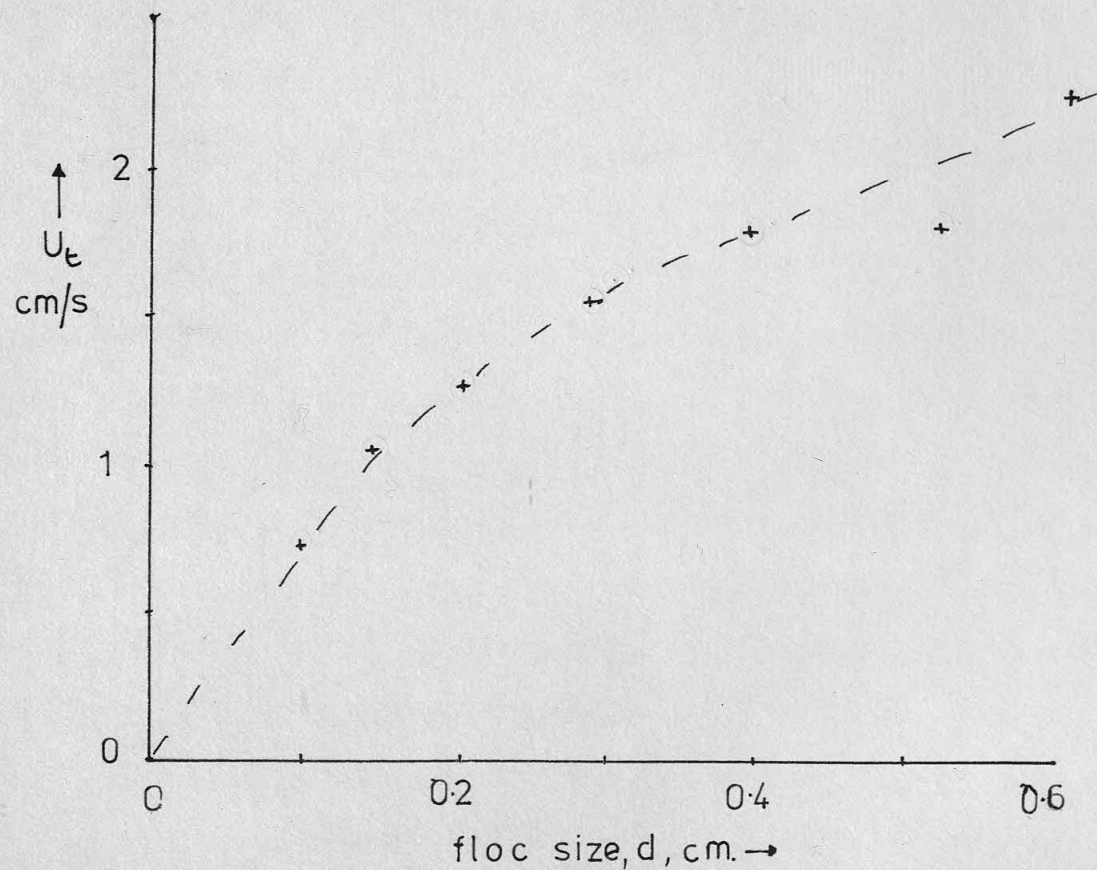


FIG. 3.7 TERMINAL VELOCITIES (CFCC 8)



The assumption of 50% voidage leads to the following values for floc density,

$$\rho_p = 0.5 \times 1 + 0.5 \times 1.07 = 1.035 \text{ g/cm}^3.$$

This may be compared to an isolated floc density, based on 80% voidage, of 1.011 g/cm^3 .

Estimates of the total floc liquid content made by other workers for various flocculent materials ranged from 63% to 99%. A 50% floc voidage leads to a total liquid content of 90%; whereas, an 80% voidage gave a value of 95% liquid content.

Precise values for floc voidages are therefore very difficult to obtain, and this should be borne in mind when calculations requiring such knowledge are attempted.

Levy (1951) considered a pellet to be an isotropic sphere and used this concept with regard to oxygen transfer considerations in structural ones.

More attention have been devoted to the models of the floc. Two main theories have been proposed for floc formation: they are cluster addition and particle aggregation.

In the cluster addition theory particles are considered to form into small clumps which then aggregate to give a floc. The following sequence of events was proposed by Smoluchowski (1917) and was later explored by Sutherland (1957) and Sutherland & Goshaw (1958). Computer calculations have been made to produce floc structures that were extremely irregular with high voidages. The simulated structure for a floc of 80% voidage is shown in Fig. 4.1 and the simulated floc voidages for various floc sizes are shown in Fig. 4.2. These flocs have voidages up to 0.8 and are generally greater than 0.5. Such voidages arise because the clusters are considered to add together in the absence of external forces, thus permitting the contact structure to remain intact.

The alternative model states the floc is built up slowly by simple particle addition. This was extensively used by Volk (1959, 1960, 1961).

CHAPTER 4

MATHEMATICAL MODELS OF MICROBIAL STRUCTURES

4.1 Introduction

An attempt has been made to describe mathematically the microbial structures discussed in Chapter 2, and to utilise the physical data of Chapter 3 in the models. Originally, it was hoped that the models would provide information on the properties and structures of microbial aggregates. Pellets and flocs, together with microbially coated solids, have been considered.

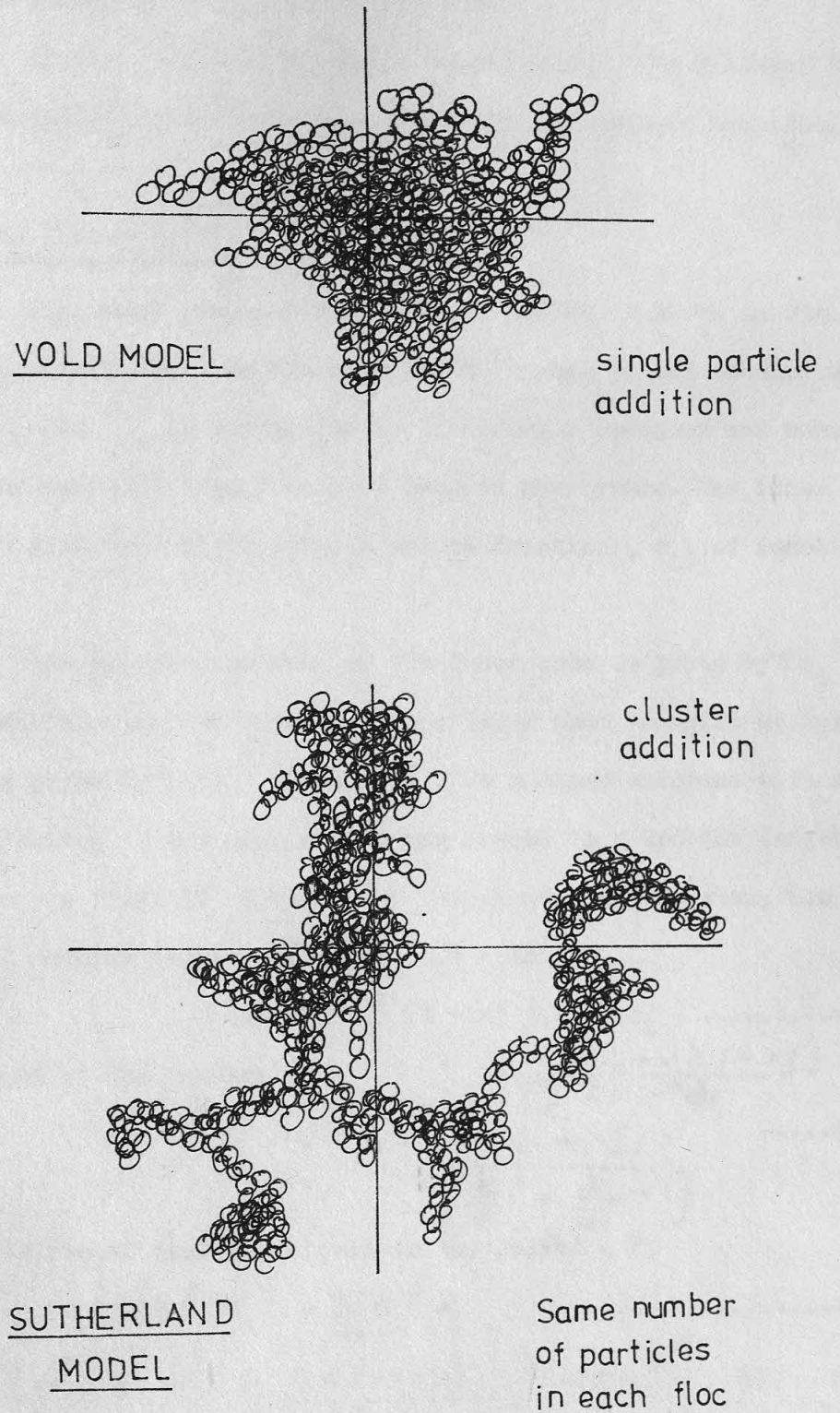
Mathematical representations of pellets are scarce in the literature. Yano et alia (1961) considered a pellet to be an isotropic sphere. However, they used this concept with regard to oxygen transfer considerations and not structural ones.

Floc structures have received more attention, the models being mainly concerned with the formation of the floc. Two main theories have been proposed for floc formation: they are cluster addition and single particle addition.

In the former, the basic particles are considered to form into small clusters which then combine to give a floc. The collision sequences for this were first proposed by Smoluchowski (1917) and were later explored by Sutherland (1967) and Sutherland & Goodarz-nia (1971), in computer simulations. This mechanism produced floc structures that were extremely open, with very high voidages. The simulated structure for a floc of 601 particles is shown in Fig. 4.1 and the predicted floc voidages for various floc sizes are shown in Fig. 4.2. These flocs have voidages upto 0.99 and are generally greater than 0.9. Such voidages arise because the clusters are considered to add together in the absence of external forces, thus permitting the contact structure to remain intact.

The alternative model where the floc is built up slowly by single particle addition has been extensively used by Vold (1959, 1960, 1963).

FIG. 4.1 FLOC SIMULATION



MATHEMATICAL MODELS OF MICROBIAL STRUCTURES

CHAPTER 4

4.1 Introduction

An attempt has been made to describe schematically the microbial structures discussed in Chapter 2, and to utilize the physical data of Chapter 3 in the models. Originally, it was hoped that the models would provide information on the properties and structures of microbial aggregates. Pellets and flocs, together with microbially coated solids, have been considered.

Mathematical representations of pellets are scarce in the literature. Yano et alia (1961) considered a pellet to be an isotropic sphere. However, they used this concept with regard to oxygen transfer considerations and not structural ones.

Floc structures have received more attention, the models being mainly concerned with the formation of the floc. Two main theories have been proposed for floc formation: they are cluster addition and single particle addition.

In the former, the basic particles are considered to form into small clusters which then combine to give a floc. The collision sequences for this were first proposed by Smoluchowski (1917) and were later explored by Sutherland (1967) and Sutherland & Goodwin (1971), in computer simulations. This mechanism produced floc structures that were extremely open, with very high voidages. The simulated structure for a floc of 601 particles is shown in Fig. 4.1 and the predicted floc voidages for various floc sizes are shown in Fig. 4.2. These flocs have voidages up to 0.99 and are generally greater than 0.9. Such voidages arise because the clusters are considered to add together in the absence of external forces, thus permitting the contact structure to remain intact.

The alternative model where the floc is built up slowly by single particle addition has been extensively used by Vold (1959, 1960, 1963).

A computer simulation using this sequence produced flocs which were more compact with lower voidages. Fig. 4.1 shows a 601 particle floc produced by this sequence and the lower voidages are illustrated in Fig. 4.2. Vold suggests that $d_{floc} = 1.13 n^{0.43}$ microns4.1.1 where n = number of particles in the floc.

In the following sections simple models for pellets, flocs and microbially-coated solids are presented and certain deductions are made.

4.2 Fungal Pellet Model

The model proposed for a fungal pellet is shown in Fig. 4.3. The d_o, d_i nomenclature is the same as in Chapter 3. The annular shell between d_o and d_i is assumed to be filled with branched and unbranched hyphae and immobile liquid trapped between the hyphae. The inner core is filled with hyphal mass and a volume fraction, e_i , of immobile liquid.

Now, the surface area of the inner core is given by πd_i^2 .

The surface area on the outside of the inner core occupied by hyphal bases is given by $k\pi d_i^2$ ($0 < k < 1$): k is assumed constant with radius. If the fraction of the hyphae with one branch is x and the length of the branch is given by f times the length of the main stem, then the

$$\begin{aligned} \text{volume of annular hyphae} &= \int_{r_i}^{r_o} \pi k d_i^2 (1 + xf) dr \\ &= \pi k d_i^2 (1 + xf) (r_o - r_i) \dots\dots\dots 4.2.1 \end{aligned}$$

$$\begin{aligned} \text{The voidage of the annulus, } e_o &= 1 - \frac{\pi k d_i^2 (r_o - r_i) (1 + xf)}{\int_{r_i}^{r_o} 4\pi r^2 dr} \\ \therefore e_o &= 1 - \frac{3K(1 + xf)}{\left[\left(\frac{d_o}{d_i}\right)^2 + \frac{d_o}{d_i} + 1\right]} \dots\dots\dots 4.2.2 \end{aligned}$$

Now the volume of immobile liquid in the pellet = V_i

$$\text{and } V = \frac{\pi}{6} (d_o^3 - d_i^3) e_o + \frac{\pi}{6} d_i^3 e_i \dots\dots\dots 4.2.3$$

$$V = \frac{\pi}{6} d_i^3 \left(e_i - 1 + \frac{3K(1 + xf)}{\left[\left(\frac{d_o}{d_i}\right)^2 + \frac{d_o}{d_i} + 1\right]} \right) + \frac{\pi d_o^3}{6} \left[1 - \frac{3K(1 + xf)}{\left[\left(\frac{d_o}{d_i}\right)^2 + \frac{d_o}{d_i} + 1\right]} \right]$$

Let the density of the hyphae = ρ_y

$$\text{Pellet density} = \rho_p = \rho_y - \frac{6V(\rho_y - \rho)}{\pi d_o^3} \dots\dots\dots 4.2.4$$

FIG 4.2 PREDICTED FLOC VOIDAGES

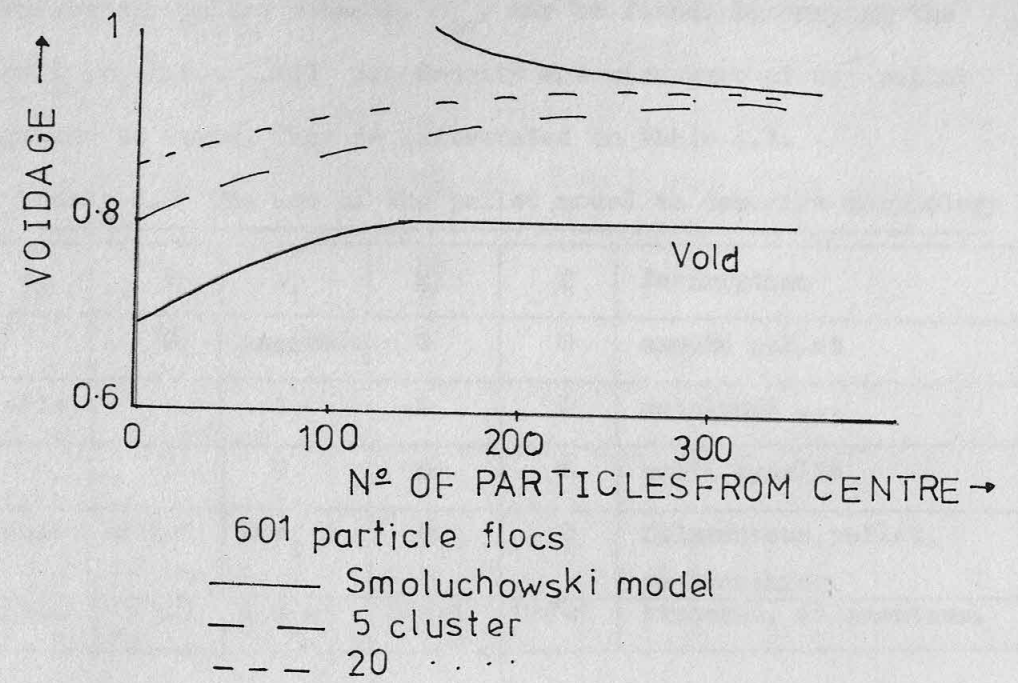
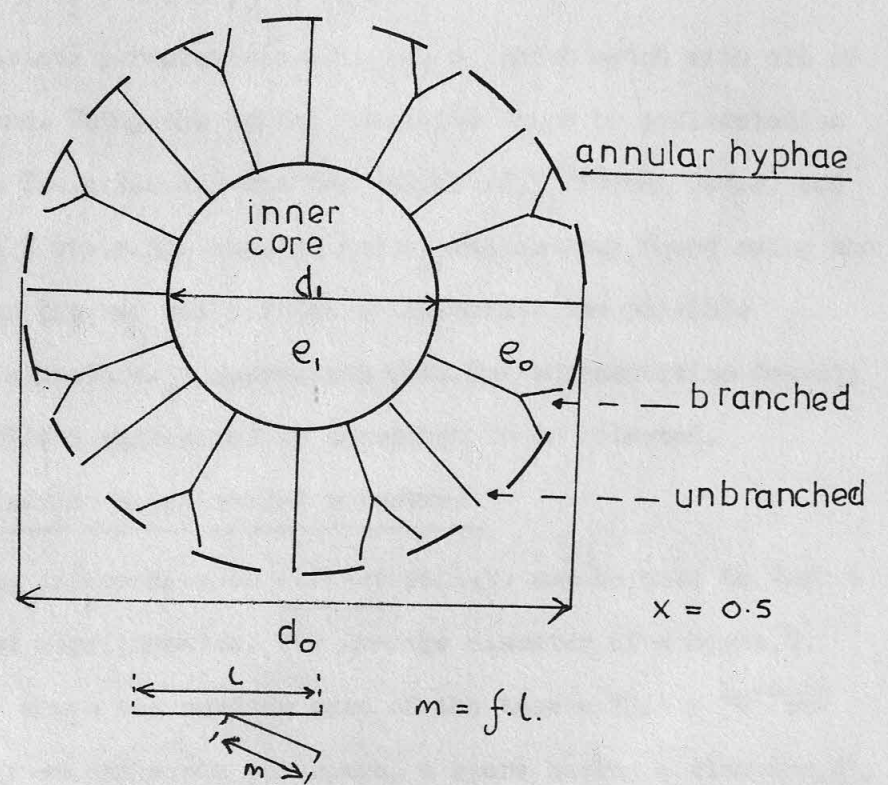


FIG. 4.3 FUNGAL PELLET MODEL



Computer simulation using this sequence produced flocs which were more compact with lower voidages. Fig. 4.1 shows a 601 particle floc produced by this sequence and the lower voidages are illustrated in Fig. 4.2. Void suggests that $d_{floc} = 1.13 \times 10^{-4}$ m. 4.1.1 where n = number of particles in the floc.

4.2 Fungal Pellet Model

The model proposed for a fungal pellet is shown in Fig. 4.3. The d_o nomenclature is the same as in Chapter 1. The annular shell between d_o and d_i is assumed to be filled with branched and unbranched hyphae and immobile liquid trapped between the hyphae. The inner core is filled with hyphal mass and a volume fraction, e_i , of immobile liquid.

Now, the surface area of the inner core is given by πd_i^2 . The surface area on the outside of the inner core occupied by hyphal mass is given by πd_o^2 ($0 < k < 1$): k is assumed constant with radius. If the fraction of the hyphae with one branch is x and the length of the branch is given by 2 times the length of the main stem, then the volume of annular hyphae = $\sum \pi k d_i^2 (1+x) dx$ 4.2.1
 $= \pi k d_i^2 (1+x) (r_o - r_i)$ 4.2.1
The volume of the annulus, e_o = $1 - \frac{\pi k d_i^2 (1+x) (r_o - r_i)}{\pi d_o^2}$ 4.2.2
 $e_o = 1 - \frac{3K(1+x)}{2} = 1 - \frac{3K}{2} (1+x)$ 4.2.2
Now the volume of immobile liquid in the pellet = V_i
and $V = \frac{\pi}{6} (d_o^3 - d_i^3) e_o + \frac{\pi}{6} d_i^3 e_i$ 4.2.3
Let the density of the hyphae = ρ_h
Pellet density = $\rho_p = \rho_h - \frac{\rho_h}{\pi d_o^3} (d_o^3 - d_i^3) e_o$ 4.2.4

$$\rho_p = \rho_y - (\rho_y - \rho) \left[e_i \left(\frac{d_i}{d_o} \right)^3 + \left(1 - \frac{3K(1+xf)}{\left[\left(\frac{d_o}{d_i} \right)^2 + \frac{d_o}{d_i} + 1 \right]} \right) \left(1 - \left(\frac{d_i}{d_o} \right)^3 \right) \right] \dots 4.2.5$$

$$\text{Also } \rho_p = \rho_y - (\rho_y - \rho) e_{av} \dots 4.2.6$$

Hence, the average pellet density, e_{av} , may be found. By varying the parameters $d_o, d_i, k, e_i, \rho_y, x, f$ the density and structure of any pellet morphology may be found. This is illustrated in Table 4.1.

Table 4.1 The use of the pellet model to describe morphology

d_o / d_i	k	e_i	x	f	Description
1	0	variable	0	0	smooth pellet
variable	1	1	0	0	autolysed ...
1	1	0	0	0	solid mycelia
variable	$0 < k < 1$	$0 < e_i < 1$	0	0	filamentous pellet, no branching.
variable	$0 < k < 1$	$0 < e_i < 1$	$0 < x < 1$	$0 < f < 1$	branched, filamentous.

The model was most readily used to evaluate structural characteristics of pellets. For a given pellet the following information may be found by physical tests or observation:

$$d_o, d_i, x, f, \rho, \rho_y, \rho_p$$

Therefore the various permutations of k and e_i which match with all of these can be found. Using the pellet densities found by sedimentation (section 3.4.4 & Table 3.4.8) and the values of ρ_y (Table 3.4.4) and estimating x and f visually, then k and e_i values were found using the model. A computer program was written to calculate the possible permutations of structure. A comparison with the sedimentation density values then enabled a corresponding structure to be selected.

Additional information about pellet structure

Existing information on A.Niger pellets may be used to form a picture of pellet configuration. The average diameter of a hypha, d, is 5×10^{-4} cm.; hence the surface area of the base = $19.6 \times 10^{-8} \text{ cm}^2$. The strain M1 gives one hypha per spore, a spore having a diameter, d',

= 7.5×10^{-4} cm. From the pellet model definition,

k = surface area of hyphal bases / area of inner core, and so $k = \frac{n \pi d^2 / 4}{\pi d_i^2}$

For the case where $d_i = 0.1$ cm. and $k = 0.02$, then the number of hyphae protruding into the outer zone is given by, $n = \frac{4 \times 0.01 \times 0.02}{25 \times 10^{-8}} = 3.2 \times 10^3$

This gives an indication of the large number of hyphae that emerge from the core of a small, "hairy" type pellet. Clearly when these hyphae branch the number on the outside could almost double.

Spore aggregates

Very little information can be obtained about the structure of the initial spore aggregate from sedimentation tests. However, a simple picture might be as follows.

Let the number of spores / aggregate = N .

The number of spores ranges from 5 to 2000, but a value of 50 is perhaps typical for a well-dispersed inoculum. For an aggregate of diameter, D and a volume fraction of spores of $(1 - e_i)$, then

$$D = (N / (1 - e_i))^{1/3} d'$$

Now the spores will be packed with hyphae in the aggregate and so assume $e_i = 0.6$. Hence, the diameter of a 50 spore aggregate will be 3.75×10^{-3} cm and the aggregate surface area will be 44.2×10^{-6} cm². Assuming the protrusion of the 50 hyphae, then $k = \frac{50 \times 19.6 \times 10^{-8}}{44.2 \times 10^{-6}} = 0.204$

Now aggregate density, $\rho_p = e_i \rho + (1 - e_i) \rho_y$, and so for

$\rho_y = 1.12$ g/cm³ (see Table 3.4.4) then $\rho_p = 1.046$ g/cm³.

This indicates a likely structure and density for such a spore aggregate.

Developed Pellets

Pellet densities calculated from the settling velocities of isolated pellets taken from well-dispersed spore cultures were compared to the possible structures predicted by the pellet model. The values taken for x and f were 0.5 and 0.333 respectively. Some comparisons for 38 h. and 16 h. pellets are shown in Fig. 4.4 & 4.5.

Also $\rho_p = \rho + (1 - e_i) \rho_y$ Hence, the average pellet density, ρ_p , may be found. By varying the parameters d_i, d, k, e_i, x, f , the density and structure of any pellet morphology may be found. This is illustrated in Table 4.1.

Table 4.1 The use of the pellet model to describe morphology

Description	f	x	e_i	k	$d_i \backslash d$
smooth pellet	0	0	variable	0	1
autolysed ...	0	0	1	1	variable
solid wocella	0	0	0	1	1
filamentous pellet, no branching	0	0	$0 < e_i < 1$	$0 < k < 1$	variable
branched, filamentous	$0 < f < 1$	$0 < x < 1$	$0 < e_i < 1$	$0 < k < 1$	variable

The model was most readily used to evaluate structural characteristics of pellets. For a given pellet the following information may be found by physical tests or observation:

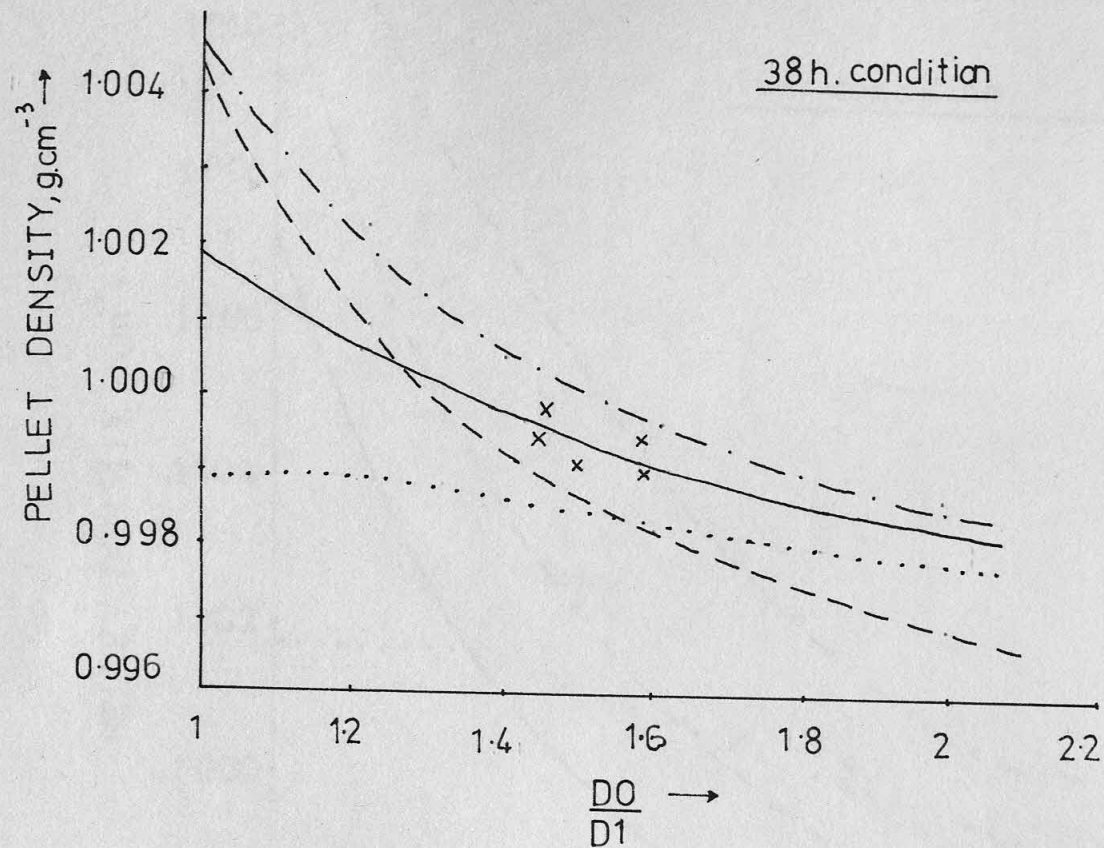
$$d_i, d, k, e_i, x, f, \rho_p$$

Therefore the various permutations of k and e_i which match with all of these can be found. Using the pellet densities found by sedimentation (section 3.4.4 & Table 3.4.8) and the values of ρ_y (Table 3.4.4) and estimating x and f visually, then k and e_i values were found using the model. A computer program was written to calculate the possible permutations of structure. A comparison with the sedimentation density values then enabled a corresponding structure to be selected.

Additional information about pellet structure

Existing information on *A. niger* pellets may be used to form a picture of pellet configuration. The average diameter of a hypha, d , is 5×10^{-4} cm; hence the surface area of the base = 19.6×10^{-8} cm². The strain M gives one hypha per spore, a spore having a diameter, d_i .

FIG.4.4 PELLET MODEL EVALUATION



	$\frac{E1}{0.9}$	$\frac{K}{0.05}$	$\frac{X}{0.5}$	$\frac{F}{0.333}$
—	0.9	0.05	0.5	0.333
- - -	0.85	0
- . - . -	0.85	0.05
.....	0.95	0.05

x from settling velocity of 38h. pellets

for 38 h. and 16 h. pellets are shown in Fig.4.4 & 4.5.

taken for x and 1 were 0.5 and 0.333 respectively. Some comparisons

to the possible structures predicted by the pellet model. The values

isolated pellets taken from well-dispersed spore cultures were compared

Pellet densities calculated from the settling velocities of

Developed Pellets

This indicates a likely structure and density for each a spore aggregate.

$$\rho_p = 1.12 \text{ g/cm}^3 \text{ (see Table 3.4.4) then } \rho_p = 1.04 \text{ g/cm}^3$$

Now aggregate density, $\rho_p = e_1 \rho + (1-e_1) \rho_v$, and so for

$$44.2 \times 10^{-8} = 0.204 \times 1.12 + (1-0.204) \times \rho_v$$

and the aggregate surface area will be $44.2 \times 10^{-8} \text{ cm}^2$. Assuming the

$e_1 = 0.6$. Hence, the diameter of a 50 spore aggregate will be $3.75 \times 10^{-3} \text{ cm}$

Now the spores will be packed with hyphae in the aggregate and so assume

$$D = (N \times (1-e_1) \times d_v)^{1/3}$$

and a volume fraction of spores of $(1-e_1)$, then

typical for a well-dispersed inoculum. For an aggregate of diameter, D

The number of spores ranges from 5 to 2000, but a value of 50 is perhaps

Let the number of spores / aggregate = N.

simple picture might be as follows.

of the initial spore aggregate from sedimentation tests. However,

Very little information can be obtained about the structure

Spore aggregates

branch the number on the outside could almost double.

the core of a small, "fuzzy" type pellet. Clearly when these hyphae

This gives an indication of the large number of hyphae that emerge from

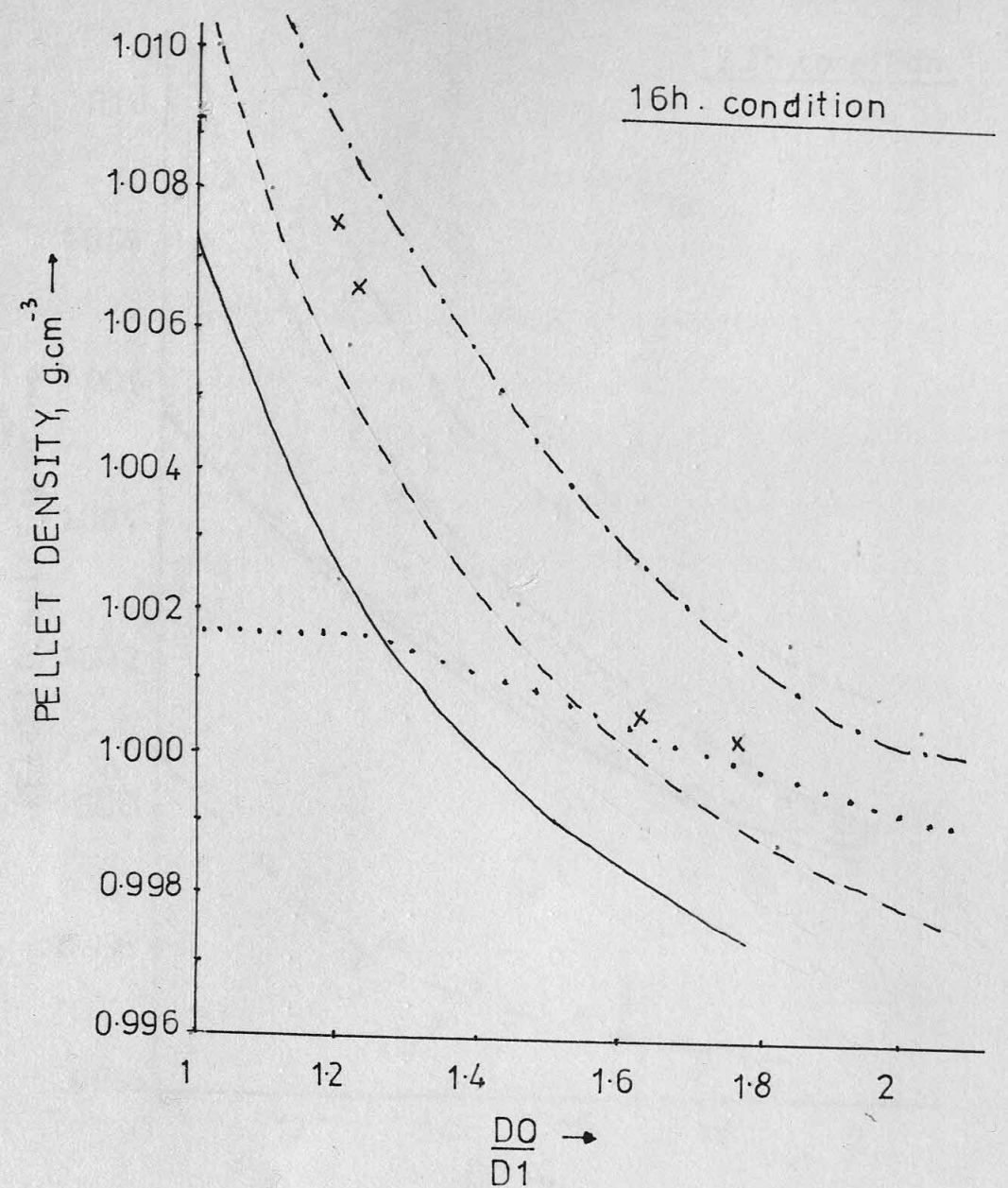
protruding into the outer zone is given by $n = 4\pi \times 10^{-8} \times 0.02 = 3.2 \times 10^3$

For the case where $d_1 = 0.1 \text{ cm}$, and $k = 0.02$, then the number of hyphae

$k = \text{surface area of hyphal bases} / \text{area of inner core}$, and so $k =$

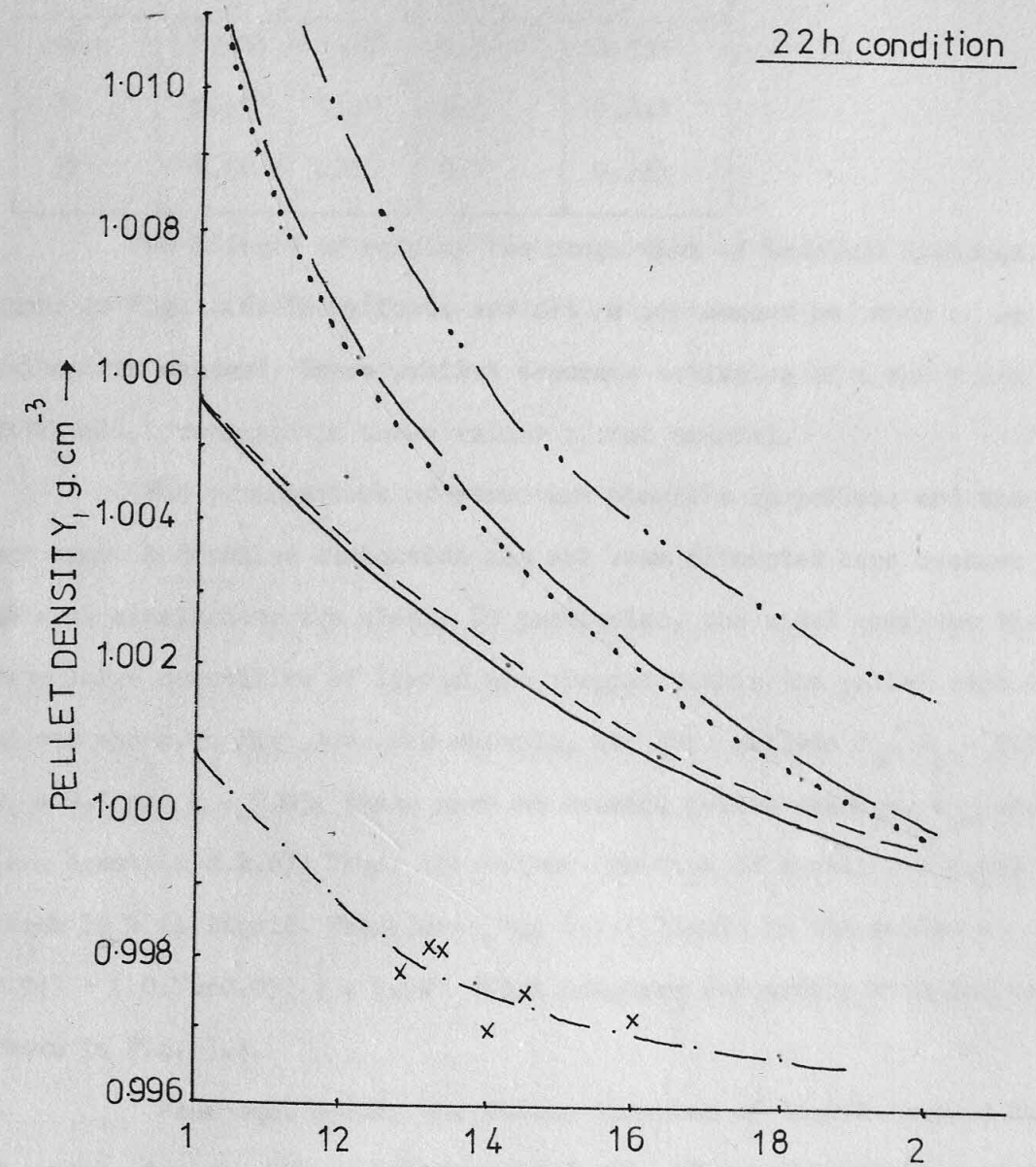
$= 7.5 \times 10^{-4} \text{ cm}$. From the pellet model definition,

FIG.45 PELLET MODEL EVALUATION



	<u>E1</u>	<u>K</u>	<u>X</u>	<u>F</u>
---	0.85	0	0.5	0.333
-.-	...	0.05
....	0.95
---	0.9	0
x	16h. pellets settling tests			

FIG. 46 PELLET MODEL EVALUATION



	$\frac{E_1}{0.9}$	$\frac{K}{0.05}$	$\frac{X}{0.5}$	$\frac{F}{0.333}$
—	0.9	0.05	0.5	0.333
- - -	0.9	..
— — —	0.85
· · · · ·	0.5	..
— · —	0.95	0
x	22h. pellet data			
— · · —	0.85	0.1

It will be seen that $e_i = 0.9$ and $k = 0.05$ was in best agreement with the 38h. pellet data. Other examples are shown in Table 4.2.

Table 4.2 Structures predicted by the pellet model

Age, h.	e_i	k	x	f
16	0.85	0.02	0.5	0.333
22	0.94	0.01	0.5	0.333
38	0.90	0.05	0.5	0.333

The effects of varying the proportion of branched hyphae, x , is shown in Fig. 4.6. The effects are not as pronounced as when e_i or k values are changed. Hence, whilst accurate estimates of x and f are difficult, precision in these values is not crucial.

The permutations of structure possible in pellets and the model are many. A detailed evaluation has not been attempted here because the general conclusions are clear. In particular, the model confirms that very large quantities of liquid are trapped within the pellet structure, as was shown in Fig. 3.4. For example, for 38h. pellets $d_o/d_i = 1.5$, $e_i = 0.9$ and $k = 0.05$; these gave an average pellet voidage, $e_{av} = 0.943$ (see equation 4.2.6). Thus, the volume fraction of mycelium = 0.057 of which 76 % is liquid. Therefore, the total liquid in the pellet = $0.943 + (0.76 \times 0.057) = 0.986$ which compares favourably with the values shown in Fig. 3.4.

From eqn. 4.2.2, the volume fraction of liquid trapped between d_o and d_i for the 38h. condition was 0.963. Thus, the relative distribution of trapped liquid and structure of a 38h. pellet ($d_o = 1.5$ cm, say) would be,

$$\text{Total pellet volume} = 1.768 \text{ cm}^3.$$

$$\text{Total trapped liquid volume} = 0.943 \times 1.768 = 1.667 \text{ cm}^3.$$

$$\text{Volume inside central core} = 0.9 \times \pi d_i^3 / 6 = 0.471 \text{ cm}^3.$$

$$\text{Volume on outside of pellet} = 0.963 \times \pi (d_o^3 - d_i^3) / 6 = 1.196 \text{ cm}^3.$$

$$\text{Volume of mycelium} = 0.101 \text{ cm}^3.$$

$$\text{Volume of dry mycelium} = 0.024 \text{ cm}^3.$$

$$\text{Number of hyphae leaving central core} = 8.015 \times 10^5.$$

$$\text{Total number of hyphae in the annular space} = 8.015 \times 10^5 (1+x) \\ = 12.02 \times 10^5$$

These calculations indicate that a considerable amount of information about the pellet can be deduced. This in turn may be useful in interpreting other experimental data, e.g. concerning rate processes.

4.3 Microbial Floc Model

Due to the transient and random nature of floc formation, a precise model cannot be formulated. However, a simple approach can yield some useful, general information. The elementary model is shown in Fig. 4.7. The floc is composed of equisized clusters and aggregates. During formation, the floc passes through several distinct stages in sequence.

Cluster formation

Now, yeast cells may be considered as oblate spheroids (minor axis = b, major axis = a). Hence, cell volume = $\pi ab^2/6$. Therefore, the voidage, e' , of a cluster (equivalent size = d_0) composed of z cells of uniform size is,

$$e' = 1 - zab^2 / d_0^3 \quad \dots\dots\dots 4.3.1$$

$$\text{Now, } \rho_y = M\rho + (1-M)\rho_s \text{ and cluster density } \rho' = (1-e')\rho_y + e'\rho \\ \therefore \rho' = zab^2(1-M)(\rho_s - \rho) / d_0^3 + \rho \quad \dots\dots\dots 4.3.2 \\ = (1-e')(1-M)(\rho_s - \rho) + \rho$$

Aggregate Formation

Suppose that an aggregate of N of these clusters of equivalent diameter, D , forms and that the volume fraction of liquid trapped in the cluster network = e'' .

Therefore, aggregate density, $\rho_{ag} = e''\rho + (1-e'')\rho'$, where $e'' = 1 - d_0^3 N / D^3$

$$\rho_{ag} = \rho + \frac{d_0^3 N}{D^3} (\rho' - \rho) \\ = \rho + \frac{d_0^3 N}{D^3} \left[\frac{zab^2}{d_0^3} (1-M)(\rho_s - \rho) \right] \\ = \rho + \frac{Nzab^2}{D^3} (1-M)(\rho_s - \rho)$$

Table 4.2 Structures predicted by the pellet model

Age, h.	e'	k	x	z
16	0.85	0.02	0.5	0.333
22	0.94	0.01	0.5	0.333
38	0.90	0.05	0.5	0.333

The effects of varying the proportion of branched hyphae, x , is shown in Fig. 4.6. The effects are not as pronounced as when e' or k values are changed. Hence, whilst accurate estimates of k and e' are difficult, prediction in these values is not crucial. The permutations of structure possible in pellets and the model are many. A detailed evaluation has not been attempted here because the general conclusions are clear. In particular, the model confirms that very large quantities of liquid are trapped within the pellet structure, as was shown in Fig. 3.4. For example, for 38h. pellets $e' = 0.90$, $k = 0.05$, $x = 0.5$, $z = 0.333$ these gave an average pellet voidage, $e_v = 0.943$ (see equation 4.2.6). Thus, the volume fraction of mycelium = 0.057 of which 76% is liquid. Therefore, the total liquid in the pellet = $0.943 + (0.057 \times 0.057) = 0.986$ which compares favourably with the values shown in Fig. 3.4.

From eqn. 4.2.2, the volume fraction of liquid trapped between d_0 and d_1 for the 38h. condition was 0.963. Thus, the relative distribution of trapped liquid and structure of a 38h. pellet ($d_0 = 1.5 \mu\text{m}$, say) would be, Total pellet volume = 1.768 cm^3 . Total trapped liquid volume = $0.943 \times 1.768 = 1.667 \text{ cm}^3$. Volume inside central core = $0.9 \times 1.768 = 0.159 \text{ cm}^3$. Volume on outside of pellet = $0.963 \times 1.768 = 1.698 \text{ cm}^3$. Volume of mycelium = 0.101 cm^3 . Volume of dry mycelium = 0.024 cm^3 . Number of hyphae leaving central core = 8.015×10^5 .

$$\rho_{ag} = \rho + (1-e')(1-e'')(1-M)(\rho_s - \rho) \dots\dots\dots 4.3.3$$

Similarly, if these large aggregates join to form a larger aggregate of voidage, e''' , then its density will be,

$$\rho_p = \rho + (1-e')(1-e'')(1-e''')(1-M)(\rho_s - \rho)$$

For multiple aggregation with the same voidage,

$$\rho_p = \rho + (1-e)^a (1-M)(\rho_s - \rho) \dots\dots\dots 4.3.4$$

Now photomicrographs show yeast cells to pack closely: hence, for each cluster or aggregate a voidage of 0.4 (say) may be taken

$$\text{i.e. } e' = e'' = e''' = e^{iv} = 0.4$$

Taking the values $M = 0.8$; $\rho_s = 1.32 \text{ g/cm}^3$; $\rho = 0.996 \text{ g/cm}^3$, then the density of each aggregation unit will be,

a	$\rho_p, \text{g/cm}^3$	e, unit voidage
1	1.0348	0.40
2	1.0192	0.643
3	1.0099	0.786
4	1.0043	0.872
5	1.0009	0.925
6	0.9989	0.955
8	0.9970	0.985
10	0.9964	0.994

(see Fig. 4.8)

$$e = (\rho_y - \rho_p) / (\rho_y - \rho)$$

where $\rho_y = 1.061 \text{ g/cm}^3$

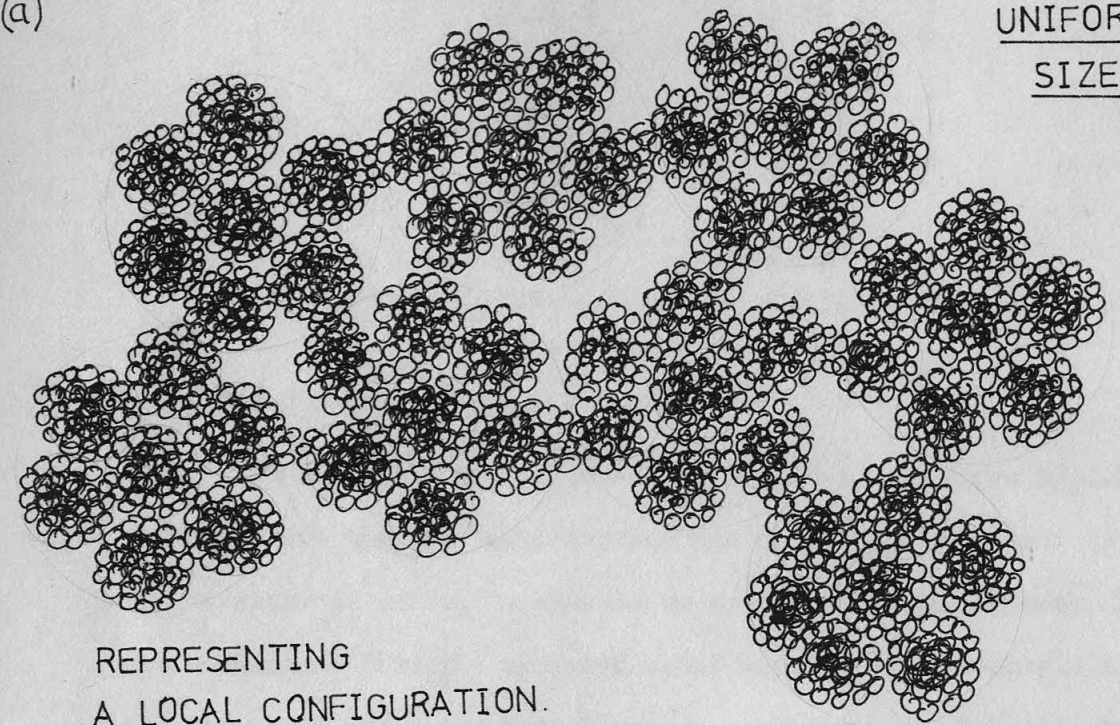
Table 4.3 Floc properties predicted by floc model for
uniform units of local voidage = 0.4

It is unlikely that at each aggregation stage the flocculated units would be of equal size. They would probably have a size distribution (see Fig. 4.7). Now when particles of varying sizes are packed together the voidage is less than for uniform spheres (Van Vlack, 1964), (a minimum value of $e = 0.15$ has been observed for a mixture of large size distribution). Hence, assuming each aggregation voidage = 0.2, then the results as shown in Table 4.4 are obtained.

FIG.4.7 FLOC MODELS

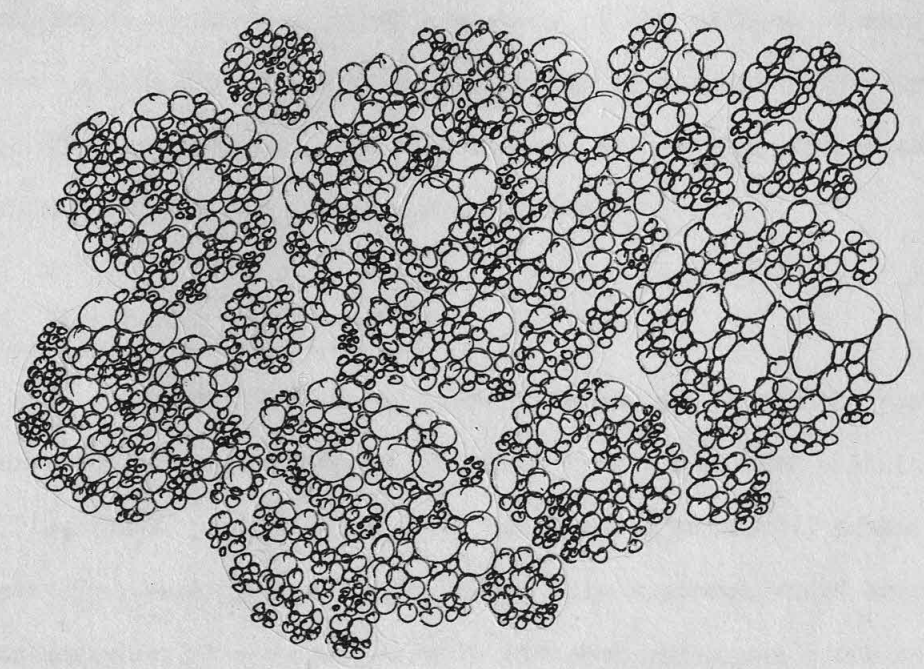
(a)

UNIFORM
SIZE



REPRESENTING
A LOCAL CONFIGURATION.
EACH UNIT SURROUNDED BY OTHERS

(b)



LARGE SIZE DISTRIBUTION

Similarly, if these large aggregates join to form a larger aggregate of voidage e'''' , then its density will be,

$$\rho_p = \rho + (1-e')((1-e'')((1-e''')((1-M)(\rho_p - \rho)))$$

for multiple aggregation with the same voidage,

$$\rho_p = \rho + (1-e)^n((1-M)(\rho_p - \rho))$$

Now photomicrographs show yeast cells to pack closely; hence for each cluster or aggregate a voidage of 0.4 (say) may be taken

$$i.e. e' = e'' = e''' = e'''' = e \text{ iv } = 0.4$$

Taking the values $M = 0.8$; $\rho_s = 1.32 \text{ g/cm}^3$; $\rho = 0.996 \text{ g/cm}^3$, then the density of each aggregation unit will be,

n	$\rho_p \text{ g/cm}^3$	e , unit voidage
1	1.0348	0.40
2	1.0192	0.643
3	1.0099	0.786
4	1.0043	0.875
5	1.0009	0.925
6	0.9989	0.955
8	0.9970	0.985
10	0.9964	0.994

Table 4.3 Floc properties predicted by floc model for

uniform units of local voidage = 0.4

It is unlikely that at each aggregation stage the flocculated units would be of equal size. They would probably have a size distribution (see Fig. 4.7). Now when particles of varying sizes are packed together the voidage is less than for uniform spheres (Van Vlack, 1964), (a minimum value of $e = 0.15$ has been observed for a mixture of large size distribution). Hence, assuming each aggregation voidage = 0.2, then the results as shown in Table 4.4 are obtained.

Table 4.4 Floc properties predicted by the floc model
for non-uniform units, voidage = 0.2

a	ρ_p , g/cm ³	e
1	1.0478	0.20
2	1.0375	0.362
3	1.0292	0.489
4	1.0226	0.591
5	1.0172	0.674
6	1.013	0.738
8	1.0069	0.832
10	1.0029	0.894

The effect is quite pronounced, although voidages of 0.2 would only occur where the size distribution was large. The assessment of the exact structure of a floc is clearly an extremely difficult task. The author recognises that the proposed model may not be an accurate simulation of the floc building mechanism. However, observation indicated that yeast flocs were relatively compact units, whose voidage could alter with environment. This model permits a study of the effects of variable voidage to be made and is thus especially useful in examining the structure of a settling suspension. The model shows how voidage alters as floc size alters or compressive forces are applied.

4.4 Microbially Coated Solids

The possibility of using a fermenter where the particles of microorganism coat a support base has been considered (Atkinson et alia, 1972). The objective of this is to minimise microbial washout and to generally speed up the fermentation. This approach would only be worth consideration if a fermenter with attached organisms contained more organisms than one containing microbial flocs or pellets suspended in the medium.

Consider $J \text{ cm}^3$ volume containing spheres of diameter = $j \text{ cm}$.

with a coating thickness = $(j_0 - j)/2$.

Now, the volume of the spheres = $J(1-e)$, where e is based on the coated spheres and the number of coated balls = $J(1-e) \cdot 6/j_0^3$

Consequently the total volume of coating is given by,

$$\frac{J(1-e)}{\pi j_0^3} \times \frac{\pi}{6} (j_0^3 - j^3) = \frac{(j_0^3 - j^3)}{j_0^3} J(1-e) \dots\dots\dots 4.4.1$$

By contrast, in a suspension of flocs the volume of organisms = $J(1-e')$,

where e' is based on centrifuged organism.

For the coated system to be preferred then the ratio:

$$\text{volume of flocs / volume of coating} \leq 1;$$

$$\text{i.e. } \frac{(1-e')j_0^3}{(j_0^3 - j^3)(1-e)} = \frac{(1-e')j^3}{(j_0^3 - j^3)(1-e'')} \leq 1 \dots\dots\dots 4.4.2$$

where e'' is based on un-coated spheres.

Consider 0.2 cm glass spheres coated with yeast. For systems that are just fluidised, $e' \approx 0.8$; $e'' \approx 0.45$ (see Chapter 5).

For the systems to be equivalent, then $0.2 j^3 = 0.55 (j_0^3 - j^3)$

and thus $j_0 = 0.222 \text{ cm}$. (i.e. coating thickness must be 0.011 cm.)

Experiments were performed to check if yeast would attach itself to ballotini. 0.2 cm. ballotini were placed in a fermenter containing growing yeast and were left for 3 days. A physically-limited yeast, CFCC83, did not coat the glass balls, but a fermentation-limited yeast, CFCC8, attached well. In the latter case the balls became embedded in a yeast paste, which, whilst stable, would not give an even flow distribution in a continuous fermenter, (see Plate 4.1).

In certain situations microbially-coated solids may have an advantage over free-floating microbial aggregates. The rate of fermentation may be increased due to improvements in the following factors.

- i. Microbial mass and volume, therefore more enzymes.
- ii. Exposed surface area.
- iii. Diffusion of the substrate and products through the microbial mass.

Table 4.4 Floc properties predicted by the model

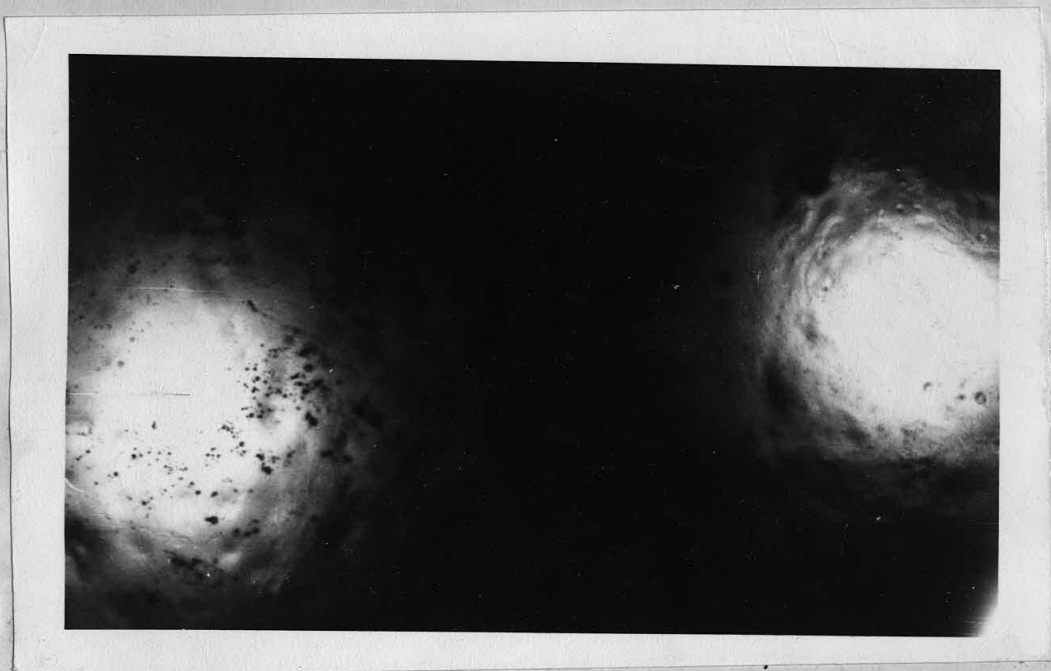
for non-uniform units, voidage = 0.2

e	$j_0, \text{ cm}$	n
0.20	1.0478	1
0.35	1.0375	2
0.48	1.0292	3
0.59	1.0226	4
0.67	1.0172	5
0.73	1.013	6
0.78	1.0099	8
0.82	1.0079	10

4.4 Microbially Coated Solids

The possibility of using a fermenter where the particles of microorganisms coat a support has been considered (Atkinson et al., 1972). The objective of this is to minimise microbial washout and to generally speed up the fermentation. This approach would only be worth consideration if a fermenter with attached organisms contained more organisms than one containing microbial flocs or pellets suspended in the medium.

PLATE 4.1 YEAST COATING 2mm. BALLOTINI



↑
BALLOTINI

↑
YEAST

Consider a volume containing spheres of diameter = j cm.
with a coating thickness = $(j_0 - j)/2$.
Now, the volume of the spheres = $j^3 (1 - e)$, where e is based on the coated
spheres and the number of coated balls = $j^3 (1 - e) \cdot \frac{4}{3} \pi$.
Consequently the total volume of coating is given by,

$$\frac{4}{3} \pi j^3 (1 - e) \cdot \frac{(j_0 - j)}{2} = \frac{4}{3} \pi j^3 (1 - e) \cdot \frac{(j_0 - j)}{2} \cdot \frac{1}{2}$$

By contrast, in a suspension of flocc the volume of organisms = $j^3 (1 - e)$,
where e' is based on centrifuged organisms.

For the coated system to be preferred then the ratio:
volume of flocc / volume of coating ≤ 1
$$\frac{j^3 (1 - e)}{\frac{4}{3} \pi j^3 (1 - e) \cdot \frac{(j_0 - j)}{2}} \leq 1$$

where e' is based on uncoated spheres.

Consider 0.2 cm glass spheres coated with yeast. For systems
that are just fluidised, $e' = 0.8$; $e' = 0.55$ (see Chapter 5).
For the systems to be equivalent, then $0.2^3 (1 - e) = 0.2^3 (1 - e')$
and thus $j_0 = 0.222$ cm. (i.e. coating thickness must be 0.011 cm).

Experiments were performed to check if yeast would attach itself
to ballotini. 0.2 cm. ballotini were placed in a fermenter containing
growing yeast and were left for 3 days. A physically-limited yeast, CEROB,
did not coat the glass balls, but a fermentation-limited yeast, CEROB,
attached well. In the latter case the balls became embedded in a yeast
paste, which, whilst stable, would not give an even flow distribution in a
continuous fermenter. (see Plate 4.1).

In certain situations microbially-coated solids may have an
advantage over free-floating microbial aggregates. The rate of fermentation
may be increased due to improvements in the following factors.
i. Microbial mass and volume, therefore more enzymes.
ii. Exposed surface area.
iii. Diffusion of the substrate and products through the
microbial mass.

FLUIDISATION AND SEDIMENTATION PHENOMENA

5.1 Introduction

The behaviour of microbial aggregates within a liquid will strongly influence the operation of a fermenter. Various factors in fermenter design depend on microbial hydrodynamics. For example, washout rates, microbial concentrations, reaction kinetics, mass transfer and microbial morphology are all controlled to varying degrees by hydrodynamic factors.

Little basic research has been done on microbial fluidisation, sedimentation and associated hydrodynamics. Yet, the successful operation of a tower fermenter, especially, requires a detailed knowledge of these factors. Liquid-solid fluidisation will occur during anaerobic, continuous fermentation and hydrodynamics will influence continuous or batch aerobic operation.

The liquid fluidisation of conventional solids, e.g. ballotini, has been well documented both theoretically and experimentally. Some tentative exploration of three-phase fluidisation has also been made using such materials. Only a few workers have investigated the fluidisation or sedimentation of microbial aggregates. In this chapter fluidisation/ sedimentation will be examined using a wide range of materials, especially microbial ones. It is hoped to illustrate the progression of behaviour from ballotini to yeast flocs^{and} to indicate the important differences in behaviour and why they occur.

5.2 Literature Survey

5.2-1 The behaviour of a single particle in an infinite medium

This represents the most basic situation in particle hydrodynamics, and is probably the most important. The classical and most easily quantified situation is that of a single, smooth and impermeable

sphere settling in a continuous medium. The fluid (in all future cases this is a liquid) exerts a drag force on the sphere given by,

$$F = C_d A \rho U_i^2 / 2 \quad \dots\dots\dots 5.2-1$$

where C_d , R' = drag coefficients & $C_d = 2R'$; ρ = liquid density ;

A = surface area of sphere ; U_i = sphere-liquid relative velocity.

The drag force relationship for this situation is shown in Fig,

5.1. Empirical equations have been deduced at various times to cover the distinctive Reynolds No. ranges.

For region (a), $Re_p < 0.2$

This is the Stokes laminar region. Stokes (1851) found that,

$$F = 3\pi \mu d U_i \text{ and that } R' / \rho U_i^2 = 12 / Re_p \quad \dots\dots\dots 5.2-2$$

For region (b), $0.2 < Re_p < 500$

In this transition region several empirical equations have been proposed. Goldstein (1929) suggested the power series,

$$R' / \rho U_i^2 = \frac{12}{Re_p} \left(1 + \frac{3}{16} Re_p - \frac{19}{1280} Re_p^2 + \frac{71}{20480} Re_p^3 \right) \dots\dots\dots 5.2-3$$

Schiller and Naumann (1933) quoted an equation,

$$R' / \rho U_i^2 = \frac{12}{Re_p} \left[1 + 0.15 Re_p^{0.687} \right] \dots\dots\dots 5.2-4$$

This was used in section 3.4-4 to evaluate pellet densities from settling data .

Allen (1900) quoted $\frac{R'}{\rho U_i^2} = \frac{K}{Re_p^{0.5}} \quad \dots\dots\dots 5.2-5$
Region (c), $500 < Re_p < 2 \times 10^5$

This is the Newton region where the drag coefficient has a constant value. $R' / \rho U_i^2 = 0.22$

Region (d), $Re_p > 2 \times 10^5$

In this very turbulent region boundary layer separation occurs very late around the sphere and thus the drag force is reduced to a value given by , $R' / \rho U_i^2 = 0.05$. These equations apply to a smooth sphere where the drag forces are strongly influenced by the behaviour of the boundary layer between the sphere and the liquid bulk.

FIG51 FRICTION FACTOR FOR SPHERES

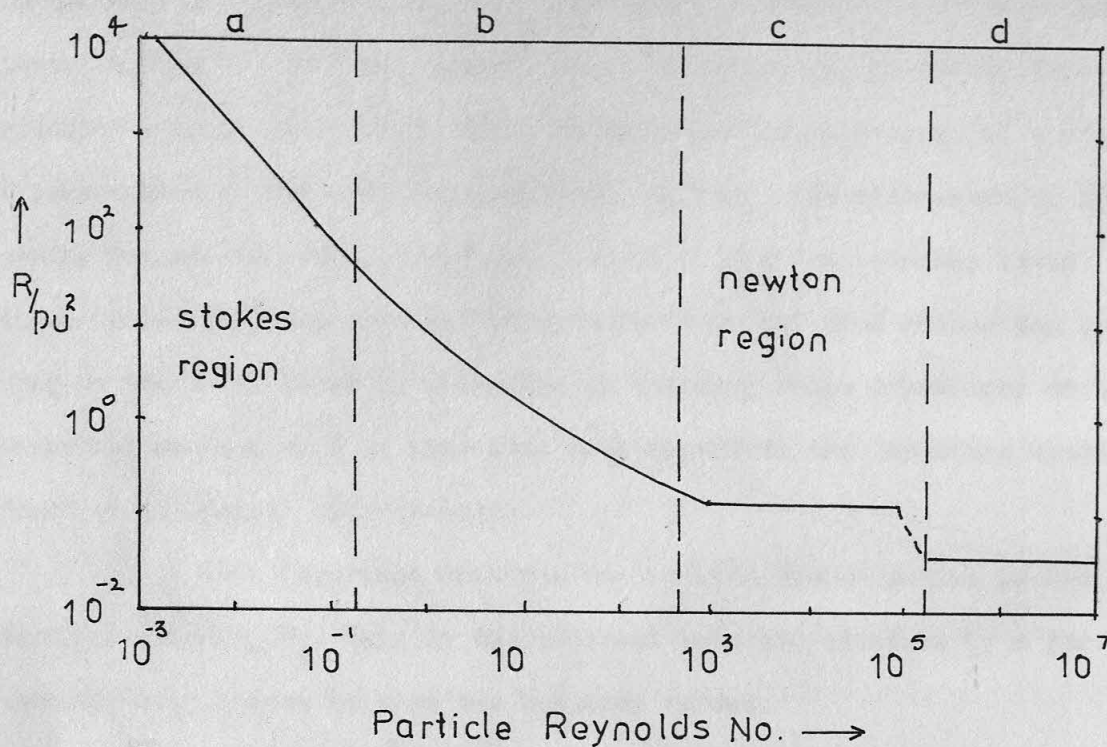
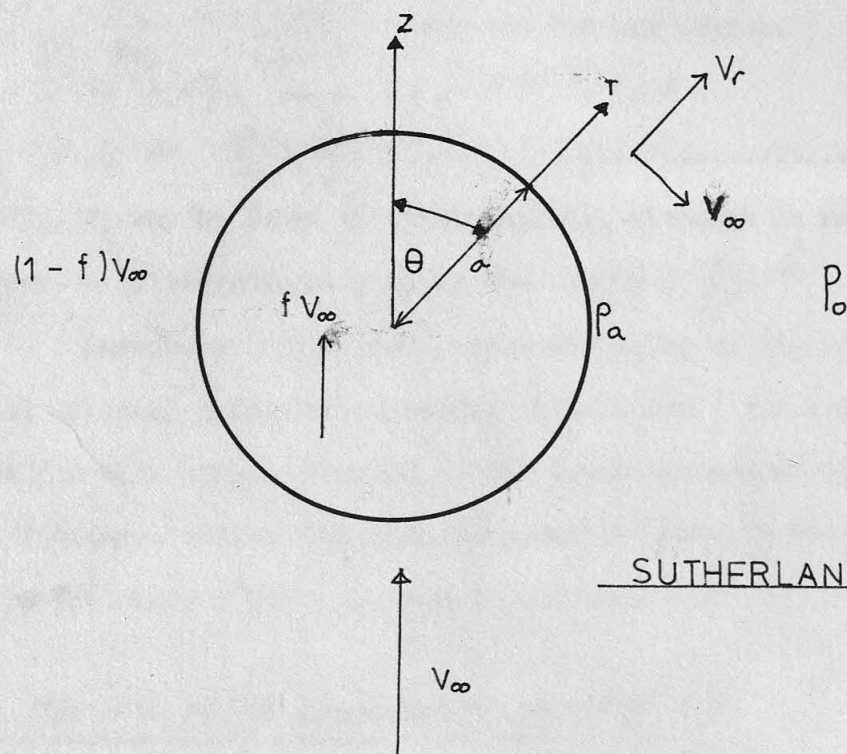


FIG52 POROUS SPHERE



SUTHERLAND-TAN MODEL

At very low Re_p the drag force is mainly due to skin friction as the boundary layer does not separate from the sphere. This situation alters as the velocity increases as there is a greater tendency for the boundary layer to separate from the sphere, with the formation of eddies. This gives rise to an increasing dominance of so-called form drag and a rapid disappearance of any skin drag. However, at very high velocities or if the sphere surface is rough, turbulence occurs within the boundary layer which tends to retard boundary layer separation and thus reduce the total drag on the body. Later in this Chapter the drag force dependency on body shape and surface will be discussed with regard to the imperfect systems found in biological hydrodynamics.

A most important criteria in particle hydrodynamics is the terminal velocity, U_t . This is the constant velocity attained by a particle when the drag forces balance the buoyancy forces.

$$\text{Thus, } C_d \frac{\pi d^2}{4} \rho \frac{U_t^2}{2} = \frac{\pi d^3}{6} (\rho_s - \rho) g$$

$$\therefore U_t^2 = \frac{4}{3} (\rho_s - \rho) g d / \rho C_d \quad \dots\dots\dots 5.2-6$$

Hence, by substituting the value of C_d for each region, U_t may be found.

$$\text{e.g. } \frac{R'}{\rho U_t^2} = \frac{12}{Re_p} = \frac{12 \mu}{U_t d \rho} \quad \text{for the laminar region.}$$

$$\therefore R' = 12 \mu / d \quad \text{and } C_d = 24 \mu / d$$

$$\therefore U_t = \frac{d^2 g (\rho_s - \rho)}{18 \mu} \quad \dots\dots\dots 5.2-7$$

Similarly, U_t may be found in other regions, although in region (b) it is necessary to solve indirectly using the function $\frac{R'}{\rho U^2} Re^2$.

Ladenburg (1907) stated that the value of the calculated terminal velocity should be corrected by a factor $(1 + 2.4d/D)$ to account for wall effect. Heywood (1948) investigated non-spherical particles and introduced a volume factor, K , to quantify them. Particle volume was given by Kd^3 where d was a projected diameter.

5.2-2 The case of the single porous particle

The porosity of microbial aggregates was discussed in Chapters 3 & 4. Clearly, any study of microbial hydrodynamics must take into account the flow of liquid relative to such porous particles.

One of the most important factors concerns the immobility of any interstitial liquid in the aggregate. Flocs and pellets contain large amounts of associated liquid and have a very loose structure. This is clear from the discussion on flocs and floc models in Chapter 4. Clearly there must be a structural configuration which is so loose and open that the occluded liquid ceases to be immobile. However, no clear quantitative criteria for this condition has been found.

Eirich and Mark (1937) investigated the settling behaviour of drilled spheres and wire-mesh bodies and deduced that the internal liquid was immobile. Sutherland and Tan (1970) attempted to produce a theoretical model of a sedimenting porous sphere. Their argument was that as a pressure drop existed across a falling sphere, then some internal flow could occur. By using Darcy's Law for the internal flow and Stokes creeping flow equations for the external liquid and equating the pressure distributions around the sphere predicted by these equations, then a permeability factor could be found. This situation is illustrated in Fig. 5.2. The permeation velocity is given by fV_∞ where $0 < f < 1$.

For the internal flow Darcy's Law gives,

$$p_a = p_o - \left(\frac{\mu}{K} f V_\infty + \rho g \right) a \cos \theta$$
 where K = sphere permeability; p_a = pressure at sphere surface; p_o = pressure in the infinite medium; a = sphere radius.

For the external flow Stokes creeping flow equations were solved to give,

$$\frac{v_r}{V_\infty} = \left[1 - \frac{3}{2} (1-f) \frac{a}{r} + \frac{1}{2} (1-f) \left(\frac{a}{r} \right)^3 \right] \cos \theta$$

$$\therefore p_a = p_o - \frac{3\mu V_\infty (1-f) \cos \theta}{2a} - \rho g a \cos \theta$$

By matching the two values of p_a at the sphere surface, then,

$$f = \frac{(3K/2a^2)}{1 + (3K/2a^2)} \dots\dots\dots 5.2-8$$

$$\text{and } U_t = 2(\rho_s - \rho)ga^2/9(1-f)\mu \dots\dots\dots 5.2-9$$

Thus, the criteria, f , provided a measure of the deviation of a porous sphere's behaviour from that of a solid body.

They used Brinkman's (1957) equation to evaluate the floc permeability, K . For very loose and open flocs they calculated that $f=0.062$

At very low Re the drag force is mainly due to skin friction as the boundary layer does not separate from the sphere. This situation alters as the velocity increases as there is a greater tendency for the boundary layer to separate from the sphere, with the formation of eddies. This gives rise to an increasing dominance of so-called form drag and a rapid disappearance of any skin drag. However, at very high velocities or if the sphere surface is rough, turbulence occurs within the boundary layer which tends to retard boundary layer separation and thus reduce the total drag on the body. Later in this Chapter the drag force dependency on body shape and surface will be discussed with regard to the imperfect systems found in biological hydrodynamics.

A most important criterion in particle hydrodynamics is the terminal velocity, U_t . This is the constant velocity attained by a particle when the drag forces balance the buoyancy forces.

$$\text{Thus, } C_D \frac{\pi a^2 \rho U_t^2}{2} = \frac{4}{3} \pi a^3 (\rho_s - \rho) g$$

$$U_t^2 = \frac{4a(\rho_s - \rho)g}{3C_D \rho}$$

Hence, by substituting the value of C_D for each region, U_t may be found.

$$\text{e.g. for the laminar region, } C_D = \frac{24}{Re} = \frac{24\mu}{aU_t\rho}$$

$$U_t^2 = \frac{a^2(\rho_s - \rho)g}{6\mu}$$

Similarly, U_t may be found in other regions, although in region (v) it is necessary to solve indirectly using the function $\frac{K}{U_t}$.

Ladenburg (1907) stated that the value of the calculated

terminal velocity should be corrected by a factor $(1 + 2.46/D)$ to

account for wall effect. Heywood (1948) investigated non-spherical particles and introduced a volume factor, K , to quantify them. Particle volume was

given by Kd^3 where d was a projected diameter.

5.2-2 The case of the single porous particle

The porosity of microbial aggregates was discussed in Chapters 3 & 4. Clearly, any study of microbial hydrodynamics must take into account the flow of liquid relative to such porous particles.

i.e. the velocity through the floc was about 6% of the approach velocity. On the basis of these calculations they concluded that the interstitial floc liquid may be regarded as immobile.

Their analysis used Stokes creeping flow equations and therefore restricted the applicability of their results to laminar flow situations. However, the main difficulty with this approach was that it used equations for flow around impermeable spheres for a situation where flow was occurring through the sphere. By directly substituting $(1-f)V_\infty$ for V_∞ in the Stokes equations they satisfied their boundary condition that $V_r = fV_\infty$ when $r=a$. However, this substitution may not be physically valid. By using the Stokes equation in this manner the rest of the analysis and its conclusions becomes questionable. Whilst the approach to the problem was interesting the model raised many questions and its quantitative aspects were thus suspect. There exists no direct evidence that flow occurs through a porous aggregate during settling. However, the evidence that it does not is far from satisfactory.

Traditionally, the convenient view has been that internal flow may be neglected. In this thesis this view will be taken. However, it is taken with the reservation that the possibility of internal flow in certain situations cannot be overlooked. Much more research in this area is required to solve this fundamental problem.

5.2-3 The effects of polymers on liquid - solid drag forces

In certain of the systems to be discussed biological polymers may be present (on the surface of the particle). These polymers are essentially polysaccharides, with associated inorganic molecules such as Sulphur. The presence of these molecules in the cell walls of yeasts and *A. Niger* has been confirmed by other workers (Robson, 1957). This was exhibited most clearly by mustard seeds, which could become covered in a sticky, sulphurous coating. The presence of this coating is shown in Plate 5.1. Its effect was to reduce the terminal velocity of the particle,

presumably by causing an increase in the drag force exerted by the liquid. Thus, most biological particle suspensions may be subject to this effect.

Now, James et alia (1970), (1971) investigated the drag on a circular cylinder in solutions of polyoxethylene. Cylinders of 0.015 to 0.036 cm. diameter were placed in a rotating fluid and the drag forces on them measured. The results are shown in Fig. 5.4. They show that for $Re_p > 2$ (i.e. turbulent flow), the drag force on the cylinder was greater than for a non-polymeric solution. Increasing polymer concentration increased this effect. Their data covered the range $2 < Re_p < 200$, but appeared almost independent of Reynolds No. Clearly, similar effects might occur with settling particles.

Polymeric drag effects have been observed in pipe flow by many workers. It was first noted by Toms (1948) and since then many people have reported similar effects notably Patterson et alia (1969), Zakin et alia (1972), Liaw et alia (1971) and McMillan et alia (1971). Basically, polymeric solutions flowing in pipes exert less drag in the turbulent regime ($Re > 2000$) than polymer-free liquids. However, in laminar flow situations this is reversed to give greater drag forces. (See Fig. 5.3).

Polyoxethylene was again generally used, although soap solution gave similar results. The viscoelastic behaviour of the polymer chain and soap micelles are thought to be responsible for this effect. The additives affect the turbulence in the boundary layer between the pipe wall and the liquid.

In passing it is noted that fish are also covered in a sticky polysaccharide material. This coating may be a natural buoyancy mechanism and it is possible that at high velocities the polymer reduces the drag to assist the fish through the water.

The presence of polymers and their effects will be discussed later in the mustard seed results section.

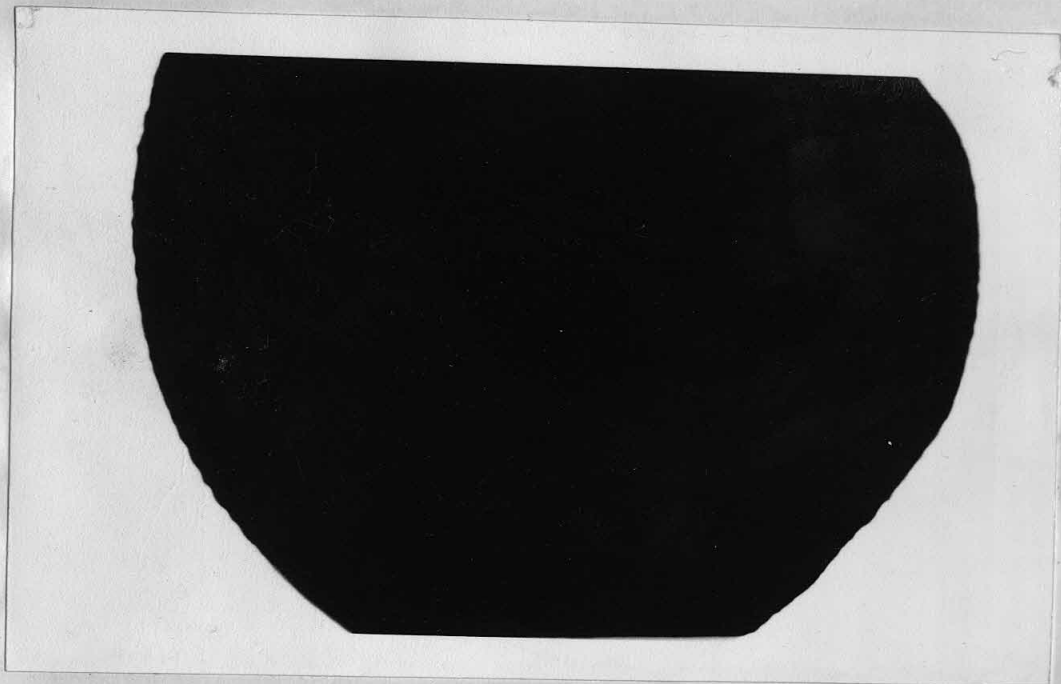
i.e. the velocity through the flow was about 1/2 of the approach velocity. On the basis of these calculations they concluded that the interstitial flow could be regarded as immobile. Their analysis used Stokes creeping flow equations and therefore restricted the applicability of their results to laminar flow situations. However, the main difficulty with this approach was that it used equations for flow around impermeable spheres for a situation where flow was occurring through the sphere. By directly substituting $(1-1/2)V_\infty$ for V_∞ in the Stokes equations they satisfied their boundary condition that $V_r = 0$ when $r = 0$. However, this substitution may not be physically valid. By using the Stokes equation in this manner the rest of the analysis and its conclusions becomes questionable. Whilst the approach to the problem was interesting the model raised many questions and its quantitative aspects were thus suspect. There exists no direct evidence that flow occurs through a porous aggregate during settling. However, the evidence that it does not is far from satisfactory. Traditionally, the convenient view has been that internal flow may be neglected. In this thesis this view will be taken. However, it is taken with the reservation that the possibility of internal flow in certain situations cannot be overlooked; Much more research in this area is required to solve this fundamental problem.

5.2-3 The effects of polymers on liquid - solid drag forces

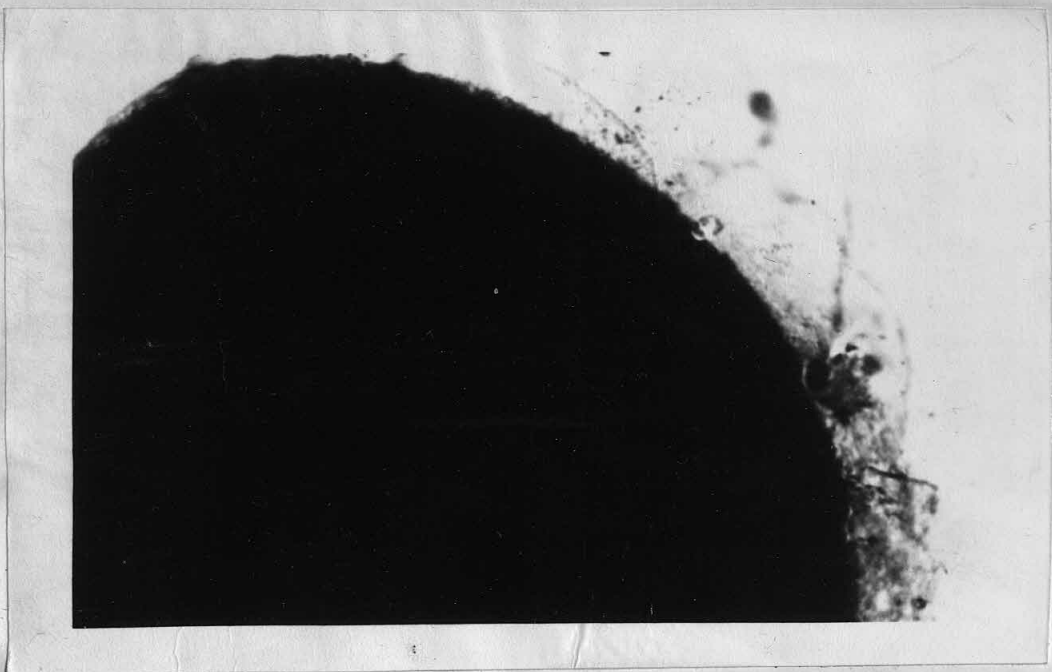
In certain of the systems to be discussed biological polymers may be present (on the surface of the particle). These polymers are essentially polysaccharides, with associated inorganic molecules such as sulphur. The presence of these molecules in the cell walls of yeasts and A. niger has been confirmed by other workers (Robson, 1977). This was exhibited most clearly by mustard seeds, which could become covered in a sticky, sulphurous coating. The presence of this coating is shown in Plate 1.1. Its effect was to reduce the terminal velocity of the particle.

PLATE 5.1 MUSTARD SEEDS

(a) UNCOATED SEED



(b) COATED SEED



presumably by causing an increase in the drag force exerted by the liquid. Thus, most biological particle suspensions may be subject to this effect.

Now, James et alia (1970), (1971) investigated the drag on a circular cylinder in solutions of polyoxethylene. Cylinders of 0.015 to 0.036 cm. diameter were placed in a rotating fluid and the drag forces on them measured. The results are shown in Fig. 5.4. They show that for $Re > 2$ (i.e. turbulent flow), the drag force on the cylinder was greater than for a non-polymeric solution. Increasing polymer concentration increased this effect. Their data covered the range $2 < Re < 800$, but appeared almost independent of Reynolds No. Clearly, similar effects might occur with settling particles.

Polymeric drag effects have been observed in pipe flow by many workers. It was first noted by Toms (1948) and since then many people have reported similar effects notably Patterson et alia (1969), Zakin et alia (1972), Law et alia (1977) and McMillan et alia (1977). Basically, polymeric solutions flowing in pipes exert less drag in the turbulent regime ($Re > 2000$) than polymer-free liquids. However, in laminar flow situations this is reversed to give greater drag forces. (See Fig. 5.3).

Polyoxethylene was again generally used, although soap solution gave similar results. The viscoelastic behaviour of the polymer chain and soap micelles are thought to be responsible for this effect. The additives affect the turbulence in the boundary layer between the pipe wall and the liquid. In passing it is noted that fish are also covered in a sticky polysaccharide material. This coating may be a natural buoyancy mechanism and it is possible that at high velocities the polymer reduces the drag to assist the fish through the water. The presence of polymers and their effects will be discussed later in the mustard seed results section.

FIG.53 DRAG REDUCTION IN PIPES

from Zakin et al [1972]

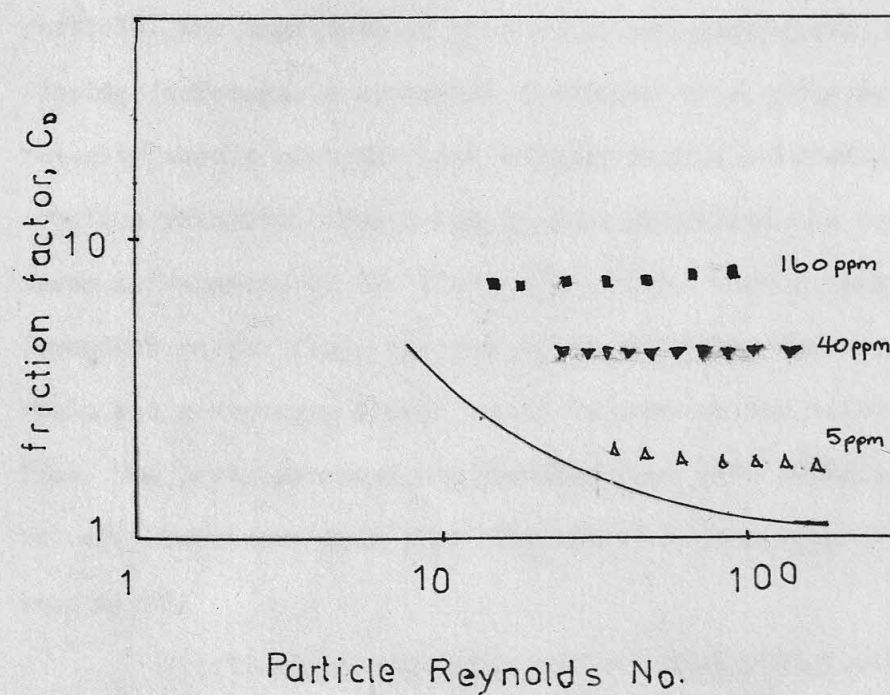
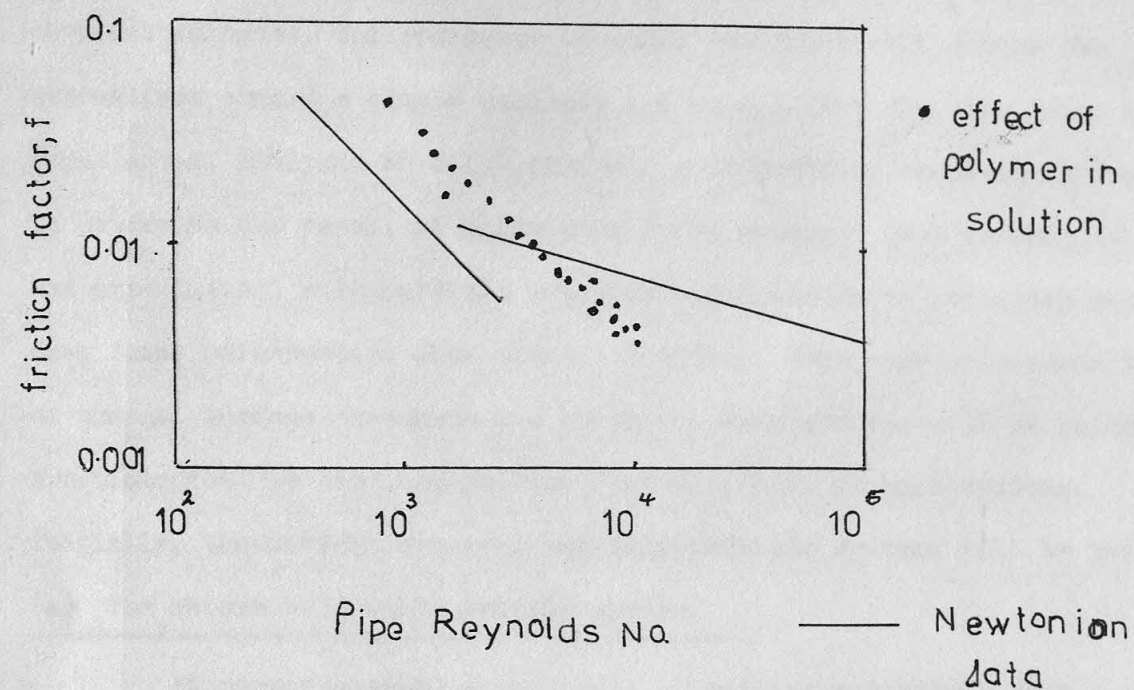


FIG.54 DRAG INCREASE FOR SPHERES

from James et al [1971]

5.2-4 Non-Biological Multiparticle Systems

5.2-4.1 Theoretical concepts

The previous three sections have discussed the behaviour of various single particle systems and have indicated the factors governing terminal velocity. The presence of other particles will change the streamlines around a single particle and thus affect the drag force it experiences. Analysis of fluidisation / sedimentation phenomena attempts to determine the result of these drag force changes. Most theoretical and experimental multiparticle research has considered particles whose drag force relationships obey classical theory. Thus, particle porosity or unusual surface phenomena are excluded. Such systems will be called non-biological to distinguish them from microbial or seed systems. Initially, theoretical concepts for multiparticle systems will be reviewed.

(a) The nature of a multiparticle system

At corresponding superficial velocities a particle in a multiparticle bed experiences a much greater drag force than an isolated particle. The magnitude of this difference increases as the particle spacing decreases. A suspension fluidised by a given upward superficial velocity should have the same voidage as one sedimenting with the same settling velocity. When a bed is just fluidised the particle buoyancy force is balanced by the fluid drag force. Then a particle becomes dependent on the fluid and not other particles for support, and the whole bed rearranges itself so as to present the least resistance to the flow. The particles separate further from each other as the flow velocity increases such that the buoyancy-drag force equilibrium is maintained.

Fluidisation mechanics indicate that concentration differences cannot exist in a bed of uniform particles. Hence, the bed is evenly distributed and stable. However, in a bed of non-uniform particles stratification will occur such that the particles with the least mass

rise to the top of the bed. Such stratification may cause concentration gradients in a bed.

(b) The quality of fluidisation

The mechanisms by which a fluidised bed is formed differ according to such characteristics as particle size, fluid-particle density difference and fluid properties. Gas-solid systems are generally "Aggregative" in that large discontinuities such as bubbles exist within the bed. These aggregative systems may be found in liquid-solid beds, also. They occur when there is a large density difference between the solid and the liquid phases, e.g. lead shot and water. "Particulate" systems are usually found in liquid-solid beds, although they can be made to occur with special gas-solid beds.

The criteria for distinguishing between these types is the Froude No., Fr , measured at the minimum fluidisation velocity, U_{mf} , which is the velocity at which the bed just fluidises.

$$\text{For Particulate beds, } Fr = U_{mf}^2 / gd < 1 \dots \dots \dots 5.2-10$$

$$\dots \text{ Aggregative } \dots \dots \dots > 1 \dots \dots \dots 5.2-12$$

Particulate systems are the ones of most interest in this study. They can exist either as beds of little motion or else may exhibit much particle motion. Generally, very low density differences between particle and fluid gives the former type.

Beds expand in a discontinuous manner because the particles on the top of the bed must move considerably further than those near the bottom. Expansion can have 3 basic modes which are,

- i. Particles fluidising progressively from the top downwards.
- ii. The bed rising en-masse and particles falling from the bottom until stability is reached.
- iii. Channels in the bed causing particles to rise up, with the rest of the bed subsiding into the gaps.

(c) Pressure Drop

The pressure drop in a fluidised bed is constant for all

velocities $> U_{mf}$. The general pressure drop relationship is shown in Fig. 5.5. Such curves may be used experimentally to determine U_{mf} as shown. Variations in packing mode can cause variations in the packed bed section of the curve.

In a fluidised bed the pressure drop equals the apparent wt. of the bed, thus, $\Delta P/\text{unit area} = (1-e)(\rho_s - \rho)Lg$ 5.2-11

(d) Minimum Fluidisation Velocity, U_{mf}

When this velocity is reached the bed passes from a packed to a fluidised state. For many uniform systems the transition is a sharp one, but for some, especially non-uniform ones, the distinction is not so apparent.

A basic approach is illustrated by Coulson & Richardson (1966). By using the Carmen-Kozeny equation for a packed bed and the pressure drop relationship for a fluidised bed they obtained,

$$\Delta P = (1-e)(\rho_s - \rho)Lg = 180 \mu S^2 L U_{mf}^2 (1-e)^2 / e^3$$

where S = surface area / unit volume of particles = $6/d$ for spheres

$$\text{For spheres, } U_{mf} = \frac{0.0055 e_{mf}^3 d^2 (\rho_s - \rho) g}{(1 - e_{mf}) \mu} \dots \dots \dots 5.2-12$$

The value of U_{mf} will therefore depend on the value of e_{mf} which is chosen.

(i.) Davidson & Harrison Model, (1963)

$$\text{This assumed } e_{mf} = 0.476, \therefore U_{mf} = \frac{0.0044 g d^2 (\rho_s - \rho)}{\mu} \dots \dots \dots 5.2-13$$

(ii.) Rowe Model, (1961)

By measuring the drag force on a sphere in an array of spheres Rowe found that drag on sphere in array / drag on isolated sphere = 68.5, at the minimum fluidisation velocity.

$$\text{Now, } C_{dt} \frac{\pi d^2 \rho U_t^2}{4} = C_{dmf} \frac{\pi d^2 \rho U_{mf}^2}{4}$$

which equates the drag forces experienced by a particle at its terminal velocity and when it just fluidises. For C_d values measured at the same Reynolds No., $C_{dmf} / C_{dt} = U_t^2 / U_{mf}^2 = 68.5$ 5.2-14

He then used a graphical approach of plotting $C_d Re_p^2$ vs. Re_p for spheres and solving for U_{mf} . He also presented an equation based on laminar flow which simply modifies the Davidson-Harrison constant from

0.00114 to 0.00081.

The Carmen-Kozeny equation used earlier is applicable to fine particles.

For large particles the Ergun equation (1952) may be used thus,

$$\frac{\Delta P}{L_{mf}} = \frac{150(1-e_{mf})^2 \mu U_{mf}}{d^2 e_{mf}^3} + \frac{1.75(1-e_{mf}) \rho U_{mf}^2}{e_{mf}^3 d}$$

Again, comparing with the fluidised bed equations for pressure drop

and substituting $Re_{mf} = U_{mf} d \rho / \mu$ and Galileo No.; $Ga = \rho(\rho_s - \rho)gd^3/\mu^2$

$$\text{then } Ga = \frac{150(1-e_{mf})}{e_{mf}^3} Re_{mf} + 1.75 \frac{Re_{mf}^2}{e_{mf}^3}$$

$$\text{Thus for } e_{mf} = 0.4, Re_{mf} = 25.7 \left(\sqrt{1 + 5.53 \times 10^{-5} Ga} - 1 \right) \dots \dots \dots 5.2-15$$

(iii.) Wen & Yu Model, (1966)

By using a particle shape factor instead of a direct value of e_{mf} , Wen & Yu obtained, $Re_{mf} = \sqrt{33.7^2 + 0.041 Ga} - 33.7 \dots \dots \dots 5.2-16$

All methods reviewed equate pressure drops in this manner. The disadvantage is that a value of e_{mf} has to be known or assumed. Thus, calculated values of U_{mf} are only approximately correct.

(e) The analysis of an expanded bed or settling suspension

The criteria for minimum fluidisation velocity has been established, but it does not indicate how the bed will behave once U_{mf} is exceeded. Fluidised or sedimenting suspensions may be characterised by measuring the superficial liquid flow rates or particle settling rates and comparing these with the voidage of the suspension. This gives a measure of the drag force variations with voidage and particle-fluid velocities. This data may be used to calculate the "voidage function" for the system.

In a fluidised bed of uniform particles the voidage is constant throughout the entire bed volume. Similarly, in a settling suspension of uniform particles the voidage is constant and equal to that at the onset of settling. However, where the suspension is not uniform and especially in flocculent systems, it is possible to have zones of different concentration. This is shown in Fig. 5.6.

FIG.55 PRESSURE DROP IN
FLUIDISED BEDS

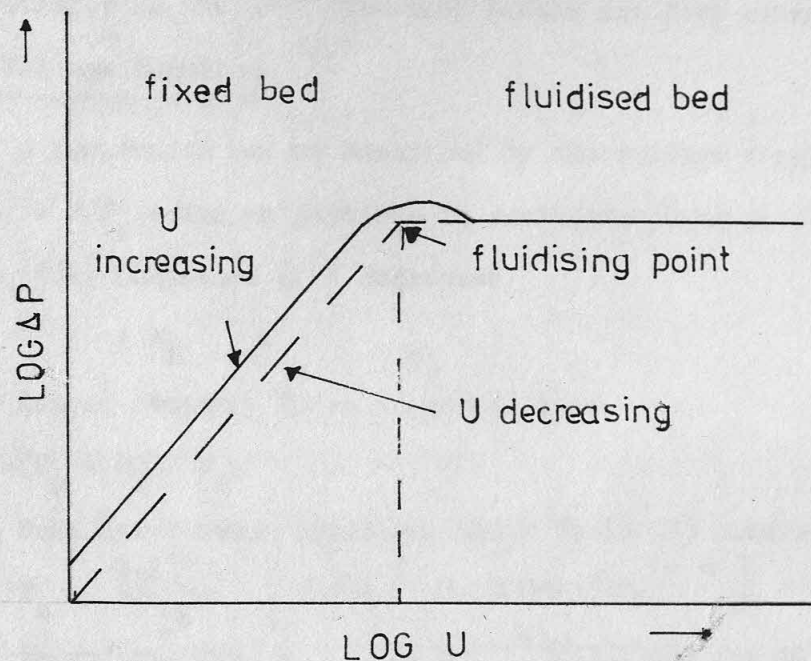
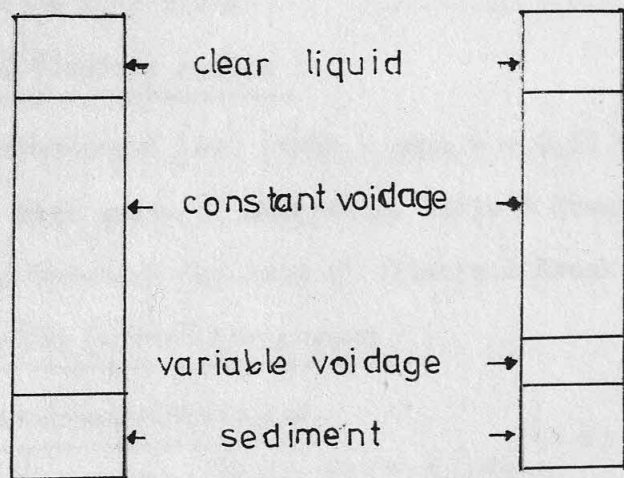


FIG.56 BATCH SETTLING



The Carman-Kozeny equation used earlier is applicable to fine particles.

For large particles the Ergun equation (1952) may be used thus,

$$\frac{\Delta P}{L} = \frac{150(1-e)^2}{e^3} \frac{U}{d_p^2} + \frac{1.75(1-e)}{e^3} \frac{U^2}{d_p}$$

Again, comparing with the fluidised bed equations for pressure drop

$$\text{then } G = \frac{150(1-e)^2}{e^3} \frac{U}{d_p^2} + 1.75 \frac{U^2}{d_p}$$

$$\text{Thus for } e_{mf} = 0.4, Re_{mf} = 22.7 \left(\sqrt{1 + 2.2 \times 10^{-5} G^2} - 1 \right) \dots \dots 2.2-12$$

(iii.) Wen & Yu Model, (1966)

By using a particle shape factor instead of a direct value of

$$e_{mf}, \text{ Wen \& Yu obtained, } Re_{mf} = \sqrt{33.7 + 0.041 G^2} - 33.7 \dots \dots 2.2-13$$

All methods reviewed equate pressure drops in this manner. The disadvantages

is that a value of e_{mf} has to be known or assumed. Thus, calculated values

of U_{mf} are only approximately correct.

(e) The analysis of an expanded bed or settling suspension

The criteria for minimum fluidisation velocity has been

established, but it does not indicate how the bed will behave once U_{mf}

is exceeded. Fluidised or sedimenting suspensions may be characterised by

measuring the superficial liquid flow rates or particle settling rates

and comparing these with the voidage of the suspension. This gives a

measure of the drag force variations with voidage and particle-fluid

velocities. This data may be used to calculate the "voidage function"

for the system.

In a fluidised bed of uniform particles the voidage is constant

throughout the entire bed volume. Similarly, in a settling suspension of

uniform particles the voidage is constant and equal to that at the onset

of settling. However, where the suspension is not uniform and especially

in flocculent systems, it is possible to have zones of different

concentration. This is shown in Fig. 56.

The upper zone remains at the original voidage and thus its settling rate is unaffected by the lower zone. However, once this zone merges into the lower ones the constant settling rate ceases and the bed settles with a varying velocity as the particles consolidate and floc structure breaks up.

(1.) The Voidage Function

A suspension may be described by the voidage function, $f(e)$, where $f(e) = F/F_s$ = drag on particle in suspension/drag on isolated particle. Generally, $f(e)$ increases as e decreases.

Now, $F + F_b = F_g$
drag force + buoyancy force = gravity force

and $f(e) = (F_g - F_b) / F_s$;

Using the Schiller-Naumann equation, Wen & Yu (1966) obtained,

$$F_s = \frac{\pi d^2 \rho U^2}{9} \left[3 Re_p^{-1} + 0.45 Re_p^{-0.31} \right]$$

therefore, $f(e) = \frac{Ga}{18 Re_p + 2.7 Re_p^{1.687}}$ for $10^{-3} < Re_p < 10^3$

Now, $f(e) = U_t / U$; and their data for glass and steel balls fluidised in water showed that, $U / U_t = e^{4.7}$

Hence, $e^{4.7} Ga = 18 Re_p + 2.7 Re_p^{1.687}$

Several workers have found that the voidage function takes the form

$$f(e) = U_t / U = e^{-n} \quad \dots\dots\dots 5.2-17$$

For $Re_{pt} < 0.2$ (laminar region)

Richardson & Zaki (1954) gave $n = 4.65$ based on their many tests with a wide range of materials. Lewis & Bowerman (1952) quoted a similar value based on the data of Wilhelm & Kwauk (1948)

For $0.2 < Re_{pt} < 500$ (transition region)

Richardson-Zaki Model

$$\text{For } 0.2 < Re_{pt} < 1 \quad n = \left(4.35 + 17.5 \frac{d}{D} \right) Re_{pt}^{-0.03} \quad \dots\dots\dots 5.2-18$$

$$\dots\dots 1 < \dots\dots < 200 \quad n = \left(4.45 + 18 \frac{d}{D} \right) Re_{pt}^{-0.1} \quad \dots\dots\dots 5.2-19$$

$$\dots\dots 200 < \dots\dots < 500 \quad n = 4.45 Re_{pt}^{-0.1} \quad \dots\dots\dots 5.2-20$$

Lewis & Bowerman quoted $n = 3.37$

For $Re_{pt} > 500$ (turbulent region)

For this region Lewis & Bowerman gave $n = 2.5$

Richardson & Zaki gave $n = 2.39$ 5.2-21

The latter also gave a correction term to account for the effect of the container on the terminal velocity. This was,

$$\log U' = \log U_t - d/D \quad \dots\dots\dots 5.2-22$$

where U' = the corrected value for the terminal velocity, U_t .

Happel Model

Happel (1958), Happel et alia (1954, 1957) developed a "Free Surface" model for laminar flow systems. His model was

$$U / U_t = \frac{3 + \frac{3}{2}(1-e)^{1/3} + \frac{3}{2}(1-e)^{5/3} - 3(1-e)^2}{3 + 2(1-e)^{5/3}} \quad \dots\dots\dots 5.2-23$$

It was based on two concentric spheres. The inner one represented a particle in a suspension. The outer sphere had a frictionless surface and the annular volume between the two was controlled by the volume of fluid / volume of particles in the bed, at a given condition. All disturbances were confined within the boundaries of the outer shell and thus a closed solution of the Navier-Stokes equation could be obtained. The solution results in the equation above which gave good experimental agreement for low voidage ($0.2 < e < 0.6$) systems, but was not so accurate for $0.6 < e < 0.95$.

Brinkman's Model

By considering a sphere embedded in a porous mass where the flow obeyed Darcy's Law, Brinkman (1947) obtained

$$U / U_t = 1 + \frac{3}{4}(1-e) \left[1 - \sqrt{\frac{8}{1-e} - 3} \right] \quad \dots\dots\dots 5.2-24$$

Obviously, the model was not rigorous because when $e = 0.33$ there can be no flow, i.e. $U / U_t = 0$.

Steinour Model

An early empirical correlation was that of Steinour (1944).

On the basis of many sedimentation tests he stated,

$$U / U_t = e^2 10^{-1.82(1-e)} \quad \dots\dots\dots 5.2-25$$

From a continuation of earlier work, Richardson & Mielke (1961) stated that for values of $e < 0.78$ then,

$$U / U_t = \frac{e^3}{6.72 (1-e)} \dots\dots\dots 5.2-26$$

Hawksley Model

Hawksley (1950) developed an equation which considered the viscosity of the suspension to be an important factor. By using the Vand (1948) equation for the viscosity of a suspension of particles, Hawksley deduced that

$$U / U_t = e^2 \exp \left(\frac{-2.5 (1-e)}{0.61 e^{0.39}} \right) \dots\dots\dots 5.2-27$$

Loeffler & Ruth Model

The settling of glass spheres was examined by them in 1959 and they stated, $U / U_t = \left(\frac{1}{e} + \frac{5.7 (1-e)}{e^3} \right)^{-1} \dots\dots\dots 5.2-28$

Oliver's Model

Oliver (1961) used Stokes stream function for a single sphere to examine the voidage function. He deduced that settling velocities were more dependent on concentration than had been previously thought. The model was, $U / U_t = e (1 - K (1-e)^{1/3}) \dots\dots\dots 5.2-29$ He thought that non-uniform suspensions were responsible for the large variation in settling results which have been found by various workers.

A different approach was adopted by Kynch (1952). This considered the effect of particle flux, j_{fs} , and solids concentration, $(1-e)$, on the sedimentation. This approach was expanded by Wallis (1969). He stated that three types of batch settling curves are possible. These are controlled by the j_{fs} vs. $(1-e)$ curves.

Type 1 would occur with uniform suspensions, where the initial voidage zone settles directly into the final sediment. Type 2 curves resemble non-uniform suspensions where various compaction zones exist; (see Fig. 5.6). The settling behaviour was explained in terms of shock waves propagating through the suspension.

(2) The Equivalent Bubble Size Model

Harrison et alia (1961) examined the differences between

aggregative and particulate beds and attempted to explain these in terms of bubble stability. They calculated the rate of rise of a bubble in a fluidised bed using a modified Davies-Taylor equation (for gas bubbles in liquids). Thus,

$$U = 0.711 g^{1/2} D_e^{1/2} \left(\frac{1 - e_{mf}}{\frac{\rho_s}{\rho_s - \rho} - e_{mf}} \right)^{1/2} \dots\dots\dots 5.2-30$$

Now, the bubble remains stable if particles are carried in its wake and therefore, $U \geq U_t$. The maximum stable bubble size is when $U = U_t$. Now, using an expression for U_t derived by Rubey (1933) then,

$$D_e / d = \pi \cdot 3 \left(\frac{U_t^2}{g d^3 \rho^2} \right) \left(\frac{\rho_s}{\rho_s - \rho} - e_{mf} \right) \left[\left(1 + \frac{9 d^3 \rho (\rho_s - \rho)}{54 \mu^2} \right)^{1/2} - 1 \right] \dots\dots\dots 5.2-31$$

Thus, when $D_e / d \leq 1$; fluidisation is particulate (liquid-solid)

$\dots\dots > 10$; $\dots\dots\dots$ aggregative (gas-solid)

$1 < \dots\dots < 10$; transition region, occurs with both systems.

A large d or $(\rho_s - \rho)$ may cause aggregative behaviour in otherwise particulate liquid systems.

(3) The Rowe Stability Criteria

An alternative approach to the investigation of bed stability was adopted by Rowe (1961). By considering the drag force on a sphere in an assembly of spheres, he found for his hexagonal array:

$$\alpha = \frac{0.68}{\delta} + 1 \dots\dots\dots 5.2-32$$

where $\alpha = F_x / F_\infty$; $\delta = x / d$; x = distance between spheres;

F_x = drag on sphere separated by x ; F_∞ = drag on isolated sphere.

From a force balance and using the Schiller - Naumann equation then the

change in velocity, Δu , needed to support a particle when separation

changes by $\Delta \delta$ is given by,

$$\Delta u = \frac{g d^2 (\rho_s - \rho)}{18 \mu (1 + 0.25 Re_p^{0.687})} \frac{0.68 \Delta \delta}{(0.68 + \delta)^2} \dots\dots\dots 5.2-33$$

The ratio $\frac{\Delta u}{\Delta \delta}$ is sensitive to $(\rho_s - \rho)$ when this is small, as is

certainly the case with microbial suspensions. The ratio is insensitive

to Reynolds No. and to particle spacing. For most fluidised systems Δu

is very much bigger than $\Delta \delta$ and consequently the separation of the particles

remains constant and thus concentration gradients in uniform beds should

not exist.

5.2-4.2 Experimental Investigations Into Multiparticle Systems

(a) Fluidisation / Sedimentation of non-flocculent material

The ease of quantifying these systems has led many workers to use them. For brevity, the main investigations into fluidisation and sedimentation using such materials are summarised in Table 5.2.1 .

A useful method of analysis was employed by Richardson & Mielke (1961), who used the technique of Harris (1959), to analyse their fluidisation / sedimentation data. The method considered the suspension to be akin to a packed bed. They used,

$$\psi = \text{friction factor} = \frac{e^3 (\rho_s - \rho) g}{5 \rho U^2} \quad \dots\dots\dots 5.2-34$$

$$Re' = \text{Blake No.} = \frac{U \rho}{\mu (1-e)} \quad \dots\dots\dots 5.2-35$$

where S = specific surface of the solids.

Their data ^{were} correlated by,

$$\psi = 3.36 Re'^{-1} \quad \text{for sedimentation / fluidisation} \quad \dots\dots 5.2-36$$

$$\psi = 5 Re'^{-1} \quad \text{for packed beds.}$$

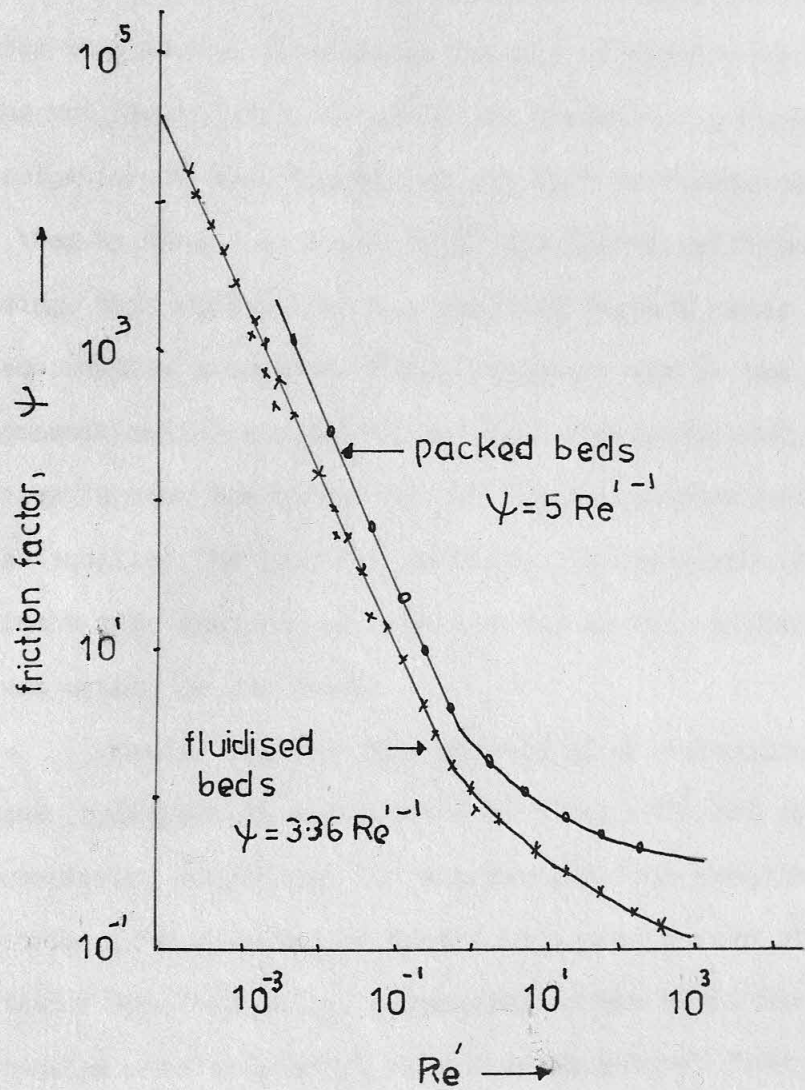
This is shown in Fig. 5.7; the friction factor for dilute suspensions being 30 % less than for packed beds. They further state, contrary to Richardson & Zaki (1954), that suspension density and not liquid density controls suspension hydrodynamics. This was confirmed by studying the settling of a mixture of two particle sizes, having the same U_t , but different densities.

(b) Fluidisation / Sedimentation of flocculent materials

Some of the earliest investigations into multiparticle systems were concerned with suspensions of flocculent material. Coe & Clevenger (1916) noted that with fine, flocculent suspensions the rate of sedimentation decreased with time and that pore flow mechanisms applied to the upward displacement of the supernatant.

One of the most comprehensive investigations into settling was conducted by Steinour (1944). He investigated both flocculent and non-flocculent materials. Tests with flocculent emery powder revealed

FIG 57 RICHARDSON-MIELKE ANALYSIS



(a) Fluidisation / Sedimentation of non-flocculent material

The ease of quantifying these systems has led many workers to use them. For brevity, the main investigations into fluidisation and sedimentation using such materials are summarised in Table 5.2.1. A useful method of analysis was employed by Richardson &

Mielke (1961), who used the technique of Harris (1959), to analyse their fluidisation / sedimentation data. The method considered the suspension

to be akin to a packed bed. They used,

$$\psi = \text{friction factor} = \frac{e}{\rho_s (1 - e)} \frac{g}{U^2}$$

$$Re' = \text{Blake No.} = \frac{U \rho_s (1 - e)}{\mu}$$

where e = specific surface of the solids.

Their data was correlated by,

$$\psi = 3.36 Re'^{-1} \quad \text{for sedimentation / fluidisation} \dots 5.2.3d$$

$$\psi = 5 Re'^{-1} \quad \text{for packed beds.}$$

This is shown in Fig. 5.7; the friction factor for dilute suspensions being 30% less than for packed beds. They further state, contrary to Richardson & Zaki (1954), that suspension density and not liquid density controls suspension hydrodynamics. This was confirmed by studying the settling of a mixture of two particle sizes, having the same U_t , but different densities.

(b) Fluidisation / Sedimentation of flocculent materials

Some of the earliest investigations into multiphase systems were concerned with suspensions of flocculent material. Coe & Clevenger (1916) noted that with time, flocculent suspensions the rate of sedimentation decreased with time and that pore flow mechanisms applied to the upward displacement of the supernatant. One of the most comprehensive investigations into settling was conducted by Steinour (1944). He investigated both flocculent and non-flocculent materials. Tests with flocculent emery powder revealed

that immobile liquid could be present with angular or flocculent material. Angular particles carried attached stagnant fluid, such that volume of liquid / volume of particles = 0.25. He stated that immobile liquid remained in the floc whilst it was settling, but during compaction of the sediment floc structure broke down and liquid flowed through them. For the latter case,
$$U = \frac{0.123 U_t (e-f)^3}{(1-f)^2 (1-e)} \quad \text{cm/s} \dots 5.2-37$$
 where the quantity of immobile liquid / unit particle volume = $f/(1-f)$ and f varied with each flocculent material.

A common flocculent system is Kaolin. Schofield et alia (1954) stated that Kaolin flocculates because of attraction between the positive edges and the negative faces of the hexagonal particles. A preliminary investigation of Kaolin settling was made by Wadsworth et alia (1956) and then by Gaudin et alia (1959). The latter confirmed Steinour's findings that supernatant was expelled through pores whose size decreased as compression proceeded. Their technique was to use X-ray absorption to measure solids concentration. This indicated that a region existed from the top to near the bottom of the suspension that had a constant voidage, which equalled the original voidage. Density gradients within the final sediment were also noted. This was due to the variation in compressive forces acting on the flocs.

Kaolin was also the subject of an investigation by Michaels & Bolger (1962), who, in addition to settling rate and composition measurements, considered the macroscopic floc behaviour. Their floc model consisted of aggregates of flocs. These could form bridges inside the container when the solids concentration was high. The properties of the suspension were related to this floc structure. They found that the total volume fraction of liquid in aggregates was 0.975.

If ϕ = volume fraction, then for Kaolin,

$$\phi_{\text{floc}} / \phi_{\text{aggregate}} = 1/3.8; \quad \phi_{\text{particle}} / \phi_{\text{floc}} = 1/10;$$

$$\phi_{\text{particle}} / \phi_{\text{aggregate}} = 1/38.$$

Thorium oxide, Kaolin and graphite suspensions were examined by Thomas (1963). The particle size range was $0.4 < d < 17 \mu$. In this size range colloidal forces play an important role in floc attraction, and as these forces may be of the same order of magnitude as shear forces they should not be neglected. He estimated that the liquid velocity through the floc was $1/20$ of the liquid velocity around it. However, no explanation of the derivation of this value was given. He quotes a parameter, α = volume of immobile liquid / volume of particles, (> 1). Thus, $\rho_{floc} = \frac{\rho_s + \alpha \rho}{(1 + \alpha)}$; & $U = U_t (1 + \alpha)^3 e^{-5.9(1 + \alpha) \phi_{s,0.5}}$ 5.2-38 The above equation applies to the hindered settling of dilute flocculent suspensions. They were found to be Non-Newtonian and could be correlated using a Bingham plastic model.

The only work on the fluidisation of flocculent aggregates that has come to the author's attention was reported by Henszelmann et alia (1967). They investigated the fluidisation / sedimentation of pigment aggregates and Kaolin, both of which formed aggregates containing a considerable amount of occluded water. This water was assumed to exist as a "liquid hull" (quote). The volume fraction of the hull varied with each pigment, but was constant and unaffected by the fluidisation rate. For Kaolin, $U = \frac{9(\rho_k - \rho) d_a^2 (1 - \frac{C_{ak} \phi_k}{\phi_a})^n}{18 \mu C_{ak}}$ 5.2-39 where ρ_k = density of Kaolin; d_a = aggregate diameter; $C_{ak} = \frac{\phi_a}{\phi_k}$; ϕ_k = volume concentration of Kaolin; U = settling velocity; ϕ_a = aggregate; e_p = volume fraction of pigment.

They used $1 - e_p = A (1 - U / U_t)^{1.5}$ to calculate the value of A . Hence, if ϕ_f = volume of liquid / volume of pigment, then this is found by $A = 0.75 / (\phi_f + 1)$ 5.2-40

The pigments were fluidised and settled in water. It was found that the bed expanded slowly, passed through a maximum after about 40 minutes and then contracted. This was explained in terms of changing aggregate diameter. An aggregate diameter, d_a , was calculated from Stokes

that immobile liquid could be present with angular or flocculent material. Angular particles carried attached stagnant fluid, such that volume of liquid / volume of particles = 0.25. He stated that immobile liquid remained in the floc whilst it was settling, but during compaction of the sediment floc structure broke down and liquid flowed through them. For the latter case, $U = \frac{0.113 U_t (e - 1)^2}{(1 - e)^2}$ 5.2-37 where the quantity of immobile liquid & unit particle volume = $1/(1 - e)$ and e varied with each flocculent material. A common flocculent system is Kaolin. Schofield et alia (1954) stated that Kaolin flocculated because of attraction between the positive edges and the negative faces of the hexagonal particles. A preliminary investigation of Kaolin settling was made by Wahaworth et alia (1956) and then by Gaudin et alia (1959). The latter confirmed Steinhilber's findings that supernatant was expelled through pores whose size decreased as compression proceeded. Their technique was to use X-ray absorption to measure solids concentration. This indicated that a region existed from the top to near the bottom of the suspension that had a constant voidage, which equalled the original voidage. Density gradients within the final sediment were also noted. This was due to the variation in compressive forces acting on the flocs. Kaolin was also the subject of an investigation by Michaels & Bolger (1962), who, in addition to settling rate and composition measurements, considered the microscopic floc behaviour. Their floc model consisted of aggregates of flocs. These could form bridges inside the container when the solids concentration was high. The properties of the suspension were related to this floc structure. They found that the total volume fraction of liquid in aggregates was 0.975.

If ϕ = volume fraction, then for Kaolin,
 $\phi_{floc} = 1/3.8$; $\phi_{particle} = 1/10$;
 $\phi_{aggregate} = 1/38$;

Law. The data presented in the paper indicated that the flocs were very open and contained large amounts of immobile liquid. This was estimated using the volume fraction of liquid in the floc, $A = \phi_f / (\phi_f + 1)$

A summary of their data is shown in Table 5.2.2.

Table 5.2.2 Pigment Properties (Henszelmann et alia)

Material	$d_{agg.}/d_p$	ϕ_f	A	$d_{agg.}, \mu$
Lead chromate	605	56.9	0.983	242
Iron oxide	1170	141.4	0.993	234
Chromium oxide	333	23.5	0.959	100

These very high values for A are similar to those reported for inorganic flocculent material by Thomas (1963) and Tambo (1967) whose work was discussed earlier in Chapter 3.

(c) Stratification Investigations

The criteria for stratification has been established by Wen & Yu (1966), Pruden et alia (1964) and Jottrand (1954). For particles of equal density these are,

- (i.) $d_1 / d_2 > 1.3$ (Wen & Yu)5.2-41
- (ii.) $(\rho_{b1} - \rho_{b2}) = (\rho_s - \rho) e_1 \left[\left(\frac{d_1}{d_2} \right)^{(3-m)mn} - 1 \right]$ (Pruden et alia) .5.2-42
- (iii.) $d_1 / d_2 > 1.41$ (Jottrand)5.2-43

where d_1 = diameter of larger particle; $m = 1$, in Stokes region;
 d_2 = smaller; $= 2$, in Newton region;
 n is governed by the Richardson-Zaki equation.

ρ_b = zone bulk density.

Pruden et alia suggested that the driving force for stratification was $(\rho_{b1} - \rho_{b2})$ and not d_1 / d_2 . A low density zone of small particles rested on a high density zone of large particles.

Following his 1952 fluidisation studies, Jottrand, in his 1954 paper, gave the critical voidage below which stratification would not occur

$$e_c = \frac{3mn}{3-m+3mn} \dots\dots\dots 5.2-46$$

Stokes region, $m=1$, $n=4.65$, $e_c = 0.875$.

Table 5.2.1 A Summary of investigations into non-flocculent, non-biological fluidisation / sedimentation

Authors	Date	Nature	Materials	Conclusions
Steinour	1944	Sedimentation	Tapioca + glass balls	$U = \frac{d^2(\rho_s - \rho)g}{18\mu} e^{1.82(1-e)} \quad (5.2-44)$
Richardson & Zaki	1954	Fluidisation / Sedimentation	Many systems $\frac{1}{4}$ " steel cubes to 1.8×10^{-2} cm. divinyl benzene	$\frac{U}{U_t} = e^n \dots (5.2-18)$ $2.39 < n < 4.65$ depending on Re_{pt}
Hanratty et alia	1957	ditto	steel + glass spheres	$U = \frac{(\rho_s - \rho)gd^2e^2}{18\mu \exp\left[\frac{2.5(1-e)}{1-39/4(1-e)}\right]} \quad (5.2-45)$
Loeffler & Ruth	1959	ditto	glass spheres in ethylene glycol $\rho_s = 2.69 \text{ g cm}^{-3}$ $0.01 < d < 0.5 \text{ cm}$	$U = \left(\frac{e^3/(1-e)}{2K + \frac{e^2}{(1-e)}} \right) \frac{d^2(\rho_s - \rho)g}{18\mu} \quad (5.2-46)$
Trupp	1968	Fluidisation	High Re_p systems (500-14000) $2.5 < \rho_s < 11.3 \text{ g cm}^{-3}$ $0.12 < d < 0.97 \text{ cm}$	$U = 0.826 U_t e^{1.18} \quad (5.2-47)$
Wilhelm & Kwauk	1948	ditto	Lead shot, sand, catalyst in water $1.13 < \rho_s < 10.8 \text{ g cm}^{-3}$ $0.03 < d < 0.5 \text{ cm}$	The importance of Fr, Ga, and other factors
Lewis & Bowermann	1952	ditto	similar to above.	$\frac{U}{U_t} = e^n \quad 2 < Re_{pt} < 500$ $n = 3.37$ $Re_{pt} > 500; n = 2.5$
Jottrand	1952	ditto	fine sand, for $Re_{pt} < 0.5$ $20 < d < 113 \mu$	$\frac{U}{U_t} = e^{5.6}$
Lewis et alia	1949	Fluidisation	glass balls $0.005 < d < 0.06 \text{ cm}$	$\frac{U}{U_t} = e^{4.65}$
Godard & Richardson	1969	ditto	used other data.	$\frac{U_t}{U_{mf}} = 80 \quad Ga < 1$ $\dots = 10 \quad Ga > 10^5$ U_{mf} based on Ergun or Carman eqns

law. The data presented in the paper indicated that the flocc were very open and contained large amounts of immobile liquid. This was estimated using the volume fraction of liquid in the flocc, $A = \phi_1 / (\phi_1 + 1)$. A summary of their data is shown in Table 5.2.2.

Table 5.2.2 Flocc Properties (Banerjee et alia)

Material	$d_{agg} \mu$	ϕ_1	A	$d_{agg} \mu$
Lead chromate	605	26.9	0.983	242
Iron oxide	1170	141.4	0.993	234
Chromium oxide	333	23.2	0.959	100

These very high values for A are similar to those reported for inorganic flocculent material by Thomas (1963) and Tambo (1967) whose work was discussed earlier in Chapter 3.

(c) Stratification Investigations

The criteria for stratification has been established by Wen & Yu (1966), Pruden et alia (1964) and Jottrand (1954). For particles of equal density these are:

$$(i.) \quad d_1 \setminus d_2 > 1.3 \quad (\text{Wen \& Yu}) \quad \dots \dots \dots 5.2-41$$

$$(ii.) \quad \left[\frac{d_1}{d_2} \right]^{(2-m)} \left[\frac{\rho_1 - \rho}{\rho_2 - \rho} \right] = (1.6 - 1.9) \quad (\text{Pruden et alia}) \quad \dots \dots \dots 5.2-42$$

$$(iii.) \quad d_1 \setminus d_2 > 1.41 \quad (\text{Jottrand}) \quad \dots \dots \dots 5.2-43$$

where d_1 = diameter of larger particles; $m = 1$ in Stokes region; $m = 2$ in Newton region; d_2 = smaller
 n is governed by the Richardson-Zaki equation.

ρ_p = some bulk density.

Pruden et alia suggested that the driving force for stratification was $(\rho_1 - \rho_2)$ and not $d_1 \setminus d_2$. A low density zone of small particles rested on a high density zone of large particles.

Following his 1952 fluidisation studies, Jottrand, in his 1954 paper, gave the critical voidage below which stratification would not occur

$$e_c = \frac{3m}{3-m} \quad \text{Stokes region, } m=1, \quad e_c = 0.675$$

Newton region $m = 2$, $n = 2.39$, $e_c = 0.935$.

This suggested that stratification occurred only in very well fluidised systems, which was contrary to the observations that it occurred continuously once the minimum fluidisation velocity was exceeded, (i.e. $e = 0.45$).

The concentrations of different particle species in a liquid fluidised bed were measured by Kennedy & Breton (1966). They obtained these concentrations at different bed heights and liquid flows. A mixture of 0.1cm. and 0.2cm. ballotini were fluidised using water or glycol.

Smith (1965) developed a theoretical model based on Happel's free surface model to predict the settling rates of multisized particle suspensions. The model was most applicable at high d_1 / d_2 ratios.

(d) Investigations into fluidised bed motions

Several workers have investigated solids motion and liquid mixing in fluidised beds. Similar techniques were used. These consisted of creating a fluidised bed where both particles and liquid have the same refractive index. Hence, by marking selected particles or activating a dye within the liquid conditions in the bed may be studied.

Handley et alia (1961) matched the refractive indices of soda glass particles fluidised by Methyl Benzoate ($\rho_s / \rho = 2.3$). By following a marker particle they found that particulate fluidisation can be of two types (a) Uniform fluidisation, which was characterised by random particle motion and a uniform dynamic pressure distribution.

(b) Non-Uniform fluidisation, with bulk solids circulation.

This latter type was induced by bad distributor design. The random motion was explained by rising fluid pockets and falling particle pockets.

Their technique was copied by workers at Swansea University. Both Carlos & Richardson (1968) and Latif & Richardson (1972) used soda glass in Dimethyl phthalate solution.

Table 2.2.1 A Summary of investigations into non-fluidisation / non-biological fluidisation / sedimentation

Authors	Date	Nature	Materials	Conclusions
Steinour	1944	Sedimentation	Glass balls	$U = 4 \frac{(\rho_s - \rho) g d_p^2}{18 \mu}$ (2.2-44)
Richardson & Zaki	1954	Fluidisation / Sedimentation	Many systems 1/2" steel cubes to 1.8x10 ⁻² cm. divinyl benzene	$\frac{U}{U_m} = e^{-(1.75 - 0.615 \frac{U_m}{U})}$ (2.2-45)
Handley et alia	1957	ditto	steel + glass spheres	$U = 1.75 \frac{(\rho_s - \rho) g d_p^2}{18 \mu}$ (2.2-46)
Loeffler & Rath	1959	ditto	Glass spheres in ethylene glycol ($\rho_s = 2.8 \rho_m$) 0.014 to 0.5 cm.	$U = \left(\frac{e^2 (1 - e)^2}{2 K_0 e} \right) \frac{(\rho_s - \rho) g d_p^2}{18 \mu}$ (2.2-47)
Trapp	1968	Fluidisation	High Re systems (200-14000) 2.5x10 ⁻³ to 1.3 cm. 0.12 to 0.97 cm.	$U = 0.02 \frac{(\rho_s - \rho) g d_p^2}{18 \mu}$ (2.2-48)
Wilhelm & Wenk	1948	ditto	Lead shot, sand, catalyst in water 0.03x10 ⁻³ to 0.8 cm. 0.03x10 ⁻³ to 0.5 cm.	The importance of Re, d_p , and ρ other factors
Lewis & Bowermann	1952	ditto	similar to above.	$U = e^{-(1.75 - 0.615 \frac{U_m}{U})}$ (2.2-49)
Jottand	1952	ditto	fine sand, for Re < 0.5 20x10 ⁻³ to 1.3 cm.	$\frac{U}{U_m} = e^{-(1.75 - 0.615 \frac{U_m}{U})}$ (2.2-50)
Lewis et alia	1949	Fluidisation	Glass balls 0.005 to 0.06 cm.	$\frac{U}{U_m} = e^{-(1.75 - 0.615 \frac{U_m}{U})}$ (2.2-51)
Gohar & Richardson	1969	ditto	used other data.	$\frac{U}{U_m} = 10^{-0.15 \frac{U_m}{U}}$ (2.2-52)

A marker particle was darkened by gamma radiation and was followed photographically. Carlos et alia used 0.9cm. spheres and Latif et alia used 0.6cm. spheres. The latter investigated a larger voidage range ($0.55 < \epsilon < 0.95$) than Carlos. Their findings were generally identical. They found that particles rose in the centre and fell near the walls. The bed was anisotropic, i.e. more particles travel faster upwards than downwards.

Vanecek et alia (1968) used the technique of Ryan et alia (1967) and Hummel (1967). A square box was fitted around the column and filled with liquid to remove any optical curvature effects. Apparatus, particles and liquids all had the same refractive index. A narrow beam of light was then used to illuminate sections of the bed for photography. Perspex (Lucite) spheres, $0.6 < d < 1.2$ cm., were fluidised with a Napthalene/Decalene mixture. Point voidages were measured at various sections of the bed, which revealed that at a given flowrate most of the bed was at constant voidage.

This technique was extended by Allen & Smith (1971). Here a dye activated by pulses from a Ruby laser was used to measure liquid velocities and flow patterns. Aggregative behaviour was noted with spheres of 1cm. diameter and at high bed voidage (high flowrates).

Voidage non-homogenities were measured by Volpicelli et alia (1966). Using various systems such as steel and water & plastic and water they observed particle circulation. They concluded that point voidages vary considerably in time and space within most systems.

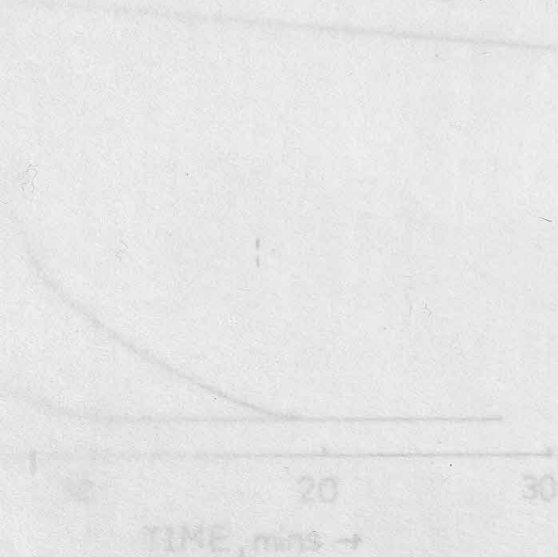
The random motion and non-homogenities observed were explained by Lawson and Hasset (1967) as being due to parvoid propagation. They define these as "striae discontinuities of low particle concentration rising in close sequence". Parvoid motion was followed photographically in a bed of 0.15 cm. glass spheres. Parvoid rise velocity was 1.5 to 3 times greater than superficial liquid velocity. Four zones in the bed were identified and these are shown in Fig. 5.8.

From the bottom upwards,

- (a) Static zone
- (b) Labile zone, where the particles are touching.
- (c) High density dispersion zone, with solids circulation.
- (d) Low with random solids motion and parvoids.

In addition to the investigations made on real fluidised beds several workers have tried to create controlled and artificial particle arrangements for drag studies. This usually involves the creation of arrays of spheres fixed in position within a matrix so as to give a specific pattern of packing. The drag force on a test sphere within the array ^{is} ~~was~~ then measured.

Martin et alia (1951) performed some early experiments by clamping ball bearings between plates. Rowe and Henwood (1961) mounted spheres in a matrix and measured the drag on the test sphere by means of the deflection of a wire. A detailed examination of this topic was made by Gunn and Malik (1966, 1967). They constructed various packing arrangements by threading spheres onto rods, and the drag forces for each arrangement ^{were} ~~was~~ calculated from the pressure drop.



A marker particle was darkened by gamma radiation and was followed photographically. Carlos et alia used 0.9cm. spheres and latex et alia used 0.6cm. spheres. The latter investigated a larger voidage range (0.25 < ϵ < 0.95) than Carlos. Their findings were generally identical. They found that particles rose in the centre and fell near the walls. The bed was anisotropic, i.e. more particles travel faster upwards than downwards. Vanacek et alia (1968) used the technique of Ryan et alia (1967) and Hummel (1967). A square box was fitted around the column and filled with liquid to remove any optical distortion effects. Apparatus, particles and liquids all had the same refractive index. A narrow beam of light was then used to illuminate sections of the bed for photography. Perspex (Lucite) spheres, 0.6 < d < 1.2cm., were fluidised with a Naphthalene-Decalene mixture. Point voidages were measured at various sections of the bed, which revealed that at a given flowrate most of the bed was at constant voidage. This technique was extended by Allen & Smith (1971). Here a dye activated by pulses from a Ruby laser was used to measure liquid velocities and flow patterns. Aggregative behaviour was noted with spheres of 1cm. diameter and at high bed voidage (high flowrates). Voidage non-homogeneities were measured by Volpceli et alia (1966). Using various systems such as steel and water & plastic and water they observed particle circulation. They concluded that point voidages very considerably in time and space within most systems. The random motion and non-homogeneities observed were explained by Lawson and Hassett (1967) as being due to parvoid propagation. They define these as "striate discontinuities of low particle concentration rising in close sequence". Parvoid motion was followed photographically in a bed of 0.15 cm. glass spheres. Parvoid rise velocity was 1.5 to 3 times greater than superficial liquid velocity. Four zones in the bed were identified and these are shown in Fig. 5.8.

FIG 5.8 MOTION IN A LIQUID FLUIDISED BED [Lawson & Hassett, 1967]

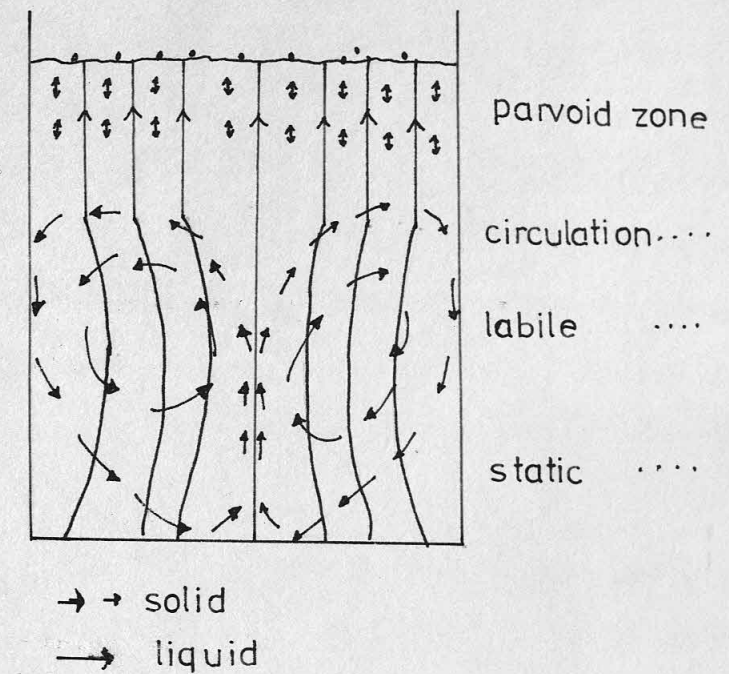
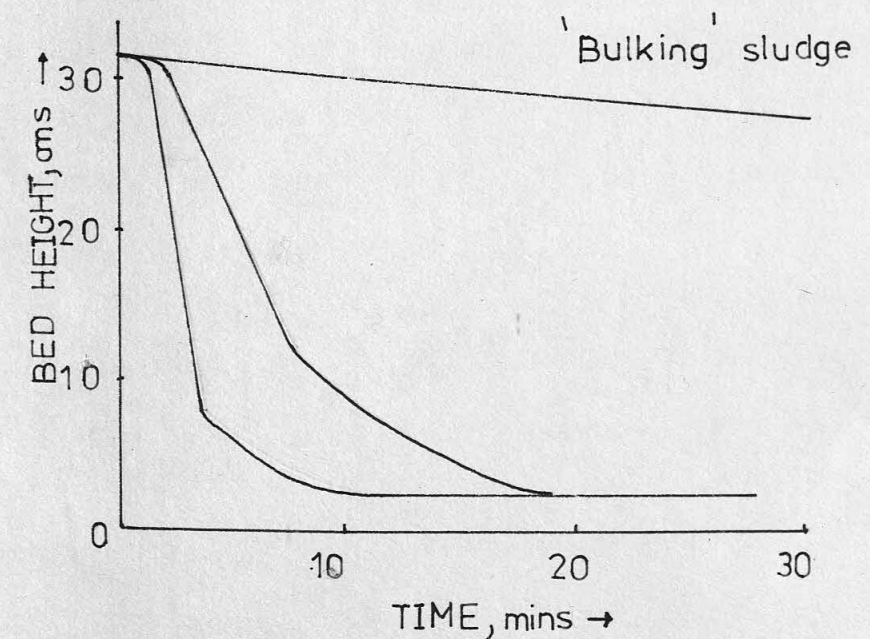


FIG 5.9 ACTIVATED SLUDGE SETTLING
from Aiba et al, 1971.



5.2-5 Biological Multiparticle Systems

Introduction

In the previous section the behaviour of conventional multiparticle systems was examined. These suspensions are easily quantified, but it must be noted that flocculent materials did present difficulties in establishing the nature of the floc units. This led to uncertainties as to the exact behaviour of these units in suspension. The quantitative problem is the main difficulty in working with biological systems. Whilst microorganisms have been used for many years by technologists, very little is known about the behaviour of microbial suspensions. Any tests that have been performed have been with sedimentation phenomena.

(a) Yeast Investigations

Perhaps the most extensively investigated organism has been yeast. As mentioned in Chapter 3, Haddad et alia (1953) settled individual yeast cells to determine their density. They made use of Stokes Law and terminal velocity measurements, but did not question the validity of using Stokes Law to calculate the drag on the cell. Akin et alia (1965) examined the sedimentation of a flocculent yeast, *S. Carlsbergensis*. Their tests were performed using a 1.5 cm. x 120cm. tube which was water jacketed to maintain constant temperature. 0.1 N phthalate buffer solution ($2.4 < \text{pH} < 5.65$) and 10g. of filtered yeast per 100ml. were used for the tests. They measured settled height of bed vs. time and report three stages in the settling process.

- (i) Agglutination, where the flocs form prior to settling.
- (ii) Constant settling period, where the suspension settles at a constant rate maintaining its initial voidage.
- (iii) Packing, where the bed consolidates very slowly with breakdown in floc structure.

They examined the effects of temperature and pH on the settling of a constant composition suspension. They observed that at constant temperature (10°C) the yeast would not settle if the pH was less than 3.8.

Above this value flocs formed and the settling rate was rapid. Increasing pH had little effect on the settling rate and no effect on the packing rate. At a constant pH of 4.15 the settling rate increased appreciably with increasing temperature in the range 3 to 15°C. No significant temperature was found similar to the pH effect above. Below 7°C larger flocs were formed than at higher temperatures. However, the dependence of liquid physical properties on temperature was clearly more important. Whilst this study revealed some interesting facts the omission of concentration effects limits the use of the data for further hydrodynamic study.

Prior to the author's investigations, Miam (1969) conducted preliminary tests into the fluidisation / sedimentation of a fermentation-limited yeast, *S. Cerevisiae* (CFCC3). Tests were performed in measuring cylinders of 250 to 500 cm³ capacity and the yeast was suspended in an acetate buffer of pH = 4.7. For the fluidisation tests a 2" diameter tube was used, with tap water as the liquid phase. The arrangement was very simple. The weight of yeast was expressed as centrifuged wet weight. The sedimentation tests examined the effects of tube diameter, initial height of suspension and concentration on the settling. Fluidisation presented problems of bed stability which was observed to fluctuate considerably with changing flow conditions. Bed height vs. flowrate was measured at different concentrations.

These data were analysed by Greenshields and Smith (1971). They assumed that the Richardson-Zaki equation applied to the suspension and from this they estimated the terminal velocity and hence, diameter of an average floc. This gave a floc diameter of about one half of that observed. Floc densities were calculated assuming a floc density of 0.38. Thus, $U = K e^{4.4}$, where $K \div U_t = 0.54$ cm/s.

They discussed the complications of stratification and variable density differences which might arise in a continuous tower fermenter and indicated that reality might present totally different conditions from those found

Introduction

In the previous section the behaviour of conventional multiparticle systems was examined. These suspensions are easily quantified, but it must be noted that flocculent materials did present difficulties in establishing the nature of the floc units. This led to uncertainties as to the exact behaviour of these units in suspension. The quantitative problem is the main difficulty in working with biological systems. Whilst microorganisms have been used for many years by technologists, very little is known about the behaviour of microbial suspensions. Any tests that have been performed have been with sedimentation phenomena.

(a) Yeast Investigations

Perhaps the most extensively investigated organism has been yeast. As mentioned in Chapter 3, Haddad et alia (1973) settled individual yeast cells to determine their density. They made use of Stokes law and terminal velocity measurements, but did not question the validity of using Stokes law to calculate the drag on the cell. Kohn et alia (1962) examined the sedimentation of a flocculent yeast, *S. Cerevisiae*. Their tests were performed using a 1.5 cm x 120 cm tube which was water jacketed to maintain constant temperature. 0.1 N phosphate buffer solution (2.4 < pH < 5.6) and 10g of filtered yeast per 100ml were used for the tests. They measured settled height of bed vs. time and report three stages in the settling process.

- (i) Agitation, where the floc form prior to settling.
- (ii) Constant settling period, where the suspension settles at a constant rate maintaining its initial voidage.
- (iii) Packing, where the bed consolidates very slowly with breakdown in floc structure.

They examined the effects of temperature and pH on the settling of a constant composition suspension. They observed that at constant temperature (10°C) the yeast would not settle if the pH was less than 3.8.

experimentally. The analysis, whilst far from rigorous, attempted merely to highlight the problems involved with this work.

(b) Filamentous Fungi

Aiba et alia (1964) performed settling tests on several different organisms. Their objective was to determine the equivalent size of the cells or aggregates by using a modified Stokes equation. Some of this work was discussed previously in Chapter 3. The suspensions were S.Cerevisiae, Serratia Marcescens, Streptomyces Griseus and Activated sludge. Volume fractions were defined by the volume of sediment obtained after prolonged gravity settling or centrifugation. The distance travelled by the interface was plotted vs. time to give the settling velocity. The diameters observed and calculated for the yeast were very close and suggest that the strain was non-flocculent. In the case of S.Griseus, a filamentous organism, the calculated size was nearly twice that observed. Large quantities of liquid were found to be bound into the filamentous network. Settling data for the activated sludge gave an equivalent size of about 80 microns.

(c) Activated Sludge

The settling behaviour of activated sludge has been used for some time as a quantifying criteria. Mohlmann (1934) first defined the Settling Volume Index (SVI) to characterise sludges.

$$SVI = \text{settled volume} / MLSS = \text{cm}^3 / \text{g.}$$

where settled volume = volume obtained after 30 mins. settling of 1 litre of sludge; MLSS = dry wt. of organisms / unit volume of sludge.

The qualitative aspects of activated sludge were reviewed by Pipes (1967). The basics of this review are presented below acting as an introduction to activated sludge phenomena.

Normally, activated sludge consists of bacteria embedded in a gelatinous matrix giving a floc-like structure. Yeast cells, protozoa, nematodes, rotifers and crustaceans may also be found. The composition of the sludge therefore prohibits a structural definition such as might be

used for fungal pellets. It is the balance in proportion of these organisms which gives the sludge its characteristics. Sludge can be classified into 3 types. These are;

- i. Rapid settling. In this case the bulk of the sludge settles leaving some material in the supernatant. For these sludges $50 < \text{SVI} < 200$ cm^3/g . and the floc size ranges from 50 to 500 microns.
- ii. Floating. If gas bubbles become trapped in the material or the components of the sludge have a density less than the liquid, the sludge will float or else sink and then float.
- iii. Bulking. These sludges will not settle to any appreciable extent. Pipes stated that this was due to its composition and not its concentration. The phenomena was not related to poor flocculation, but to a high filamentous to non-filamentous material ratio. Thus, "sphaerotilus" bulking sludge has an SVI between 100 & 2000 and contains large amounts of filamentous material; whereas, "zoogloeal" sludge contains much flocculent material and large amounts of immobilised liquid.

Following his initial tests on activated sludge in 1964, Aiba et alia (1971) conducted further tests on different sludges. Their results are shown in Fig.5.9. The tests were performed in a 6.3cm. diameter tube with the liquid pH = 7.

If U = interfacial velocity, cm/min; U' = settling velocity, cm/s;
 c = volume fraction of sediment obtained after 30 minutes settling;

ρ_p = floc density, g/cm^3 .

Then, $U' = U / (60(1-c))$.

and $U_t = U (1 + K c^{1/3})$ and $d_e = \left(\frac{18 U_t \mu}{g (\rho_p - \rho)} \right)^{1/2} \dots \dots \dots 5.2-48$

Using a value of $\rho_p = 1.003 \text{ g}/\text{cm}^3$ found in earlier tests the values of d_e were calculated.

For rapid settling sludges; $d_e = 750 \mu$

For bulking sludges ; $d_e = 100 \mu$

They stated that sludge flora and fauna influenced settling, as was stated by Pipes. If the organisms were attached to the flocs rapid settling

experimentally. The analysis, whilst far from rigorous, attempted merely to highlight the problems involved with this work.

(d) Filamentous Fungi

Aiba et alia (1964) performed settling tests on several different organisms. Their objective was to determine the equivalent size of the cells or aggregates by using a modified Stokes equation. Some of this work was discussed previously in Chapter 3. The suspensions were *S. cerevisiae*, *Gerrardia marcescens*, *Streptomyces griseus* and activated sludge. Volume fractions were defined by the volume of sediment obtained after prolonged gravity settling or centrifugation. The distance travelled by the interface was plotted vs. time to give the settling velocity. The diameters observed and calculated for the yeast were very close and suggest that the strain was non-filamentous. In the case of *S. griseus*, a filamentous organism, the calculated size was nearly twice that observed. Large quantities of liquid were found to be bound into the filamentous network. Settling data for the activated sludge gave an equivalent size of about 80 microns.

(e) Activated Sludge

The settling behaviour of activated sludge has been used for some time as a quantifying criteria. Mohlmann (1934) first defined the Settling Volume Index (SVI) to characterise sludges.

$$\text{SVI} = \frac{\text{settled volume} / \text{mass}}{\text{g}} \times 100$$
where settled volume = volume obtained after 30 mins. settling of 1 litre of sludge; mass = dry wt. of organisms / unit volume of sludge.
The qualitative aspects of activated sludge were reviewed by Pipes (1967). The basis of this review are presented below acting as an introduction to activated sludge phenomena.
Normally, activated sludge consists of bacteria embedded in a gelatinous matrix giving a floc-like structure. Yeast cells, protozoa, nematodes, rotifers and crustaceans may also be found. The composition of the sludge therefore prohibits a structural definition such as might be

occurred; whereas, if the organisms were free-swimming the settling was retarded.

The most relevant research performed using activated sludge was by Edeline et alia (1969). Using a scale model of a water treatment tower they fluidised sludge flocs and attempted to relate the behaviour to the Richardson-Zaki equation. The most difficult measurement was, of course, the floc liquid content and thus, bed voidage. They used several approaches amongst which were centrifuged wet wt. and tracer residence time. The first underestimated the floc volume and the second overestimated it, due to channeling effects. They found, on the basis of the tracer method, that the bed voidage decreased towards the bottom. However, the general conclusion which was drawn was that the value of "n" in the Richardson-Zaki equation was much larger than had been found using non-biological materials.

Their data correlated with $U / U_t = e^n$; where $12 < n < 27$ 5.2-49

Settled bed voidages were found to be high (0.8 to 0.9) and the average floc density was 1.003 g/cm^3 , similar to that found by Aiba et alia (1971).

They also compared their results with an equation proposed by Bond (1966) for floc settling. This reduced to

$$U / U_t = 2.8 e^{0.667} - 1.8 \text{5.2-50}$$

which is impractical for $e < 0.52$, their data ^{were} only comparable for $e > 0.8$.

(d) The Sedimentation of Blood

Whilst, not totally relevant to the work in this thesis, an interesting study of the settling of red blood cells in suspension was made by Meyer (1973). He observed long initial aggregation times, followed by the rapid settling of the erythrocyte network. This aggregate network was held together by surface macromolecules and required large shear forces to break it down. This work followed an earlier more elementary investigation by Kermack (1929) who analysed blood cell settling data using Stokes Law modified ^{by the use of} using the suspension viscosity.

(e) Investigations using Herbs and Plants

The Russians have examined a system which is a link between conventional and biological materials. This is a bed of plant material. The original purpose of this work was to develop better equipment for the extraction of medicinal compounds from herbs. Quantifying the material was again the major problem.

The investigations have been performed by Zamorvera et alia (1964,1961) and Rakhman-Zade et alia(1971). The latter extended the work of the former. Really, the studies are concerned with the flow of fluid through restrained beds of plant material; although, Rakhman-Zade ^{has} does performed some tests with unrestrained beds. Zamorvera et alia have tested Belladonna leaves, cabbage and Hawthorn berries; together with unswollen and swollen cone neddles, Ephedra and Anabasis leaves. They plotted pressure gradient versus water flowrate.

Rakhman-Zade et alia used an approach based on the average terminal velocity for the material, which included Pachycarpine and anabasine herbs, thyme, cotton, peppermint and lily-of-the-valley leaves. 1cm³ of material was settled to find the mean terminal velocity; which would not be the same as a normally accepted terminal velocity as there were many particles present. Their values of "e" ranged from 0.46 to 0.7 for roots or leaves respectively. The bed pressure drop was higher for leaves than for roots .

(d) The Sedimentation of Blood

Whilst, not totally relevant to the work in this thesis, an interesting study of the settling of red blood cells in suspension was made by Meyer (1973). He observed long initial aggregation times, followed by the rapid settling of the erythrocyte network. This aggregate network was held together by surface macromolecules and required large shear forces to break it down. This work followed an earlier more elementary investigation by Kermack (1929) who analysed blood cell settling data using Stokes law modified using the suspension viscosity.

5.3 Experimental Equipment and Techniques

This investigation into fluidisation and sedimentation phenomena used widely different materials. It was imperative that the equipment used for the tests should produce a uniform distribution of liquid flow and allow easy access to the internals of the equipment between tests. As the range of materials was wide, many different problems were encountered and this led to several different experimental apparatuses being constructed. A description of each arrangement now follows.

5.3-1 Equipment

The different apparatuses were as follows,

- i. 1½" and 3" diameter columns

These were constructed from QVF sections and were supported in an angle-iron framework. They were designed to have the potential for co-current gas and liquid flow, although their main use was for liquid fluidisation tests. The basic design was common to both and is shown in Fig. 5.10 and Plate 5.2. A common air and liquid feed arrangement was used and this, too, is shown in Fig. 5.10. A series of rotameters were used such that a wide range of liquid flows could be covered. The liquid used was water which was pumped from stainless steel holding tanks to the columns via a Stuart-Turner centrifugal pump. Accurate flowrates could be maintained using a series of needle valves. The liquid flow was usually operated in closed circuit, a mesh filter being placed over the feed tank to remove any particles eluting from the column. A wire mesh screen was used to support the bed and to separate it from the distributor section.

Good distribution of the liquid flow was essential in such tests as these. Several systems were tried, but the most successful was the one shown in Fig. 5.10. The liquid entered through a feed pipe which was fitted with a cross shaped distributor pipe drilled with 1/16" holes. The liquid was thus forced downwards and outwards through the holes from whence it flowed upwards through a Berl saddle packing to the bed above. Injection of tracer dye into this arrangement indicated that the flow

Injection of tracer dye into this arrangement indicated that the flow
 The liquid was thus forced downwards and outwards through the holes from
 the one shown in Fig. 5.10. The liquid entered through a feed pipe which
 tests as these several systems were tried, but the most successful was
 Good distribution of the liquid flow was essential in such
 used to support the bed and to separate it from the distributor section.
 to remove any particles eluting from the column. A wire mesh screen was
 operated in closed circuit, a mesh filter being placed over the feed tank
 maintained using a series of needle valves. The liquid flow was usually
 via a Stant-Turner centrifugal pump. Accurate flowrates could be
 water which was pumped from stainless steel holding tanks to the columns
 that a wide range of liquid flows could be covered. The liquid used was
 and this, too, is shown in Fig. 5.10. A series of rotameters were used such
 Fig. 5.10 and Plate 5.2. A common air and liquid feed arrangement was used
 fluidization tests. The basic design was common to both and is shown in
 co-current gas and liquid flow, although their main use was for liquid
 an angle-iron framework. They were designed to have the potential for
 These were constructed from DVP sections and were supported in
 1. $\frac{1}{2}$ " and 3" diameter columns

The different apparatus were as follows,

5.3-1 Equipment

being constructed. A description of each arrangement now follows.

were encountered and this led to several different experimental apparatus
 between tests. As the range of materials was wide, many different problems
 liquid flow and allow easy access to the internals of the equipment
 equipment used for the tests should produce a uniform distribution of
 phenomena used widely different materials. It was imperative that the
 This investigation into fluidization and sedimentation

KEY

- a - storage tank
- b - filter
- c - speed control
- d - pump
- e - rotameters
- f - air sinter
- g - cross distributor
- h - wire screen
- i - viewing box
- j - 3" column
- k - air rotameter
- l - gauge
- m - reducer

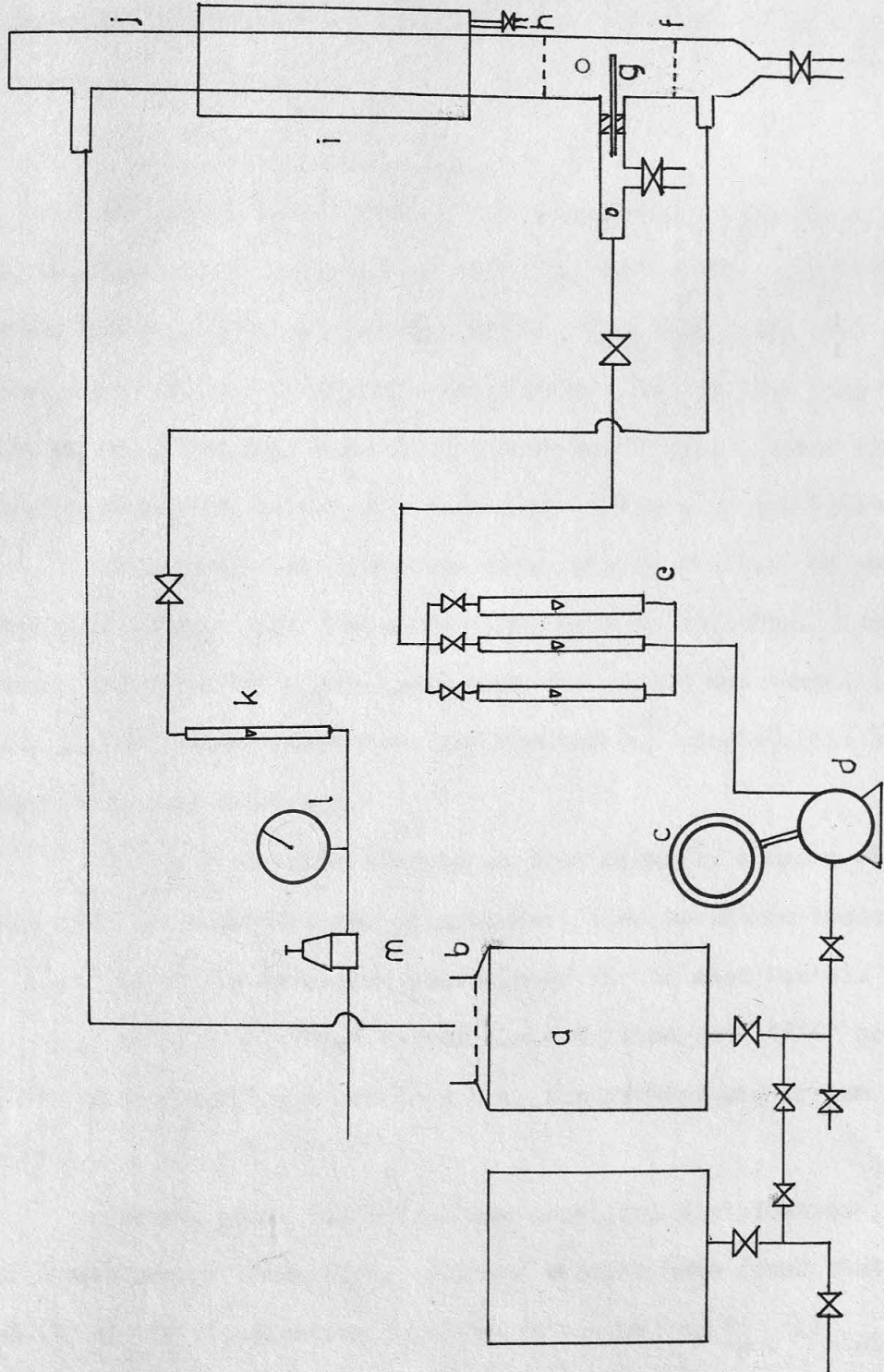


FIG 50 3" DIA. COLUMN & ANCILLARIES

passing through the wire screen was uniform and therefore suitable for fluidisation tests.

The saddles rested on a sintered metal air distributor. Injection points were located in the column by means of bulkhead fittings placed in holes drilled through the glass. Tracer dyes could then be injected by hypodermic syringe into the bed. A plastic box was fitted around part of the column to remove curvature distortion from photographic studies. The gap between the box and the column was filled with water to assist in this purpose.

ii. Two-Dimensional Bed

To permit better visual and photographic clarity of a fluidised bed, two-dimensional beds may be used. For this work, the two-dimensional bed was constructed from perspex, and the opposite faces were glued and bolted together. The distributor section and bed section were bolted together using flanges. A support screen was placed between these inside rubber gaskets. The arrangement is shown in Fig.5.11 and Plate 5.3.

Relatively low flowrates were used in the bed. It was also found that a dense distributor packing, such as ballotini, caused the adjacent plates to be forced apart when the liquid was pumped into the column. Thus, the following distributor arrangements ^{were} ~~was~~ adopted, (the bed being supported by one of them).

(a) A wire gauze covered on both sides by a nylon filter cloth which acted as a support and distributor (used in Diakon tests).

(b) A 100 mesh wire gauze (used in the seed tests).

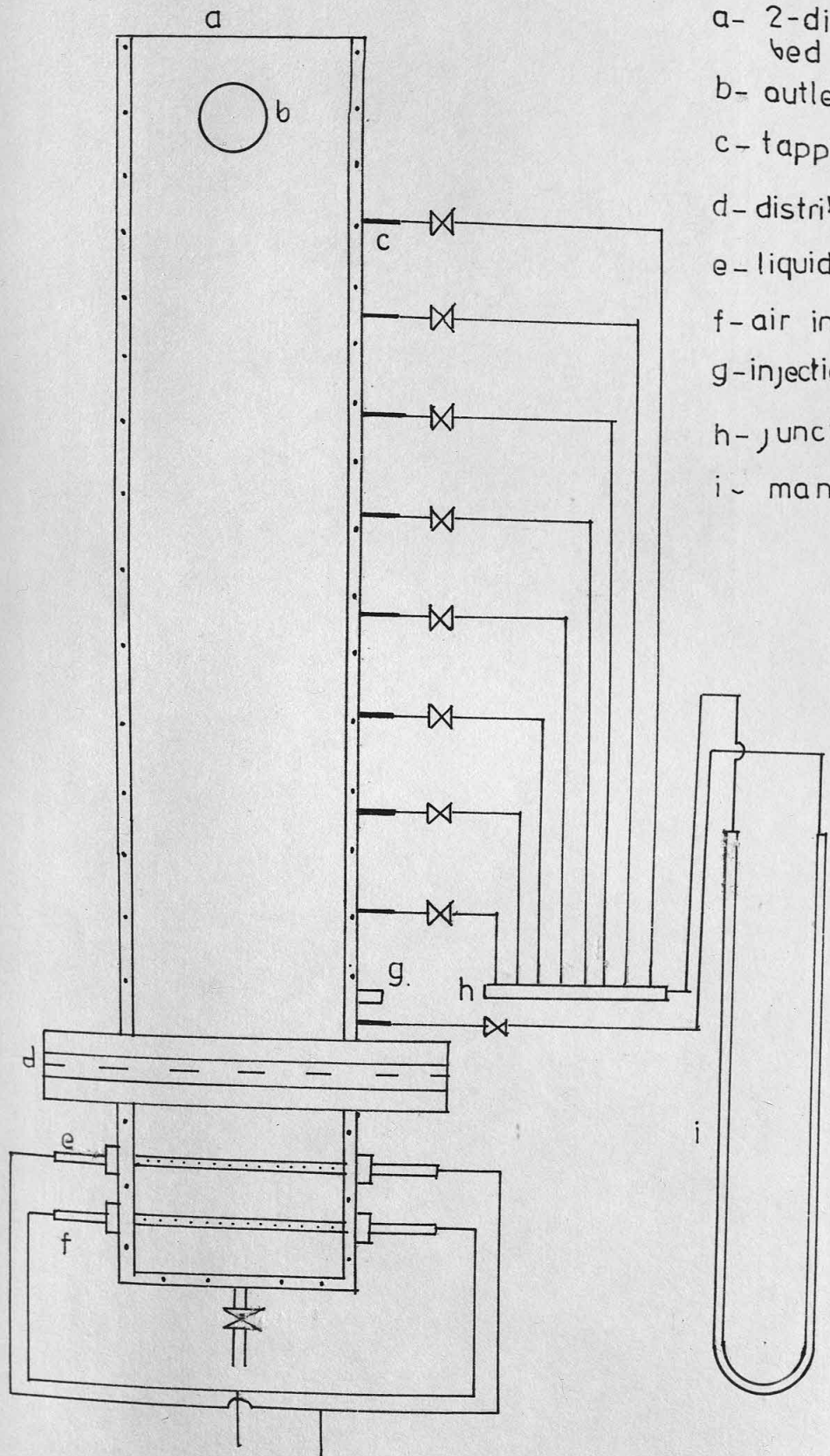
(c) A 1/16" thick copper plate drilled with 1/16" holes on a 3/16" square pitch (this acted as both distributor and screen in the seed tests).

Arrangements (a) & (c) gave excellent distribution, although (b) caused severe channelling. Several workers have found that the quality of the fluidisation depended ^s on the ratio $\Delta P_{\text{bed}} / \Delta P_{\text{distributor}}$.

FIG 511 TWO-DIMENSIONAL BED

KEY

- a- 2-dimensional bed 6" x 6"
- b- outlet pipe 2" O.D.
- c- tapping 1/8" I.D.
- d- distributor/screen
- e- liquid inlet 3/8" I.D.
- f- air inlet
- g- injection point
- h- junction
- i- manometer



passing through the wire screen was uniform and therefore suitable for

fluidization tests.

The sand was tested on a standard metal air distributor.

Injection points were located in the column by means of ball valves.

Fittings placed in holes drilled through the glass. Tracer dyes could then

be injected by hypodermic syringe into the bed. A plastic box was fitted

around part of the column to remove curvature distortion from photographic

studies. The gap between the box and the column was filled with water

to assist in this purpose.

11. Two-Dimensional Bed

To permit better visual and photographic clarity of a fluidized

bed, two-dimensional beds may be used. For this work, the two-dimensional

bed was constructed from plexiglas, and the opposite faces were lined and

bolted together. The distributor section and bed section were bolted

together using flanges. A support screen was placed between these inside

rubber gaskets. The arrangement is shown in Fig. 5.11 and Plate 5.3.

Relatively low flow rates were used in the bed. It was also

found that a dense distributor packing, such as ballotini, caused the

adjacent plates to be forced apart when the liquid was pumped into the column.

Thus, the following distributor arrangement was adopted, (the bed being

supported by one of them).

(a) A wire gauze covered on both sides by a nylon filter cloth

which acted as a support and distributor (used in fluidization tests).

(b) A 100 mesh wire gauze (used in the seed tests).

(c) A 1/16" thick copper plate drilled with 1/16" holes on a

3/16" square pitch (this acted as both distributor and screen in the seed

tests).

Arrangement (a) & (c) gave excellent distribution, although

(b) caused severe channeling. Several workers have found that the

quality of the fluidization depends on the ratio of distributor

PLATE 5.2 3" DIAMETER COLUMN

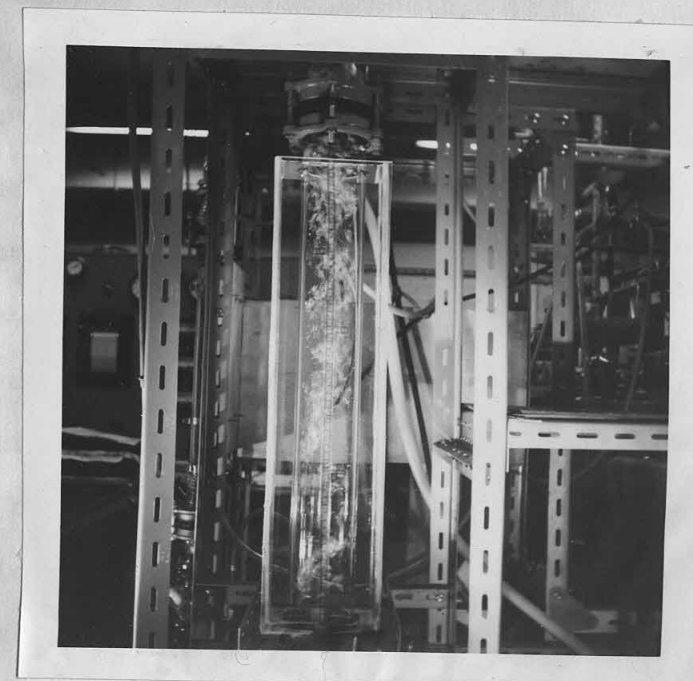
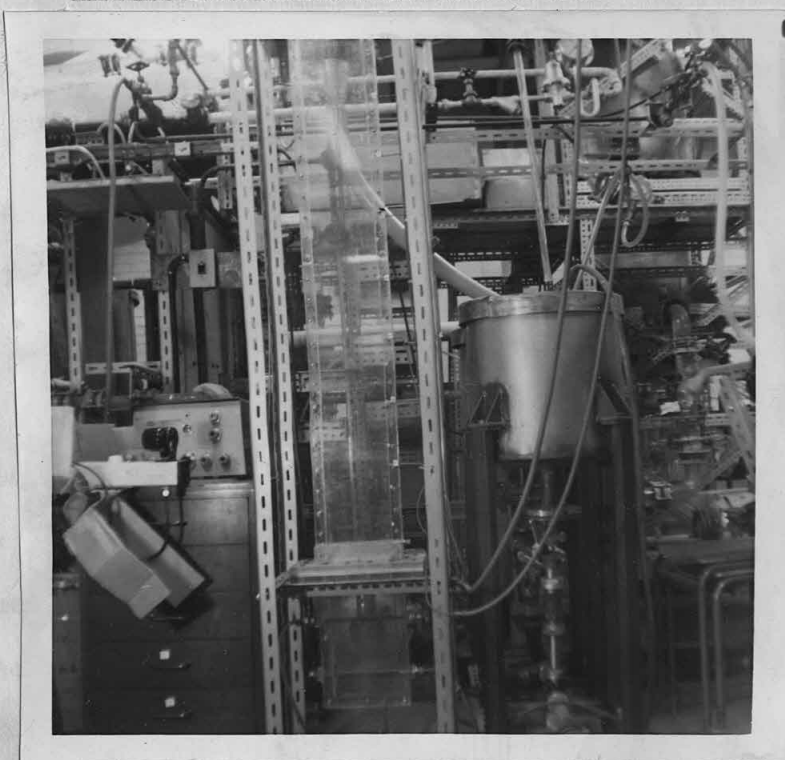


PLATE 5.3 TWO-DIMENSIONAL BED



This has been shown to be a function of bed length to column diameter. For large ratios of length to diameter the distributor pressure drop should be much greater than that for the bed. This explains why arrangements (a) & (c) were so satisfactory, the pressure drops through beds of materials tested being fairly small.

The liquid entered the column through a $\frac{3}{8}$ " diameter pipe drilled with $\frac{1}{16}$ " holes. For liquid fluidisation tests only one pipe was used, provisions existing for another pipe to be used as an air distributor. A flow straightner made from wire mesh packing was fitted between the screen and the pipe. The liquid was pumped into the column using the previous centrifugal pump arrangement. The pump was fitted with a variable speed control for pumping at very low flowrates. For some tests this was replaced by a DCL micropump described later. The holding tanks used for the previous columns were used and the water flow was again closed-circuit, using the filter, ^{being used} to remove any eluted ^{had} particles.

A thermometer was fitted into the side of the column using bulkhead fittings and injection ports were used as in the previous case. The pressure drop through the bed was measured using a water / carbon tetrachloride U-tube manometer. Eight tappings were located in the sides of the column and these were connected to a common junction unit. Tappings were isolated using clips, such that only one needed to be monitored at any one time. A tapping just above the support screen constituted the other arm of the manometer. A wire gauze fitted over the ends of each tapping prevented particles from entering into the system.

iii. 3.2 cm. Column (C1/55 equipment)

The quantities of microorganism that could be grown for testing were relatively small. Additionally, the experimental procedure required that the temperature should be accurately controlled, ^{had} buffer solutions ~~to~~ be used and the accurate removal of microorganism after the tests. Thus, the best solution was to use a small scale arrangement that could be readily dismantled. For this purpose an arrangement was constructed

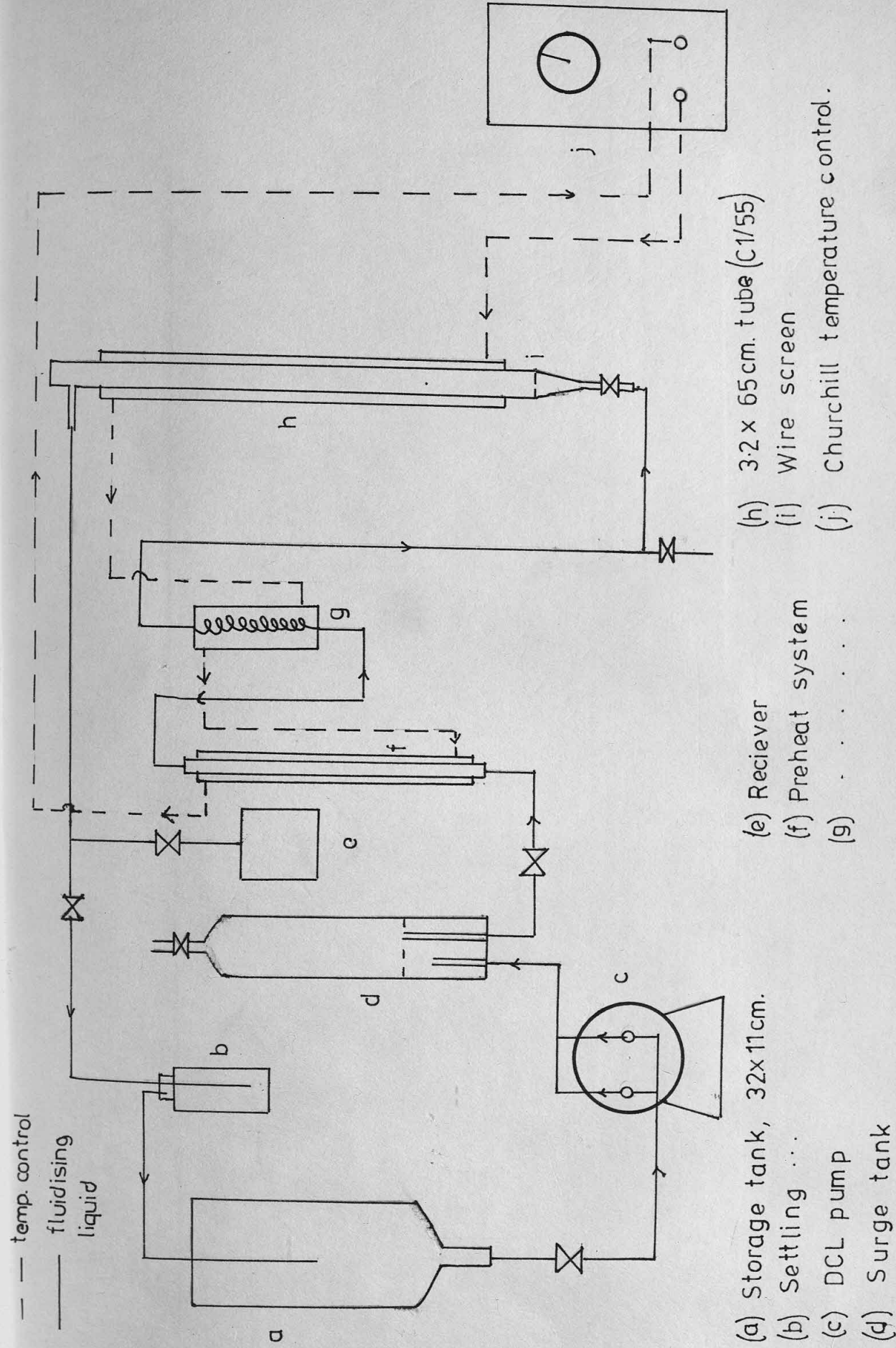
from Quickfit and associated glassware.

The notation C1/55 refers to the Leibig condenser unit which served as the fluidisation column. The internal diameter of this unit was 3.2cm., with an effective length of 65cm. A wire gauze on the bottom of the tube served as a support screen. A condenser was chosen for the ease of temperature control which is an important factor when using microorganisms, especially flocculent ones. A "Churchill" temperature control and pump unit circulated the water through the condenser-jacket and the liquid feed was preheated by passing it through a smaller condenser and a coiled heat exchanger prior to entry into the 32cm. tube. A good flow distribution was achieved using a tapered entry section. The liquid feed was often a buffer solution and this was pumped from a storage vessel using a DCL Series II micropump. This pump had two size 4 heads, each with a capacity of 3 litres /h. and a variable throughput controlled by a micrometer gauge which adjusted the stroke length. The pump was calibrated using water and was found to perform accurately over a long time. The feed passed through a feed tank prior to entry into the preheat section. Closed-circuit flow could be used and in this instance the flow leaving the 3.2cm. column passed through a settling chamber (a Dreschel bottle), prior to returning to the feed tank. This arrangement proved most satisfactory for the tests on microorganisms. The arrangement is shown in Fig. 5.12 and Plate 5.4. The microorganisms were grown in the 1½ litre fermenters discussed earlier in Chapter 3 and shown in Plate 3.1.

iv. Measuring Cylinders

The sedimentation tests were performed using either the apparatus previously discussed or a 250ml. or 500ml. measuring cylinder. The dimensions of the 500ml. cylinder were 4.55cm. diameter by 30 cm. length. This was placed in a water bath to maintain constant temperature.

FIG 512 MICROBIAL FLUIDISATION APPARATUS (3.2 cm. TUBE)



This was placed in a water bath to maintain constant temperature. dimensions of the 500ml. cylinder were 4.5cm. diameter by 30 cm. length. previously discussed as a 250ml. or 500ml. measuring cylinder. The sedimentation tests were performed using either the apparatus

iv. Measuring Cylinders

fermenters discussed earlier in Chapter 3 and shown in Plates 3.1. in Fig. 5.12 and Plate 5.4. The microorganisms were grown in the 15 litre satisfactory for the tests on microorganisms. The arrangement is shown prior to returning to the feed tank. This arrangement proved most the 3.2cm. column passed through a settling chamber (a Fresnel bottle). Closed-circuit flow could be used and in this instance the flow leaving The feed passed through a feed tank prior to entry into the preheat section. calibrated using water and was found to perform accurately over long time. by a micrometer gauge which adjusted the stroke length. The pump was each with capacity of 3 litres /h. and a variable throughput controlled vessel using a DCL Series II micropump. This pump had two size 4 heads. liquid feed was often a buffer solution and this was pumped from a storage. A good flow distribution was achieved using a tapered entry section. The condenser and a coiled heat exchanger prior to entry into the 32 cm. tube. and the liquid feed was preheated by passing it through a smaller control and pump unit circulated the water through the condenser-jacket microorganisms, especially flocculent ones. A "Churchill" temperature ease of temperature control which is an important factor when using of the tube served as a support screen. A condenser was chosen for the was 3.2cm. within effective length of 65cm. A wire gauge on the bottom appeared as the fluidisation column. The internal diameter of this unit The notation C1/55 refers to the Japig condenser unit which from Quikfit and associated glassware.

PLATE 5.4

3.2cm. COLUMN UNIT

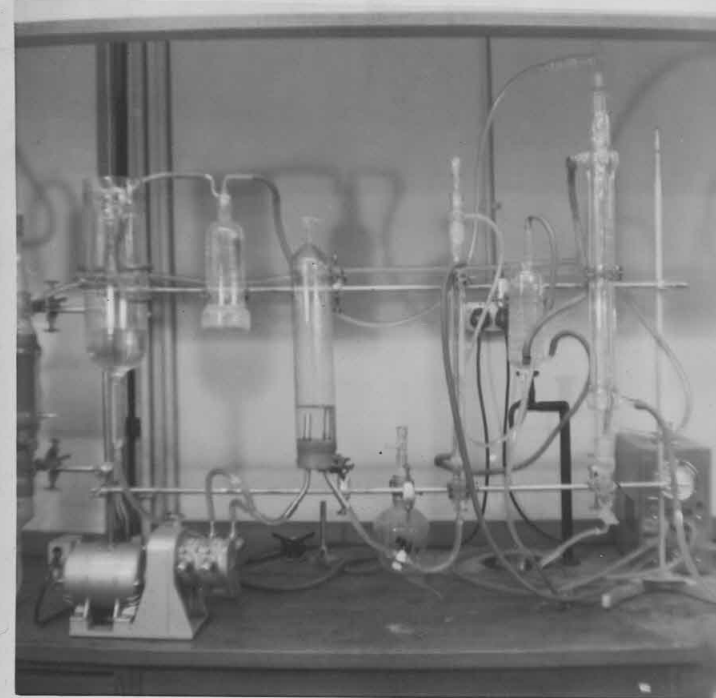
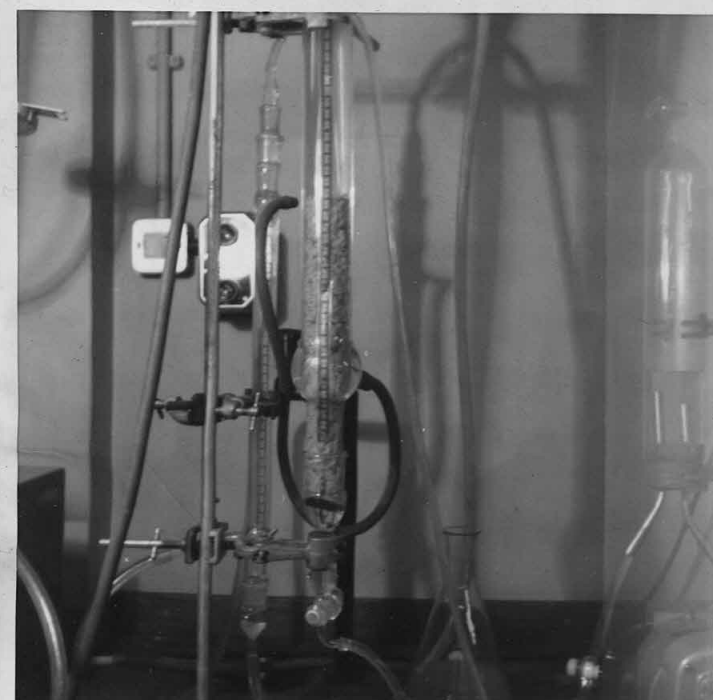


PLATE 5.5

FLUIDISED BED OF YEAST



5.3-2 Experimental Materials and Methods

5.3-2.1 Materials

The physical properties of the materials used in the tests were as follows.

i. Ballotini

Several sizes of closely sized ballotini were used, thus,

Diameter, cm.	Density, g/cm ³
0.2	2.68
0.3	2.40
0.6	2.45

These densities and those of subsequent materials were determined using a specific gravity bottle and tap water.

ii. Diakon

Diakon consists of perspex particles and was supplied by Griffin & George Ltd., Birmingham. In its commercial state the material has a size range $300 < d < 1200$ microns. The material was therefore sieved and two size fractions were used, which were $0.0655 \text{ cm} \pm 0.0055 \text{ cm}$. and $0.055 \text{ cm} \pm 0.005 \text{ cm}$. Density determinations on diakon were complicated ^{since} by,

- (a) some beads were hollow,
- (b) air was trapped between the particles and
- (c) electrostatic forces created difficulties of adhesion.

To overcome these problems the material was fluidised and the less dense material eluted off. Density measurements were then made on a sample that had remained in the bed. Care was taken to remove any trapped air bubbles, which was accomplished by stirring the material. The density of "solid" diakon was 1.16 g/cm^3 , and the density of a mixture of "solid" and hollow particles was 1.12 g/cm^3 .

iii. Mustard Seed

The batch of seeds obtained for these tests had a close size range. The sieve analysis of dry seeds is given below in Table 5.3-1.

Table 5.3-1 Sieve analysis of dry seeds

Size range, μ	3353-2411	2411-2360	2360-2000	2000-1700
Weight fraction, X	0.022	0.013	0.721	0.244
d average, μ	2882	2385.5	2180	1850
X / d ;	0.00764	0.00544	0.3307	0.1319

$$\therefore X / d = 0.47568 \text{ and } 1/\sum X/d = d_{\text{mean}} = 2102 \text{ microns.}$$

The density of this mixture was 1.118 g/cm^3 . In certain tests the seeds were used without size selection. In later tests a size fraction was taken. This was $d = 0.218 \text{ cm} \pm 0.018 \text{ cm}$. The density of this fraction was found to be 1.093 g/cm^3 .

Now, when the seeds were placed in water they were observed to swell. This caused the physical properties of the dry state to alter. To follow this swelling process seeds were attached to an indented microscop slide, and covered with water. The diameter of the seed was measured under the microscope at various time intervals. It was observed that after 4 h. soaking the seeds attained a constant steady state diameter. Distilled water was found to swell the seeds more than tap water. This supported the idea that osmosis was the cause of the swelling.

The ratio $d_{\text{final}}/d_{\text{initial}}$ was found to be nearly constant for all seeds examined. The values were (a) Tap water $d_f/d_i = 1.31$
(b) Distilled water $d_f/d_i = 1.35$

Using this ratio and assuming that water enters the seed and that no material leaves it, the density of the seed may be found thus,

$$\begin{aligned} \text{Let } d_f/d_i &= z \text{ and } \rho_s = \text{density of dry seed, } \rho = \text{density of water} \\ \therefore \text{Wt. of seed material/wt. of water} &= \frac{\pi d^3 \rho_s}{\pi d^3 (z^3 - 1) \rho} \\ \therefore \text{Wt. of one swollen particle} &= \frac{\pi d^3 (\rho_s + (z^3 - 1) \rho)}{6} \\ \text{and particle volume} &= \frac{\pi d^3 z^3}{6} \\ \therefore \text{Density of swollen seed} &= \rho_p = \frac{\pi d^3 (\rho_s + (z^3 - 1) \rho)}{\pi z^3 d^3 / 6} \\ \text{Hence, seed density} &= \frac{\rho_s + (z^3 - 1) \rho}{z^3} \end{aligned} \quad \dots\dots\dots 5.3-1$$

If the weight of the dry seeds = x , then the weight of the swollen seeds is given by $x (1 + (z^3 - 1) \rho / \rho_s)$ 5.3-2

Hence, for 0.218cm. seeds in tap water, the properties of the swollen state are $d = 0.286\text{cm.}$ and $\rho_p = 1.042 \text{ g/cm}^3$.

The difficulties of measuring the physical properties of a material which reacts to its surrounding fluid will now be apparent. In the case of the seeds the problems have a satisfactory solution. As will be apparent from the chapter on the properties of microbial aggregates the solutions are not so forthcoming for microorganisms.

iv. Microorganisms

The complex properties of the various organisms have already been discussed in Chapter 3. The application of this data to fluidisation and sedimentation will be shown later in the relevant sections.

5.3.2.2 Experimental Methods

The techniques used, the measurements taken and the test preparations made were, as follows

i. Ballotini

This material has been a favourite for liquid fluidisation experiments for many years. Consequently, its behaviour is well documented. The purpose of using ballotini, therefore was that it provided a situation that enabled the equipment and techniques to be evaluated.

Ballotini was fluidised with water in the $1\frac{1}{2}$ " column. A known weight of beads was placed in the column and the bed height was measured for various liquid flowrates. The water temperature was measured and the unit was operated on closed-circuit flow. These tests were performed with 0.2, 0.3 & 0.6cm. ballotini, starting with a large flowrate and decreasing it progressively.

ii. Diakon

Tests were performed using the two size fractions of 0.0655cm.

Table 5.3-1 Sieve analysis of dry seeds

Size range, μ	Weight fraction, X	d average, μ	X/d
2000-2500	0.024	2180	0.011
2500-3000	0.073	2385	0.031
3000-3500	0.023	2885	0.008
3500-4000	0.004	3885	0.001
4000-4500	0.004	4385	0.001
4500-5000	0.004	4885	0.001
5000-5500	0.004	5385	0.001
5500-6000	0.004	5885	0.001
6000-6500	0.004	6385	0.001
6500-7000	0.004	6885	0.001
7000-7500	0.004	7385	0.001
7500-8000	0.004	7885	0.001
8000-8500	0.004	8385	0.001
8500-9000	0.004	8885	0.001
9000-9500	0.004	9385	0.001
9500-10000	0.004	9885	0.001
10000-10500	0.004	10385	0.001
10500-11000	0.004	10885	0.001
11000-11500	0.004	11385	0.001
11500-12000	0.004	11885	0.001
12000-12500	0.004	12385	0.001
12500-13000	0.004	12885	0.001
13000-13500	0.004	13385	0.001
13500-14000	0.004	13885	0.001
14000-14500	0.004	14385	0.001
14500-15000	0.004	14885	0.001
15000-15500	0.004	15385	0.001
15500-16000	0.004	15885	0.001
16000-16500	0.004	16385	0.001
16500-17000	0.004	16885	0.001
17000-17500	0.004	17385	0.001
17500-18000	0.004	17885	0.001
18000-18500	0.004	18385	0.001
18500-19000	0.004	18885	0.001
19000-19500	0.004	19385	0.001
19500-20000	0.004	19885	0.001
20000-20500	0.004	20385	0.001
20500-21000	0.004	20885	0.001
21000-21500	0.004	21385	0.001
21500-22000	0.004	21885	0.001
22000-22500	0.004	22385	0.001
22500-23000	0.004	22885	0.001
23000-23500	0.004	23385	0.001
23500-24000	0.004	23885	0.001
24000-24500	0.004	24385	0.001
24500-25000	0.004	24885	0.001
25000-25500	0.004	25385	0.001
25500-26000	0.004	25885	0.001
26000-26500	0.004	26385	0.001
26500-27000	0.004	26885	0.001
27000-27500	0.004	27385	0.001
27500-28000	0.004	27885	0.001
28000-28500	0.004	28385	0.001
28500-29000	0.004	28885	0.001
29000-29500	0.004	29385	0.001
29500-30000	0.004	29885	0.001
30000-30500	0.004	30385	0.001
30500-31000	0.004	30885	0.001
31000-31500	0.004	31385	0.001
31500-32000	0.004	31885	0.001
32000-32500	0.004	32385	0.001
32500-33000	0.004	32885	0.001
33000-33500	0.004	33385	0.001
33500-34000	0.004	33885	0.001
34000-34500	0.004	34385	0.001
34500-35000	0.004	34885	0.001
35000-35500	0.004	35385	0.001
35500-36000	0.004	35885	0.001
36000-36500	0.004	36385	0.001
36500-37000	0.004	36885	0.001
37000-37500	0.004	37385	0.001
37500-38000	0.004	37885	0.001
38000-38500	0.004	38385	0.001
38500-39000	0.004	38885	0.001
39000-39500	0.004	39385	0.001
39500-40000	0.004	39885	0.001
40000-40500	0.004	40385	0.001
40500-41000	0.004	40885	0.001
41000-41500	0.004	41385	0.001
41500-42000	0.004	41885	0.001
42000-42500	0.004	42385	0.001
42500-43000	0.004	42885	0.001
43000-43500	0.004	43385	0.001
43500-44000	0.004	43885	0.001
44000-44500	0.004	44385	0.001
44500-45000	0.004	44885	0.001
45000-45500	0.004	45385	0.001
45500-46000	0.004	45885	0.001
46000-46500	0.004	46385	0.001
46500-47000	0.004	46885	0.001
47000-47500	0.004	47385	0.001
47500-48000	0.004	47885	0.001
48000-48500	0.004	48385	0.001
48500-49000	0.004	48885	0.001
49000-49500	0.004	49385	0.001
49500-50000	0.004	49885	0.001
50000-50500	0.004	50385	0.001
50500-51000	0.004	50885	0.001
51000-51500	0.004	51385	0.001
51500-52000	0.004	51885	0.001
52000-52500	0.004	52385	0.001
52500-53000	0.004	52885	0.001
53000-53500	0.004	53385	0.001
53500-54000	0.004	53885	0.001
54000-54500	0.004	54385	0.001
54500-55000	0.004	54885	0.001
55000-55500	0.004	55385	0.001
55500-56000	0.004	55885	0.001
56000-56500	0.004	56385	0.001
56500-57000	0.004	56885	0.001
57000-57500	0.004	57385	0.001
57500-58000	0.004	57885	0.001
58000-58500	0.004	58385	0.001
58500-59000	0.004	58885	0.001
59000-59500	0.004	59385	0.001
59500-60000	0.004	59885	0.001
60000-60500	0.004	60385	0.001
60500-61000	0.004	60885	0.001
61000-61500	0.004	61385	0.001
61500-62000	0.004	61885	0.001
62000-62500	0.004	62385	0.001
62500-63000	0.004	62885	0.001
63000-63500	0.004	63385	0.001
63500-64000	0.004	63885	0.001
64000-64500	0.004	64385	0.001
64500-65000	0.004	64885	0.001
65000-65500	0.004	65385	0.001
65500-66000	0.004	65885	0.001
66000-66500	0.004	66385	0.001
66500-67000	0.004	66885	0.001
67000-67500	0.004	67385	0.001
67500-68000	0.004	67885	0.001
68000-68500	0.004	68385	0.001
68500-69000	0.004	68885	0.001
69000-69500	0.004	69385	0.001
69500-70000	0.004	69885	0.001
70000-70500	0.004	70385	0.001
70500-71000	0.004	70885	0.001
71000-71500	0.004	71385	0.001
71500-72000	0.004	71885	0.001
72000-72500	0.004	72385	0.001
72500-73000	0.004	72885	0.001
73000-73500	0.004	73385	0.001
73500-74000	0.004	73885	0.001
74000-74500	0.004	74385	0.001
74500-75000	0.004	74885	0.001
75000-75500	0.004	75385	0.001
75500-76000	0.004	75885	0.001
76000-76500	0.004	76385	0.001
76500-77000	0.004	76885	0.001
77000-77500	0.004	77385	0.001
77500-78000	0.004	77885	0.001
78000-78500	0.004	78385	0.001
78500-79000	0.004	78885	0.001
79000-79500	0.004	79385	0.001
79500-80000	0.004	79885	0.001
80000-80500	0.004	80385	0.001
80500-81000	0.004	80885	0.001
81000-81500	0.004	81385	0.001
81500-82000	0.004	81885	0.001
82000-82500	0.004	82385	0.001
82500-83000	0.004	82885	0.001
83000-83500	0.004	83385	0.001
83500-84000	0.004	83885	0.001
84000-84500	0.004	84385	0.001
84500-85000	0.004	84885	0.001
85000-85500	0.004	85385	0.001
85500-86000	0.004	85885	0.001
86000-86500	0.004	86385	0.001
86500-87000	0.004	86885	0.001
87000-87500	0.004	87385	0.001
87500-88000	0.004	87885	0.001
88000-88500	0.004	88385	0.001
88500-89000	0.004	88885	0.001
89000-89500	0.004	89385	0.001
89500-90000	0.004	89885	0.001
90000-90500	0.004	90385	0.001
90500-91000	0.004	90885	0.001
91000-91500	0.004	91385	0.001
91500-92000	0.004	91885	0.001
92000-92500	0.004	92385	0.001
92500-93000	0.004	92885	0.001
93000-93500	0.004	93385	0.001
93500-94000	0.004	93885	0.001
94000-94500	0.004	94385	0.001
94500-95000	0.004	94885	0.001
95000-95500	0.004	95385	0.001
95500-96000	0.004	95885	0.001
96000-96500	0.004	96385	0.001
96500-97000	0.004	96885	0.001
97000-97500	0.004	97385	0.001
97500-98000	0.004	97885	0.001
98000-98500	0.004	98385	0.001
98500-99000	0.004	98885	0.001
99000-99500	0.004	99385	0.001
99500-100000	0.004	99885	0.001

$X/d = 0.47588$ and $1/3 X/d = 0.15863$ mean $d = 2102$ microns.

The density of this mixture was 1.118 g/cm^3 . In certain tests the seeds were used without size selection. In later tests a size fraction was taken. This was $d = 0.218 \text{ cm}$. The density of this fraction was found to be 1.093 g/cm^3 .

Now, when the seeds were placed in water they were observed to swell. This caused the physical properties of the dry state to alter. To follow this swelling process seeds were attached to an indented microscope slide, and covered with water. The diameter of the seed was measured under the microscope at various time intervals. It was observed that after 4 h. soaking the seeds attained a constant steady state diameter.

Distilled water was found to swell the seeds more than tap water. This supported the idea that osmosis was the cause of the swelling.

The ratio $d_{\text{final}}/d_{\text{initial}}$ was found to be nearly constant for all seeds examined. The values were (a) Tap water $d_f/d_i = 1.31$

(b) Distilled water $d_f/d_i = 1.35$

Using this ratio and assuming that water enters the seed and that no material leaves it, the density of the seed may be found thus:

Let $d_f/d_i = z$ and $\rho_s = \text{density of dry seed}$, $\rho = \text{density of water}$

Wt. of seed material/wt. of water = $\frac{\pi d_i^3 \rho_s}{\pi d_f^3 \rho} = \frac{1}{z^3}$

Wt. of swollen particle = $\frac{\pi d_f^3 \rho}{6} = \frac{\pi d_i^3 \rho_s}{6} z^3$

Density of swollen seed = $\rho = \frac{\pi d_i^3 \rho_s}{\pi d_f^3} z^3 = \frac{\rho_s}{z^3}$

Hence, seed density = $\frac{\rho_s}{z^3} = \frac{\rho_s}{(d_f/d_i)^3}$

and 0.055cm.. The material was fluidised using water in the 3" column, the two-dimensional bed and the 3.2cm. tube. Settling tests were also performed in the two-dimensional bed.

Diakon presented many difficulties during the initial tests. This was because electrostatic and surface tension forces caused the particles to aggregate together, to attach to air bubbles and to the walls of the equipment. The presence of fine particles in the suspension also led to a hazy, indeterminate upper boundary to the bed. Consequently, the bed required considerable preparation prior to the tests. The bed material was weighed and then poured into the test section which already contained some liquid, this prevented aggregation on the sides of the equipment. A detergent solution was then poured into the suspension and the particles were left in this solution for some minutes. The detergent had the action of freeing the particles from the air bubbles by altering surface tension forces. This detergent was then washed from the column by flushing using the pump. The fine particles were elutriated and collected at this stage. These were weighed and the true bed weight found. This treatment gave a bed which was free from aggregates and stratification effects.

During fluidisation the water temperature was noted and the bed height recorded for each flowrate. For the tests in the two-dimensional bed the pressure drop across the bed was measured using the water/carbon tetrachloride manometer. The nearest tapping in the column to the top of the bed was opened and the difference in height on the manometer arms was noted. Visual and photographic observations were made during the tests.

Settling measurements were taken by fluidising the suspension to a given height, noting that height and then shutting down the pump. The fall of bed height against time was then noted. This method gave a suspension free of any liquid motion that might be present in a suspension shaken in a tube prior to settling.

If the weight of the dry seeds = x , then the weight of the swollen seeds is given by $x(1 + \frac{V_s}{V_d})$ Hence, for 0.218cm. seeds in tap water, the properties of the swollen state are $d = 0.286$ cm. and $\rho = 1.042$ g/cm³.

The difficulties of measuring the physical properties of a material which reacts to its surrounding fluid will now be apparent. In the case of the seeds the problems have a satisfactory solution. As will be apparent from the chapter on the properties of microorganisms, aggregates the solutions are not so forthcoming for microorganisms.

iv. Microorganisms

The complex properties of the various organisms have already been discussed in Chapter 3. The application of this data to fluidisation and sedimentation will be shown later in the relevant sections.

5.3.2.2 Experimental Methods

The techniques used, the measurements taken and the test preparations made were, as follows:

1. Belloini

This material has been a favourite for liquid fluidisation experiments for many years. Consequently, its behaviour is well documented. The purpose of using Belloini, therefore was that it provided a situation that enabled the equipment and techniques to be evaluated. Belloini was fluidised with water in the 1½" column. A known weight of seeds was placed in the column and the bed height was measured for various liquid flowrates. The water temperature was measured and the unit was operated on closed-circuit flow. These tests were performed for 0.2, 0.3 & 0.6cm. Belloini, starting with a large flowrate and decreasing it progressively.

ii. Diakon

Tests were performed using the two size fractions of 0.055cm.

In the two-dimensional bed a nylon filter cloth screen was used; in all other units a very fine wire mesh screen supported the particles. Hysteresis was investigated by measuring the bed height with both increasing and decreasing flowrates during the fluidisation.

iii. Mustard Seeds

The seeds were fluidised in the $1\frac{1}{2}$ " 3" and 3.2cm. columns and in the two-dimensional bed. Water was used as the fluidising liquid, and only swollen seeds were tested. A known weight of dry seeds was placed in a beaker of water and allowed to soak for a given time. The liquid was then discarded and the seeds poured into the test column which contained water. The seeds were then washed by pumping water through the bed. When this was complete the bed was altered to closed-circuit flow and the bed height versus flowrate measurements taken. Bed pressure drops were measured in the two-dimensional bed as for the diakon tests. Wire mesh screens were used to support the seeds in all tests, except where a drilled plate distributor/screen was used in the two-dimensional bed.

Sedimentation tests were performed after fluidising to a given height. The seeds were also sedimented in 500ml. cylinders. In this case a known weight of seeds were placed in the tube and left to soak for a given time. The liquid was then decanted and fresh liquid used to wash the seeds. After several washings the suspension height was measured and the liquid in the tube shaken to suspend the particles uniformly. The tube was placed vertically and the fall of bed height vs. time noted. The suspension volume was then altered and the test repeated several times.

In all tests the water temperature was noted. The effect of different soaking times, size distributions and hysteresis were examined. The latter was especially difficult as a consolidated bed of seeds fluidised unevenly due to aggregation.

iv. Kaolin

A limited number of sedimentation tests were performed on this much investigated material. A known weight of kaolin was placed in a 500ml. cylinder containing a given volume of water at a known temperature. The suspension was dispersed by agitation and then the bed height was measured vs. time. This was repeated for several different volumes.

v. Aspergillus Niger

The primary purpose of this whole investigation was to examine the behaviour of microbial suspensions. The difficulties in quantifying such material ^{have} ~~has~~ already been discussed and these problems were equally apparent in hydrodynamic testing. For the materials so far discussed, the weight of particles in suspension was easily found by direct weighing. This is not possible for microbial suspensions because of their variable wet state. Therefore, an indirect method was used based on the microbial properties obtained earlier.

In the case of A. Niger the dry weight of the bed was measured and knowing the amount of liquid associated with the pellets an estimate of the effective wet weight and volume could be made. For certain tests an estimate of the average terminal velocity was made by timing the fall of an isolated pellet in water, at a known temperature, several times. A more accurate average could be obtained by extrapolation or regression of the voidage vs. flowrate data. Initially, the A. Niger pellets were tested in the two-dimensional bed using the DCL micropump and the drilled plate distributor. In later tests, the 3.2 cm. column was used where a more constant liquid temperature could be achieved. Water was used in both cases. A suspension of pellets was poured into the column and water was pumped through the bed. When the bed was stably fluidised to the maximum height the flowrate was measured and then progressively decreased. At the completion of the tests the pellets were removed from the column and the dry weight determined.

Sedimentation tests were performed in 250ml. cylinders using similar techniques to those above. It was essential that the bed reached equilibrium before any measurements were taken. In the case of microbial suspensions and A. Niger particularly, this could take upto 30 minutes. It was noted that the ^{various} particular materials took progressively longer to reach equilibrium, the order being ballotini, diakon, seeds, yeast and A. Niger. Several different pellet morphologies were tested.

vi. Yeasts

For the yeast tests the bed weight was found indirectly from the centrifuged wet weight. Fluidisation tests were performed in the 3.2 cm. tube; settling tests in a 500ml. cylinder. Due to the flocculent nature of the organism strict pH and temperature control was necessary. Therefore for fluidisation the liquid temperature was controlled using a jacket around the column and a Churchill temperature regulator.

In the settling tests the cylinder was placed in a water bath at the appropriate temperature. pH was controlled by using a buffer solution as the suspension medium. Usually, the pH was 4.7; the composition of the buffer being

Glacial Acetic acid	4.05 g/l.
Sodium Acetate	6.8 ...
Hydrated Calcium Sulphate	0.5 g/l.

The specific gravity of this solution was measured using a 25ml. density bottle at the appropriate temperature. The pH was varied for certain tests by altering the ratios of the above chemicals. The procedure for fluidisation tests in the 3.2cm. tube was as follows.

The acetate buffer was prepared and then some of it was pumped into the 3.2cm. tube. A known weight of centrifuged yeast was then suspended in buffer and poured in to the column, whilst a low flowrate of buffer passed through the column. This ensured that there was no blocking of the distributor due to the yeast packing down over the wire screen. Fine particles in the suspension were collected after elution and reweighed.

iv. Kaolin

A limited number of sedimentation tests were performed on this much investigated material. A known weight of kaolin was placed in a 500ml. cylinder containing a given volume of water at a known temperature. The suspension was dispersed by agitation and then the bed height was measured at time. This was repeated for several different volumes.

v. Aspergillus Niger

The primary purpose of this whole investigation was to examine the behaviour of microbial suspensions. The difficulties in quantifying such material has already been discussed and these problems were equally apparent in hydrodynamic testing. For the materials so far discussed, the weight of particles in suspension was easily found by direct weighing. This is not possible for microbial suspensions because of their variable wet state. Therefore, an indirect method was used based on the microbial properties obtained earlier.

In the case of A. Niger the dry weight of the bed was measured and knowing the amount of liquid associated with the pellets an estimate of the effective wet weight and volume could be made. For certain tests an estimate of the average terminal velocity was made by timing the fall of an isolated pellet in water at a known temperature, several times. A more accurate average could be obtained by extrapolation or regression of the volume vs. flowrate data. Initially, the A. Niger pellets were tested in the two-dimensional bed using the DCP micropump and the fluidised state distributor. In later tests, the 322 cm. column was used where a more constant liquid temperature could be achieved. Water was used in both cases. A suspension of pellets was poured into the column and water was pumped through the bed. When the bed was stably fluidised to the maximum height the flowrate was measured and then progressively decreased. At the completion of the tests the pellets were removed from the column and the dry weight determined.

Thus, a uniform bed whose behaviour could be measured was produced (see Plate 5.5). Bed height versus flowrate measurements were taken using the decreasing flowrate technique. The effects of temperature and pH on the fluidisation were measured for various yeast strains. A similar procedure in the settling tests was followed as before.

vii. Activated Sludge

A limited number of settling tests were performed with the sludge. The sludge was placed in a 1000ml. cylinder and the suspension height vs. time measured. The liquid temperature was measured and the suspension was filtered and the dry weight found. The experiments were repeated using different dry weights of sludge.

vi. Yeasts

Several different pellet morphologies were tested.

For the yeast tests the bed weight was found indirectly from the centrifuged wet weight. Fluidisation tests were performed in the 3.2 cm. tube; settling tests in a 500ml. cylinder. Due to the flocculent nature of the organism strict pH and temperature control was necessary. Therefore for fluidisation the liquid temperature was controlled using a jacket around the column and a Churchill temperature regulator.

In the settling tests the cylinder was placed in a water bath at the appropriate temperature. pH was controlled by using a buffer solution as the suspension medium. Usually, the pH was 4.7; the composition of the buffer being

Glacial Acetic acid 4.05 g/l.

Sodium Acetate 6.8 ...

Hydrated Calcium Sulphate 0.5 g/l.

The specific gravity of this solution was measured using a 25ml. density bottle at the appropriate temperature. The pH was varied for certain tests by altering the ratios of the above chemicals. The procedure for fluidisation tests in the 3.2cm. tube was as follows.

The acetate buffer was prepared and then some of it was pumped into the 3.2cm. tube. A known weight of centrifuged yeast was then

suspended in buffer and poured in to the column, whilst a low flowrate of buffer passed through the column. This ensured that there was no blocking of the distributor due to the yeast packing down over the wire screen.

The particles in the suspension were collected after elution and reweighed.

5.4 Experimental Results and Analysis

The results of the fluidisation and sedimentation tests on each material so far mentioned will now be discussed and analysed. Detailed results may be found in Appendix A.

Throughout the presentation certain theoretical and empirical expressions will be used. Whilst they have already been discussed in the Literature survey, they are summarised below for convenience.

5.4-1 Summary of the relevant equations

1. Calculation of the terminal velocity, U_t

The function $C_{dt} Re_t^2 = \frac{4}{3} \frac{d^3 \rho g (\rho_s - \rho)}{\mu^2}$ was evaluated. Then Re_t and hence U_t was found using the plot $C_{dt} Re_t^2$ vs. Re_t . (see 5.2-6).

2a. Minimum Fluidisation Velocity, U_{mf}

Four methods are available, the first two based on the Carmen-Kozeny equation.

$$\text{Now, } U_{mf} = \frac{0.0055 e_{mf}^3 d^2 (\rho_s - \rho) g}{(1 - e_{mf}) \mu} \quad (\text{see 5.2-12})$$

$$\text{and i. } U_{mf} = \frac{0.0044 g d^2 (\rho_s - \rho)}{\mu} \quad \text{Davidson-Harrison, } e_{mf} = 0.476$$

$$\text{ii. } U_{mf} = \frac{0.0081 g d^2 (\rho_s - \rho)}{\mu} \quad \text{Rowe 2, } e_{mf} = 0.435 \quad (5.2-13).$$

$$\text{iii. } Re_{mf} = \sqrt{33.7^2 + 0.041 G_a} - 33.7 \quad \text{Wen-Yu, based on Ergun eqn.,} \\ (\text{see 5.2-16}).$$

$$\text{iv. } \frac{C_{Dmf}}{C_{Dt}} = \frac{U_t^2}{U_{mf}^2} = 68.5 \quad \text{Rowe 1, (see 5.2-14).}$$

2b. Fluidisation Equations

The principal equations considered are,

$$\begin{aligned} \text{i. Richardson-Zaki model} \quad U / U_t &= e^n \\ n &= (4.45 + 18 d/D) Re_{pt}^{-0.1} \quad 1 < Re_{pt} < 200 \\ n &= 4.45 Re_{pt}^{-0.1} \quad 200 < Re_{pt} < 500 \\ n &= 2.39 \quad Re_{pt} > 500 \\ n &= 4.65 \quad 0.2 < Re_{pt} \\ \log U' &= \log U_t - d/D \quad (\text{see 5.2-18 to 5.2-22}). \end{aligned}$$

ii. Happel model

$$\frac{U}{U_t} = \frac{3 - \frac{1}{2}(1-e)^{1/3} + \frac{1}{2}(1-e)^{5/3} - 3(1-e)^2}{3 + 2(1-e)^{5/3}} \quad (\text{see 5.2-23}).$$

3a. Pressure Drop across the bed

$$\Delta P = (\rho_s - \rho)g(1-e)A = \frac{W(\rho_s - \rho)g}{\rho_s} \quad (\text{see 5.2-11}).$$

3b. Friction Factor plots

These are based on the Richardson-Mielke plots.

$$\psi = \frac{e^3(\rho_s - \rho)g}{5\rho U^2} \quad (\text{see 5.2-34,35})$$

$$Re' = \frac{U\rho}{5\mu(1-e)}$$

4a. Froude No. criterion

$$Fr = U_{mf}^2 / gd \quad ; < 1 \text{ for particulate systems, (see 5.2-10).}$$

4b. Equivalent Bubble size

Using the Harrison - DeKock equation, where $D/d < 1$ for particulate systems

$$\frac{De}{d} = 71.3 \left(\frac{\mu^2}{gd^3\rho^2} \right) \left(\frac{\rho_s - \rho}{\rho_s - \rho_{mf}} - e_{mf} \right) \left[\left(1 + \frac{gd^3\rho(\rho_s - \rho)}{54\mu^2} \right)^{1/2} - 1 \right] \quad (\text{see 5.2-31}).$$

4c. Bed Stability

Using the criterion of Rowe.

$$\frac{\Delta U}{\Delta \delta} = \frac{gd^2(\rho_s - \rho)}{18\mu(1 + 0.25 Re_p^{0.687})} \times \frac{0.68}{(0.68 + \delta)^2} \quad (\text{see 5.2-33}).$$

5. Stratification Criteria

In certain beds stratification is possible. The criteria developed for this are given below. Let the largest particle be represented by 1.

i. $d_1 / d_2 > 1.3$ or 1.41 for stratification, based on Wen-Yu

or Jottrand respectively.

ii. $(\rho_{b1} - \rho_{b2}) = (\rho_s - \rho) e_1 \left(\left(\frac{d_1}{d_2} \right)^{(3-m)m} - 1 \right)$ based on Pruden, (see 5.2-41 to 5.2-43).

For each material all or some of the above criteria will be evaluated. The majority of the results will be presented in graphical form, sample results being given in tabular form in Appendix A.

Results and Analysis for Individual Materials

5.4-2 Ballotini Results

Using this classical material, water fluidisation tests were performed in the 1½" column on 0.2, 0.3 & 0.6 cm. diameter particles. For such systems, the bed voidage may be calculated using

$$e = 1 - W / AL \rho_s \dots\dots\dots 5.4.1$$

For the appropriate fluid conditions the particle terminal velocities were calculated as follows,

Table 5.4.1 Ballotini Terminal Velocities

Size, cm.	Re _{pt}	U _t , cm/s.
0.2	540	29.4
0.3	1050	36.1
0.6	3000	51.8

1. The effect of U on voidage

The results for all particle sizes are shown in Fig. 5.13 and given in Appendix A. The results were seen to be in good agreement with the Richardson-Zaki equation. The index "n" was in all cases = 2.39, as Re_{pt} was always greater than 500. The wall effect correction was found thus,

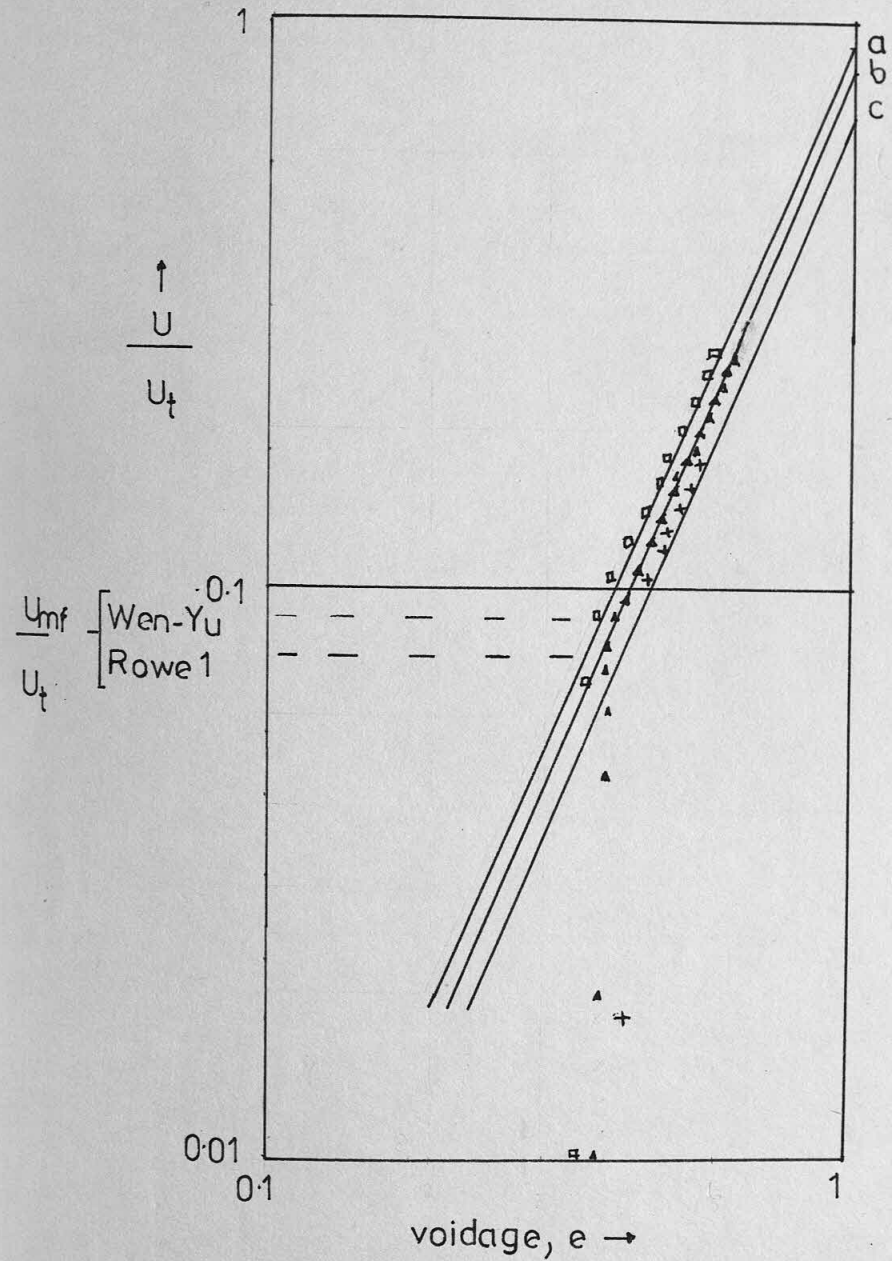
Table 5.4.2 Wall-effect correction for Ballotini

Size, cm.	d / D	U' / U _t at e = 1
0.2	0.053	0.89
0.3	0.079	0.84
0.6	0.158	0.70

2. U_{mf} values and Froude No.

The values for the minimum fluidisation velocity were computed using the various methods and compared to the observed value. Froude No. values are also shown in Table 5.4.3. The results indicate that the methods using the laminar flow Carmen-Kozeny equation (i.e. Rowe 2 & Davidson-Harrison) do not give accurate results when the flow is turbulent.

FIG 13 BALLOTINI FLUIDISATION



Richardson-Zaki	Data
a 0.2 cm ballotini	□
b 0.3	▲
c 0.6	+

n=239

2.4.2 Ballotini Results

Using this classical material, water fluidisation tests were performed in the 18" column on 0.2, 0.3 & 0.6 cm. diameter particles. For such systems, the bed voidage may be calculated using

$$e = 1 - W / A \rho_s$$

For the appropriate fluid conditions the particle terminal velocities were calculated as follows,

Table 2.4.1 Ballotini Terminal Velocities

Size, cm.	Re _{pt}	U _t , cm/s.
0.2	240	29.4
0.3	1020	36.1
0.6	3000	51.8

1. The effect of U on voidage

The results for all particle sizes are shown in Fig. 2.13 and given in Appendix A. The results were seen to be in good agreement with the Richardson-Zaki equation. The index "n" was in all cases = 2.39, as Re_{pt} was always greater than 500. The wall effect correction was found

Table 2.4.2 Wall-effect correction for Ballotini

Size, cm.	U _t / U _t at e = 1	U _t / U _t at e = 1
0.2	0.92	0.92
0.3	0.97	0.97
0.6	0.98	0.98

2. U_{mf} values and Fronds No.

The values for the minimum fluidisation velocity were computed using the various methods and compared to the observed value. Fronds No. values are also shown in Table 2.4.3. The results indicate that the methods using the laminar flow Carman-Kozeny equation (i.e. Rowe 2 & Richardson-Zaki) do not give accurate results when the flow is turbulent.

The Ergun based formula (Wen-Yu) was the more consistently accurate for ballotini. The values of e_{mf} are also much lower than those used by Rowe or Davidson, who assumed $0.43 < e_{mf} < 0.476$;whereas the results indicated $0.35 < e_{mf} < 0.43$.

Table 5.4.3 Ballotini Minimum Fluidisation Velocity

d, cm.	U_{mf} , cm/s.				Froude No.	e_{mf} expt.
	experiment	Rowe1	Rowe2	Wen-Yu		
0.2	2.53	1.80	4.87	2.27	0.033	0.355
0.3	3.18	2.72	9.65	3.15	0.034	0.39
0.6	5.44	5.2	39.5	5.25	0.050	0.43

The fluidisation was clearly particulate as $Fr < 1$. Visually the fluidisation did not appear smooth, as waves were seen passing through the bed of particles.

3. Bed pressure drop and Friction Factor

The theoretical fluidised bed pressure drop for the 0.3 cm. ballotini was $\Delta P_b = 175g \text{ gcm/s}^2$. This would give a differential manometer height of 25.7 cm. CCl_4 .

The Richardson-Meilke analysis was evaluated thus,

Now, for 0.3cm. ballotini the specific surface of solids, $S = 6/0.3$
 $= 20 \text{ cm}^2/\text{cm}^3$. Hence, $\psi = \frac{e^3(2.4-1)g}{20 U^2} = 68.67 e^3 / U^2$
 and $Re' = \frac{U}{20 \times 0.01 (1-e)} = 5 U / (1-e)$

The results are shown in Table 5.4.4 and in Fig. 5.14 and may be compared with the proposed equations. It can be seen that the results for the fluidised bed agree very well with the proposed correlation. However, a marked deviation occurs when the bed ceases to be fluidised.

4. The Quality of the fluidisation

(i) For 0.3 & 0.6 cm. ballotini the equivalent bubble sizes are given by the Harrison-DeKock equation as,

Size, cm.	De , cm.
0.3	0.0043
0.6	0.0102

(ii) The Rowe stability criterion for the 0.3cm. ballotini system may be evaluated ^{for} the condition where all the particles are touching, i.e. $x/d = \delta = 0$ and just being fluidised, $U = U_{mf}$. Thus, $\frac{\Delta U}{\Delta \delta} = 150$ for this condition. This implies that for the ballotini systems used the particle concentration was uniform all through the bed.

Table 5.4.4 Richardson-Meilke analysis - Ballotini, 0.3cm.

U cm/s	e	Re'	ψ
7.4	0.577	87.47	0.241
7.1	0.566	81.8	0.247
6.8	0.554	76.23	0.253
6.2	0.533	66.38	0.270
5.03	0.487	49.02	0.313
4.44	0.455	40.73	0.328
3.85	0.424	33.42	0.353
3.55	0.405	29.83	0.362
3.4	0.397	28.19	0.372
2.66	0.388	21.73	0.566
1.48	0.382	11.97	1.748
0.74	0.382	5.99	6.990

5. Stratification

An elementary experiment was performed to investigate stratification in a bed consisting of the three sizes of ballotini. Known weights of the three sizes were mixed and then fluidised in the $1\frac{1}{2}$ " column. Bed height and flowrate readings were taken.

For a given flowrate the total bed height was predicted by summing the bed heights for each size that was predicted by the Richardson-Zaki equation.

$$\text{For component } i, L_i = \frac{x_i}{(1-e_i)A\rho_s} \dots\dots\dots 5.4.2$$

Example

For $U = 7.4$ cm/s., then

$$i. \text{ 0.2cm. particles } x = 500g; \rho_s = 2.68 \text{ g/cm}^3$$

$$U/U_t = 0.252 ; e = 0.58 \text{ from Richardson-Zaki, } \therefore L = 39.31\text{cm}$$

The diagram based formula (Wen-Yu) was the more consistently accurate for ballotini. The values of e are also much lower than those used by Rowe or Davidson, who assumed $0.43 < e < 0.476$; whereas the results indicated $0.35 < e < 0.43$.

Table 5.4.3 Ballotini Minimum Fluidisation Velocity

d, cm	U _{mf} , cm/s	U _{mf} , cm/s			e _{mf}
		Wen-Yu	Rowe	experiment	
0.2	2.53	1.80	4.87	2.27	0.352
0.3	3.18	2.72	9.62	3.12	0.39
0.6	5.44	5.2	39.2	5.25	0.43

The fluidisation was clearly particulate as first. Visually the fluidisation did not appear smooth, as waves were seen passing through the bed of particles.

3. Bed pressure drop and friction factor

The theoretical fluidised bed pressure drop for the 0.3 cm. ballotini was $\Delta P = 1752 \text{ g/cm}^2 \text{ s}^2$. This would give a differential manometer height of 25.7 cm. CO₂.

The Richardson-Meilke analysis was evaluated thus,

$$\text{Now, for 0.3cm. ballotini the specific surface of solids, } S = 6/0.3 = 20 \text{ cm}^2/\text{cm}^3. \text{ Hence, } \psi = \frac{e^2(1-e)^{-1.75}}{20 \times 1.75} = 0.27 \times 10^{-2} \text{ and } Re' = \frac{U}{20 \times 0.3(1-e)} = 5.7(1-e)$$

The results are shown in Table 5.4.4 and in Fig. 5.14 and may be compared with the proposed equations. It can be seen that the results for the fluidised bed agree very well with the proposed correlation. However, a marked deviation occurs when the bed ceases to be fluidised.

4. The quality of the fluidisation

(i) For 0.3 & 0.6 cm. ballotini the equivalent bubble sizes are given by the Harrison-Leck equation as,

d _b , cm	d _{eq} , cm
0.0043	0.3
0.0102	0.6

ii. 0.3cm. particles

$$x = 200g ; \rho_s = 2.4 \text{ g/cm}^3 ;$$

$$U / U_t = 0.205 ; e = 0.56 ; L = 16.42 \text{ cm.}$$

iii. 0.6 cm particles

$$x = 200g ; \rho_s = 2.45 \text{ g/cm}^3 ;$$

$$U / U_t = 0.143 ; e = 0.52 ; L = 15.1 \text{ cm.}$$

Hence, the total predicted height = 70.83 cm.

The experimentally observed height at $U = 7.4 \text{ cm/s}$ was 71 cm.

Similarly, at $U = 5.62 \text{ cm/s}$, the predicted height was 62.1cm and the observed height was 62 cm.

$$\text{Now, } d_b / d_a = 3/2 = 1.5 \text{ and } d_c / d_b = 6/3 = 2$$

Hence, $d_{\text{large}} / d_{\text{small}} = 1.3 \text{ or } 1.41.$

Therefore, the criteria for stratification to occur are satisfied.

Ideally, the particles should be of equal density for this criterion to apply. However, the smallest particle has also the highest density and hence, the particle size at the top of the bed was higher than at the bottom. These results suggest that the criteria of particle size ratios is probably correct. They also indicate that each size fraction behaved independently of the others. Three distinct size zones were formed each obeying its own fluidisation equation. Each zone also fluidised at the predicted U_{mf} for that size.

A stratified bed therefore consists of zones graded by size (or more generally by terminal velocity). The particles with the lowest terminal velocity rest on the top. Each zone fluidises independently of the others and obeys the equations appropriate to a uniform bed of that size.

By considering the bed in total, a comparison with a uniformly sized bed was made. Now, 900g of beads were fluidised with water.

The average properties of the bed were found as follows

$$d(\text{average}) = \frac{(500 \times 0.2) + (200 \times 0.3) + (200 \times 0.6)}{900} = 0.31 \text{ cm.}$$

$$\text{and } \rho_s(\text{average}) = \frac{(500 \times 2.68) + (200 \times 2.4) + (200 \times 2.45)}{900} = 2.57 \text{ g/cm}^3$$

The average U_t was 38.7 cm/s. The Richardson-Zaki index was $n = 2.39$

Table 2.4.4 Richardson-Zaki index analysis - Ballotini, 0.3cm.

U cm/s	e	Re	ψ
7.4	0.577	87.41	0.241
7.1	0.566	81.8	0.247
6.8	0.554	76.23	0.253
6.5	0.533	66.38	0.270
6.03	0.487	49.02	0.313
4.44	0.452	40.73	0.328
3.85	0.424	33.42	0.353
3.55	0.402	29.88	0.362
3.4	0.397	28.19	0.372
2.66	0.368	21.73	0.566
1.48	0.382	11.97	1.148
0.74	0.382	7.99	6.990

Stratification

An elementary experiment was performed to investigate stratification in a bed consisting of the three sizes of ballotini. Known weights of the three sizes were mixed and then fluidised in the 15" column. Bed height and flowrate readings were taken.

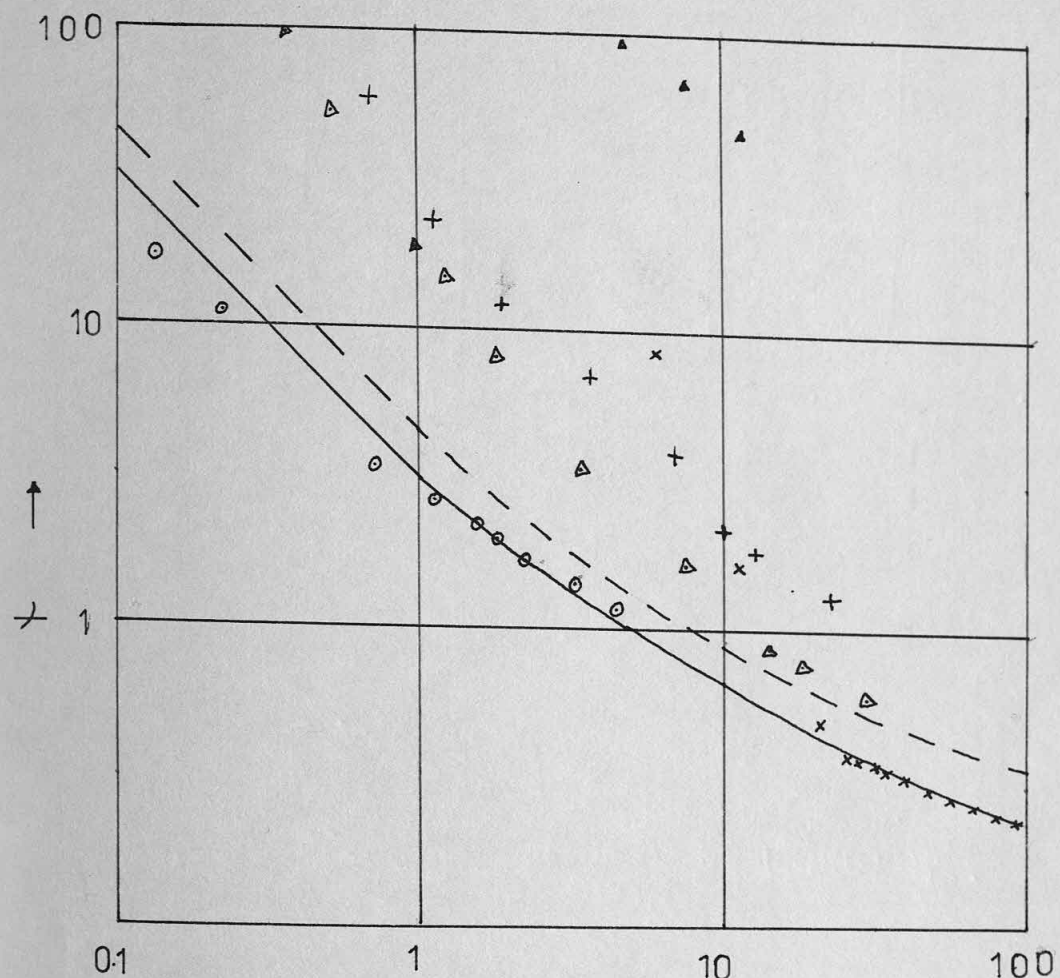
For a given flowrate the total bed height was predicted by assuming the bed heights for each size that was predicted by the Richardson-Zaki equation.

For component i , $U_i = (1 - e_i) A R_i$

For $U = 7.4 \text{ cm/s}$, then

i. 0.3cm. particles $x = 200g ; \rho_s = 2.4 \text{ g/cm}^3$

FIG 5-14 FRICTION FACTOR, ψ vs. BLAKE NO.



BLAKE NO. Re' →

— fluidisation $\psi = 3.36 Re'^{-1}$

- - - packed bed $\psi = 5 Re'^{-1}$

× 0.3 cm. ballotini

o 0.055 cm. diakon

Δ 0.286 cm. seeds < 8 hrs. soak

+ >

▲ CFCC 34 yeast

The average U_f was 38.7 cm/s. The Richardson-Zaki index was $n = 2.35$ and ρ_a (average) = $\frac{(700 \times 1.2) + (200 \times 1.4) + (100 \times 1.6)}{1000} = 1.27$ g/cm³ and ρ (average) = $\frac{(200 \times 0.2) + (200 \times 0.4) + (200 \times 0.6)}{600} = 0.4$ g/cm³. Hence, the total predicted height = 70.83 cm.

At $U_f = 0.143$: $e = 0.92$; $L = 12.1$ cm.

At $U_f = 0.205$: $e = 0.76$; $L = 16.42$ cm.

At $U_f = 0.300$: $e = 0.4$; $L = 2.4$ cm.

Hence, the total predicted height = 70.83 cm.

Similarly, at $U = 2.62$ cm/s, the predicted height was 62.1 cm and the observed height was 62 cm.

Now, $d_p / d_a = 3/2 = 1.5$ and $d_p / d_a = 6/3 = 2$.

Hence, $d_{large} / d_{small} = 1.3$ or 1.61 .

Therefore, the criteria for stratification to occur are satisfied. Ideally, the particles should be of equal density for this criterion to apply. However, the smallest particle has also the highest density and hence, the particle size at the top of the bed was higher than at the bottom. These results suggest that the criteria of particle size ratios is probably correct. They also indicate that each size fraction behaved independently of the others. Three distinct zones were formed each obeying its own fluidisation equations. Each zone also fluidised at the predicted U_f for that size.

A stratified bed therefore consists of zones graded by size (or more generally by terminal velocity). The particles with the lowest terminal velocity rest on the top. Each zone fluidises independently of the others and obeys the equations appropriate to a uniform bed of that size.

By considering the bed in total, a comparison with a uniformly sized bed was made. Now, 300g of beads were fluidised with water. The average properties of the bed were found as follows

ρ (average) = $\frac{(200 \times 0.2) + (200 \times 0.4) + (200 \times 0.6)}{600} = 0.4$ g/cm³

and ρ_a (average) = $\frac{(700 \times 1.2) + (200 \times 1.4) + (100 \times 1.6)}{1000} = 1.27$ g/cm³

The results revealed that the stratified bed had a voidage greater than that predicted by the Richardson-Zaki equation based on the average properties. This deviation, whilst small, may be common to stratified systems. This will be examined further for other materials.

Summary

The experimentation using ballotini was limited because this material has been fully investigated by others. The results were seen to be in good agreement with the equations in the Literature. This was to be expected, as the equations were derived from work using this or similar material. The data obtained ~~down~~, however, serve as a comparison with that obtained for less well documented systems examined later.

The object of these tests was to observe general trends for an easily quantified material. This was why 0.6cm balls were fluidised in a 1.27cm. diameter tube, a system with a large wall effect which, nevertheless, confirmed the validity of the Richardson-Zaki relationship.

Whilst all systems examined in the ballotini tests were particulate there ~~was~~ ^{were} considerable differences visually in the ~~appearance~~ ^{fluidisation}. An increase of a factor of 2 in the diameter produced an increase of 2.38 times the equivalent bubble size, a change which was apparent visually, the larger particles fluidising less smoothly.

5.4.3 Diakon Results

For this material the following tests were performed,

Fluidisation	3" column	2-dimensional	3.2cm. tube
550 micron	Yes	Yes	Yes
655	Yes	No	No
Sedimentation			
550 micron	No	Yes	No

Fluidisation Tests

1 550 micron particles

i. Fluidisation in 3" column

Several tests were made including some for bed hysteresis.

This was observed to be only significant at low flowrates. The agreement with Richardson-Zaki was very good and the results are shown in Fig. 5.16 and in Appendix A.

ii. Fluidisation in 2- Dimensional bed

Diakon was fluidised by water using a nylon cloth support / distributor. The bed was fluidised using both the decreasing and increasing flowrate procedures. The density of the particles was 1.16 g/cm^3 . The pressure drop across the bed was measured at each flowrate. The results are shown in Fig. 5.17 and given in Appendix A.

1 The effect of U on voidage

The equations of Richardson and Zaki were evaluated in two ways. This was because two possible diameters may have applied to the bed. The first was the sectional diameter of $6" = 15.24 \text{ cm}$. However, the hydraulic mean diameter may have also been correct.

(a) Based on $D = 15.24 \text{ cm}$.

Here $d / D = 0.0036$; $\therefore n = 3.64$ & $U' / U_t = 0.99$ at $e=1$.

(b) Based on H.M.D.

The hydraulic mean diameter for the bed = 2.34cm.

Hence, $d / D = 0.0234$; $\therefore n = 3.91$ & $U' / U_t = 0.95$.

These equations together with all the results for the fluidisation of 550 μ diakon in the 2-dimensional bed are shown in Fig. 5.17.

It can be seen that the data has a slope of $n = 3.64$. Hence, the thin bed behaves exactly as if it were a tube of 6" diameter. Diakon again fluidises exactly in accordance with the predictions of Richardson-Zaki, Rowe & Wen and Yu, excepting for the transition area. This lay in a region between the packed and the fully-fluidised bed and did not obey the Richardson-Zaki equation. The bed appeared to pass through two transition points. The first occurred at the value of U_{mf} , the next when the curve altered slope to agree with the Richardson-Zaki prediction. This region was observed in all Diakon tests and probably represents an intermediate state between the packed and fluidised conditions. No hysteresis was observed, and the theoretical U_t was 1.6 cm/s.

Whilst the Richardson-Zaki model appears to be satisfactory for diakon, other fluidisation models may be compared to the data.

These were, (a) Happel's model
$$\frac{U}{U_t} = \frac{3 - \frac{2}{3}(1-e)^{1/3} + \frac{2}{3}(1-e)^{5/3} - 3(1-e)^2}{3 + 2(1-e)^{5/3}}$$

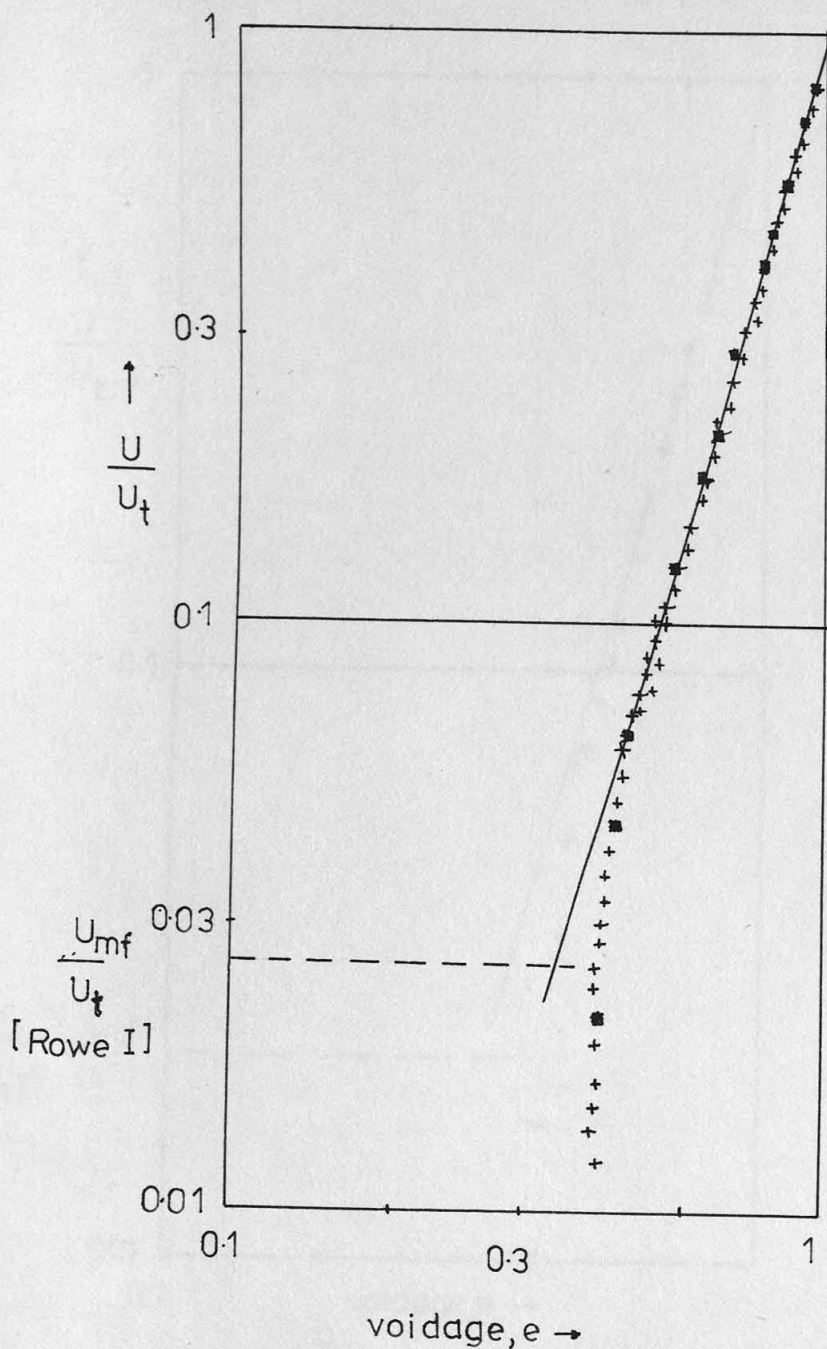
(b) Hawksley-Vand model
$$\frac{U}{U_t} = \frac{e^2}{\exp \left[\frac{2.5(1-e)}{0.61e + 0.39} \right]}$$

(c) Richardson-Mielke model
$$\frac{U}{U_t} = \frac{e^3}{6.72(1-e)}$$

These are shown in Table 5.4-5 and in Fig. 5.17, and may be compared to the accurate model $U / U_t = e^{3.64}$.

From the form of these other three models it was seen that they predicted the same curve irrespective of the system, whereas, Richardson-Zaki varied with each different bed condition. Happel's model was a very bad fit to the diakon data. The others were closer but still not as accurate as Richardson-Zaki. The Richardson-Mielke model had the obvious disadvantage of $U / U_t > 1$.

FIG. 5. 50.065cm. DIAKON FLUIDISED IN 3" DIA. TUBE



Richardson-Zaki $n = 3.66$

+ Data $\rho = 1.123 \text{ g/cm}^3$
 x " " $\rho = 1.16$

(d) Based on H.M.D.

The hydraulic mean diameter for the bed = 2.34cm.

Hence, $d/D = 0.0234$; $n = 3.91$ & $U/U_t = 0.95$.

These equations together with all the results for the fluidisation of

250-diakon in the 2-dimensional bed are shown in Fig. 5.17.

It can be seen that the data has a slope of $n = 3.66$. Hence,

the thin bed behaves exactly as if it were a tube of 6" diameter. Diakon

again fluidises exactly in accordance with the predictions of Richardson-

Zaki, Rowe & Wen and Yu, excepting for the transition area. This lay in a

region between the packed and the fully-fluidised bed and did not obey

the Richardson-Zaki equation. The bed appeared to pass through two

transition points. The first occurred at the value of U/U_t , the next when

the curve altered slope to agree with the Richardson-Zaki prediction.

This region was observed in all Diakon tests and probably represents

an intermediate state between the packed and fluidised conditions.

No hysteresis was observed, and the theoretical U_t was 1.6 cm/s.

Whilst the Richardson-Zaki model appears to be satisfactory

for Diakon, other fluidisation models may be compared to the data.

These were, (a) Happel's model $\frac{U}{U_t} = \frac{3 - \frac{2}{3}(1-e)^{1/3} + \frac{2}{3}(1-e)^{2/3} - 3(1-e)^{5/3}}{3 + 2(1-e)^{2/3}}$

(b) Hawkey-Vand model $\frac{U}{U_t} = \frac{e^2}{\exp[2.5(1-e) + 0.6(1-e)^2]}$

(c) Richardson-Millie model $\frac{U}{U_t} = \frac{e^2}{(e-0.12)(1-e)}$

These are shown in Table 5.4-5 and in Fig. 5.17, and may be compared to

the accurate model $U/U_t = e^{3.66}$.

From the form of these other three models it was seen that they

predicted the same curve irrespective of the system, whereas, Richardson-

Zaki varied with each different bed condition. Happel's model was a

very bad fit to the Diakon data. The others were closer but still not as

accurate as Richardson-Zaki. The Richardson-Millie model had the obvious

disadvantage of $U/U_t > 1$.

FIG. 5.16 0.055cm. DIAKON - 3" DIA. COLUMN

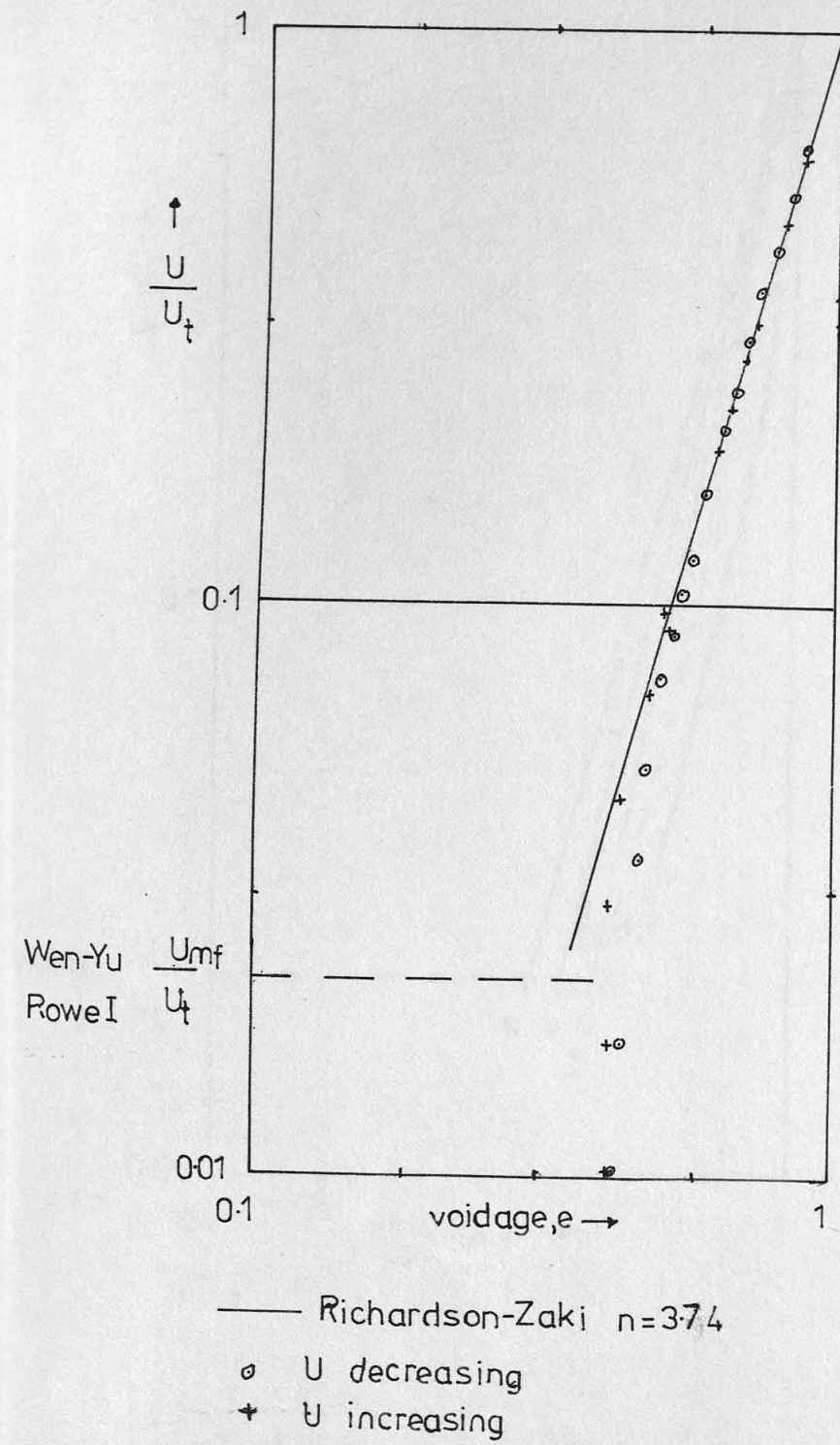


FIG. 5.17 0.055 cm. DIAKON - 2-DIMENSIONAL BED

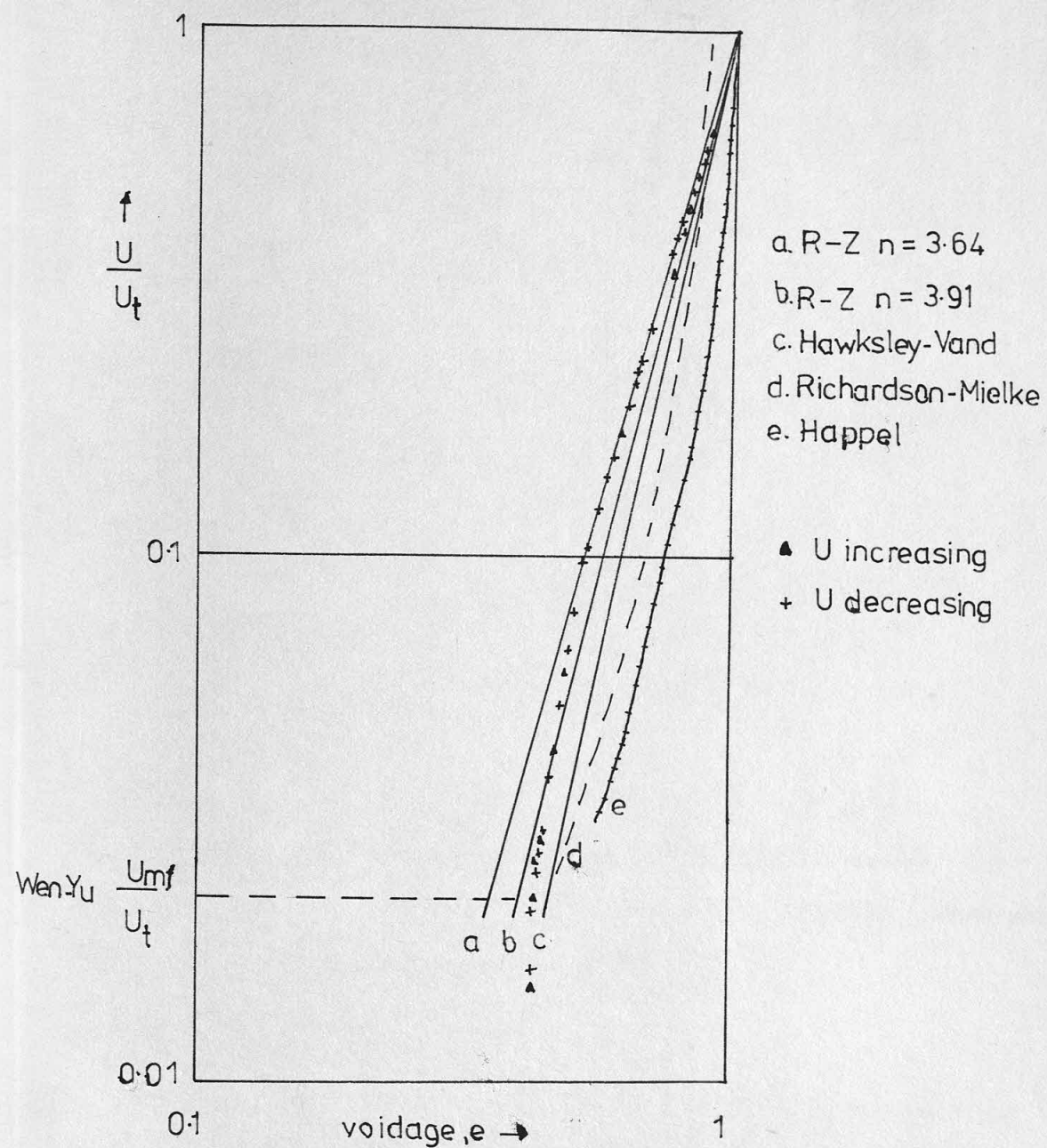


Table 5.4-5 Hydrodynamic Models

'e' values chosen	U / U _t predicted			
	Happel	Hawksley-Vand	Richardson-Mielke	Richardson-Zaki
0.4	0.012	0.015	0.0159	0.044
0.5	0.025	0.041	0.0372	0.091
0.6	0.052	0.096	0.0804	0.166
0.7	0.092	0.196	0.1701	0.283
0.8	0.174	0.362	0.3810	0.450
0.9	0.315	0.620	1.0848	0.680
1.0	1.0	1.0	∞	1.0

2. U_{mf} and Froude No.

The observed value of U_{mf} was 0.036 cm/s. This was compared with the predicted values,

i. Rowe 1

$$Re_{mf} = 0.2; U_{mf} = 0.036 \text{ cm/s}; U_{mf} / U_t = 0.0226.$$

ii. Rowe 2

$$U_{mf} = 0.039 \text{ cm/s}; U_{mf} / U_t = 0.0244.$$

iii. Wen-Yu

$$Re_{mf} = 0.2; U_{mf} = 0.036; U_{mf} / U_t = 0.0226.$$

The theoretical prediction was very accurate for these laminar flow systems. The value of the Froude No. was 0.000024, indicating that the fluidisation was smoother than for the ballotini.

3. Bed pressure drop and Friction Factor

The pressure drop across the bed was measured several times for both increasing and decreasing flowrates. The results are shown in Fig. 5.18. They have the same basic shape as in Fig. 5.5 which was taken from the literature. In all readings taken the bed weight was 400g. Hence, the pressure drop should have been

$$\Delta P_G = 55.86 \text{ g cm s}^{-2} = 55.86 \text{ grams.}$$

This gives a manometer reading of 4.7 cms. CCl_4 , where,

$$h = \frac{\Delta P_G}{(\rho_{\text{CCl}_4} - \rho_{\text{H}_2\text{O}}) g} \quad (\rho_{\text{CCl}_4} = 1.595 \text{ g/cm}^3)$$

The observed average value of ΔP_b was 8.5 % higher than calculated for the fully-fluidised bed. A peak of maximum pressure was observed at $U = 0.063 \text{ cm/s}$, i.e. $U / U_t = 0.039$. There followed a reactionary drop in ΔP_b until a steady state was reached at $U / U_t = 0.084$. Before the maximum ΔP_b peak was reached the pressure curve ceased to be linear when $U / U_t = 0.032$.

The transition between $0.032 < U/U_t < 0.084$, corresponds approximately with the transition between packed and fully-fluidised states shown in Fig. 5.17. Ideally, this region should not be present. It was, however, a recurring feature with the low density diakon system and proved to be even more important in systems of even lower density.

Friction factor plots were drawn using the Richardson-Mielke criteria.

$$\psi = \frac{e^3 g}{U^2} (1.16 - 1) \times \frac{0.055}{6} = 1.439 e^3 / U^2$$

$$Re' = \frac{U}{(1-e)} \frac{0.055}{0.01 \times 6} = 0.9167 U / (1-e)$$

Table 5.4-6 Diakon Friction Factors (550 μ)

U, cm/s	e	Re'	ψ
0.834	0.847	4.997	1.257
0.759	0.818	3.823	1.367
0.642	0.776	2.627	1.631
0.584	0.756	2.194	1.823
0.409	0.667	1.126	2.553
0.300	0.607	0.699	3.576
0.133	0.499	0.243	10.11
0.058	0.433	0.094	34.73
0.028	0.416	0.044	132.1

These results are shown in Fig. 5.14. They lay in a different region to the ballotini results. For $Re' > 1$, the diakon showed good agreement with the Richardson-Meilke results. For $Re' < 1$, the value of ψ was less than predicted at corresponding values of Re' . This corresponds with the deviation observed from Richardson-Zaki in this region.

Table 5.4-5 Hydrodynamic Models

a' values	U / U _t \ Predicted			
	Richardson-Zaki	Happel	Hawkey-Vand	Richardson-Mielke
0.4	0.012	0.012	0.012	0.012
0.5	0.025	0.041	0.041	0.0375
0.6	0.052	0.096	0.096	0.0804
0.7	0.092	0.196	0.196	0.1701
0.8	0.174	0.362	0.362	0.3810
0.9	0.312	0.620	0.620	1.0818
1.0	1.0	1.0	1.0	∞

2. U_{mf} and Fronde No.

The observed value of U_{mf} was 0.036 cm/s. This was compared

with the predicted values,

i. Rowe 1

$$Re'_{mf} = 0.2; U_{mf} = 0.036 \text{ cm/s}; U_{mf} / U_t = 0.0226$$

ii. Rowe 2

$$U_{mf} = 0.039 \text{ cm/s}; U_{mf} / U_t = 0.0244$$

iii. Wen-Yu

$$Re'_{mf} = 0.2; U_{mf} = 0.036; U_{mf} / U_t = 0.0226$$

The theoretical prediction was very accurate for these laminar flow systems. The value of the Fronde No. was 0.00024, indicating that the fluidisation was smoother than for the ballotini.

3. Bed pressure drop and Friction Factor

The pressure drop across the bed was measured several times

for both increasing and decreasing flowrates. The results are shown in Fig. 5.12. They have the same basic shape as in Fig. 5.5 which was taken from the literature. In all readings taken the bed weight was 400g. Hence,

the pressure drop should have been

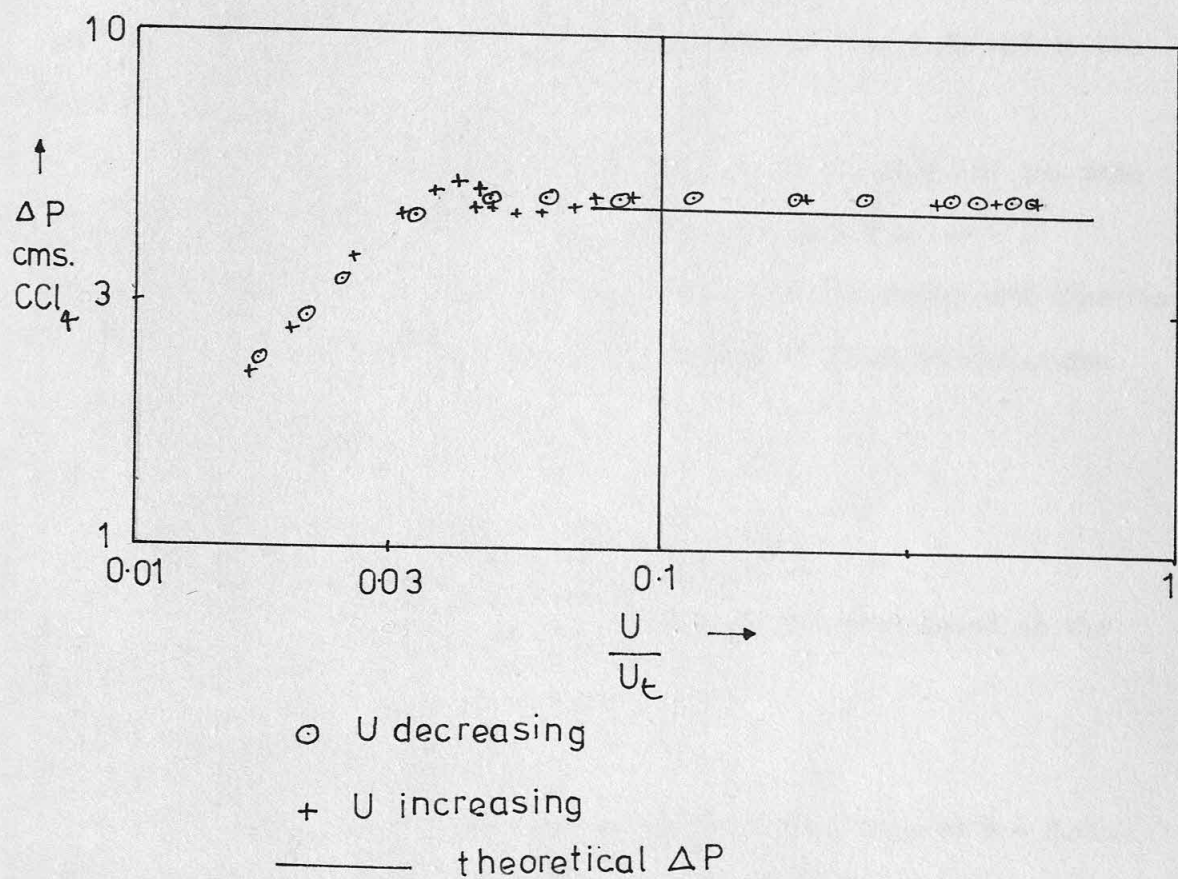
$$\Delta P = 52.866 \text{ gms} = 52.866 \text{ grams}$$

This gives a manometer reading of 4.7 cms. CGF, where,

$$h = \frac{\Delta P}{\rho g} = \frac{52.866}{1.242 \times 9.81} = 4.37 \text{ cms}$$

FIG. 5.18

PRESSURE DROP ACROSS BED OF DIAKON (0.055cm.)
FLUIDISED IN TWO DIMENSIONAL BED



$U, \text{ cm/s}$	e	Re'	ψ
0.028	0.416	0.044	132.1
0.058	0.433	0.094	34.73
0.133	0.499	0.1243	10.11
0.300	0.607	0.699	3.576
0.409	0.667	1.156	2.553
0.584	0.756	2.194	1.823
0.642	0.776	2.627	1.631
0.759	0.818	3.823	1.367
0.834	0.847	4.997	1.257

Table 5.4-6 Diakon Friction Factors (250°)

$$Re' = \frac{U}{(1-e)} \times \frac{0.055}{0.01 \times 0.001} = 0.917 U / (1-e)$$

$$\psi = \frac{e^3}{U^2} (1-e) \times \frac{0.055}{0.01 \times 0.001} = 1.439 e^3 / U^2$$

These results are shown in Fig. 5.14. They lay in a different region to the ballottini results. For $Re' > 1$, the diakon showed good agreement with the Richardson-Melke results. For $Re' < 1$, the value of ψ was less than predicted at corresponding values of Re' . This corresponds with the deviation observed from Richardson-Zaki in this region.

Friction factor plots were drawn using the Richardson-Melke criteria. and proved to be even more important in systems of even lower density. was, however, a resonating feature with the low density diakon system states shown in Fig. 5.17. Ideally, this region should not be present. It approximately with the transition between packed and fully-fluidised The transition between $0.032 < U/U_c < 0.084$, corresponds

$U/U_c = 0.032$. maximum ΔP peak was reached the pressure curve ceased to be linear when in ΔP until a steady state was reached at $U/U_c = 0.084$. Before the $U = 0.063 \text{ cm/s}$, i.e. $U/U_c = 0.032$. There followed a reactionary drop for the fully-fluidised bed. A peak of maximum pressure was observed at The observed average value of ΔP was 8.5% higher than calculated

4. The Quality of fluidisation

The equivalent bubble size, D_e , was calculated thus,
For diakon, $d = 0.055 \text{ cm}$; $e_{mf} = 0.416$; $\rho_s = 1.16 \text{ g/cm}^3$.

$$D_e / d = 0.0396, \text{ i.e. } D_e = 0.0022 \text{ cm.}$$

The value of D_e / d was 17 % less than that obtained for the ballotini.
This confirmed that the diakon bed, with its lower density difference, fluidised more smoothly than the ballotini.

iii. Fluidisation in the 3.2 cm. tube (C1/55)

These tests were to check upon this equipment when testing particles of this size. The results are shown in Fig. 5.20 and in the Appendix A .

The terminal velocity was calculated as 1.6 cm/s and for this column $d / D = 0.0174$. Hence, Richardson-Zaki gave $U/U_t = e^{3.77}$. The results obtained were in good agreement with the theory and therefore the 3.2 cm. tube could be used with confidence in later fluidisation tests.

2 655 micron particles in the 3" column

The results are plotted in Fig. 5.15, and are tabled in the Appendix A .

1. The effect of U on voidage

The Richardson-Zaki equation was evaluated to give $n = 3.66$, with intercept $U'/U_t = 0.98$, where $U_t = 1.58 \text{ cm/s}$. The results were found to be in good agreement with this correlation.

2. U_{mf} and the Froude No.

The observed value of U_{mf} was 0.0395 cm/s. This was compared to

Rowe 1 $U_{mf} = 0.0395 \text{ cm/s}$; Rowe 2 $U_{mf} = 0.041 \text{ cm/s}$;

Wen-Yu $U_{mf} = 0.032 \text{ cm/s}$.

The value of the Froude No. was 0.00002.

FIG. 519 0.055cm. DIAKON SETTLING- 2 DIMENSIONAL BED

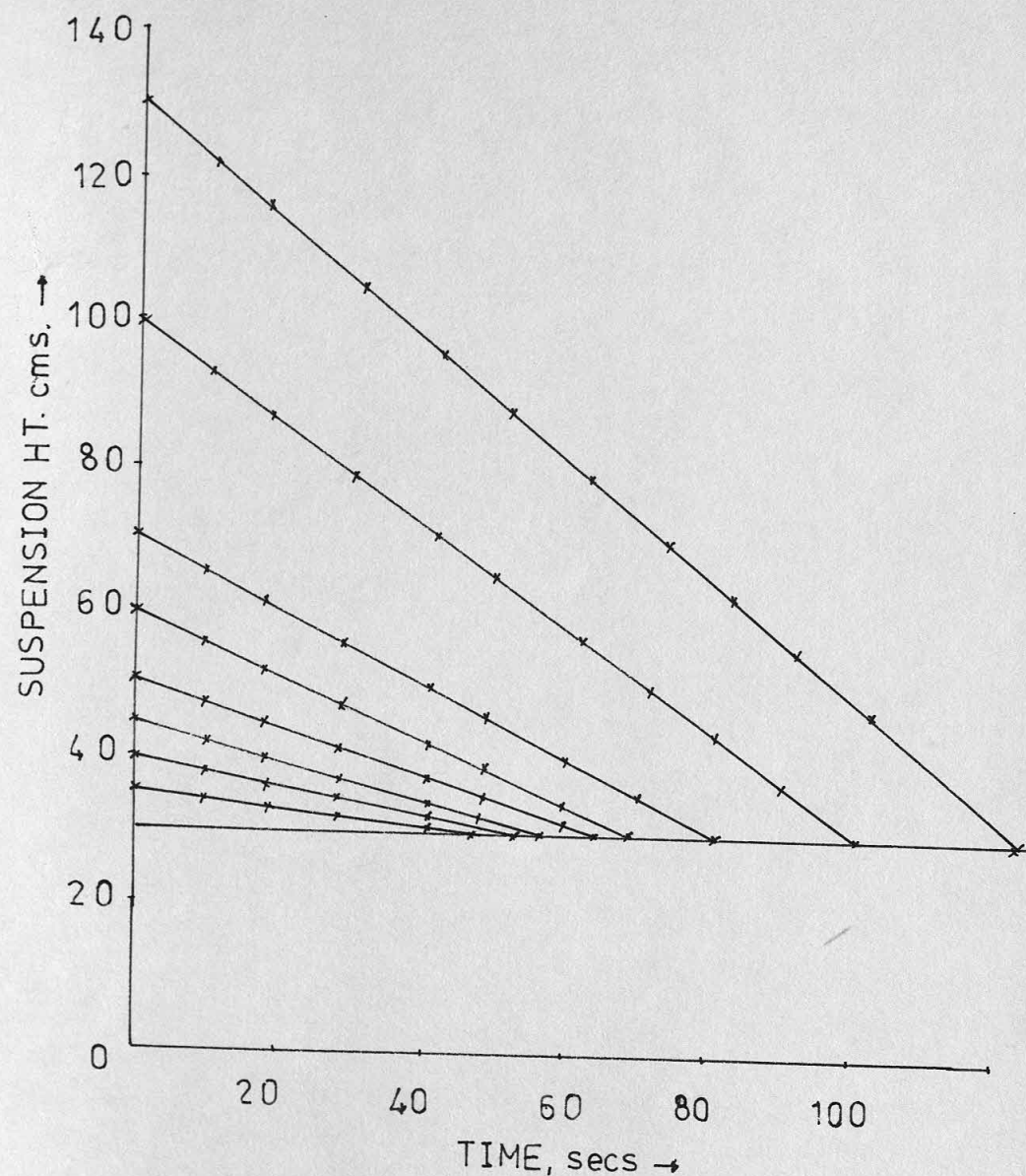
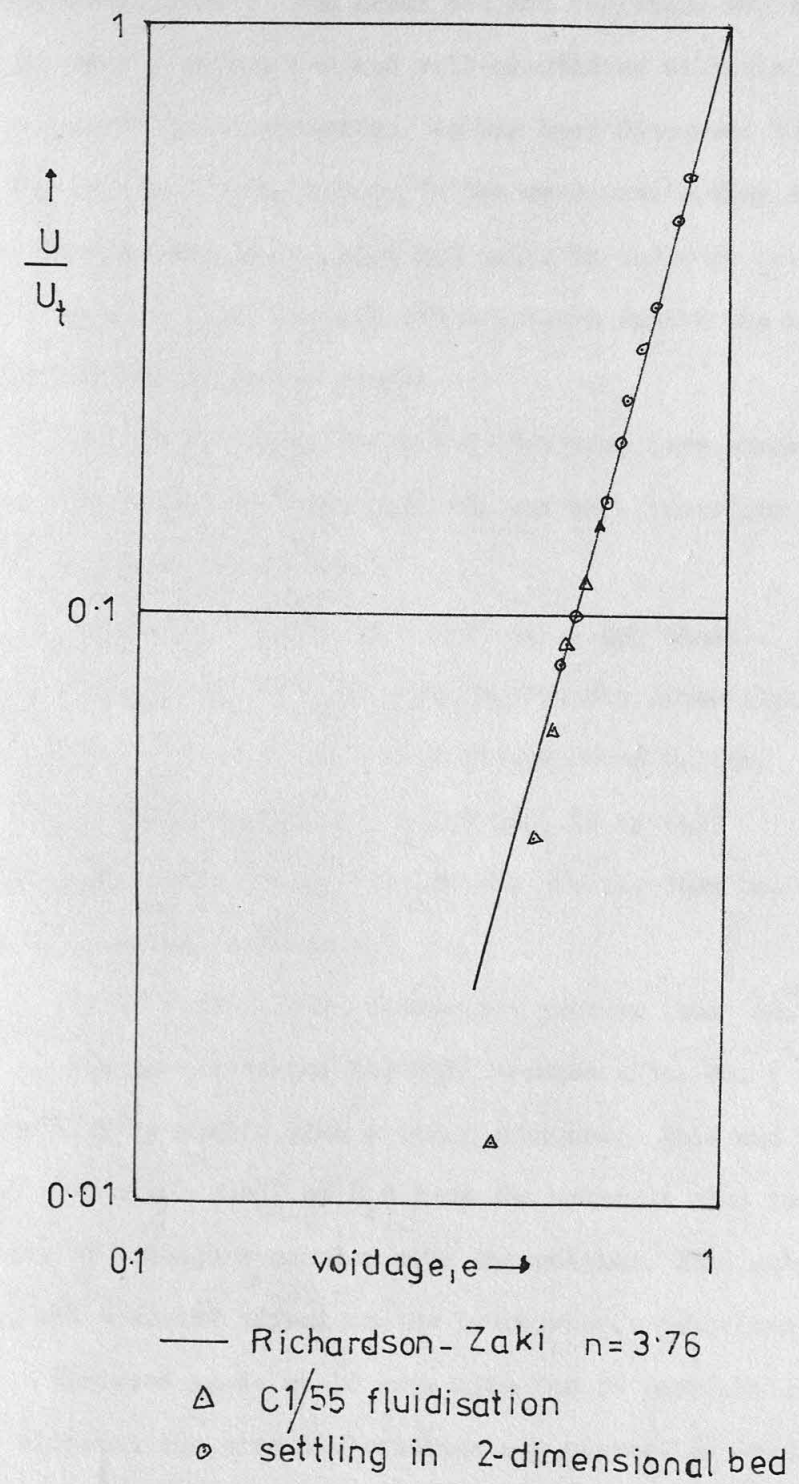


FIG 5.20 0.055 cm. DIAKON SEDIMENTATION



5.4.4 Mustard Seed Results

Introduction

The two previous materials discussed did not interact with their liquid environment. The seeds did and therefore represent a link between the easily understood and well-quantified ballotini or diakon systems and microbial suspensions. As has been discussed the seeds became swollen when placed in tap water. In the crude state they had a size distribution. Four categories of seed bed could be and were investigated. To maintain a logical order through the materials tested the seed systems will be analysed in the following order;

(a) Sieved seeds, $d = 0.218 \pm 0.018$ cm. (dry state).

The seeds were soaked for less than 8h. and were, therefore, uncoated. This state is shown in Plate 5.1.

(b) Unsieved seeds, $d = 0.21$ cm. (dry state).

These were also soaked for less than 8h. The dry state size range was $0.17 < d < 0.33$ cm; although, few were greater than 0.24 cm.

(c) Sieved seeds, $d = 0.218$ cm. (as in (a))

These were soaked for various periods all greater than 8h. and were thus coated, as is shown in Plate 5.1.

(d) Unsieved seeds, soaked for greater than 8h.

The 8h. criterion was made because after 8h. (approx.) the seeds were lightly coated with a tacky substance. This was thought to be a polysaccharide; the smell of H_2S from the solution also indicated the possibility of a sulphur complex with the polymer. This substance, as will be shown, had a marked effect on the hydrodynamic behaviour of the seeds.

Unsieved seeds would have also led to possible stratification effects, although the size distribution was narrow. The seeds systems therefore may be used to simulate both microbial and conventional systems.

The condition of the seeds did not alter between attaining the steady state after 4h. soaking and the onset of polymer emission after 8h.

A. Uncoated, Uniformly sized seeds , d = 0.286 cm.

Tests were performed in the two-dimensional bed , unless stated. The dry state properties were $d = 0.218 \text{ cm}$; $\rho_s = 1.093 \text{ g/cm}^3$.

Now, the swollen diameter, $d' = zd = 1.31d = 0.286 \text{ cm}$.
and the density of the swollen seed = $\rho_p = \frac{\rho_s + (z^3 - 1) \rho}{z^3} = 1.042 \text{ g/cm}^3$.

Bed Voidage

Now, the voidage of a bed of swollen seeds of dry weight = $x \text{ g}$ is given by , $e = \frac{1 - x [1 + (z^3 - 1) \rho / \rho_s]}{A L \rho_p} \dots\dots\dots 5.4.3$

$$\text{hence, } e = 1 - \frac{x z^3}{A L \rho_s} \dots\dots\dots 5.4.4$$

Fluidisation

Known dry weights of seeds were fluidised using water in the two-dimensional bed with a drilled plate distributor. The results were obtained for decreasing and increasing flow situations. Bed pressure drop was monitored using the CCl_4 manometer.

Sedimentation

These tests were performed by fluidising the bed to a given height and then timing the rate of fall against zero flow, as for diakon. The settling curves are shown in Fig. 5.21. It was observed that whilst the seeds fell at constant rate for most of the settling , a consolidation occurred before the final condition was attained. This was unlike the diakon (compare with Fig. 5.19). This bed consolidation occurred in all seed tests, irrespective of their condition. It gave rise to certain characteristics of pressure drop and hysteresis; the degree of bed consolidation affecting both. This behaviour was similar , but less marked, to microbial suspensions and showed again that the seeds were the ideal material for investigating the transition between microbial and usual materials.

The bed voidage was calculated on the basis of the initial bed height before settling. The constant rate of settling was measured and

the results are summarised in Appendix A. The final consolidated voidage after several hours was $e = 0.375$. Fully consolidated beds were fluidised to examine the effects of this consolidation on the subsequent fluidisation. A marked hysteresis was found at low flowrates, together with a larger bed pressure drop. All of these fluidisation/sedimentation results are shown in Fig. 5.22. The pressure drop results are shown in Fig. 5.25.

The pressure drop curves were seen to be different from the classical type (i.e. diakon). When the bed was fully fluidised the bed pressure drop was independent of flowrate and past history. However, bed consolidation had a marked effect on the initial ΔP values. No "hump" in the curve was observed, but the pressure drop during expansion was greater than during contraction.

1. The effects of U on voidage

The results were compared with the Richardson-Zaki model. This was evaluated using both the column diameter and the hydraulic mean value.

i. Based on $D = 15.2$ cm.

$d/D = 0.0188$ and for the seeds $1 < Re_{pt} < 200$;

$$\text{hence, } n = (4.45 + 18d/D) / Re_{pt}^{0.1} \dots\dots\dots 5.2.19$$

Therefore, for $U_t = 4.14$ cm/s, then $n = 3.02$, $U'/U_t = 0.956$.

ii. Based on $HMD = 2.35$ cm

$d/D = 0.122$ and hence, $n = 4.18$ with $U'/U_t = 0.755$.

These curves are plotted in Fig. 5.22. It may be seen that the model based on the HMD correlated the data reasonably well, whereas the other model underestimated the voidage. Diakon showed the reverse behaviour, probably because the particle size was much smaller. Happel's model did not fit the data, but Hawksley-Vand gave reasonable agreement.

2. U_{mf} and the Froude No.

Estimates of U_{mf} were difficult to make due to the effects of the consolidation. A transition in behaviour was observed between $0.04 < U/U_t < 0.05$ and also the bed pressure drop began to stabilise in this region. Hence, this was considered to be the onset of fluidisation.

FIG521

0.286 cm SEEDS [-8 hrs.] SETTLING IN 2-DIMENSIONAL BED
(uncoated uniform size)

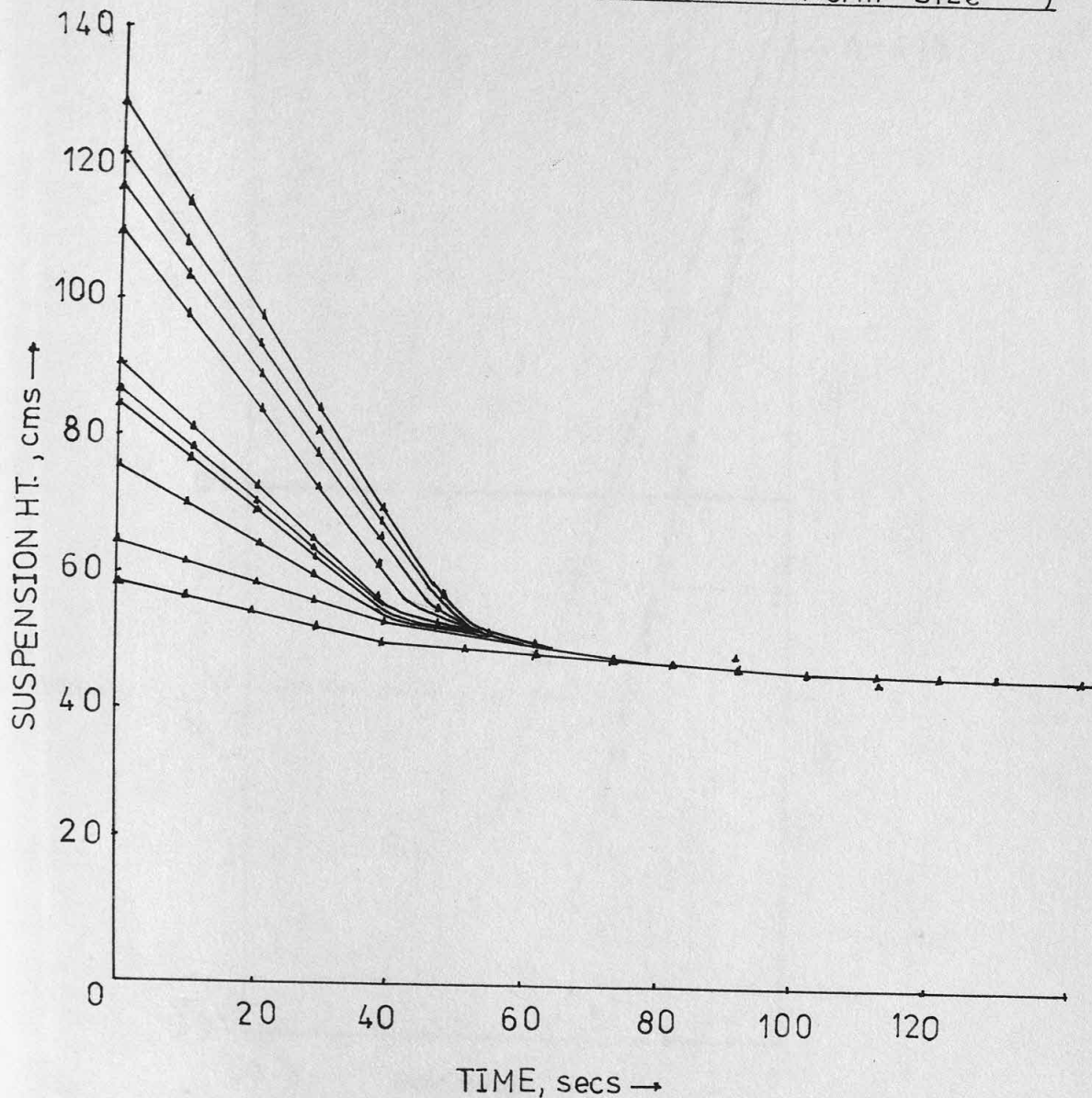
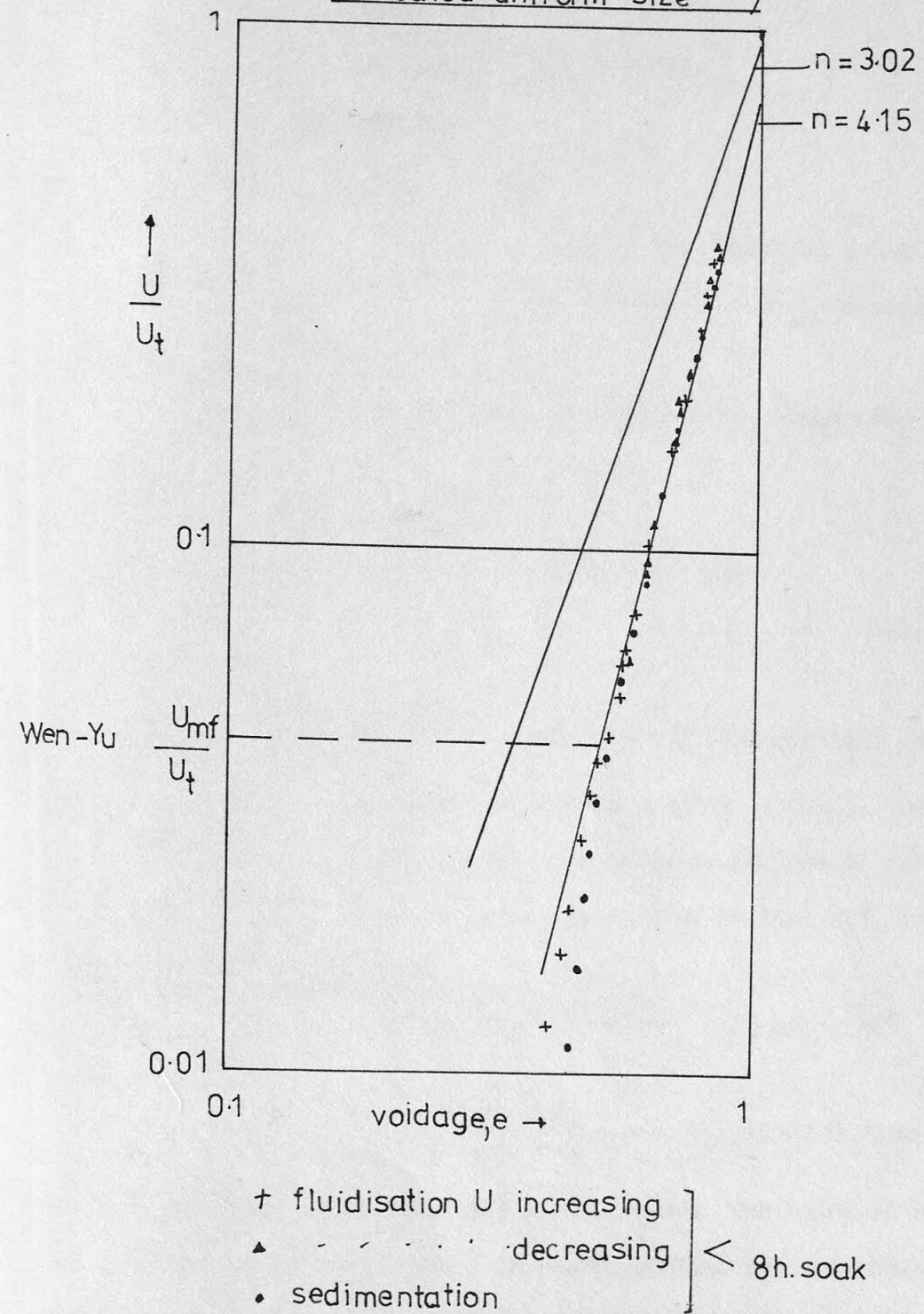


FIG 5.22 0.286cm. SEEDS IN 2-DIMENSIONAL BED
(uncoated uniform size)



The theoretical values of U_{mf}/U_t were,

i. Wen-Yu method

$$Ga = 7.65 \times 10^3; \quad Re_{mf} = 4.4; \quad U_{mf} = 0.178 \text{ cm/s}; \quad U_{mf}/U_t = 0.043.$$

ii. Rowe 1 method

$$Re_{mf} = 3.35; \quad U_{mf} = 0.137 \text{ cm/s}; \quad U_{mf}/U_t = 0.033.$$

iii. Rowe 2 method

$$U_{mf} = 0.285 \text{ cm/s}; \quad U_{mf}/U_t = 0.069.$$

The Wen-Yu equation was the more accurate, the other two being outside the observed transition region. Again, the value of Re_{mf} was higher than permissible in these other two models.

Taking $U_{mf} = 0.18 \text{ cm/s}$, the value of the Froude No. was 0.00011.

3. Pressure drop and Friction Factor

The weight of the wet seeds was found by,

$$W = x (1 + (z^3 - 1) \rho/\rho_s) \dots\dots\dots 5.3.2$$

$$= 2.14 x.$$

$$\text{Hence, as } \Delta P_b = \frac{W(\rho_p - \rho)g}{\rho_p}, \text{ then the bed pressure drop in the tests}$$

would be 22.63g, which gave a manometer reading of 1.9 cm. CCl_4 .

This calculated value was much less than the observed one of 2.8 cm.

Richardson-Mielke analysis was applied to this bed, the particles being considered spheres. Thus,

$$\psi = \frac{e^3 g (1.042 - 1) \times 0.286}{U^2 \times 6} = 1.962 e^3 / U^2$$

$$Re' = \frac{U \times 0.286}{(1 - e) \times 0.01 \times 6} = 4.767 U / (1 - e)$$

These are shown in Table 5.4.7 and in Fig. 5.14. The value of the Friction Factor was considerably in excess of that for conventional materials at corresponding Blake Nos. This reflects the high ΔP values discussed previously.

Table 5.4.7 Richardson-Mielke for uncoated, sieved seeds

U, cm/s	e	Re'	ψ
1.33	0.805	32.51	0.5886
1.03	0.754	19.96	0.7848
0.91	0.731	16.13	0.8829
0.525	0.658	7.32	1.9620
0.209	0.537	2.15	6.7690
0.133	0.514	1.30	15.009
0.057	0.465	0.51	60.430
0.027	0.437	0.23	215.33

4. The Quality of fluidisation

The equivalent bubble size was found by taking $e = 0.52$ and using the appropriate equation. This gave $D_e/d = 0.19$, i.e. $D_e = 0.054$ cm. This high value for D_e/d occurs because of the small density difference between the liquid and the swollen seeds. This result suggests two possibilities:

- The equation, which originated from studies of gas/solid and aggregative liquid fluidised systems, may not apply to very low density difference systems.
- The liquid bubbles are comparatively large for such systems despite the apparently smooth fluidisation.

The Rowe stability criterion was evaluated for $\delta = 0$ and $Re = Re_{mf}$ to give; $\frac{\Delta \psi}{\Delta \delta} = 18.3$ for $Re_{mf} = 4.5$. This was compared to the value of 150.1 for 0.3 cm. ballotini. Clearly, it was possible for voidage differences to be maintained in the bed without total structural collapse.

Once the bed was fully fluidised, then this ratio fell considerably. The bed of seeds fluidised such that particle separation was often unusually large in certain areas, the particles aggregating in others. Whilst the overall voidage was accurately predicted by the Richardson-Zaki model, the presence of void pockets could have been explained by the unusually large D_e/d values and the ability of the bed to maintain such

pockets as shown by the Rowe criterion.

Regression Analysis

In the sections that follow some doubt may be raised as to the validity of classical hydrodynamic theory, because of flocculence, polymer or stratification effects. Hence, the true value of the terminal velocity and the index, n , were found using a least squares regression analysis on the data for each suspension. The "BASIC" programme which was used for this evaluation is shown in Fig.5.23. The accuracy of this method was tested by analysing the diakon data, the regression of which was in good agreement with theory.

B. Uncoated, Multisized seeds, $d = 0.275$ cm.

The dry state properties of the unsieved seeds were average diameter = 0.21cm., $\rho_s = 1.118 \text{ g/cm}^3$. Therefore, the swollen state diameter was 0.275cm with a density = 1.052 g/cm^3 . The results are shown in Appendix A.

1. The effect of U on voidage

For these seeds the calculated value of U_t , based on $d = 0.275$ cm., was 4.8 cm/s. The value of U_t found by regression of the data was 3.92 cm/s., which was the value of U_t used in the Appendix A for these seeds. The results were compared to the Richardson-Zaki prediction and were seen not to agree, as is shown in Fig.5.24. The high voidages observed in this system were also seen in fluidisation tests using the 3.2cm. tube and in sedimentation tests. The deviations were due to the size distribution of the seeds and not to peculiar drag effects. The observed lower value of U_t and the higher voidages at a given flowrate suggested that the small particles had a profound influence on the macroscopic behaviour of the bed. The data could be correlated by $U/U_t = e^{5.57}$.

Table 5.4.7 Richardson-Zaki for uncoated, sieved seeds

U , cm/s	e	Re	ψ
1.33	0.805	32.51	0.5886
1.03	0.754	19.96	0.7848
0.91	0.731	16.13	0.8829
0.525	0.658	7.32	1.3620
0.209	0.537	2.12	6.7690
0.133	0.514	1.30	12.009
0.057	0.465	0.51	60.430
0.027	0.437	0.23	212.33

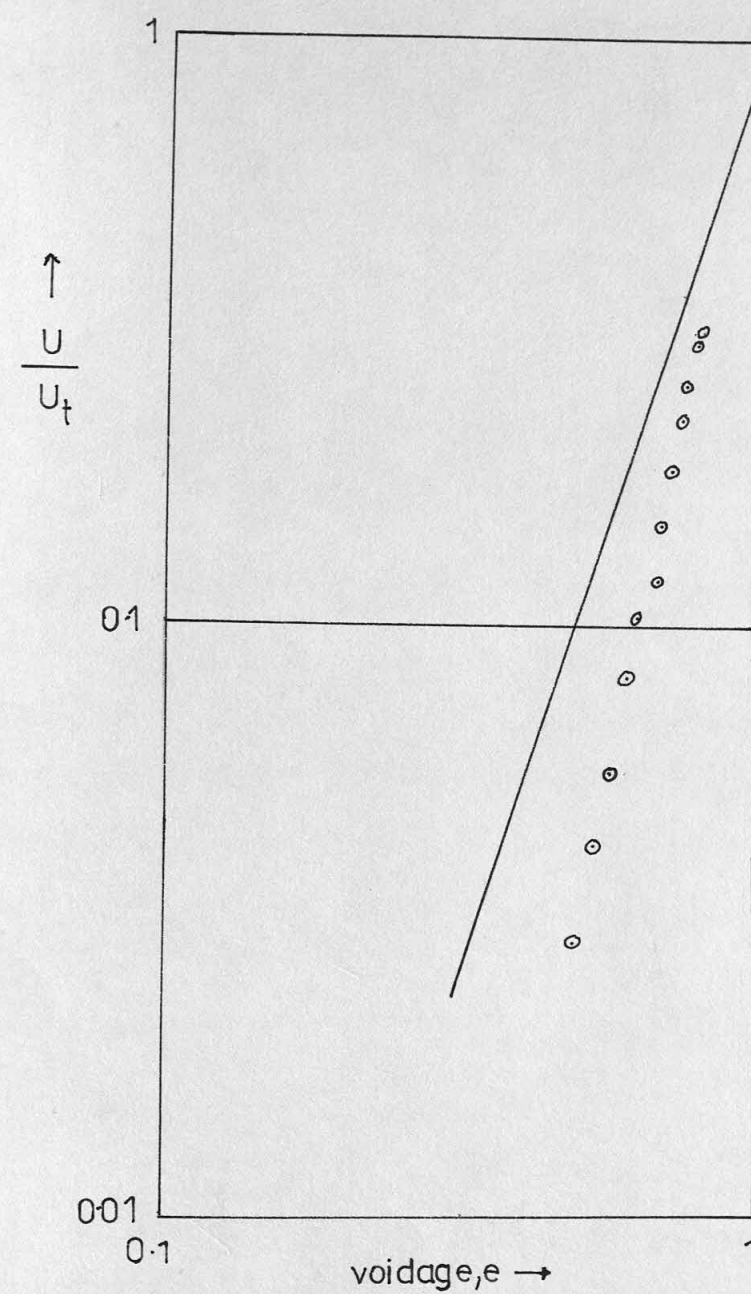
FIG. 5.23.A REGRESSION PROGRAM

```

50 X2=0
60 X3=0
70 X4=0
80 Y2=0
90 Y3=0
110 READ N
120 FOR J=1,N
130 READ A,B
140 X=LOG(A)
150 Y=LOG(B)
160 X2=X2+X*X
170 Y2=Y2+Y*Y
180 X3=X3+X*X*X
190 X4=X4+X*X*X*X
200 Y3=Y3+Y*Y*Y
210 NEXT J
220 X5=X3-N*X2*X2
230 M=(X4-N*X2*Y2)/X5
240 S2=Y3-N*Y2*Y2-M*M*X5
250 V=S2/(N-2)*X5
260 E=V*.5
270 C=Y2-M*X2
280 RESTORE
290 READ N
292 FOR J=1,N
300 READ A,B
310 X=LOG(A)
320 Y6=M*X+C
330 B6=EXP(Y6)
340 PRINT A,B,B6
350 NEXT J
360 PRINT
370 PRINT "SLOPE";1/M;" + OR - ";E/M*.2;"INTERCEPT";EXP(-C/M)
380 END

```


FIG. 5.24 0.275cm seeds IN 3" COLUMN
(uncoated multisized)



— Richardson-Zaki
 ○ 3" column fluidisation
 based on experimental U_t } < 8h soak

2. Stratification Effects

The particle size range for this section was shown in section 5.3-2.1. All particles were assumed to have a density of 1.052 g/cm^3 . the properties of the bed were thus,

Table 5.4.8 Stratified, uncoated seeds; physical properties

number	d, cm. (dry)	d, cm. (wet)	Re_t	U_t , cm/s
1	0.12	0.157	40.5	2.58
2	0.17	0.223	84	3.77
3	0.21	0.275	132	4.8
4	0.335	0.439	315...	7.17

Thus, $d_4/d_1 = 2.79$; $d_2/d_1 = 1.42$; $d_3/d_2 = 1.24$; $d_4/d_3 = 1.60$. and $U_{t4}/U_{t1} = 2.78$; $U_{t2}/U_{t1} = 1.46$; $U_{t3}/U_{t2} = 1.27$; $U_{t4}/U_{t3} = 1.49$.

The various stratification criteria proposed are that for segregation to occur then, $d_a/d_b > 1.4$ or $U_{ta}/U_{tb} > 2$.

The multisized seed system certainly fulfills these requirements overall. However, this system is different from the previously investigated segregated beds in that it consists of a continuous spectrum of particle sizes whereas previously the beds have been composed of a few discrete sizes. This and the low solid-liquid density difference may explained the large deviations caused by the particle size distribution.

C. Coated, Uniformly sized seeds, $d = 0.286 \text{ cm}$.

The sieved seeds were allowed to soak for periods greater than 8h. Whilst the seed diameter did not appreciably alter a sticky substance coated the seeds. Fluidisation tests with the flowrate decreasing were performed in the two-dimensional bed, using water. The results are shown in Appendix A.

1. The effect of U on voidage

The value of U_t was theoretically 4.04 cm/s . The value found

from the data was 2.95 cm/s. The Richardson-Zaki equation, based on the HMD and the theoretical U_t , was evaluated to give $n = 4.16$ with $U'/U_t = 0.755$. This model underestimated the actual voidage at corresponding U/U_t values. The deviation was consistent and quite marked.

Seeds were soaked for 17h. and for 90h.; fluidisation tests being performed on both and settling tests on the former only. All results are shown in Fig. 5.26. The data ^{were} very consistent for all situations and indicated that a stable particle state was achieved during this prolonged soaking. The theoretical terminal velocity was used in this correlation.

2. U_{mf} values

The minimum fluidisation velocity appeared to be 0.17 cm/s.

The theory of Wen & Yu predicted that $U_{mf} = 0.174$ cm/s.

3. Pressure drop and Friction Factor

The theoretical bed pressure drop should have been $\Delta P/W = 0.041$. The pressure drop was considered in this manner in order to compare the pressure drops for all seed states. Now,

$$\Delta P/W = \frac{\Delta P}{\propto [1 + (z^3 - 1) \rho/\rho_s]} \dots\dots\dots 5.4.5$$

where W = mass of wet seeds, g., and ΔP is in grams.

The results are shown in Table 5.4.9 and in Fig. 5.25.

Table 5.4.9 Bed pressure drops for coated, sieved seeds

Seeds condition	$\Delta P/W$	U/U_t , actual
0.286cm, 17h. W = 642g.	0.0704	0.193
	0.0704	0.123
	0.0685	0.086
	0.0650	0.043
	0.0650	0.034
	0.0575	0.024
	0.0496	0.013
	0.0427	0.010
0.286cm., 5h. W = 525g.	0.0635	0.321
	0.0635	0.249

Table 5.4.9 (continued)

Seed condition	$\Delta P/W$	U/U_t , actual
as before	0.0635	0.220
	0.0635	0.081
	0.0612	0.050
	0.0567	0.040
	0.0499	0.025
	0.0453	0.017
	0.0340	0.010

Data from the previous section A is included for comparison. The value of $\Delta P/W$ was consistently larger for the coated seeds and was considerably more than the theoretical value. This was especially true at low flowrates although the difference became less at high flowrates.

The Richardson-Mielke curves were evaluated and are shown in Table 5.4.10

Table 5.4.10 Richardson-Mielke for coated, sieved seeds

U , cm/s	e	Re'	ψ
0.730	0.740	13.38	1.492
0.642	0.736	12.54	2.057
0.560	0.728	9.81	2.414
0.425	0.703	6.82	3.774
0.286	0.639	3.78	6.258
0.184	0.583	2.10	11.48
0.115	0.551	1.22	24.82
0.069	0.515	0.678	56.29
0.027	0.465	0.241	270.6

This is shown in Fig. 5.14. The values are higher than for uncoated seeds as would have been expected considering the large ΔP values obtained with the coated seeds.

Discussion

All this information indicated that the presence of the polysaccharide coating modified the hydrodynamic behaviour of the particles. The actual terminal velocity of the seeds appeared to be 34 % lower than the theoretical value. The higher pressure drop in the fluidised bed also

from the data was 2.25 cm/s. The Richardson-Mielke equation, based on the

0.730 This model underestimated the actual velocity at corresponding

U/U_t values. The deviation was constant and quite marked.

Seeds were soaked for 17h, and for 90h, fluidisation tests being performed on both and settling tests on the former only. All results

are shown in Fig. 5.26. The data was very constant for all situations

and indicated that a stable particle state was achieved during this

pre-soaked soaking. The theoretical terminal velocity was used in this

correlation.

2. U values

The minimum fluidisation velocity appeared to be 0.17 cm/s.

The theory of Wen & Yu predicted that $U_{mf} = 0.174$ cm/s.

3. Pressure drop and friction factor

The theoretical bed pressure drop should have been $\Delta P/W = 0.041$

The pressure drop was considered in this manner in order to compare the

pressure drops for all seeds states. Now,

$$\Delta P/W = \frac{\rho U^2}{2} \left[1 + \frac{150(1-e)}{Re' e} \right]$$

where W = mass of wet seeds, g, and ΔP is in grams.

The results are shown in Table 5.4.9 and in Fig. 5.25.

Table 5.4.9 Bed pressure drops for coated, sieved seeds

Seeds condition	$\Delta P/W$	U/U_t , actual
0.286cm, 17h, $W = 642g$	0.0704	0.193
	0.0704	0.123
	0.0685	0.086
	0.0650	0.043
	0.0650	0.034
	0.0575	0.024
	0.0496	0.013
	0.0427	0.010
0.286cm, 90h, $W = 525g$	0.0635	0.321
	0.0635	0.249

FIG. 5.25

FLUIDISED MUSTARD SEEDS - BED PRESSURE
DROP FOR DECREASING U

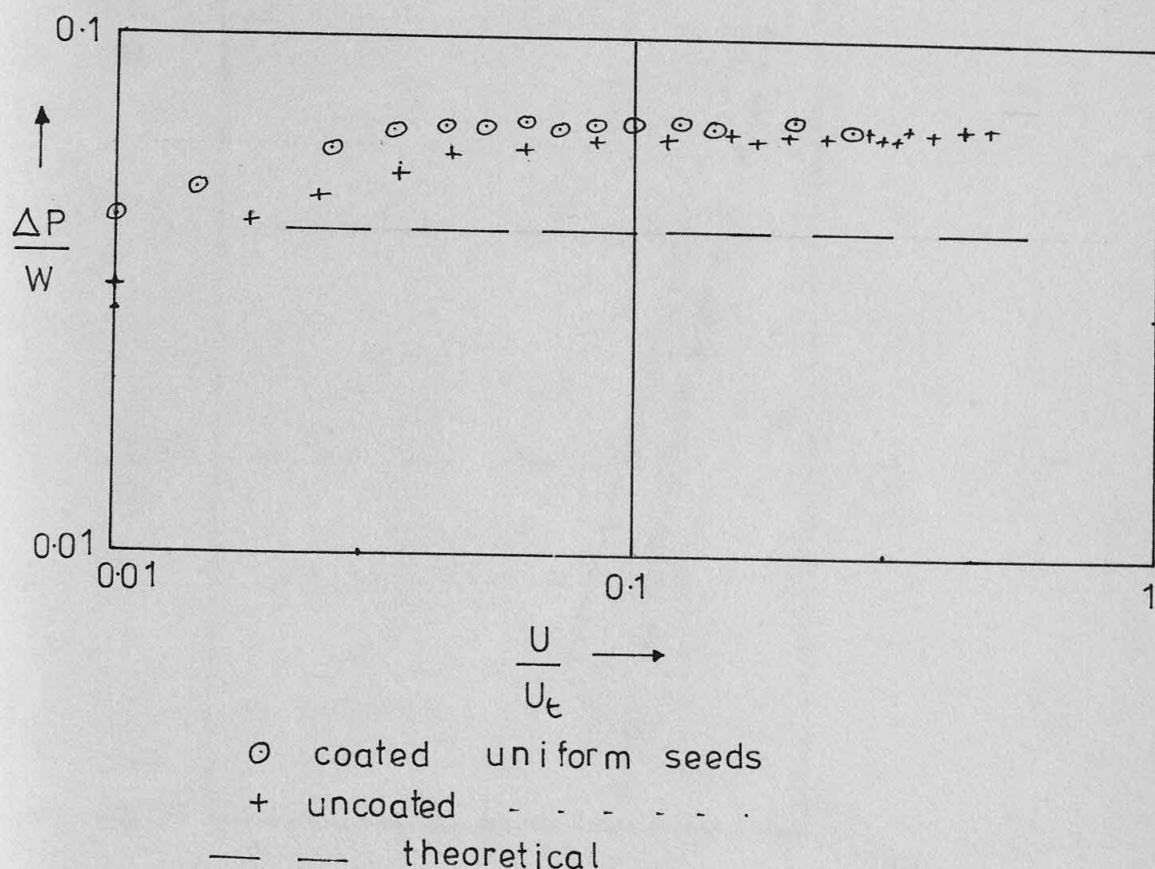


Table 5.4.9 (continued)

Bed condition	$\Delta P/W$	U/U_t , actual
as before	0.0635	0.0220
	0.0635	0.0301
	0.0612	0.0500
	0.0567	0.0400
	0.0499	0.0325
	0.0453	0.017
	0.0340	0.010

Let us now compare the previous section A is included for comparison. The value of $\Delta P/W$ was consistently larger for the coated seeds and was considerably more than the theoretical value. This was especially true at low flow rates, although the difference became less at high flow rates.

The Richardson-Zaki curves were evaluated and are shown in

Table 5.4.10

Table 5.4.10 Richardson-Zaki for coated, uncoated seeds

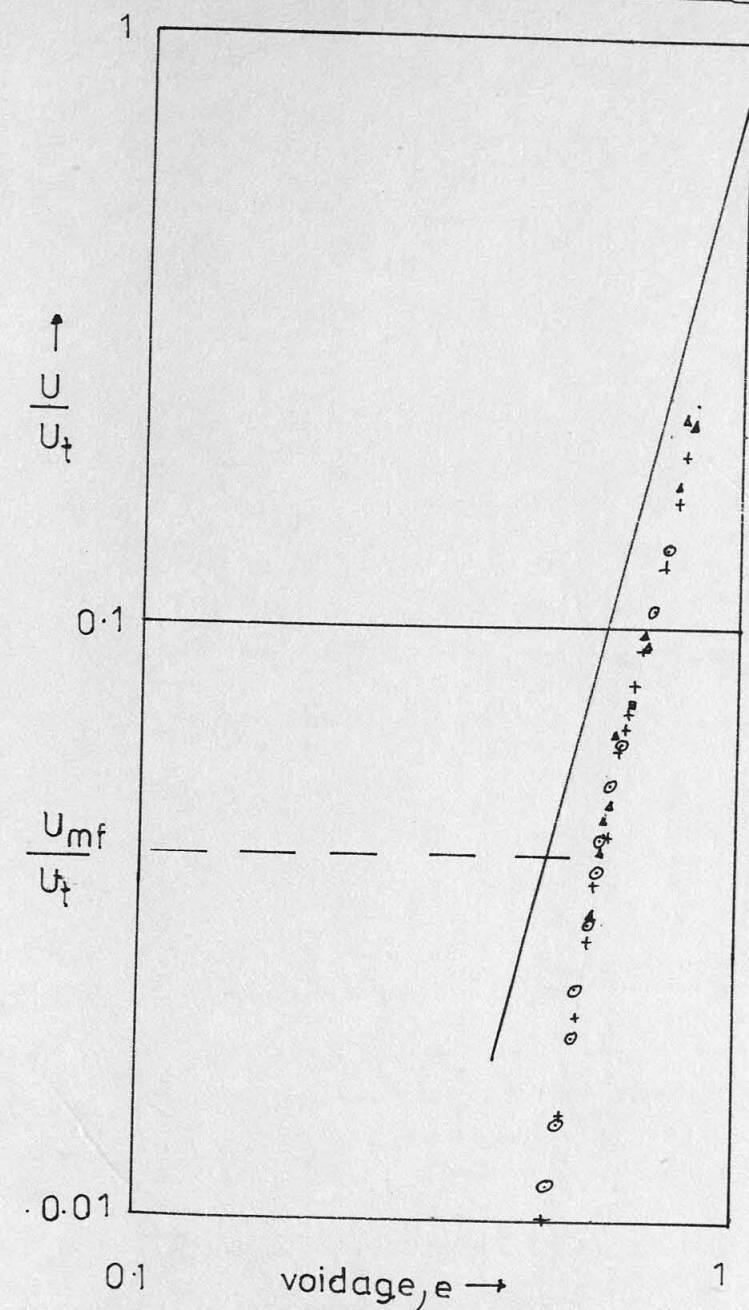
U , cm/s	e	Re	ψ
0.730	0.740	13.38	1.492
0.642	0.736	12.54	2.057
0.560	0.728	9.81	2.414
0.425	0.703	6.82	3.774
0.286	0.639	3.78	6.258
0.184	0.583	2.10	11.48
0.115	0.551	1.22	24.82
0.069	0.515	0.678	56.29
0.027	0.465	0.241	270.6

This is shown in Fig. 5.14. The values are higher than for uncoated seeds as would have been expected considering the large ΔP values obtained with the coated seeds.

Discussion

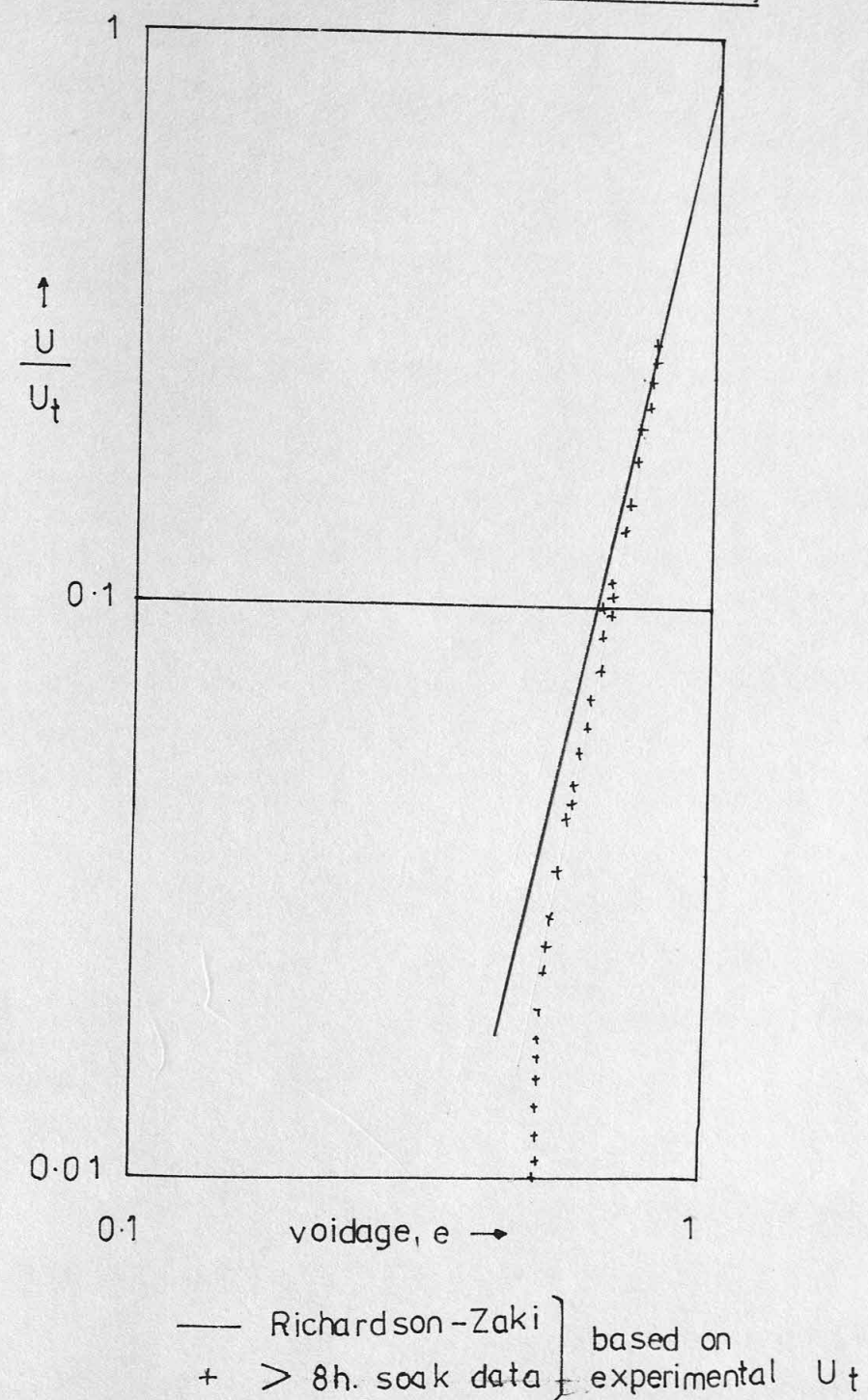
All this information indicated that the presence of the polyacrylate coating modified the hydrodynamic behaviour of the particles. The actual terminal velocity of the seeds appeared to be 34% lower than the theoretical value. The higher pressure drop in the fluidised bed also

FIG. 5.26 0.286cm SEEDS IN 2-DIMENSIONAL BED
(coated uniform size)



— Richardson-Zaki
 + 17h soak fluidisation
 ▲ sedimentation
 ⊙ 90h ... fluidisation
 based on theoretical U_t

FIG. 5.27 0.286cm SEEDS IN 2-DIMENSIONAL BED
(coated uniform size)



suggested that the prescence of the polysaccaride increased the drag force on the particle. Similar findings for non-biological systems were discussed in the Literature survey.

The effects of replotting the data using the actual terminal velocity is shown in Fig. 5.27. As was expected the data lay nearer to the Richardson-Zaki prediction, but ~~was~~ ^{were} not in agreement with it as ~~was~~ ^{were} the data for the uncoated seeds. No wall effect was included in the plot because use of the actual terminal velocity had already taken this into account. The data ~~was~~ ^{were} correlated with $U/U_t = e^{5.6}$ ~~with~~ ^{and} $U'/U_t = 1$.

Particles experiencing drag forces greater than the theoretical cannot be expected to obey that theory. Happel's model did not fit the data shown in Fig. 5.27. However, the data plotted in Fig. 5.26 (using the theoretical U_t) did approximate to Happel's model. The Hawksley-Vand, Richardson-Zaki and Richardson-Mielke models gave reasonably accurate predictions of the curve once the bed was fully fluidised ($U/U_t > 0.1$). These models were, however, consistent in their underestimation of the voidage at lower flowrates.

D. Coated, Multisized seeds, $d = 0.275\text{cm}$.

Tests on seeds in this condition were performed in the $1\frac{1}{2}$ " & 3" diameter columns. Seed soak times were approximately 15h. The results are shown in Appendix A and in Fig. 5.28.

1. The effect of U on voidage

The theoretical terminal velocity for 0.275cm seeds was 4.8cm/s. The Richardson-Zaki model was $U/U_t = e^{3.17}$ with $U'/U_t = 0.92$. The actual value of the terminal velocity found from the data was 3 cm/s. The data ~~was~~ ^{were} compared to the theoretical models discussed before and the effects of plotting the data using both U_t values may be observed.

2. U_{mf} values

Minimum fluidisation velocities were calculated as follows,

$$U_{mf} = 0.217 \text{ cm/s} ; U_{mf} / U_t = 0.045 ; (\text{Rowe 1})$$

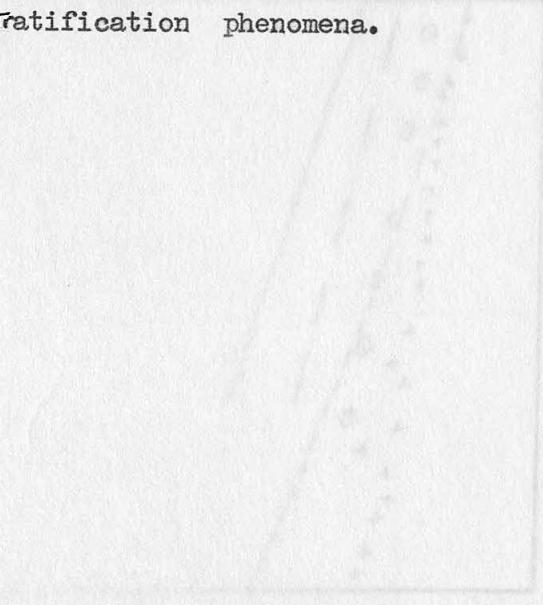
$$U_{mf} = 0.217 \dots \dots \dots ; (\text{Wen-Yu})$$

$$U_{mf} = 0.315 \dots \dots \dots = 0.066 ; (\text{Rowe 2})$$

The fluidisation of this particular seed state was affected by a combination of stratification and drag force effects, such as would be found in a microbial suspension. Polymer drag effects appeared to affect the terminal velocity value, which varied thus,

Situation	U_t , cm/s
Theoretical value	4.8
Multisized suspension	3.92
Multisized suspension with biopolymer.	3.0

The overall behaviour of the bed appeared to be predominantly controlled by the stratification phenomena.



The overall behaviour of the bed appeared to be predominantly controlled by the stratification phenomena.

— Richardson - Zaki
 — — Hawksley
 - - - - Happel
 + based on theoretical U_t
 ○ experimental ...

5.4.5 Kaolin - A flocculent, non-biological system

Introduction

This inorganic flocculent material has been ^{the} subject of much investigation. It therefore serves as a link material between the well understood non-flocculent and the flocculent microbial systems. A few simple settling tests were performed and the results analysed as for previous materials.

15g. of kaolin were placed in a 500 cm³ measuring cylinder containing water at 21°C. Suspensions of varying concentrations were settled and the settling rates estimated. The density of kaolin was measured using a specific gravity bottle and was found to be 1.68 g/cm³. The pH of the suspension was 7. The settling curves for kaolin are shown in Fig. 5.29a. Slight agglomeration lag times were observed, but the settling lines revealed a constant rate of settling for the free-settling period.

The data ~~were~~ analysed initially using the assumption of Michaels & Bolger (1962) that the volume of floc / volume of particles = 10 for kaolin in water. This was, although not stated, based on the assumption that the Richardson-Zaki equation applied to the suspension. Regression of the data gave $U_t = 0.067$ cm/s and the analysis is shown in Table 5.4.11 and in Fig. 5.29b.

Table 5.4.11 Kaolin sedimentation analysis

U cm/s	e	U/U _t
0.0033	0.405	0.050
0.0047	0.554	0.070
0.0072	0.642	0.108
0.0156	0.745	0.233
0.0236	0.797	0.354

The Richardson-Zaki equation was used with a value $n = 4.65$. Laminar conditions were assumed as this would apply for floc sizes less than 300 microns. Michaels & Bolger reported floc sizes ranging between 50 to 350 microns.

Fig. 5.29b shows that the results were in good agreement with the theory when the ratio floc volume / particle volume = 10 was assumed. This agreement merely shows that the present results are in good agreement with those of Michaels & Bolger. It does not prove that kaolin obeys the Richardson-Zaki equation as this was implicit in the use of the Michaels & Bolger floc structure.

The effects of floc structure breakdown may be seen in Fig. 5.29b. At low U/U_t values the results suggested that liquid was being forced out of the flocs at high concentrations. Indeed, after 3 days settling the volume of the sediment was 40 cm^3 . Clearly the floc structure had broken down such that floc/particle volume = 4.48, assuming zero voidage for the sediment. Obviously, the floc structure depends on the environment.

Michaels & Bolger reported that flocs tend to become spherical and of constant size in a flow field. Gaudin et alia (1958), using X rays, showed that a zone of constant voidage, equal to the initial one, existed in a settling kaolin suspension. This justified the assumption which was the basis of the settling data analysis.

The ratio taken by Michaels & Bolger gave a floc voidage of 0.9. Using a floc voidage of 0.5, then the particle/floc volume ratio = $\frac{1}{2}$. The results were reanalysed using this new structure and are shown in Fig. 5.29b. The voidages are seen to be considerably greater than was previously the case and this illustrates the criticality of floc structure assumptions.

Using the Michaels & Bolger floc voidage of 0.9, then floc density in water = $\rho_p = 0.9 \times 0.998 + 1.68 \times 0.1 = 1.066 \text{ g/cm}^3$. Now, the floc model (eqn. 4.3.4) gives

$$\rho_p = \rho + (1-E)^a (1-M) (\rho_s - \rho)$$

As the floc particles do not contain liquid then $M = 0$.

$$\frac{\rho_p - \rho}{\rho_s - \rho} = (1-E)^a$$

and taking $E = 0.4$, then $a = 4.5$. (i.e. between 4 & 5 aggregations have occurred to build up the floc).

Introduction

This inorganic flocculent material has been subject of much investigation. It therefore serves as a link material between the well understood non-flocculent and the flocculent microbial systems. A few settling tests were performed and the results analysed as for various materials.

15g. of kaolin were placed in a 500 cm³ measuring cylinder containing water at 21°C. Suspensions of varying concentrations were settled and the settling rates estimated. The density of kaolin was measured using a specific gravity bottle and was found to be 1.68 g/cm³. The pH of suspension was 7. The settling curves for kaolin are shown in Fig. 5.29a. Slight agglomeration lag times were observed, but the settling lines showed a constant rate of settling for the free-settling period. The data were analysed initially using the assumption of Michaels & Bolger (1962) that the volume of floc / volume of particles = 10. This was, although not stated, based on the assumption that the kaolin was in water. This was, although not stated, based on the assumption that the Richardson-Zaki equation applied to the suspension. Regression of the data gave $U_t = 0.067 \text{ cm/s}$ and the analysis is shown in Table 5.4.11 in Fig. 5.29b.

Table 5.4.11 Kaolin sedimentation analysis

U/U_t	ϵ	$U \text{ cm/s}$
0.050	0.402	0.0033
0.070	0.524	0.0047
0.108	0.642	0.0072
0.233	0.747	0.0156
0.324	0.797	0.0236

The Richardson-Zaki equation was used with a value $n = 4.5$. Under conditions were assumed as this would apply for floc sizes less than 50 μ . Michaels & Bolger reported floc sizes ranging between 50 to 100 μ .

FIG. 5.29A KAOLIN SEDIMENTATION CURVES

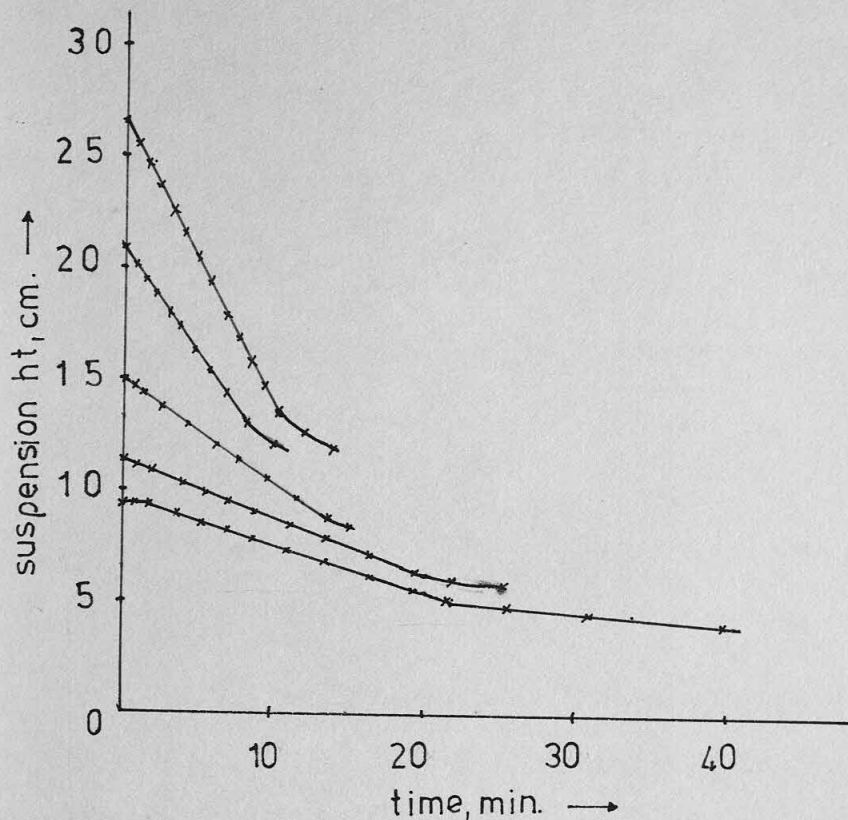


FIG. 5.29B KAOLIN SETTLING.

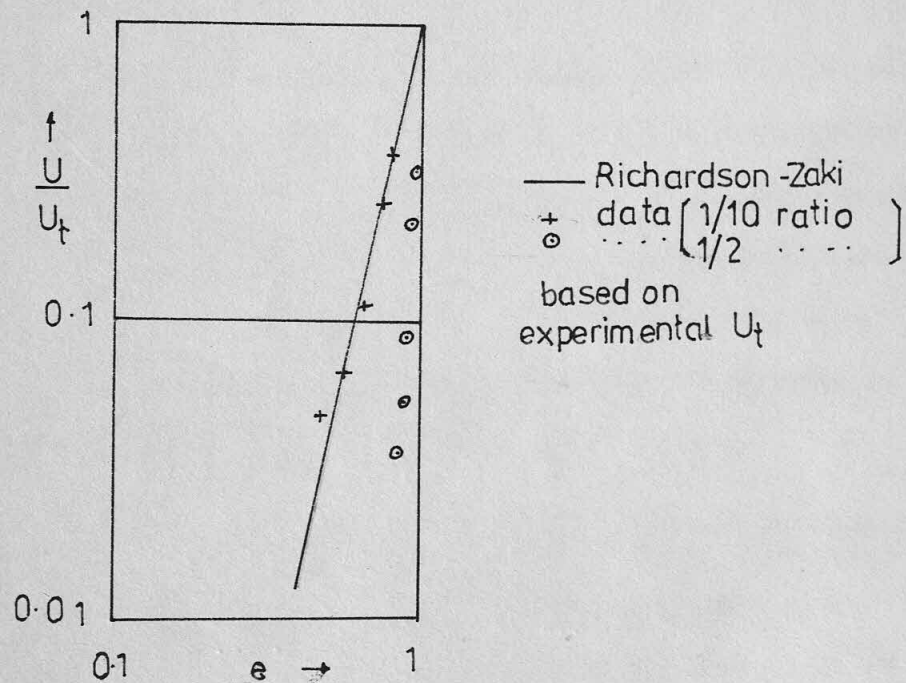


Fig. 5.29b shows that the results were in good agreement with the theory when the ratio floc volume / particle volume = 10 was assumed. The agreement merely shows that the present results are in good agreement with those of Michaels & Bolger. It does not prove that kaolin obeys the Richardson-Zaki equation as this was implicit in the use of the Michaels & Bolger floc structure.

The effects of floc structure breakdown may be seen in Fig. 5.29b. At low U/U_t values the results suggested that liquid was being forced out of the flocs at high concentrations. Indeed, after 3 days settling the volume of the sediment was 40 cm³. Clearly the floc structure had broken down such that floc/particle volume = 4.48, assuming zero voidage for the sediment. Obviously, the floc structure depends on the environment. Michaels & Bolger reported that flocs tend to become spherical of constant size in a flow field. Gaudin et alia (1958), using X rays, showed that a some of constant voidage, equal to the initial one, existed in a settling kaolin suspension. This justified the assumption which was the basis of the settling data analysis.

The ratio taken by Michaels & Bolger gave a floc voidage of 0.9. Using a floc voidage of 0.9, then the particle/floc volume ratio = $\frac{1}{10}$. The results were reanalysed using this new structure and the shown in Fig. 5.29b. The voidages are seen to be considerably greater than was previously the case and this illustrates the criticality of floc structure assumptions.

Using the Michaels & Bolger floc voidage of 0.9, then floc density in water = $\rho_p = 0.9 \times 0.998 + 1.62 \times 0.1 = 1.066 \text{ g/cm}^3$. The floc model (eqn. 4.3.4) gives

$$\rho_p = \rho + (1-E) \rho_s (1-M) (1-E)^{-1}$$

the floc particles do not contain liquid then $M = 0$.

$$\frac{\rho_p - \rho}{\rho_s - \rho} = \frac{1-E}{1-E} = 1$$

taking $E = 0.4$, then $a = 4.5$. (1.0. between 4 & 5 aggregations have occurred to build up the floc).

The assumption of Michaels & Bolger, i.e. that Richardson-Zaki equations could be applied to the suspension, was probably erroneous because the kaolin suspension was multisized and therefore subject to stratification effects. Such effects, as shown by the mustard seed work, can cause some deviation from theoretical settling for low density solids. This would result in the floc voidage estimate falling from the value of 0.9 to a value of 0.8 (say).

5.4.6 The Results for Aspergillus Niger

Introduction

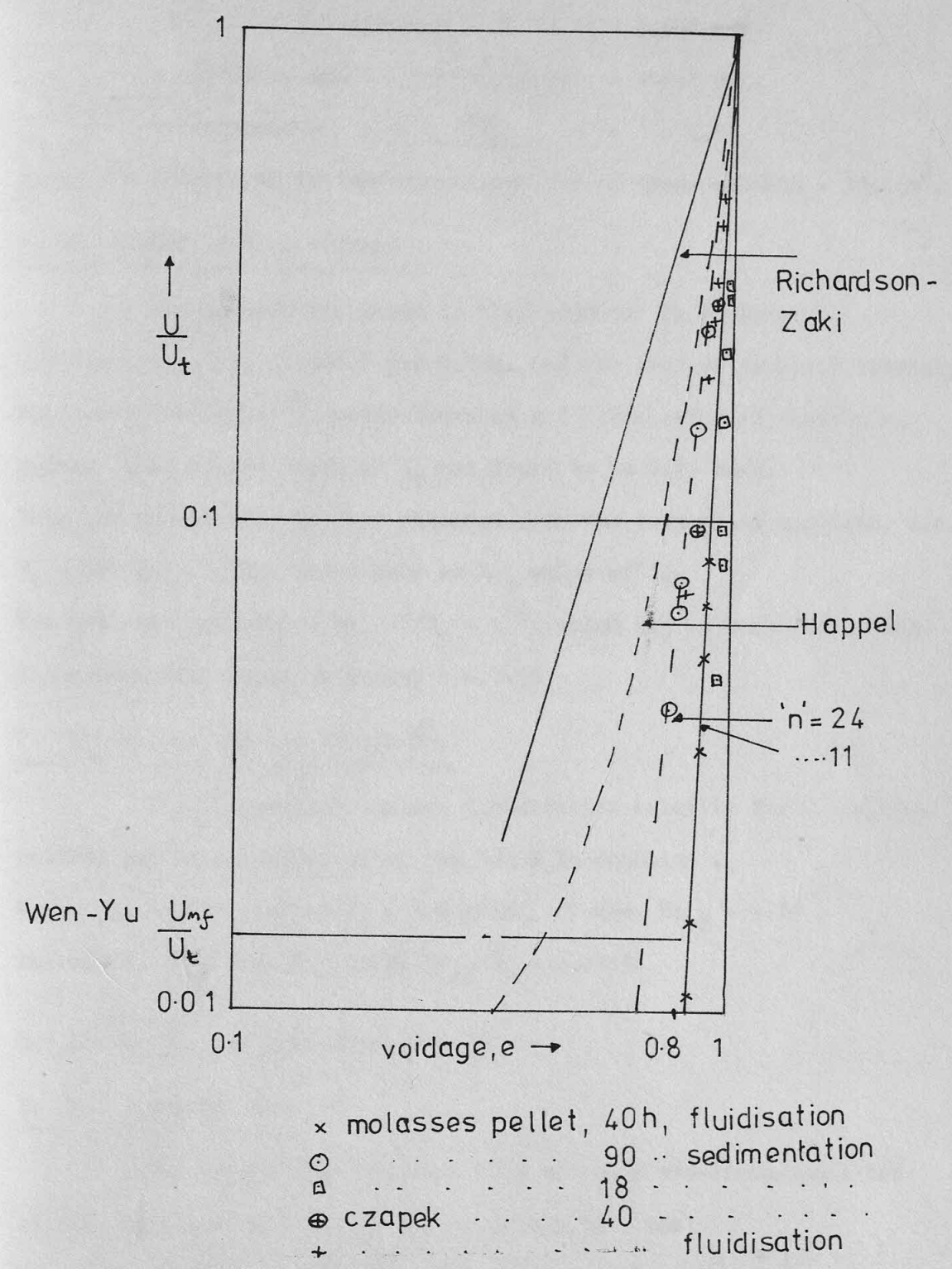
A mould pellet retains its size and structure over a limited period of time (say 2h.), but over an extended period it completely changes in size and structure. A suspension of such pellets at a given growth time contains particles of varying size, but similar structure and density. The investigations outlined in Chapter 3 enabled the structure of a pellet to be accurately estimated. Furthermore, as individual pellets could be handled without disruption, the average terminal velocity for the suspension could be measured. Therefore, A.Niger suspensions could be accurately characterised, unlike kaolin or other flocculent material.

Fluidisation tests were performed using water and the two-dimensional bed or 3.2 cm. tube. Sedimentation tests were performed in measuring cylinders. Different morphologies were investigated.

A. Fluidisation of Molasses-grown pellets in the 2-dimensional bed

Fluidisation tests were performed on 40h. molasses - grown pellets, whose morphology was described in Chapter 3. The dry weight of mycelium in suspension was 3.5g. Water was the liquid phase.

FIG.5.30 ASPERGILLUS NIGER FLUIDISATION



The assumption of Michaels & Bolger, i.e., that Richardson-Zaki equation could be applied to the suspension, was probably erroneous because the kaolin suspension was multistage and therefore subject to a fluidisation effect. Such effects, as shown by the mustard seed work, can cause some deviation from theoretical settling for low density solids. This would result in the flocc voidage estimate falling from the value of 0.9 to a value of 0.8 (say).

5.4. The Results for Aspergillus Niger

Introduction

A mould pellet retains its size and structure over a limited period of time (say 2h.), but over an extended period it completely changes its size and structure. A suspension of such pellets at a given growth time contains particles of varying size, but similar structure and density. The investigations outlined in Chapter 3 enabled the structure of a pellet to be accurately estimated. Furthermore, as individual pellets could be handled without disruption, the average terminal velocity for the suspension could be measured. Therefore, A. Niger suspensions could be accurately characterised, unlike kaolin or other flocculent material. Fluidisation tests were performed using water and the two-dimensional bed or 3.2 cm. tube. Sedimentation tests were performed in measuring cylinders. Different morphologies were investigated.

A. Fluidisation of Molasses-grown pellets in the 2-dimensional bed

Fluidisation tests were performed on 40h. molasses - grown pellets whose morphology was described in Chapter 3. The dry weight of molasses in suspension was 3.5g. Water was the liquid phase.

Bed voidage

For pellets of greater than 35h. growth the mycelial density was 1.24 g/cm^3 (see Fig. 3.1) and the total liquid content was 98.5 % (approx. ; see Fig. 3.4). The suspension voidage was therefore found from

$$\text{Volume of dry mycelium} = 3.5/1.24 = 2.822 \text{ cm}^3$$

$$\therefore \text{pellet volume} = \frac{2.822}{(1 - 0.985)} = 188.2 \text{ cm}^3$$

$$\therefore \text{voidage, } e = 1 - \frac{188}{19.9L} = 1 - 9.46 / L$$

where L = bed length in two-dimensional bed of cross-section = 19.9 cm^2 .

1. The effect of U on voidage

The results are shown in Fig. 5.30 and in Appendix A.

The average pellet diameter was 0.2cm. and the average terminal velocity was determined from 15 measurements in a 1 litre cylinder containing water. The average value of U_t was found to be 0.71 cm/s.

This may be compared to that obtained from the regression analysis, i.e.

$U_t = 1.1 \text{ cm/s}$. This value gave an Re_t value of 22.

The data was correlated by $U/U_t = e^{24}$, which may be compared to the Richardson-Zaki equation index, $n = 3.56$

2. U_{mf} values and the Froude No,

The theoretical minimum fluidisation velocity for 0.2cm, 40h. pellets may be evaluated using the Wen & Yu equation .

Now, $Ga = 313$, taking $\rho_p = 1.0 \text{ g/cm}^3$. Hence, $Re_{mf} = 0.19$.

Therefore, $U_{mf} = 0.0095 \text{ cm/s}$; $U_{mf}/U_t = 0.0133$.

The Froude No. was therefore 4×10^{-7}

3. Bed Pressure Drop

The theoretical pressure drop across a two-dimensional bed of 40h. molasses pellets, of dry wt.; $x = 3.5\text{g}$, was

$$\Delta P = \frac{W (\rho_p - \rho) g}{\rho_p} = \frac{x g (\rho_p - \rho)}{\rho_s (1 - A)}$$

$$\therefore \text{ as } \rho_p = \rho_s (1 - A) + \rho A$$

$$\text{then, } \Delta P = \frac{-167 \times 9 (\rho_s - \rho)}{\rho_s}$$

Now, $\rho_s = 1.24 \text{ g/cm}^3$, and therefore $\Delta P = 0.689 \text{ g cm s}^{-2}$

Using the $\text{CCl}_4/\text{H}_2\text{O}$ manometer, $h = 0.058 \text{ cm. CCl}_4$

4. The Quality of Fluidisation

An evaluation of the Rowe stability criterion, based on the previous U_{mf} value, gave $\frac{\Delta U}{\Delta \delta} = 1.19$. This indicates the high degree of voidage differences that could be locally maintained throughout such a bed.

B. The Fluidisation of Czapek-grown pellets

Pellets grown on a different medium to the previous one were fluidised in the 3.2 cm. tube. The medium was Czapek with a plant growth hormone added. The medium composition included,

Sucrose = 90 g/l.; $\text{NH}_4(\text{SO}_4)_2 = 2.6 \text{ g/l.}$; $\text{MgSO}_4 = 0.5 \text{ g/l.}$;

$\text{KCl} = 0.5 \text{ g/l.}$; $\text{ZnSO}_4 = 0.05 \text{ g/l.}$;

This medium gave a different morphology to the previous one because it was of poorer quality to the molasses medium. The pellets that developed were small, fairly smooth and had a high density of hyphae packing with $d_0/d_1 = 1$. The liquid content was determined from sedimentation tests as in section 3.4.4. These revealed that the pellets had liquid contents slightly higher than for the correspondingly sized molasses pellets.

In the tests in the 3.2 cm. tube, water was used as the liquid phase and 0.73g dry wt. of mycelium was used with the following properties, density = 1.24 g/cm^3 ; average water content = 96.5%; $d_{\text{average}} = 0.07 \text{ cm.}$ The results are shown in Fig. 5.30 and in Appendix A. Regression analysis gave $U_t = 0.13 \text{ cm/s}$ and the data correlated with an index, $n = 13.5$.

Czapek pellets were also tested using sedimentation. These tests were performed in a 250ml. cylinder and the settling curves are shown in Fig. 5.31. They are also shown in comparison with the fluidisation

tests in Fig.5.30. Clearly, the different morphology of Czapek pellets led to different hydrodynamic behaviour. The compactness of the Czapek type caused them to fluidise more like smooth spheres than the more ragged molasses pellets.

C. Sedimentation of Molasses-grown Pellets

Sedimentation tests were performed on 18h. ("hairy" morphology) and older, autolysed pellets. These tests were carried out in 250 ml. measuring cylinders. The average value for the terminal velocity was determined using a 1 l. cylinder. The water temperature in all tests was 26°C.

Now, for the 18h. pellets $U_{t.av.} = 0.14$ cm/s; $d_{av.} = 0.12$ cm.

for the autolysed pellets 1.42 0.4 ...

The settling curves are shown in Fig. 5.31.

Bed Voidage

Example

For the autolysed pellets, dry wt. of mycelium in suspension = 2.26 g and mycelial density = 1.24 g/cm³. Therefore, volume of dry mycelium = 2.26/1.24 = 1.822 cm³.

Now, from Table 3.4.3 liquid content of wet mycelium = 78 %.

Hence, the volume of wet mycelium = 8.28 cm³.

If 75 % of the autolysed pellet is liquid in the central cavity then pellet volume = 8.28/0.25 = 33.1 cm³ and therefore suspension voidage is

$$e = 1 - 33.1 / \text{suspension volume.}$$

Sample analyses are shown in Fig. 5.30 and in Appendix A.

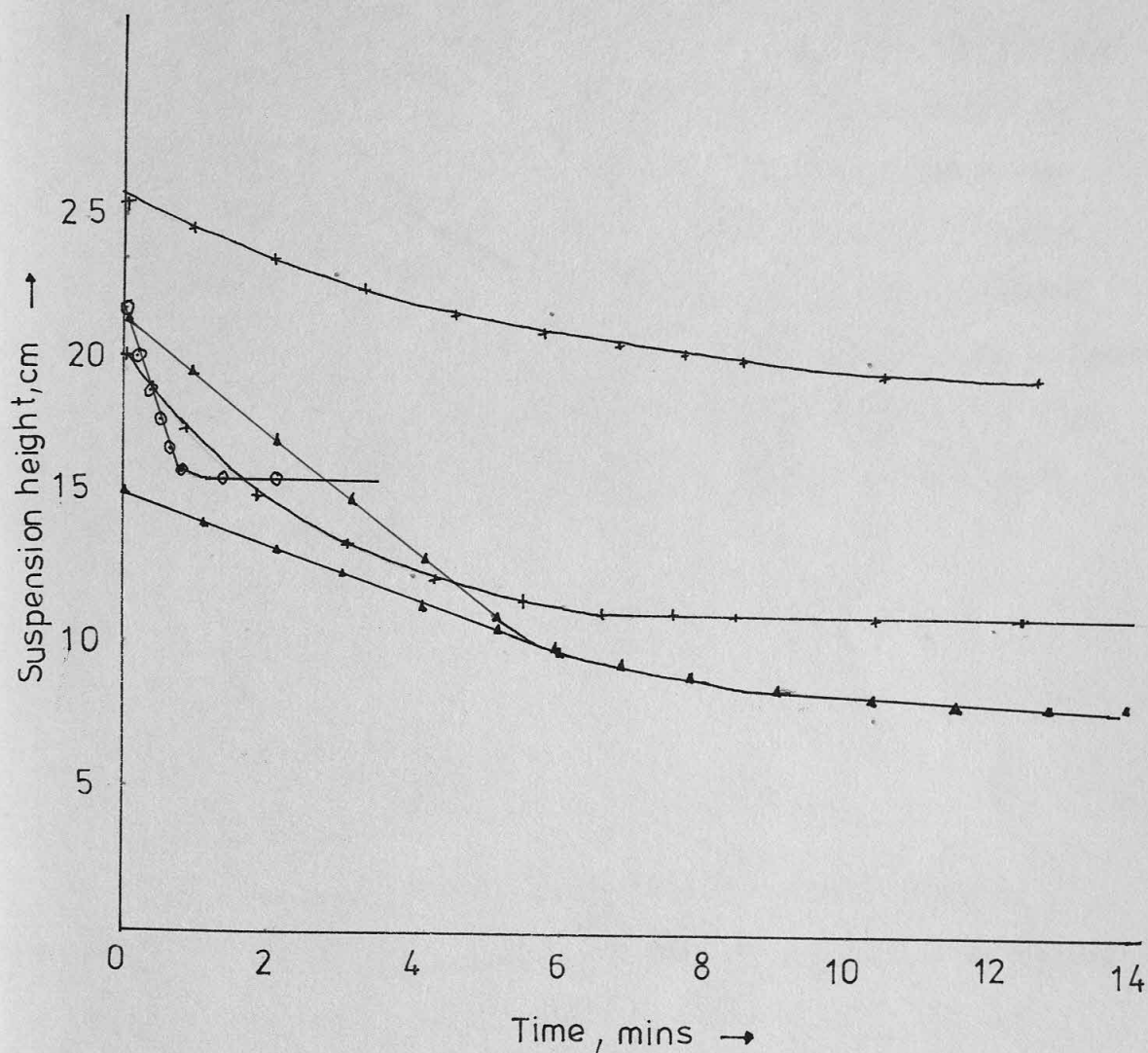
"Hairy" pellets were correlated by $U/U_t = e^{40}$

Autolysed $U/U_t = e^{11}$

Summary

The results are summarised in Fig. 5.30, which shows a trend that the more "hairy" the pellet the greater the value of the index, n.

FIG. 5.31 PELLET SEDIMENTATION



+ 18h molasses pellets
 o 90 - - - - -
 Δ 40 czapek

tests in Fig. 5.30. Clearly, the different morphology of Czapek pellets led to different hydrodynamic behaviour. The compactness of the Czapek type caused them to fluidise more like smooth spheres than the more irregular molasses pellets.

C. Sedimentation of Molasses-grown Pellets

Sedimentation tests were performed on 18h, ("hairy" morphology) and 40h, autolysed pellets. These tests were carried out in 250 ml. measuring cylinders. The average value for the terminal velocity was determined using a 1 l. cylinder. The water temperature in all tests was 20°C. Now, for the 18h. pellets $U_{av} = 0.14$ cm/s; $\delta_{av} = 0.12$ cm. For the autolysed pellets $U_{av} = 1.42$ cm/s; $\delta_{av} = 0.4$ cm. The settling curves are shown in Fig. 5.31.

Example For the autolysed pellets, dry wt. of mycelium in suspension = 2.26 g and mycelial density = 1.234 g/cm³. Therefore, volume of dry mycelium = $2.26/1.24 = 1.822$ cm³. Now, from Table 3.4.3 liquid content of wet mycelium = 78%. Hence the volume of wet mycelium = 8.28 cm³. If 1% of the autolysed pellet is liquid in the central cavity then pellet volume = $8.28/0.25 = 33.12$ cm³ and therefore expansion volume is $e = 1 - 33.1/33.1 = 0$.

Group analyses are shown in Fig. 5.30 and in Appendix A. "Hairy" pellets were correlated by $U/U_f = e^{1.40}$ Autolysed pellets $U/U_f = e^{1.11}$

The results are summarised in Fig. 5.30, which shows a trend that the more "hairy" the pellet the greater the value of the index, n .

This effect may well be related to the formation of mycelial networks, which are self-supporting and thus produce suspensions of high voidage as the normal rules of particle packing do not apply. Such networks would be most predominant in suspensions containing many surface hyphae.

It was a characteristic of A.Niger fluidisation that the visual transition to a fluidised state was not obviously apparent from the fluidisation data. The network effect and the low density difference for the suspension may cause the normal packed-to-fluidised transition to disappear. Beds of A.Niger do not settle to compaction against zero flowrate and therefore the concept of a minimum fluidisation velocity may be meaningless. In addition to the network effect, the significant deviation of A.Niger from theoretical fluidisation behaviour may be caused by the size distribution effects accentuated by the high buoyancy, thus giving a suspension containing a wide range of terminal velocities in relation to the size range.

5.4.7 Yeast Results

Introduction

The fluidisation of yeast may occur in a tower fermenter continuously producing beer. During this process, CO_2 gas may be evolved and changes in pH, temperature, electrolyte composition, ethanol and sugar concentrations and liquid density may take place. Since any one of these factors might influence the hydrodynamic behaviour of a yeast suspension, an investigation of yeast fluidisation in an actual fermenter would be extremely difficult. For this reason, and since very little information exists in the literature regarding yeast suspension hydrodynamics, the author has carried out some preliminary studies using simplified systems.

Fluidisation/Sedimentation Tests

Flocculent strains of yeast, typical of those used in tower fermenters, were employed in the experiments. In an attempt to regulate the flocculence all tests were performed in a liquid at constant pH, temperature and ionic composition. This liquid was the acetate buffer discussed in section 5.3. The yeast concentration was described in terms of the centrifuged wet weight. The strains tested were :

Table 5.4.12 Description of yeast strains

Code No.	Yeast strain	Comments
CFCC 8	<u>S.Cerevisiae</u>	Fermentation limited
CFCC 34
CFCC 3	Physically limited
CFCC 83	<u>S.Carlsbergensis</u>
CFCC 54	<u>S.Diaeticus</u>

Fluidisation tests were performed in the 3.2cm. column and sedimentation tests in a 500 cm³ measuring cylinder. The results are shown in detail in Appendix A. The voidage term, e , was based on an assumed floc voidage figure of 50%. The dry weight concentration, $C_m, \%$, was derived from the formula :

$$C_m = \frac{100 \times \text{Centrifuged wet wt.}}{\text{Suspension volume}} \times \frac{\text{Dry wt.}}{\text{Centrifuged wet wt.}} \quad \dots\dots 5.4.6$$

The latter ratio was taken from Table 3.4.5. The advantage of using C_m to represent concentration is that no assumptions regarding floc structure need be made. However, floc structure does affect the dry weight in suspension and this is reflected in the changes in C_m . The value of C_m may be approximately related to the liquid velocity, U , by :

$$U = \lambda C_m^{-\omega} \quad \dots\dots\dots 5.4.7$$

Examples of the values of λ & ω are shown in Table 5.4.13

Like Kaolin, the voidages of yeast suspensions are very difficult to determine because of lack of knowledge regarding floc structure. In section 3.4.5 the structure of CFCC 8 flocs was evaluated from terminal velocity measurements. However, the results obtained from these tests only apply strictly to isolated flocs. In concentrated suspensions the floc structure will be different and will probably vary with concentration.

An attempt to relate the fluidisation behaviour of yeast to that of other materials was made by assuming a constant floc voidage of 50% for all strains and conditions. This is clearly an over-simplification, but indicates probable magnitudes for the fluidisation index, n . Regression analysis of data incorporating this assumption was used to obtain the pseudo-index, n' and the pseudo-terminal velocity, U_t' . These values appear in Table 5.4.13 and some are shown in Fig. 5.32.

Overall Correlations

Although there is no systematic change in the values for n' & U_t' with pH and temperature, when all the data for a particular strain was taken together reasonably consistent values of the index, n' , are obtained, although U_t' values vary considerably with environment.

As an approximation, the following correlations may be used :

CFCC 8	$U/U_t' = e^{8.0}$
CFCC 34 $e^{11.5}$
CFCC 3 $e^{15.5}$
CFCC 83 e^{15}
CFCC 54 $e^{9.4}$

An Example

Because of the uncertainty concerning true floc structure in suspension detailed analyses of all tests were not performed. However, as an illustration of the differences between yeasts and other materials an analysis of one fluidisation run is presented in detail below.

Fluoculent strains of yeast, typical of those used in tower fermenters, were employed in the experiments. In an attempt to regulate the foaminess all tests were performed in a liquid at constant pH, temperature and ionic composition. This liquid was the acetate buffer discussed in section 5.3. The yeast concentration was described in terms of the centrifuged wet weight. The strains tested were :

Table 5.4.12 Description of yeast strains

Code No.	Yeast strain	Comments
CFCC 8	<u>S. Cerevisiae</u>	Fermentation limited
CFCC 34
CFCC 3	Physically limited
CFCC 83	<u>S. Carlsbergensis</u>
CFCC 54	<u>S. Kluyveri</u>

Fluidisation tests were performed in the 3.2cm. column and used entation tests in a 500 cm³ measuring cylinder. The results are and in detail in Appendix A. The voidage term, ϵ , was based on an assumed floc voidage figure of 50%. The dry weight concentration, C_m , was derived from the formula :

$$100 \times \text{Centrifuged wet wt.} \times \text{Dry wt.} = \text{Spun volume} \times \text{Centrifuged wet wt.}$$

The after ratio was taken from Table 5.4.5. The advantage of using C_m to present concentration is that no assumptions regarding floc structure need be made. However, floc structure does affect the dry weight in suspension and this is reflected in the changes in C_m . The value of C_m was approximately related to the liquid velocity, U , by :

$$U = \lambda C_m^{-0.47}$$

Values of the values of λ & C_m are shown in Table 5.4.13

A typical case is that of CFCC 34 in the 3.2 cm column fluidised by acetate buffer at pH = 4.75 and 20°C. The floc size ranged from 0.4 to 0.8 cm. and the floc wt./centrifuged wt. = 1.3 (see 3.4.2). Based on an assumed 50% floc voidage, floc density was 1.035 g/cm³. Consequently, suspension voidage, $e = 1 - 1.3W / (1.035 \times \text{volume})$

1. The effect of U on voidage

The results of the fluidisation tests are listed in Appendix A and data regression based on a 50% voidage gave

$$U_t' = 4.27 \text{ cm/s.}$$

$$n' = 12.5$$

Using this U_t' value, the data are compared for those of conventional solids in Fig. 5.33. The differences between the yeast results and those for beds of uniform spheres could be explained by

- i. stratification effects and
- ii. the assumption of constant floc voidage of 50%.

Now, the voidage found for the consolidated yeast bed (based on the 50% floc voidage) was 0.163. Clearly, this is far too low and suggests a change in floc structure.

If the centrifuged weight is used as the basis for estimating the suspension voidage, then the floc voidage equals 0.36. This implies that in a consolidated bed the concept of separate flocs no longer holds: indeed, the entire bed can be thought of as a single compact "floc".

2. Minimum Fluidisation velocity & Froude No.

Taking $d = 0.6 \text{ cm.}$, then from the Wen & Yu equation (5.2.16), $U_{mf} = 0.556 \text{ cm/s.}$, hence, $U_{mf}/U_t' = 0.131$ based on the regression value for U_t' . The theoretical value of U_t for this size of floc is 7.53 cm/s., hence, $U_{mf}/U_t = 0.074$. This is shown in Fig. 5.33. The value of the Froude No. based on the theoretical U_{mf} was 5.3×10^{-4} .

The terminal Reynolds No. based on the experimental terminal

velocity was 256. The observed range of Re_t for the yeasts tested was $4 < Re_t < 800$. Thus, for flocculent yeasts the applicability of Stokes Law is questionable.

As the yeast flocs do not apparently obey classical hydrodynamics then it is likely that predicted values of the minimum fluidisation velocity will be in error. U_{mf} equations based on conventional packed beds (such as the Ergun based Wen & Yu equation) are not likely to hold for another reason. When yeast flocs are just resting on one another, bridging occurs and unstable structures of high voidage are formed.

3. Pressure Drop and Friction Factor

The pressure drop through the bed, based on the 50% floc voidage, was $\Delta P_b = 26 \times 2.3 \times (1.035 - 0.996)g / 1.035 = 1.274g$. (This would have given a manometer reading of 0.27 cm. CCl_4)

The Richardson-Mielke analysis for this run is shown in Fig. 5.14 and Table 5.4.14.

Table 5.4.14 Richardson-Mielke analysis for CFCC 34

U	e	Re'	ψ
0.224	0.803	11.33	39.6
0.178	0.770	7.71	55.2
0.132	0.748	5.22	92.2
0.088	0.732	3.27	194.5
0.043	0.697	1.41	703.1
0.022	0.673	0.66	2510

4. The Quality of Fluidisation

The Rowe stability criterion, based on the theoretical U_{mf} and $\delta = 0$, gave $\frac{\Delta U}{\Delta \delta} = 26.9$ which was comparable with the mustard seed value of 19.

It is unlikely that the conventional stratification criteria (e.g. Pruden et alia, 5.4.42) would apply to the yeast suspension as the particle size range was continuous, not discrete. This stratification

effect would probably cause deviations from the Richardson-Zaki theory. To use the approach of Michaels & Bolger (i.e back-calculating the floc structure assuming the applicability of the Richardson-Zaki equation) would also be incorrect.

For the highly flocculent CFCC 34, the assumption of a 50% floc voidage was probably an underestimation. However, as the true value probably changes and is very difficult to evaluate it was considered pointless to use further floc voidage values.

General Remarks

It has always been considered that the yeast flocs inside tower fermenters operating continuously behave like a fluidised bed. However, it is possible that the yeasts in the above tests and in commercial towers are not fully fluidised in the classical sense. For many tests $U_{mf}/U_t < 0.1$, which for conventional materials would indicate that the bed is not fully fluidised. It will be remembered that both diakon and mustard seed exhibited a transition region where the bed was in an expanded-packed condition. Such a condition may exist in the yeast suspensions investigated.

Yeast is the most complex of all the materials tested, and it will be clear that such suspensions cannot be properly characterised due to lack of fundamental knowledge of a physical and microbiological nature. By making a number of assumptions it has been possible to derive a number of empirical equations that describe the fluidisation/sedimentation behaviour. Whilst these leave much to be desired, they do provide a starting point for the design of tower fermenters, as will be shown in Chapter 7.

velocity was 256. The observed range of Re_t for the yeasts tested was 4-1000. Thus, for flocculent yeasts the applicability of Stokes law is questionable. As the yeast flocs do not apparently obey classical hydrodynamic laws then it is likely that predicted values of the minimum fluidisation velocity will be in error. U_{mf} equations based on conventional packed beds (such as the Ergun based Wen & Yu equation) are not likely to hold for another reason. When yeast flocs are just starting to form, a bridge occurs and unstable structures of high voidage are formed.

Pressure Drop and Friction Factor

The pressure drop through the bed, based on the 50% floc voidage, was $\Delta P = 26 \times 2.5 \times (1.035 - 0.996) / 1.035 = 1.2746$. (This would have given a manometer reading of 0.27 cm. CO₂) The Richardson-Zaki analysis for this run is shown in Fig. 5.14 and Table 5.4.14.

Table 5.4.14 Richardson-Zaki analysis for CFCC 34

U	e	Re_t	ψ
0.022	0.673	0.66	2510
0.043	0.697	1.41	103.1
0.088	0.732	3.27	194.5
0.132	0.748	5.22	92.2
0.178	0.770	7.71	52.2
0.224	0.803	11.33	32.6

Quality of Fluidisation

The Rowe stability criterion, based on the theoretical U_{mf} and $\Delta U/\Delta z = 26$, which was comparable with the mustard seed value. It is unlikely that the conventional stratification criteria (e.g. Fruden et al., 5.4.42) would apply to the yeast suspension as the size range was continuous, not discrete. This stratification

Table 5.4.13 Yeast Fluidisation and Sedimentation Analysis

Strain	T°C	pH	U_t , cm/s.	n'	λ	ω
CFCC 8	20	4.1	0.16	3.8	0.47	1.98
	20	4.6	0.48	8.1	0.53	1.92
	25	4.65	0.31	5.3	0.54	1.55
	30	4.7	0.48	7.6	0.64	1.98
CFCC 34	16	5.3	7.46	46.8	-	-
	20	4.05	13.2	18.0	76	5.67
	20	4.75	4.27	12.5	160	5.78
	20	5.0	3.17	14.2	6	3.78
	20	5.4	3.7	14.1	12.5	4.36
	25	4.8	4.93	10.6	-	-
	30	4.15	8.98	15.1	-	-
	30	4.85	6.03	9.3	300	5.07
	30	5.1	7.03	14.9	66	5.36
	40	5.2	24.6	17.6	-	-
CFCC 3	20	4.7	18.1	14.8	570	6.13
	20	5.3	50.6	16.6	1800	6.54
	30	4.8	26.0	14.8	360	5.56
	40	4.9	627	25.4	-	-
CFCC 83	20	3.75	0.47	16.5	0.24	3.05
	20	4.1	4.27	12.5	-	-
	20	4.2	4.12	31.3	0.17	2.67
	20	4.75	2.37	16.0	3.4	4.0
	20	5.2	0.27	5.6	0.52	2.0
	25	4.8	6.44	20.1	-	-
	30	4.3	0.16	9.2	-	-
	30	4.85	13.7	22.4	60	6.67
	35	4.9	2.36	16.1	-	-
CFCC 54	25	4.9	1.71	9.35	-	-

CFCC 34 } Based on 50%
83 } fluid volume

Table 5.4.13 - Yeast Fluidisation and Sedimentation Analysis

Series	$T^{\circ}C$	U_t cm/s	n'	λ	ω
CFCC 34	20	4.1	3.8	0.41	1.98
	20	4.6	8.1	0.53	1.92
	25	4.62	2.3	0.54	1.52
	30	4.7	7.6	0.64	1.98
CFCC 83	16	2.3	46.8	-	-
	20	4.02	18.0	76	2.67
	20	4.72	15.2	180	2.78
	20	2.0	14.2	6	3.38
	20	2.4	14.1	12.2	4.36
	25	4.8	10.6	-	-
	30	4.12	12.1	-	-
	30	4.82	2.3	300	2.07
	30	2.1	14.9	66	2.36
	40	2.2	12.6	-	-
CFCC 8	20	4.7	18.1	270	6.13
	20	2.3	16.6	1800	2.24
	30	4.8	14.6	360	2.26
	40	4.9	22.4	-	-
CFCC 24	20	3.72	16.2	0.24	3.02
	20	4.1	12.2	-	-
	20	4.2	31.3	0.11	2.61
	20	4.72	16.0	3.4	4.0
	20	2.2	2.6	0.22	2.0
	25	4.8	20.1	-	-
	30	4.3	9.2	-	-
	30	4.82	22.4	60	6.67
	32	4.9	16.1	-	-
	25	4.9	22.92	-	-

FIG.5.32 YEAST FLUIDISATION

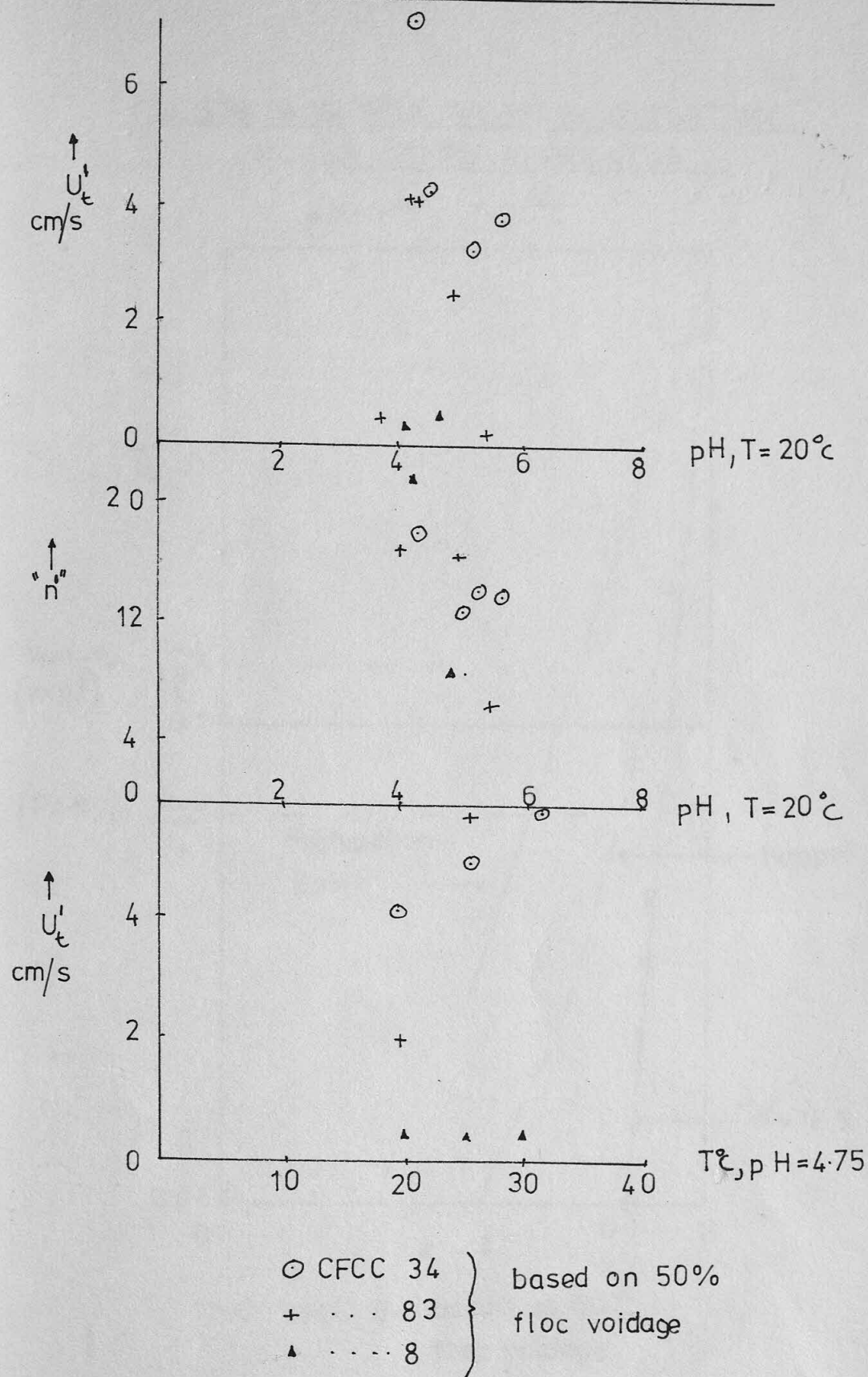
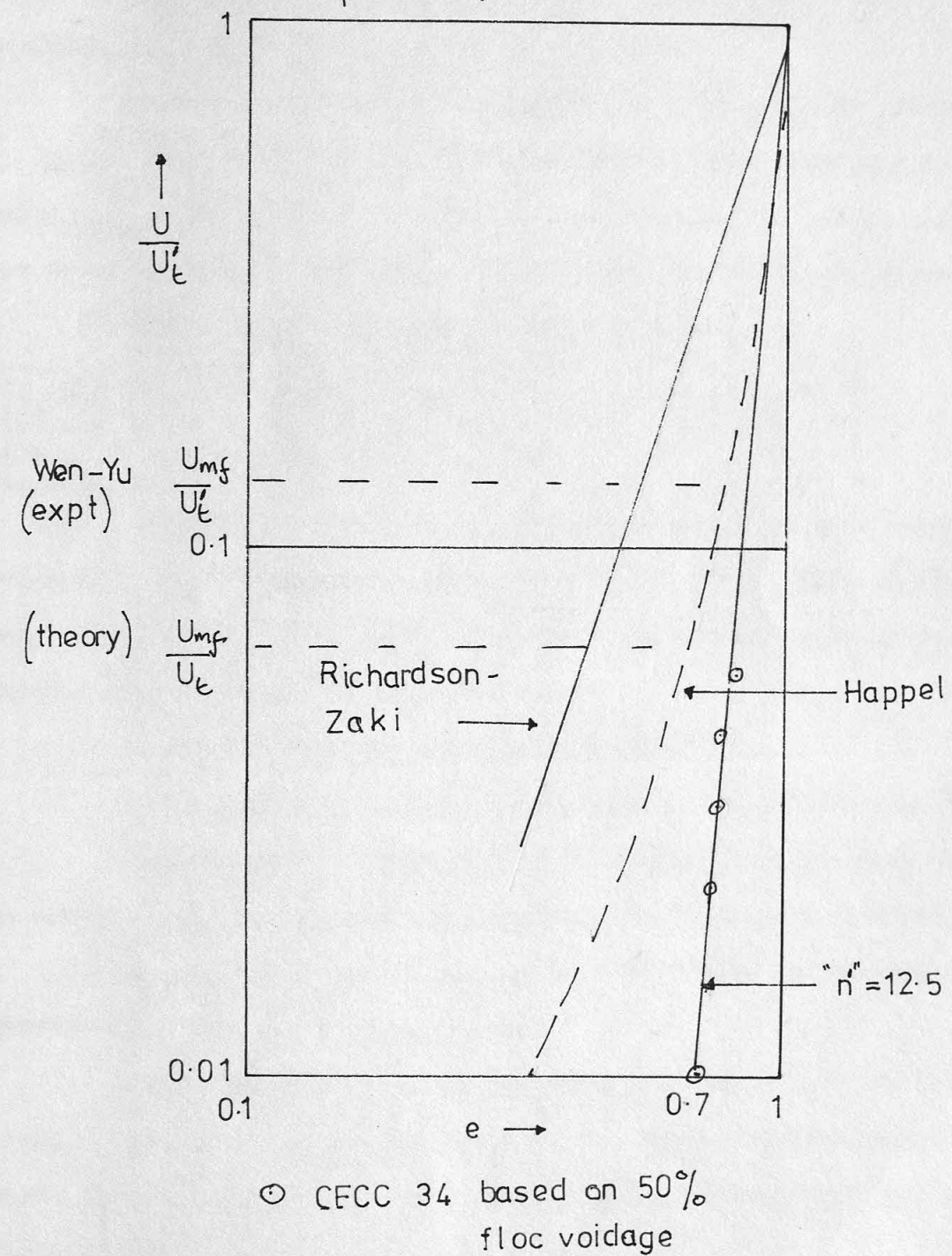


FIG. 5.33 A SAMPLE YEAST FLUIDISATION
IN C1/55 APPARATUS

$pH=4.75$, $T=20^{\circ}C$



5.4.8 Activated Sludge Results

The raw sludge as used by Mr. A. Milner (Biological Sciences) was settled in a 1000 cm³ cylinder at 20°C. After each test the dry weight of sludge in suspension was measured. The ratio of filtered wet weight to dry weight was 12.5 which indicated that the material was about 94% liquid. This was a higher value than for fungi and was probably due to the different types of organism present in the sludge.

As before , taking the floc voidage as 50%, then the floc wt. to dry wt. ratio = 25. The values for suspension voidage were based on the value $\rho_{\text{floc}} = 1.003 \text{ g/cm}^3$ (Edeline et alia ,1969). The settling curves are shown in Fig. 5.34 and sample results taken from these curves were:

Table 5.4.15 Activated Sludge Hydrodynamics

U, cm/s.	0.10	0.0925	0.0248	0.0161	0.0142	0.0125
e	0.979	0.951	0.962	0.958	0.875	0.923

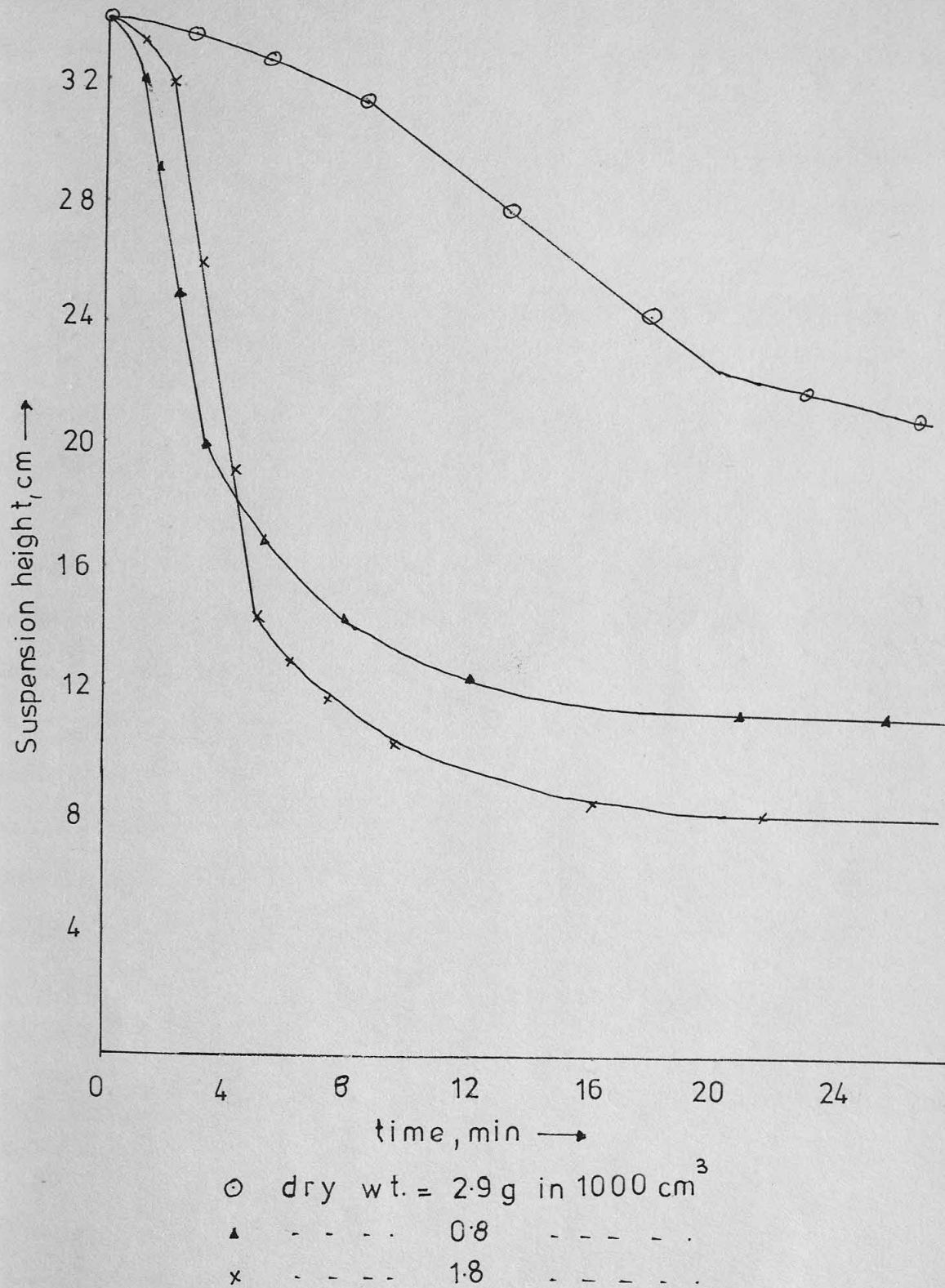
A regression analysis on the above suggested a pseudo-terminal velocity, $U_t' = 0.3 \text{ cm/s}$; and a value for n' of 39. Edeline et alia(1969) have reported values of n in the range 12 to 27. The higher value for n' obtained by the author may be due to :

- i. different sludge characteristics and
- ii. errors arising from the assumption that floc voidage was 50%.

The variability and complexity of activated sludge means that an accurate analysis is impossible. However, the high value observed for n' again indicates that the hydrodynamics of biological suspensions are different from those of other systems.

Sludges are usually characterised by the "Settled Volume Index" which is taken after 30 minutes settling. This equals settled volume / MLSS , where MLSS = dry wt. / unit sludge volume. Variations found in the index were from 127778 to 381250 cm³/g.

FIG.5-34 ACTIVATED SLUDGE SETTLING



5.4.3 Activated Sludge Results

The raw sludge as used by Mr. A. Miller (Biological Sciences) was settled in a 1000 cm³ cylinder at 20°C. After each test the dry weight of sludge in suspension was measured. The ratio of filtered wet weight to dry weight was 12.5 which indicated that the material was about 94% liquid. This is a higher value than for fungi and was probably due to the different types of organism present in the sludge.

As before, taking the free volume as 50%, then the flow rate to the wt. ratio = 25. The values for suspension volume were based on the value $V_{floc} = 1.003 \text{ g/cm}^3$ (Meline et alia, 1969). The settling curves are shown in Fig. 5.34 and sample results taken from these curves were:

Table 5.4.15 Activated Sludge Hydrodynamics

U, m/s	0.10	0.025	0.015	0.011	0.0125
σ	0.973	0.951	0.955	0.958	0.975

A regression analysis on the above suggested a pseudo-terminal velocity, $U_t' = 0.3 \text{ cm/s}$, and a value for n' of 39. Meline et alia (1969) have reported values of n in the range 12 to 27. The higher value for n' obtained by the author may be due to:

i. different sludge characteristics and

ii. errors arising from the assumption that free volume was 50%.

The variability and complexity of activated sludge means that an accurate analysis is impossible. However, the high value observed for n' indicates that the hydrodynamics of biological suspensions are different from those of other systems.

Sludges are usually characterized by the "Settled Volume Index"

which is taken after 30 minutes settling. This equals settled volume /

100 where 100 = dry wt. / unit sludge volume. Variations found in

the literature were from 12778 to 381250 cm³/g.

5.5 Summary of Fluidisation and Sedimentation work

The objective of this work was to compare conventional materials with microbiological systems. Conventional materials may be defined as suspensions of uniformly sized, smooth spheres of constant size and density which obey classical theory. Microbiological aggregates differ from these in the following ways:

i. There is a continuous size distribution which together with the mean size may change with time, temperature, pH or volume fraction of solids.

ii. Polysaccharides present at the external wall of the cells may lead to unusual drag force effects.

iii. The irregular configuration and the high immobile liquid contents of the aggregates may lead to flow pattern deviations.

iv. The particle-particle interactions caused by mycelial networks or floc bridges lead to high voidages during settling and during compaction the voidage changes. The networks, furthermore, lead to highly viscous suspensions (see Chapter 6).

v. Density differences between the continuous and dispersed phases are usually small.

Despite these differences and the difficulties they cause in predicting suspension behaviour, a regular and explicable pattern has emerged. A possible ranking of the various systems examined is shown:

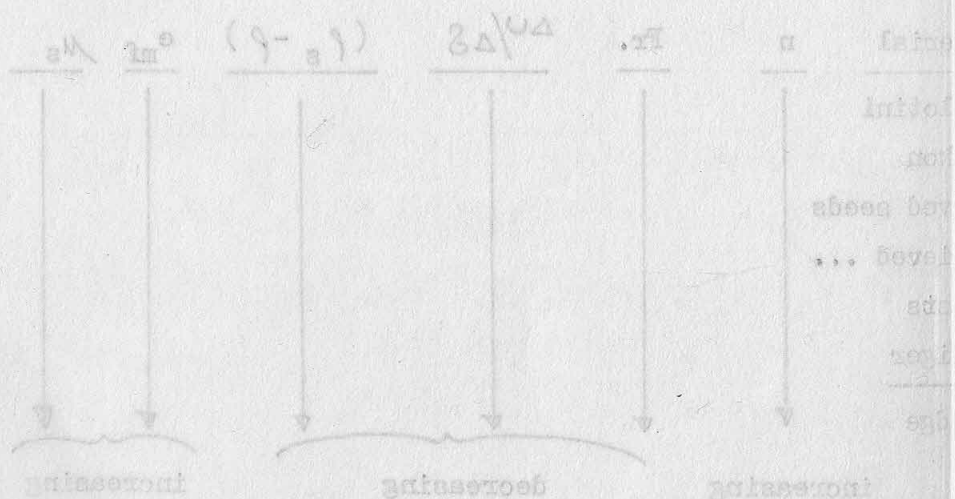
Material	n	Fr.	$\Delta U / \Delta S$	$(\rho_s - \rho)$	e_{mf}	μ_s
Ballotini						
Diakon						
Sieved seeds						
Unsieved ...						
Yeasts						
A. Niger						
Sludge						
	increasing		decreasing		increasing	

The size distribution of a suspension appears to control its behaviour. A uniform size ensures that the suspension obeys conventional theory. If a mixture of a few sizes is used deviation towards higher voidages occurs. If the size distribution is continuous a bigger deviation occurs, which may be accentuated by a low solid-liquid density difference and/or particle interactions due to mycelial or flocculent morphology.

Accurate prediction of the sedimentation/fluidisation behaviour of flocculent suspensions, in particular, is made very difficult by the variability of the floc structure. True representation of these systems may, if ever, be obtained after much more fundamental work.

The objective of this work was to compare conventional materials with biological systems. Conventional materials may be defined as suspensions of uniformly sized, smooth spheres of constant size and density which obey classical theory. Microbiological aggregates differ from these in the following ways:

- i. There is a continuous size distribution which together with the size may change with time, temperature, pH or volume fraction of solids.
 - ii. Polysaccharides present at the external wall of the cells may lead to unusual drag force effects.
 - iii. The irregular configuration and the high immobile liquid content of the aggregates may lead to flow pattern deviations.
 - iv. The particle-particle interactions caused by mycelial networks or floc bridges lead to high voidages during settling and in comparison the voidage changes. The networks, furthermore, lead to viscous suspensions (see Chapter 6).
 - v. Density differences between the continuous and dispersed phases are usually small.
- Despite these differences and the difficulties they cause in predicting suspension behaviour, sedimentation and expansion pattern has been examined. A possible ranking of the various systems examined is shown:



THE VISCOSITIES OF MICROBIAL SUSPENSIONS

6.1 Introduction.

The successful operation of a fermenter depends on achieving efficient gas/liquid mass transfer and mixing. These operations are strongly influenced by the broth viscosity. The changing morphology and biomass in a fermentation broth cause the viscosity to vary to a remarkable degree. It is hoped in this chapter to examine the rheological characteristics of microbial suspensions and relate them to theories of the viscosities of dilute suspensions of spheres.

6.2 Literature Survey

The presence of small, rigid particles in a liquid deforms flow streamlines and thus causes the suspension to have a higher viscosity than the liquid. This effect was first quantified by Einstein (1911) who stated that $\mu_r = \mu_s / \mu_o = 1 + 2.5 \phi$ 6.1 where μ_s = suspension viscosity; μ_o = liquid viscosity; ϕ = volume fraction of solids, which must include any immobilised liquid. The equation applies to rigid spheres in dilute suspension, $\phi < 0.05$.

Guth et alia (1956) modified Einstein's equation to account for higher concentrations. They obtained the following,

$$\mu_r = (1 + 0.5\phi - 0.5\phi^2) / (1 - 2\phi - 9.6\phi^2) \text{6.2}$$

This applies for $\phi < 0.08$

Moulik (1968) attempted to extend the Einstein equation by means of empirical constants varying for each suspension. However, one of the most successful approaches has been that of Vand (1948). From a theoretical analysis for rigid, non-solvated spheres he obtained,

$$\mu_r = 1 + 2.5\phi + F\phi^2 \text{6.3}$$

This equation correlated the data he obtained for 65 micron glass spheres in zinc iodide solution for $\phi < 0.25$. A value for F of 7.35 was originally quoted by Vand, but values as high as 14.1 have been reported in certain cases (Eirich, 1967). The true theoretical value is 9.15 (Eirich, 1967).

Happel (1957) modified the free surface model for a suspension described in chapter 5 (eqn.5.2-23) to obtain the following,

$$\mu_r = 1 + 5.5\phi\psi, \text{ where } \psi = \frac{4\gamma^7 + 10 - (84/11)\gamma^2}{10(1 - \gamma^{10}) - 25\gamma^3(1 - \gamma^4)} \dots\dots\dots 6.4$$

Here, γ = the ratio of inner to outer sphere diameters in the model .

A different form of equation was proposed by Thomas (1963), which he claimed was in agreement with his experimental results, viz;

$$\mu_r = 1 + 2.5\phi + 10.05\phi^2 + 0.003\exp(16.6\phi) \dots\dots\dots 6.5$$

This equation gives results which are similar to the Vand equation when F is taken as 14.1 .

6.2.1 The measurement of microbial viscosities

The importance of broth viscosity to fermenter operation has motivated the research of several workers. An early investigation made by Eirich (1936) used yeast in water and Lycoperdon bovista in tetrachloroethane. These results were later observed to agree with the Vand eqn. for $\phi < 0.14$. Non-flocculent S.Cerevisiae suspensions were tested by Koga et alia (1959) who used an Ostwald viscometer: they observed Newtonian behaviour over the concentration ranges considered. Similar techniques were used by Aiba et alia (1962). They found that the suspension viscosity was less than the figure predicted by the Einstein eqn. based on rigid spheres. However, this equation would correlate the data if soft particles were considered, i.e. $\mu_r \neq 1 + 2.5\phi$, the constant is < 2.5 , for soft particles.

Shayegan (1970) tested non-flocculent S.Cerevisiae suspensions with a Ferranti rotating cylinder viscometer. His results agreed with the Vand equation for $\phi < 0.5$, (see Fig.6.7). He observed Newtonian or occasionally dilatant behaviour. Such behaviour has not been observed with mould broths. Deindoerfer & Gaden (1955) tested Penicillium chrysogenum broths with a MacMichael viscometer. Their results suggested a transition from Newtonian to Bingham plastic behaviour after about 16h. into the fermentation, the broth viscosity increasing rapidly with

fermentation time upto a value of 200 cp. for a 1.34 g% broth (i.e. 1.34g of dry mycelium /100 ml. of suspension). This broth condition caused an 85% reduction in the oxygen uptake compared to the original medium. They also examined the changes in the surface tension of the medium, γ . They found that the γ value varied between 57 & 59 dyne/cm. in an oscillatory manner. Antifoam addition however, caused a marked reduction in γ to 52 dyne/cm.

This work was extended for other organisms by Deindorfer & West (1960). They observed Bingham behaviour for Streptomyces broths in agreement with the findings of Karow (1953). However, pseudoplastic behaviour was observed for Penicillium chrysogenum and Coniothyrium helleborio. They concluded that the Non-Newtonian behaviour was due to the rigidity of the mycelial networks.

Solomons & Perkin (1958) using a Ferranti VM viscometer found that A. Niger broths gave Bingham plastic behaviour. However, this conclusion was changed in a later paper by Solomons (1962) after using an Epprecht Rheomat 15 viscometer. He reported that A. Niger broths were pseudoplastic, but could be mistaken for Bingham if low shear rates were not investigated. Using the analysis proposed by Calderbank et alia (1959) he found $T = K \left(\frac{dv}{dy} \right)^n$ 6.6 where $n = 0.35$; $K = 172 \text{ dyne s}^n \text{ cm.}^{-2}$

Viscosities of 20,000cp. were obtained for certain A. Niger broths, indicating virtual anaerobic fermentation conditions.

Takahashi (1969) examined A. Niger broths and plotted viscosity against dry mycelial concentration. This revealed that filamentous mycelium had much higher viscosities than discrete pellets. This work will be discussed in more detail later.

Recently, Bongenaar et alia (1973) measured P. Chrysogenum broth viscosities using a six-bladed impeller transmitting to a Haake-Rotovisco viscometer. They claimed that this method overcomes the problem of wall-effects that can arise when using rotating cylinder viscometers.

They observed pseudoplastic behaviour for a broth which was taken directly out of a fermenter. Using equation 6.6 they obtained the data shown in Table 6.1.

Table 6.1 Rheological constants for A.Niger (Bongenaar et alia)

Mycelial age, h.	"n"	"K", dyne s ⁿ cm ⁻²
111	0.18	18.6
90	0.23	16.3
62	0.23	13.3
39	0.37	5.73

6.3 Experimental Method

In the following tests the measured viscosity was not always the true viscosity, but was an "apparent" one based on the relationship

$$\tau = \mu_s' (dv/dy) : \text{where } \mu_s' = \text{"apparent" viscosity.}$$

In the case of Newtonian suspensions the apparent and true viscosities are identical, i.e. $\mu_s' = \mu_s$.

The measurement of the apparent viscosity of microbial suspensions was made using a Ferranti Rotational Viscometer, Model VL, having a capacity for measuring viscosities upto 2000cp. (see Fig.6.1a). The cylinders had been modified to allow the suspension to circulate through them to ensure representative sampling. This was effected by an arrangement of holes and baffles in the cylinders. The viscometer was initially calibrated using Rape oil at a known temperature. This enabled the viscosity conversion factors for each speed (5 speeds in all), to be obtained. The shear rates quoted for each speed and cylinder were,

Table 6.2 Viscometer Data

Cylinder No.	Gear No.	Shear Rate, s ⁻¹
VLA	5	950
	4	791
	3	628
	2	475
	1	318

Table 6.2 (cont.)

Cylinder No.	Gear No.	Shear Rate, s ⁻¹
VLB	5	328
	4	274
	3	217
	2	164
	1	110
VLC	5	204
	4	170
	3	135
	2	102
	1	68

The microbial suspensions were placed in beakers of various capacities (500 to 1000cm³). These were then placed in a water bath at 30±0.5°C and allowed to reach that temperature. The apparent viscosity of the suspension was then measured, the rotation of the cylinders being sufficient to maintain the particles in suspension. In certain cases the rheological characteristics were measured by obtaining the apparent viscosity at various shear rates. Otherwise, the apparent viscosity was measured at a fixed shear rate.

6.3.1 A.Niger tests

The changing morphology of this organism required the viscosity to be tested at various fermentation times. Hence, samples were taken directly from the fermenter and the changes in apparent viscosity and mycelial dry weight with time were observed. Additionally, for each sample time the change of apparent viscosity with dry weight concentration was observed; tests being made at a number of different shear rates. Water was used as the suspension fluid.

6.3.2 Yeast

The morphology of yeast does not change appreciably with time; hence, samples were not taken from the fermenter at various stages during growth. At the end of the fermentation the yeast was centrifuged and its weight measured. Samples were then transferred into known volumes of water

They observed pseudoplastic behaviour for a broth which was taken direct out of a fermenter. Using equation 6.6 they obtained the data shown in Table 6.1.

Table 6.1 Rheological constants for A.Niger (Bongenaar et al.)

Mycelial age, h.	"n"	"K", dyne s cm ⁻²
111	0.18	18.6
90	0.23	16.3
62	0.23	13.3
39	0.37	5.73

6.3 Experimental Method

In the following tests the measured viscosity was not always the true viscosity, but was an "apparent" one based on the relationship $\eta_a = \eta_s (6v/\dot{\gamma})$ where η_a = "apparent" viscosity.

In the case of Newtonian suspensions the apparent and true viscosities are identical, i.e. $\eta_a = \eta_s$.

The measurement of the apparent viscosity of microbial suspensions

was made using a Ferranti Rotational Viscometer, Model VP, having a

capacity for measuring viscosities up to 2000cp. (see Fig. 6.1a). The

cylinders had been modified to allow the suspension to circulate through

them ensure representative sampling. This was effected by an

arrangement of holes and baffles in the cylinders. The viscometer was

initially calibrated using rape oil at a known temperature. This enabled

the viscosity conversion factors for each speed (5 speeds in all) to

be obtained. The shear rates quoted for each speed and cylinder were,

Table 6.2 Viscometer Data

Cylinder No.	Gear No.	Shear Rate, s ⁻¹
VLA	5	950
	4	791
	3	628
	2	475
	1	318

or acetate buffers of differing pH. The effects of shear rate, pH and concentration were investigated for various yeast strains.

6.4 Results and Analysis

6.4.1 A.Niger Results

6.4.1.1 The variation of apparent viscosity with morphology and biomass concentration

The results were obtained using cylinder VLC, gear 5, giving a shear rate of 204 s^{-1} . The suspension temperature was 30°C .

Table 6.3 Variation of A.Niger suspension apparent viscosity with concentration and time (morphology).

Fermentation time, h.	Apparent viscosity, cp	Dry mycelial wt; g %
24	244	1.36
	49.7	0.57
	18.8	0.36
	9.4	0.25
	4.04	0.15
	10.2	0.26
	17.5	0.32
29	118	0.86
	40.4	0.45
	25.6	0.39
	13.5	0.22
	44.4	0.55
	32.2	0.70
	28.2	0.54
38	175	1.47
	70	0.86
	35	0.66
	16.2	0.45
	202	0.95
	93	0.80
90	110	1.26
	271	2.08
	75	0.97
	48	0.87
	24	0.74

Table 6.2 (cont.)

Cylinder No.	Gear No.	Shear Rate, s^{-1}
VIB	2	328
	4	274
	3	217
	2	164
	1	110
VLC	2	204
	4	170
	3	135
	2	102
	1	68

The microbial suspensions were placed in beakers of various sizes (500 to 1000 ml). These were then placed in a water bath at $30 \pm 0.5^\circ\text{C}$ and allowed to reach that temperature. The apparent viscosity of the suspension was then measured, the rotation of the cylinders being sufficient to maintain the particles in suspension. In certain cases the rheological characteristics were measured by obtaining the apparent viscosity at various shear rates. Otherwise, the apparent viscosity was measured at a fixed shear rate.

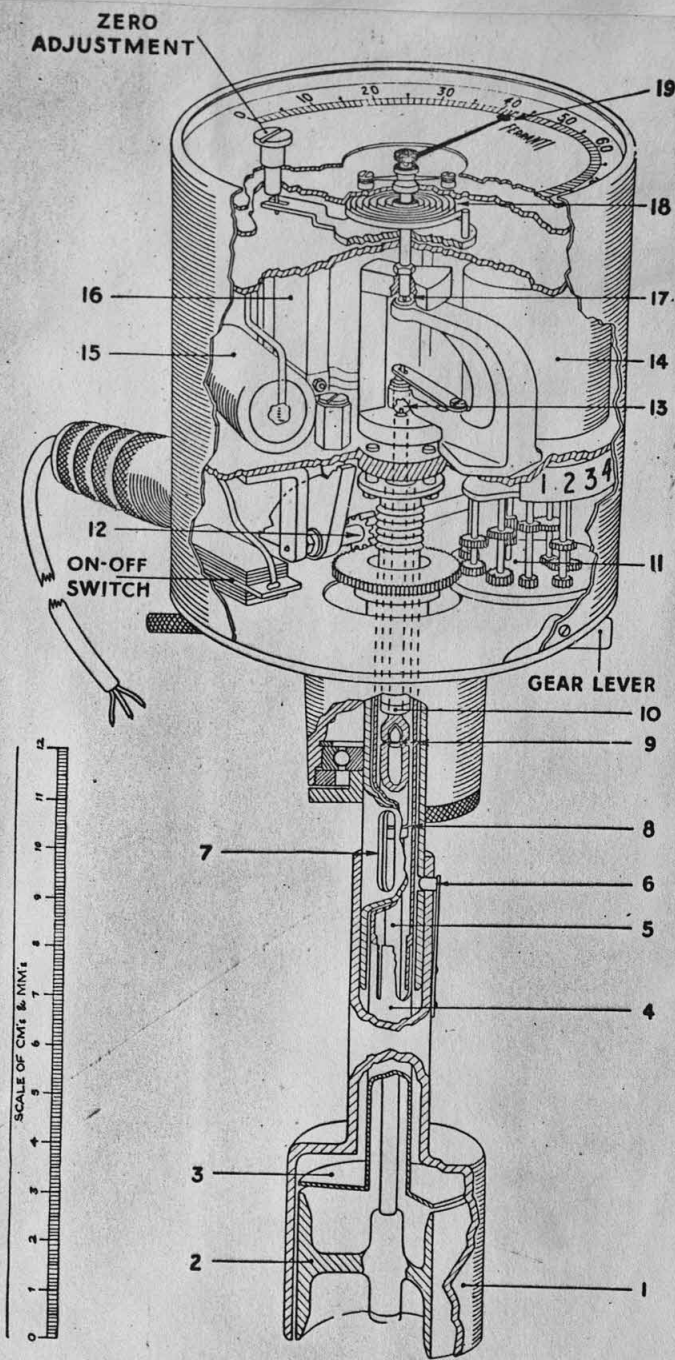
6.3.1 A.Niger tests

The changing morphology of this organism required the viscosity to be tested at various fermentation times. Hence, samples were taken directly from the fermenter and the changes in apparent viscosity and mycelial dry weight with time were observed. Additionally, for each sample time the change of apparent viscosity with dry weight concentration was observed; tests being made at a number of different shear rates.

6.3.2 Yeast

The morphology of yeast does not change appreciably with time; hence samples were not taken from the fermenter at various stages during growth. At the end of the fermentation the yeast was centrifuged and its weight measured. Samples were then transferred into known volumes of water

FIG. 61^A FERRANTI VISCOMETER, MODEL VL



KEY

No.	ITEM	
1	OUTER CYLINDER	10 STEADY BEARING
2	INNER CYLINDER	11 TURRET GEAR BOX
3	GUARD RING	12 INNER CYLINDER LOCKING MECHANISM
4	GUARD RING SUPPORT TUBE (DETACHABLE)	13 SPRING LOADED SECONDARY BEARING
5	INNER CYLINDER SPINDLE	14 SYNCHRONOUS MOTOR
6	OUTER CYLINDER QUICK RELEASE ATTACHMENT	15 PHASING CONDENSER
7	INNER CYLINDER RELEASE APERTURE	16 TRANSFORMER
8	INNER CYLINDER	17 MAIN JEWELLED BEARING
9	QUICK RELEASE SYSTEM	18 TORQUE SPRING
		19 VISCOSITY INDICATING POINTER

or see the effects of differing η . The effects of shear rate, $\dot{\gamma}$, and

concentration were investigated for various yeast strains.

6.4 Results and Analysis

6.4.1 A. Niger Results

6.4.1.1 The variation of apparent viscosity with morphology and biomass concentration

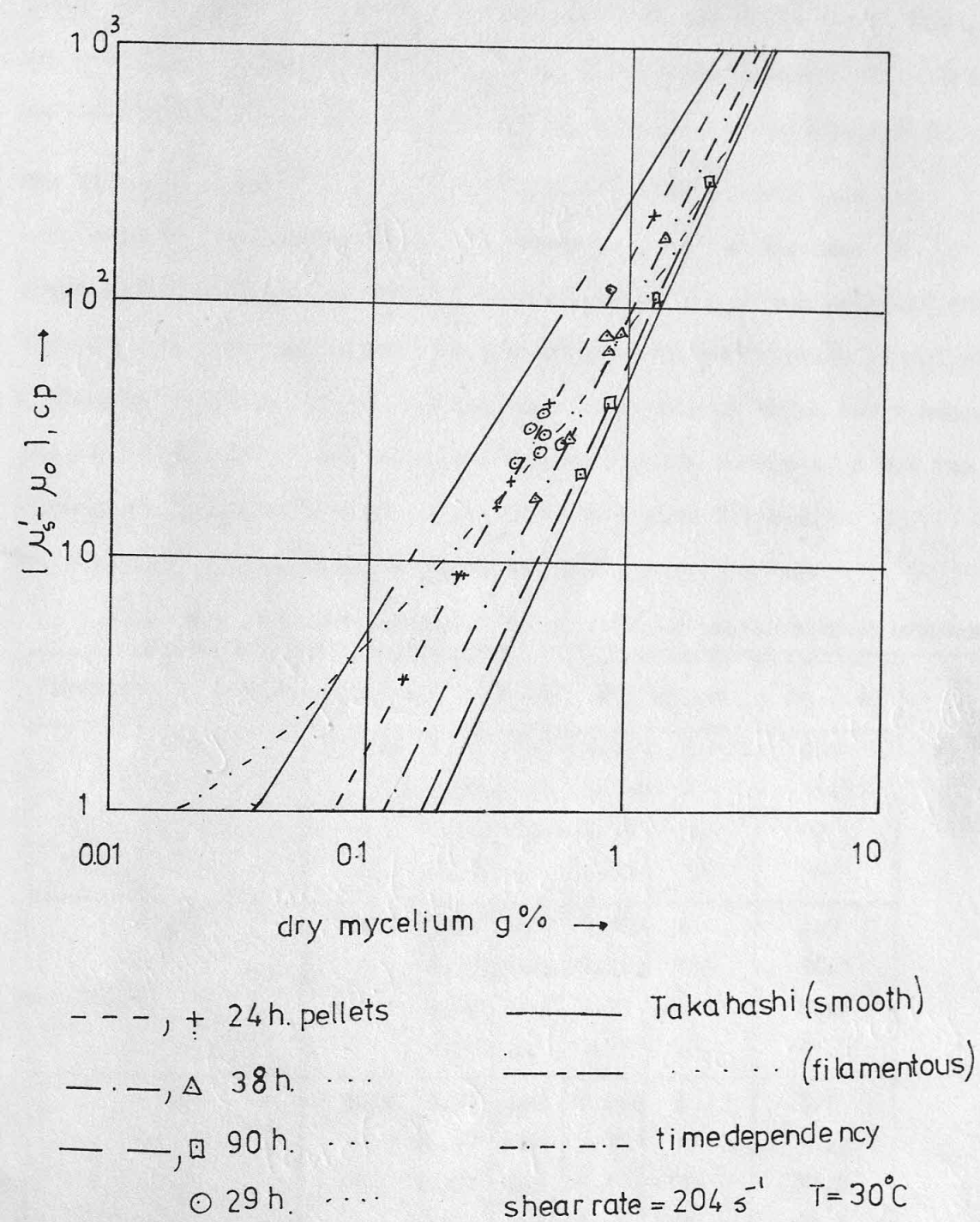
The results were obtained using cylinder VLG, gear 5, giving a shear rate of 204 s^{-1} . The suspension temperature was 30°C .

Table 6.3 Variation of A. Niger suspension apparent viscosity

with concentration and time (morphology).

Apparent viscosity, cp	Apparent viscosity, cp	Apparent viscosity, cp
1.36	244	24
0.57	49.7	25
0.36	18.8	26
0.25	9.4	27
0.15	4.04	28
0.26	10.2	29
0.32	17.2	30
0.86	118	31
0.45	40.4	32
0.39	25.6	33
0.22	13.2	34
0.22	44.4	35
0.70	32.2	36
0.24	28.2	37
1.47	172	38
0.86	70	39
0.66	32	40
0.45	16.2	41
0.25	202	42
0.80	93	43
1.26	110	44
2.08	211	45
0.97	75	46
0.87	48	47
0.74	24	48

FIG. 6.1⁸ EFFECT OF A. NIGER MORPHOLOGY ON VISCOSITY



These results are plotted in Fig. 6.1b. They were compared with those of Takahashi (1969). Whilst the overall comparison seemed favourable it should be noted that Takahashi did not quote the shear rate at which his data was obtained. The general trend of filamentous pellets having greater apparent viscosities than smooth pellets may be observed.

The dry mycelial weights were converted to actual pellet volumes using the information outlined in section 3.4-4 and Table 3.4-2. Thus, if x = dry mycelial wt. /100ml. ; then, ϕ = volume fraction of pellets in suspension, and $\phi = \frac{x}{\rho_s(1-A)100} \dots\dots\dots 6.7$

The values obtained for A only applied where the pellets were not subjected to compression. When this occurred, as was the case in concentrated suspensions, then some immobilised liquid was squeezed out. Fluidisation tests suggested that the maximum volume fraction of pellets (ϕ) was 0.25. Hence, it was assumed that once this ϕ value was reached the pellets began to lose some immobilised liquid. Values of x and the corresponding apparent viscosities were taken from Table 6.3.

The value of μ_o was that for water at 30°C, i.e. 0.81 cp.

Table 6.4 A.Niger apparent viscosities and suspension fractions

Fermentation time, h.	$\rho_s, g/cm^3$	A	$x, g\%$	ϕ	μ_s', cp	μ_s' / μ_o
24	1.29	0.98	0.2	0.078	6.4	7.9
		0.98	0.4	0.155	23	28.5
		0.98	0.65	0.25	56	69
		0.97	1	0.25	135	167
38	1.24	0.985	0.2	0.108	4	4.9
		0.985	0.4	0.215	13	16.1
		0.985	0.47	0.25	18	22.2
		0.977	0.7	0.25	40	49.5
90	1.24	0.97	0.2	0.054	3	3.7
		0.97	0.4	0.108	10	12.4
		0.97	0.6	0.161	22	27.2
		0.97	0.93	0.25	53	65.5
		0.96	1.2	0.25	90	111

These are compared with the existing theories for suspension viscosities in Fig. 6.2. The data listed in Table 6.5 were used in this figure.

Table 6.5 Theories for the viscosity of suspensions

ϕ		$\mu_r = \mu_s / \mu_o$		
	Einstein (eqn. 6.1)	Thomas (eqn. 6.5)	Happel (eqn. 6.4)	Vand (eqn. 6.3)
0.05	1.125	-	1.281	-
0.10	1.25	1.37	1.605	1.32
0.20	1.5	1.99	2.486	1.79
0.30	1.75	3.1	3.942	2.41
0.40	2.0	5.89	6.621	3.18
0.50	2.25	16.91	12.20	4.09
0.60	2.5	70.62	-	5.15
0.80	3.0	-	-	7.7
1.00	3.5	-	-	10.85

(The Vand equation was evaluated using $F = 7.35$.)

The results for A. Niger, which are typical of those observed for mycelial broths, do not agree with existing viscosity theories, which cannot account for the rigidity of hyphal networks. Even though the values for ϕ are only estimates this overall conclusion is still valid.

6.4.1.2 Rheological characteristics of A. Niger

The variation of apparent viscosity with shear rate was measured for samples taken at 28 & 38h. The results are summarised in Table 6.6 and shown in Fig. 6.3.

In Table 6.6, $\tau = \mu_s' (dv/dy)$ and for a Bingham plastic,

$$\tau = \tau_o + \eta \frac{dv}{dy} \dots\dots\dots 6.8$$

For a Pseudoplastic fluid,

$$\tau = K (dv/dy)^n \dots\dots\dots 6.6$$

The 28h. pellets appeared to behave like a Bingham suspension with

$$\tau = 9 + 0.27 (dv/dy) \dots\dots\dots 6.9$$

The 38h. sample appeared to be pseudoplastic. This suggested that the broth became increasingly Non-Newtonian as the fermentation proceeded,

These results are plotted in Fig. 6.1b. They were compared with those of Takahashi (1969). Whilst the overall comparison seemed favourable it should be noted that Takahashi did not quote the shear rate at which his data was obtained. The general trend of filamentous pellets having greater apparent viscosities than smooth pellets may be observed. The dry mycelial weights were converted to actual pellet volumes

using the information outlined in section 3.4.4 and Table 3.4.2. Thus, if μ_s = dry mycelial wt./100ml.; then, ϕ = volume fraction of pellets in suspension, and $\phi = \frac{X}{2(1-A)}$ 6.7 The values obtained for A only applied where the pellets were not subjected to compression. When this occurred, as was the case in compressed suspensions, then some immobilised liquid was squeezed out. Elutriation tests suggested that the maximum volume fraction of pellets (ϕ) = 0.25. Hence, it was assumed that once this ϕ value was reached the pellets began to lose some immobilised liquid. Values of x and the corresponding apparent viscosities were taken from Table 6.3.

The value of μ_o was that for water at 30°C, i.e. 0.81 cp.

Table 6.4 A. Niger apparent viscosities and suspension fractions

Permeation time, h.	ϕ	$x, \%$	$\mu_s', \text{cp.}$	μ_s' / μ_o
24	0.25	0.25	1.25	1.55
	0.25	0.4	0.98	1.21
	0.25	0.65	0.98	1.21
	0.25	1	0.97	1.20
38	0.25	0.25	1.24	1.54
	0.25	0.4	0.98	1.21
	0.25	0.47	0.98	1.21
	0.25	0.7	0.97	1.20
30	0.25	0.25	1.24	1.54
	0.25	0.4	0.97	1.20
	0.25	0.6	0.97	1.20
	0.25	0.93	0.97	1.20
	0.25	1.2	0.96	1.19

as was found by Deindoerfer et alia (1955). The constants in equation 6.6 were found by linearising the data in Table 6.6. Thus, for the 38h. pellets

$$\tau = 37 (dv/dy)^{0.43} \dots\dots\dots 6.10$$

This was comparable with the results of Bongenaar et alia (1973) for *P.Chrysogenum*. Values of 172 & 0.35 reported by Solomons (1962) were for 4.5 g% *A.Niger* broth which contained much more biomass than the 38h. sample.

Table 6.6 *A.Niger* Rheology and Morphology

Age, h.	Biomass, g%	μ_s' , poise	Shear rate, s^{-1} (dv/dy)	Shear stress, τ , dyne/cm ²
38	1.47	1.75	204	357
		2.01	170	341.7
		2.34	135	315.9
		2.70	102	275.4
		3.29	68	223.7
28	0.54	0.28	204	57.1
		0.29	135	39.2
		0.35	68	23.8

6.4.1.3 Apparent viscosity variation during fermentation

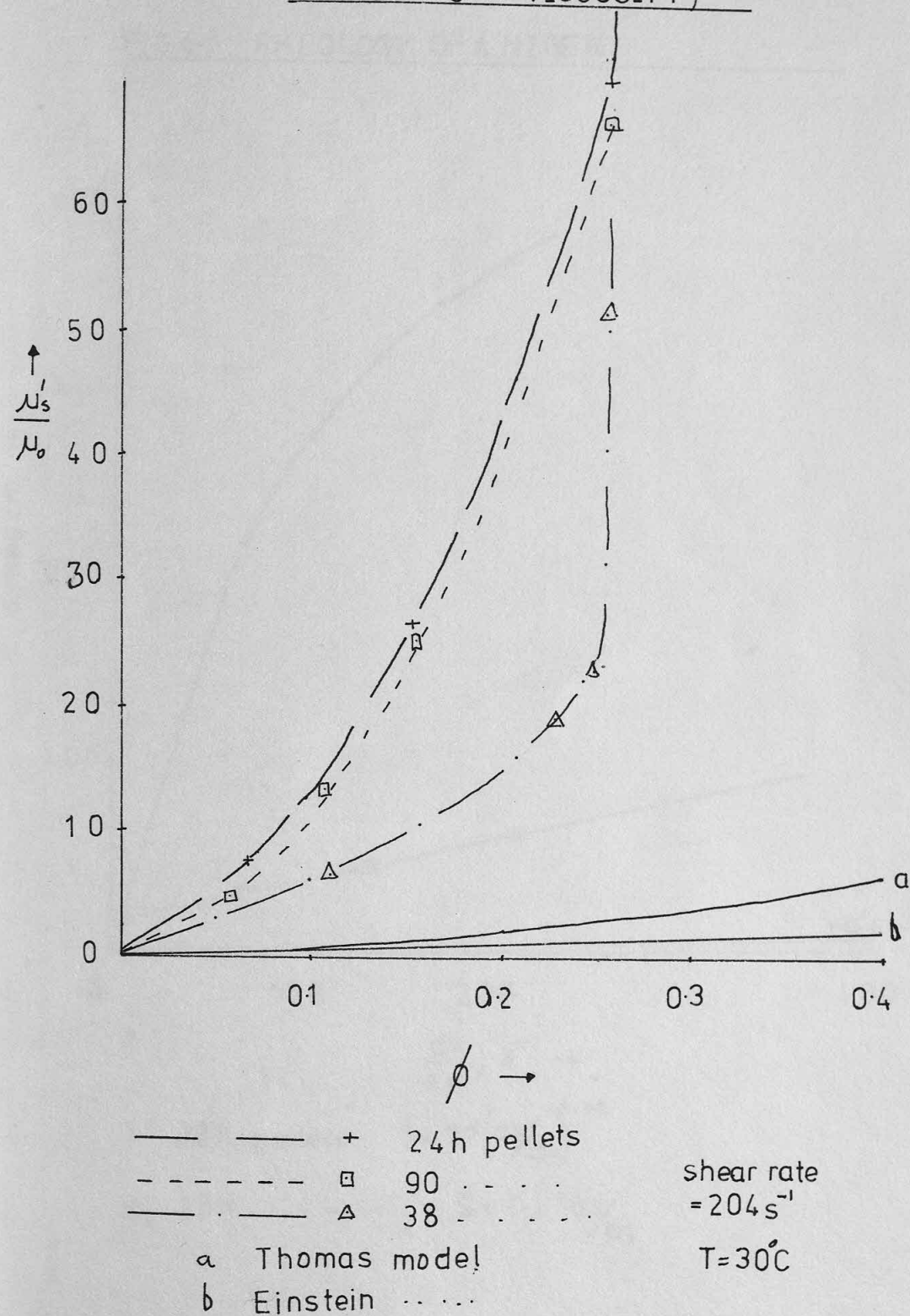
The apparent viscosity and dry mycelial weight were measured with time during the course of a fermentation (see Table 6.7).

Table 6.7 Time variations of apparent viscosity for *A.Niger*

Fermentation time, h.	Apparent viscosity, cp	Dry wt., g%
0	0.87	0
14	1.45	0.017
19	5.3	0.086
25	17.5	0.32
28	28.2	0.54
30	36.3	0.56
40	91.5	0.78

The results are shown in Fig.6.4. They suggest an exponential increase in apparent viscosity with time throughout most of the growth cycle. These results ~~were~~ ^{are} similar to those of Deindoerfer & West (1960).

FIG. 6.2 RHEOLOGY OF A. NIGER SUSPENSIONS
(SUSPENSION VISCOSITY)



as was found by Deindorfer et alia (1972). The constants in equation 6.6 were found by linearizing the data in Table 6.6. Thus, for the 38h. pellets $\tau = 37 \text{ (dyne/cm}^2\text{)}^{0.43}$ 6.10

This was comparable with the results of Borgmann et alia (1973) for *S. cerevisiae*. Values of 172 ± 0.35 reported by Solomon (1962) were for *S. cerevisiae* broth which contained much more biomass than the 38h.

Table 6.6 A. Niger Rheology and Morphology

Time, h.	Biomass, %	μ_0 , poise	Shear rate, s^{-1} (dyne/cm ²)	Shear stress, τ (dyne/cm ²)
38	1.47	1.75	204	357
		2.01	170	341.7
		2.34	135	315.9
		2.70	102	275.4
		3.29	68	223.7
28	0.54	0.28	204	27.9
		0.29	135	30.8
		0.32	68	23.8

Table 6.7 Time variations of apparent viscosity for A. Niger

The apparent viscosity and dry mycelial weight were measured with the course of a fermentation (see Table 6.7).

Time, h.	Apparent viscosity, cp	Dry wt., %
0	0.07	0
14	1.45	0.017
19	2.3	0.066
25	17.5	0.32
28	28.2	0.54
30	36.3	0.55
40	41.5	0.78

The results are shown in Fig. 6.4. They suggest an exponential increase in apparent viscosity with time throughout most of the growth cycle. These results were similar to those of Deindorfer & Hart (1969).

FIG.6.3 RHEOLOGY OF A. NIGER

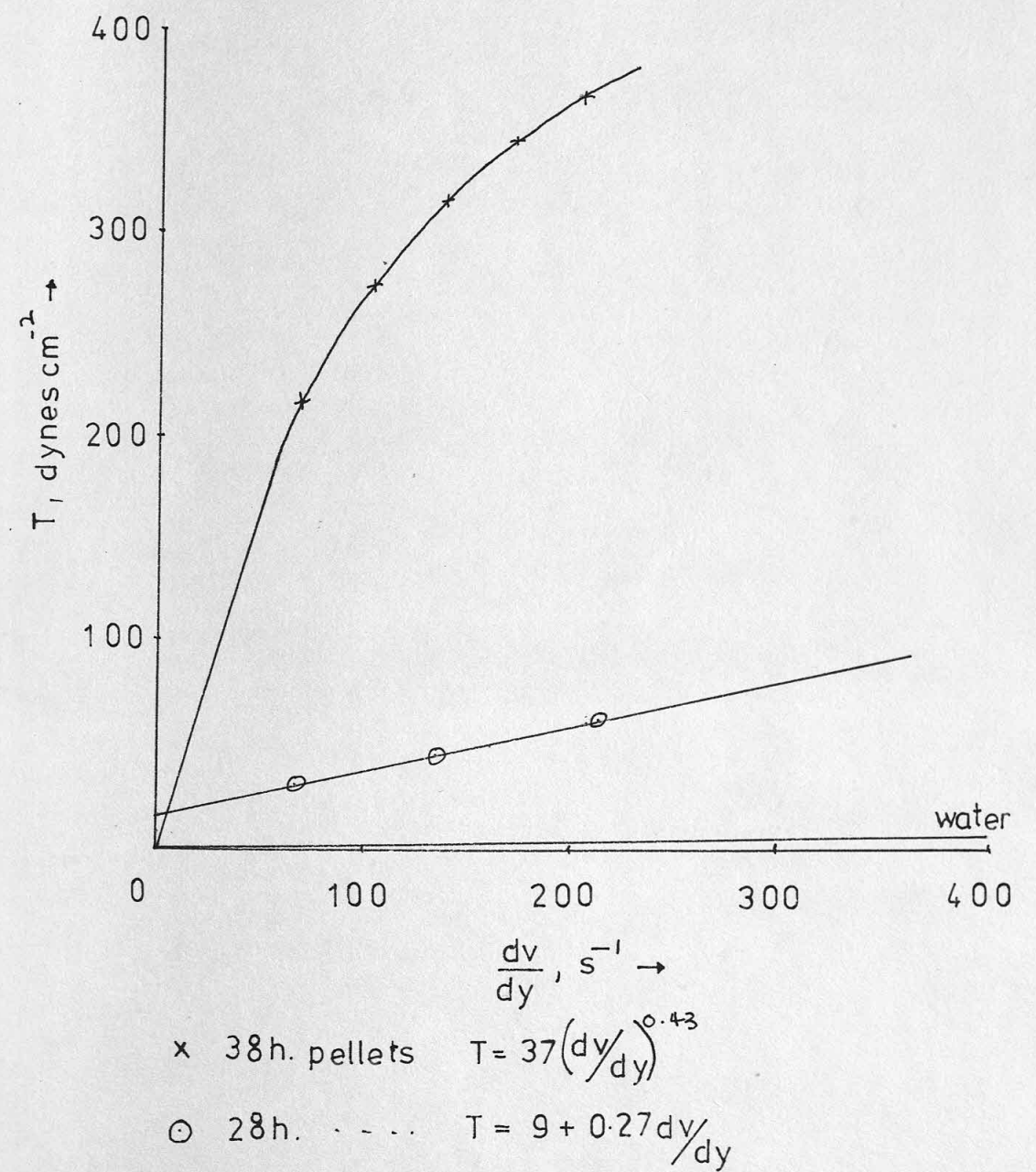


FIG. 64 A. NIGER VISCOSITY vs. TIME

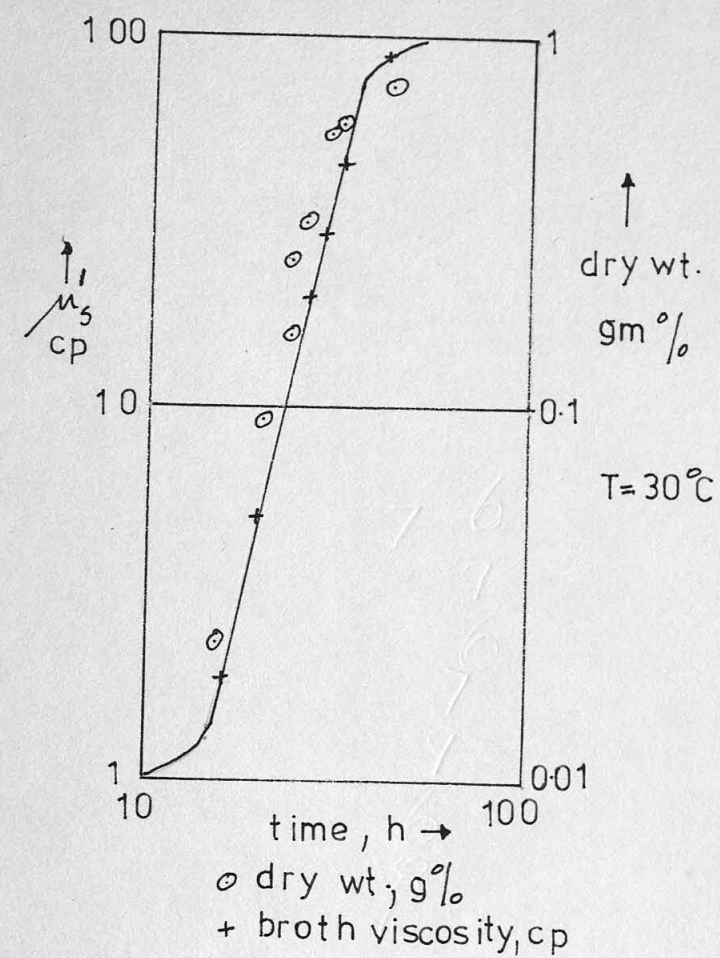
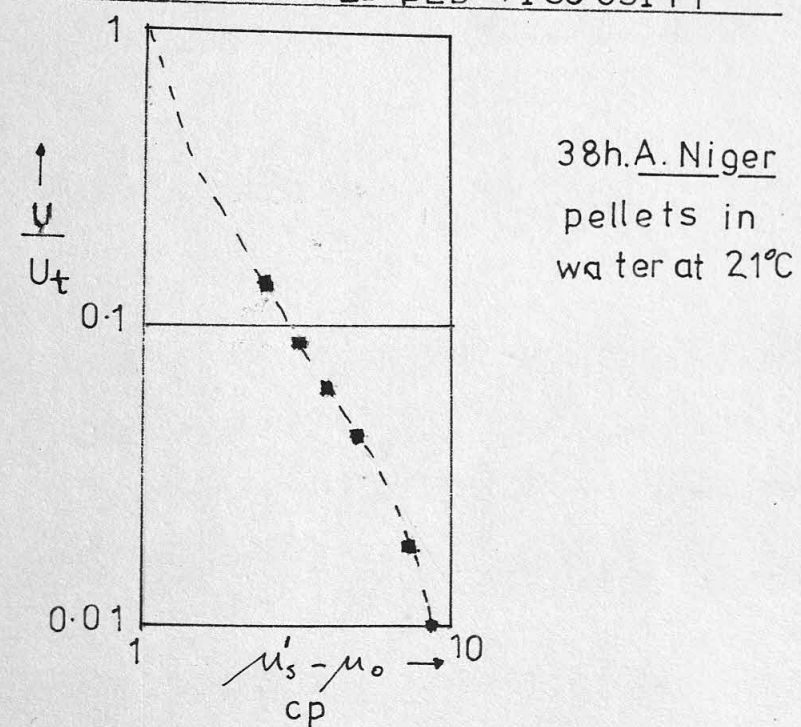


FIG. 65 FLUIDISED BED VISCOSITY



The time variation of apparent viscosity is also included in Fig.6.1b, illustrating that both morphology and concentration contributed to the apparent viscosity change.

6.4.1.4 Fluidised bed viscosities

A liquid fluidised bed is merely a suspension of particles and thus will have a viscosity whose value depends on the solids concentration and thus the liquid flowrate. As an illustration of the variation of apparent viscosity with flowrate, the data from the 40h. molasses pellets in the two-dimensional bed (see Chapter 5) was analysed.

The dry weight in the bed was 3.5g and thus at each voidage the dry weight concentration could be calculated. From Fig.6.1, the apparent viscosity corresponding with each dry wt. concentration was found for 40 h. pellets. The results are shown in Fig.6.5 and Table 6.8.

Table 6.8 A.Niger fluidised bed viscosity variations

Bed volume, cm ³	e	Dry wt., g%	($\mu_s' - \mu_o$), cp	U / U_t
1810	0.896	0.193	2.6	0.120
1740	0.892	0.201	2.9	0.096
1570	0.880	0.223	3.6	0.072
1380	0.864	0.254	4.7	0.048
1160	0.839	0.302	6.9	0.024
1100	0.828	0.319	7.6	0.018
1020	0.815	0.344	8.8	0.006
985	0.809	0.356	9.6	0.0

6.4.2 Yeast Results

The apparent viscosity of various yeast suspensions was measured at 30°C using the VLA cylinders. A known centrifuged weight was suspended in a given volume of water or buffer and the apparent viscosity measured. The strains used were S.Carlsbergensis CFCC 83, S.Cerevisiae CFCC 8 & 34.

It was probable that the high shear field in the viscometer annulus caused the flocs to form into their basic low voidage cluster

FIG.66 YEAST CONCENTRATION vs. VISCOSITY

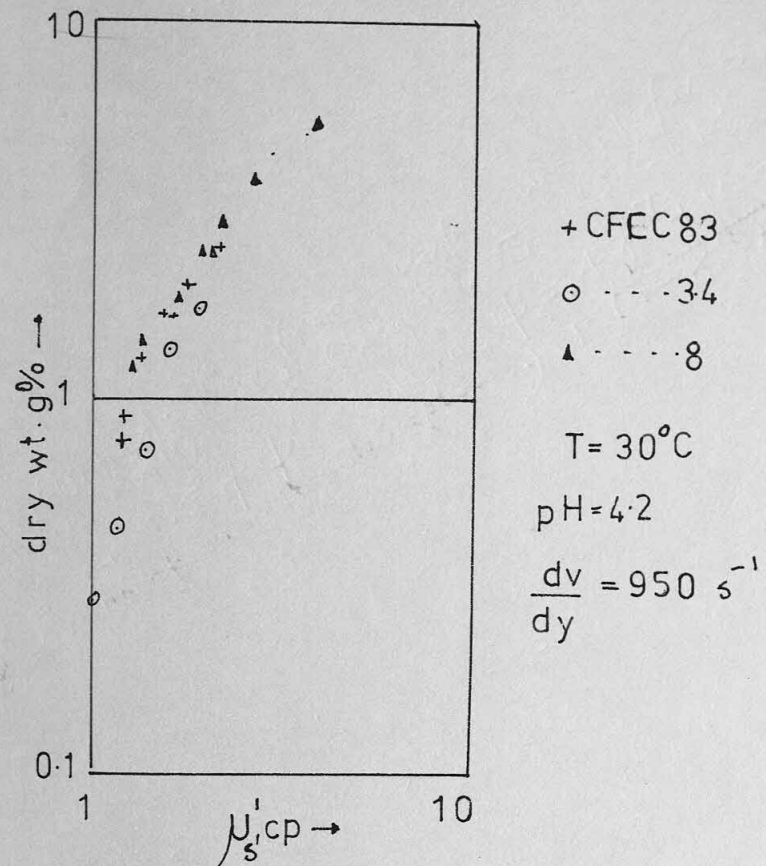
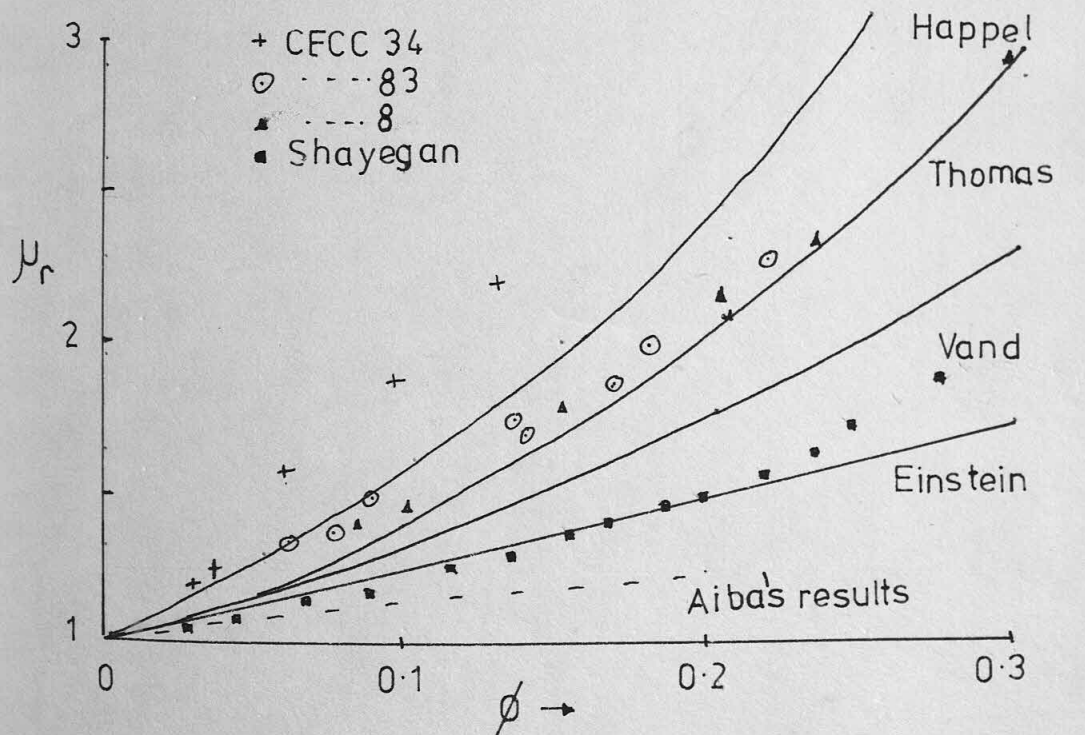


FIG.67 VISCOSITY OF YEAST SUSPENSIONS



The time variation of apparent viscosity is also included in Fig. 6.6, illustrating that both morphology and concentration contributed to the apparent viscosity change.

Table 6.8 A. Niger fluidized bed viscosity variations

A liquid fluidized bed is merely a suspension of particles and will have a viscosity whose value depends on the solids concentration and thus the liquid flowrate. As an illustration of the variation of apparent viscosity with flowrate, the data from the 40% molasses pellets in the two-dimensional bed (see Chapter 5) was analyzed. The dry weight in the bed was 3.5% and thus at each voidage the dry weight concentration could be calculated. From Fig. 6.1, the apparent viscosity corresponding with each dry wt. concentration was found for 40% molasses. The results are shown in Fig. 6.5 and Table 6.8.

Volume, cm ³	Dry wt., %	$(\mu' - \mu'_0) \times 10^{-2}$	μ' / μ'_0
1810	0.896	0.193	0.120
1740	0.892	0.201	0.098
1570	0.880	0.223	0.075
1380	0.864	0.254	0.048
1160	0.833	0.302	0.024
1100	0.828	0.319	0.018
1020	0.815	0.344	0.006
995	0.809	0.356	0.0

Table 6.8 A. Niger fluidized bed viscosity variations

The apparent viscosity of various yeast suspensions was measured at 30°C using the VLA cylinders. A known centrifugal weight was suspended in a given volume of water on pulley and the apparent viscosity measured. The strains used were S. Carlsbergensis CFEC 83, S. Cerevisiae CFEC 34.

It was probable that the high shear field in the viscometer caused the flocs to form into their basic low voidage cluster

configuration. Therefore, a floc voidage of 50 % was assumed and the data of section 3.4.2 was used. The dry wt. of yeast per 100ml. and the floc suspension volume fractions were thus evaluated.

A sample test on CFCC 83 at pH = 4.2, T = 30°C have the results shown in Table 6.9. For CFCC 83, the dry wt. /centrifuged wt. = 0.19.

Table 6.9 Sample viscosity results for a physically- limited yeast

Centrifuged wt. g.	Suspension volume, cm ³	Dry material g %	ϕ	μ_s , cp	$\frac{\mu_s}{\mu_o}$	$\frac{dv}{dy}$, s ⁻¹	τ , dyne/cm ²
36.4	400	1.73	0.132	1.52	1.88	318	4.83
				1.46	1.80	475	6.94
				1.41	1.74	791	11.15
				1.34	1.65	950	12.73
44.5	335	2.52	0.193	2.07	2.56	318	6.58
				1.91	2.36	475	9.07
				1.83	2.26	791	14.48
				1.75	2.16	950	16.63
44.5	900	0.94	0.072	1.30	1.60	318	4.13
				1.24	1.53	475	5.89
				1.19	1.47	791	9.41
				1.12	1.38	950	10.64

The results for the three strains are shown in Figs. 6.6 to 6.9.

6.4.2.1 Dry material concentration vs. Apparent viscosity

This data is shown in Fig. 6.6. The results were independent of any assumptions concerning floc structure and they revealed that the results for the highly flocculent yeast CFCC 34 were significantly different from the less flocculent yeasts. The corresponding apparent viscosity for CFCC 34 was greater than the others, a similar trend being observed in Fig. 6.7.

6.4.2.2 Relative viscosity vs, Volume fraction of solids

These results are shown in Fig. 6.7. The results, based on a 50 % floc voidage, compared favourably with the Thomas and Happel equations for CFCC 8 & 83. The relative viscosity values were much less than for

mycelial suspensions, but were greater than those for non-flocculent yeasts (e.g. the results of Shayegan and Aiba et alia). As CFCC 34 gave greater viscosities than any others it appears that the corresponding apparent viscosity increases with increasing flocculence. For $\phi > 0.08$ the results may be correlated with the Vand equation when $F \approx 16$.

6.4.2.3 Rheological Properties

The shear rate vs. shear stress diagrams for the yeasts are shown in Fig. 6.8 .They suggest that the suspensions are Newtonian for $\phi < 0.06$ and slightly pseudoplastic for higher concentrations. This suggests that for yeasts the true and apparent viscosities are very similar. Linearising the τ vs. $\frac{dv}{dy}$ values given in Table 6.9 the pseudoplastic equation constants were as follows;

ϕ	K , dyne s ⁿ cm ⁻²	n
0.072	0.028	0.869
0.132	0.035	0.867
0.193	0.056	0.836

6.4.2.4 Effect of pH on viscosity

This is illustrated in Fig. 6.9 for CFCC 83 at 30°C over a pH range of 6.2 to 4.2 for a constant yeast volume fraction (0.092), in suspension. A maximum viscosity at pH = 5.3 was observed which may correspond to the optimum pH for flocculation.

6.5 Conclusions

Flocculent yeast and mycelial suspensions showed pseudoplastic behaviour at high concentrations. At low concentrations Bingham or Newtonian behaviour was observed. Mycelial suspensions had apparent viscosities much greater than flocculent yeasts which in turn had greater viscosities than non-flocculent yeasts. Flocculent yeasts behaved in reasonable agreement with the Happel and Thomas equations, whereas, none of

the existing theories can be used to correlate the data for mycelial suspensions.

Morphological changes were observed to affect the apparent viscosity, the highest viscosities being observed with filamentous pellets. Concentration and morphological changes caused the apparent viscosity of mycelial broths to increase rapidly with fermentation time. Increasing flocculence and factors affecting flocculence were found to have a considerable influence on the viscosity of yeast suspensions.

Aeration of mycelial suspensions of A.Niger would be very inefficient after about 25h. fermentation time due to the high apparent viscosity of the suspensions. Similarly, the power required to mix mycelial suspensions would increase rapidly during the fermentation. From about 35h. onwards the A.Niger fermentation performed by the author (see Chapters 3 & 7) would probably be largely anaerobic with very little mixing occurring. This suggests that after a relatively short fermentation time, the suspension should be diluted so as to promote faster biomass production.

Mycelial suspensions, but were greater than those for non-flocculent yeasts (e.g. the results of Bagnall and Ellis at pH 5.0 for CERO 34 gave greater viscosities than any others it appears that the corresponding apparent viscosity increases with increasing flocculence. For 0.03 the results may be correlated with the Vand equation when $n = 10$.

6.4.2.3 Pseudoplastic Properties

The shear rate vs. shear stress diagrams for the yeasts are shown in Fig. 6.6. They suggest that the suspensions are Newtonian for $\dot{\gamma} > 100$ s⁻¹ and slightly pseudoplastic for higher concentrations. This suggests that for yeasts the true and apparent viscosities are very similar. The values given in Table 6.9, the pseudoplastic equation constants were as follows:

n	K , dyne s ⁿ cm ⁻²	$\dot{\gamma}_0$
0.068	0.028	0.075
0.067	0.032	0.132
0.038	0.056	0.193

6.4.2.4 Effect of pH on viscosity

This is illustrated in Fig. 6.9 for CERO 83 at 30°C over a pH range of 2 to 4.2 for a constant yeast volume fraction (0.032), in suspension. A maximum viscosity at pH = 3.2 was observed which may correspond to the optimum pH for flocculation.

6.5 Conclusions

Flocculent yeast and mycelial suspensions showed pseudoplastic behaviour at high concentrations. At low concentrations Bagnall and Ellis (1961) showed that mycelial suspensions had apparent viscosities much greater than flocculent yeasts which in turn had greater viscosities than non-flocculent yeasts. Flocculent yeasts behaved in reasonable agreement with the Bagnall and Ellis equations, whereas none of

FIG.68 RHEOLOGY OF YEAST SUSPENSIONS

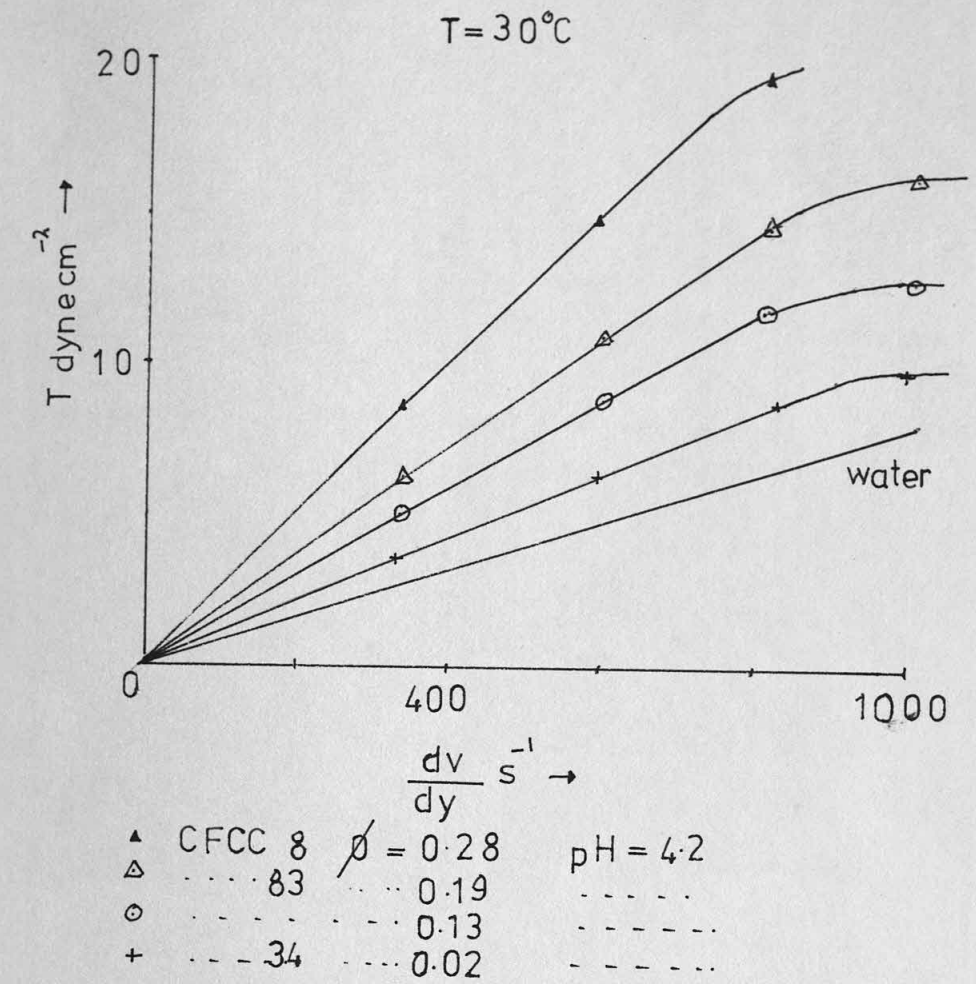
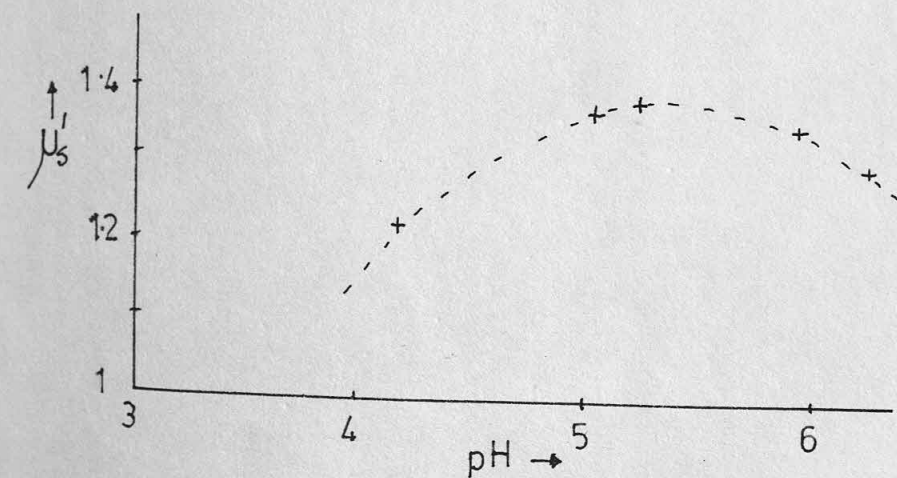


FIG.69 VISCOSITY vs. pH FOR CFCC 83

$T = 30^{\circ}\text{C} \quad \frac{dv}{dy} = 950 \text{ s}^{-1} \quad \phi = 0.09$



CHAPTER 7

THE DESIGN AND OPERATION OF TOWER FERMENTERS

7.1 Introduction

The previous chapters have described work which has been aimed at measuring certain basic properties and understanding the behaviour of microbial aggregates. Where possible, comparisons between these aggregates and conventional engineering materials were made. This revealed that microbial systems behave differently from the usual systems due, in the main, to the peculiarities of the aggregate itself (i.e. density, morphology and sensitivity to environment). However, the tests and results described previously are not strictly applicable to operating tower systems. Two main factors were absent. These are:

- i. the gas phase and
- ii. the presence of fermenting sugars and associated metabolites.

Thus in using information from earlier chapters the modifying effects of the above should be taken into account when dealing with actual fermenters.

7.2 The presence of a gas phase

A suspension in a fermenter may be in contact with a gas phase from two sources :

- i. CO_2 evolved as small bubbles and
- ii. external air introduced for aeration/mixing.

If these two occur separately as in ethanol production, then their separate effects will be different. However, if external air is introduced throughout the process then it will be present in much greater volume.

7.2.1 Literature Review on Gas-Liquid Fluidisation

Many workers have recently investigated the effects of cocurrent

gas and liquid flow through a bed of solids. The solids used have been conventional fluidisation materials, e.g. ballotini, sand and lead-shot. Generally, air and water have been the fluid phases used in experimental work. Thus, the direct applicability of this work to fermenters using microbial aggregates is limited.

A leading worker has been Østergaard (1965, 1966, 1968, 1970, 1972). He presented an excellent review of this topic in 1968. For brevity, the general principles of three phase fluidisation will be discussed

1. The hold-up of the gas phase

The presence of solids affects the gas hold-up, as does the flowrate of liquid; and, with gas-liquid systems, hold-up depends on gas velocity. Particles of less than 0.1 cm. cause a reduction in hold-up, but particles greater than 0.3 cm. give a higher hold-up, than solids-free systems. (Viswanathan et alia , 1965).

Østergaard and Michelson (1970) summarised their data as follows

Particle size	Gas Hold-up
0.025cm ballotini	$K U_g^{0.88}$
0.10	$K' U_g^{0.78}$
0.60	$K'' U_g^{0.93}$
no ballotini	$K''' U_g^{1.05}$

Gas hold-up was found to decrease with increasing U_L in the solids-free systems and when 0.6cm ballotini was used . But the reverse relationship was found using the smaller ballotini, which also lead to intense mixing in both the gas and liquid phases.

2. The hold-up of the solids phase

Knowing the gas hold-up , the solids hold-up (and hence, liquid hold-up) may be found from expansion measurements. Stewart and Davidson (1964) and Østergaard et alia (1966) state that :

- bed expansion increases as U_L increases , and
- expansion is considerably decreased in the presence of the

gas phase.

The reduction caused by the introduction of gas increased as the initial expansion increased and was most marked in the case of small particle suspensions (see Fig. 7.1). For large ($>0.3\text{cm.}$) particles bed expansion can increase on introducing the gas phase. Stewart et alia (1964), Østergaard (1965), Efremov et alia (1970) and Vail et alia (1970) all presented theories to predict the total hold-up and the individual hold-ups.

Wake structure

Qualitatively, the contraction of the bed in certain instances was ascribed to the acceleration of the wake liquid and consequent deceleration of the extra-wake liquid. This reduction in liquid velocity causes the particles to move closer thereby causing a reduction in bed height. Rigby and Capes (1970) investigated wake properties and found that wake/bubble volume ratio

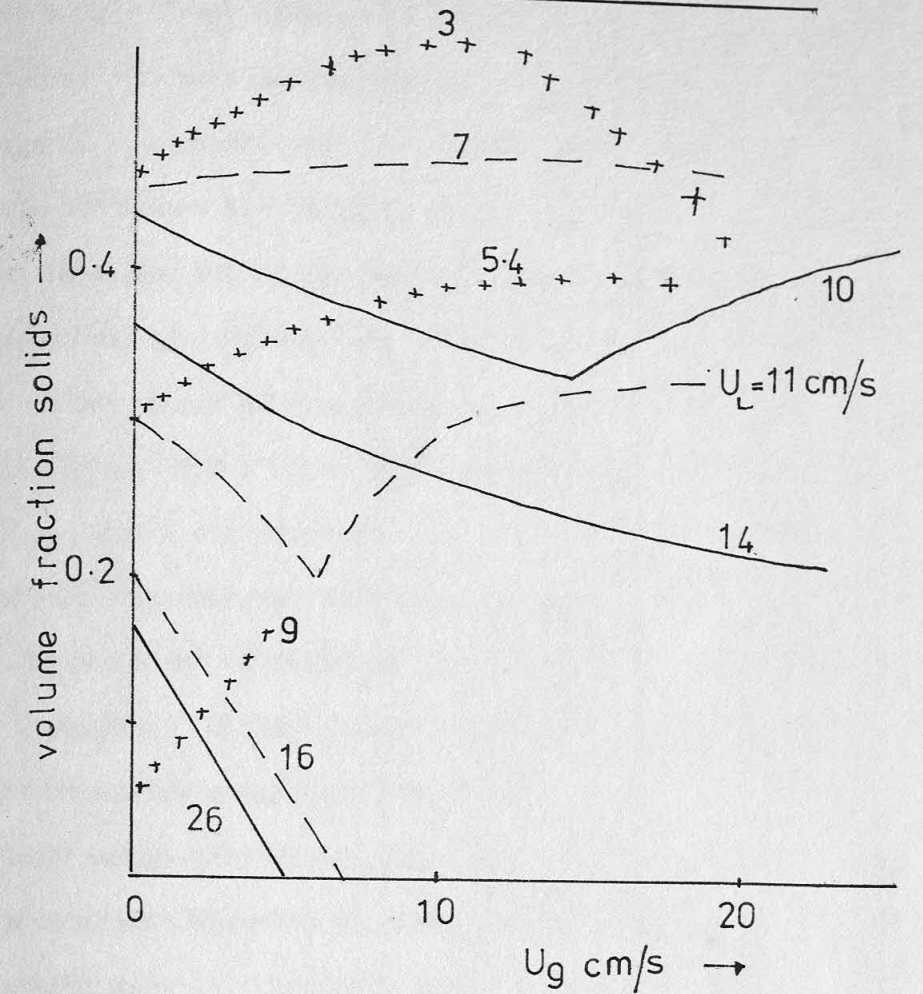
- i. increased as d or U_L increased
- ii. increased as U_G decreased.

The wake was free from particles and the vortices contained particles at a lower concentration than the rest of the bed. However, changing the density of the solids can affect this behaviour (see Fig. 7.2).

Zero liquid flow

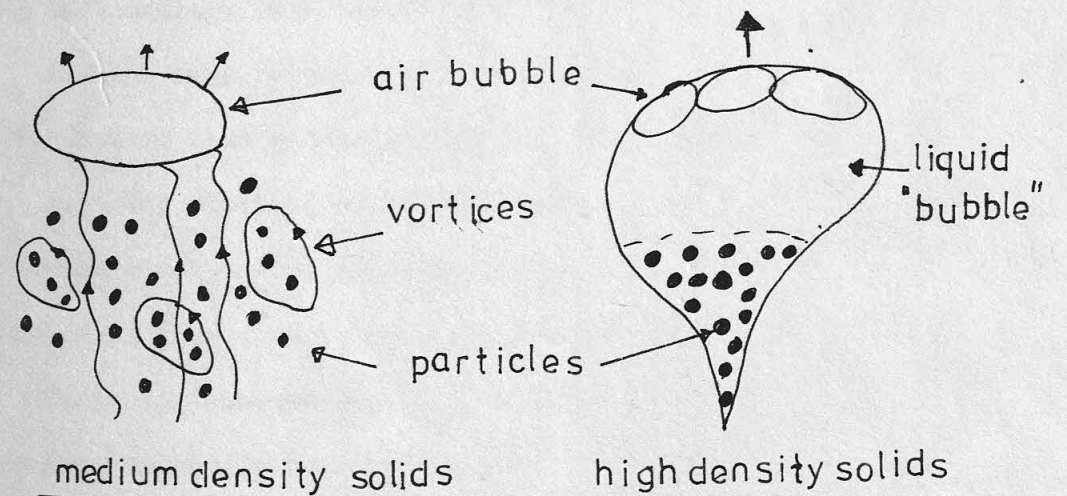
When no liquid is flowing the system is known as a "bubble column slurry system" (Østergaard, 1968). An important characteristic of these systems is the gas rate required to maintain an even distribution of solids in suspension. As might be expected, this is controlled by the amount of solids in suspension. This critical gas velocity has been measured by Kolbel et alia (1964), Kato (1963) and Roy et alia (1964). The latter workers defined a critical solids hold-up and showed how this was related to gas velocity, particle size and the physical properties of the system.

FIG.7.1 THREE PHASE SYSTEMS



— 0.6 cm. ballotini from Østergaard
 - - 0.3 " " & Michelson, 1970
 + + 0.1 " " " "

FIG.7.2 WAKE STRUCTURES



The reduction caused by the introduction of gas increased as the initial expansion increased and was most marked in the case of small particles (see Fig. 7.1). For large (>0.3cm.) particles bed expansion can increase on introducing the gas phase. Stewart et alia (1965), Østergaard (1965), Efremov et alia (1970) and Vail et alia (1970) all presented theories to predict the total hold-up and the individual hold-up.

Qualitatively, the contraction of the bed in certain instances was ascribed to the acceleration of the wake liquid and consequent deceleration of the extra-wake liquid. This reduction in liquid velocity causes particles to move closer thereby causing a reduction in bed height. Higby and Gapes (1970) investigated wake properties and found that wake volume ratio
 1. increased as U_L increased
 2. increased as U_g decreased.

The wake was free from particles and the vortices contained particles at a lower concentration than the rest of the bed. However, changing the density of the solids can affect this behaviour (see Fig. 7.2).

When no liquid is flowing the system is known as a "bubble column" or "system" (Østergaard, 1968). An important characteristic of these systems is the gas rate required to maintain an even distribution of solids in suspension. As might be expected, this is controlled by the amount of solids in suspension. This critical gas velocity has been measured by Kato et alia (1964), Kato (1963) and Roy et alia (1964). The latter workers defined a critical solids hold-up and showed how this was related to gas velocity, particle size and the physical properties of the system.

7.2.2 Qualitative observations, made by the author, with low-density solids

Tests were first made using fluidised beds of mustard seed. Single bubbles of air were introduced via a hypodermic syringe. The effect of the passage of the bubble was to produce a temporary bed contraction. Particles were entrained in the wake of the bubble and were lifted for some distance from the top of the bed before returning. Considerable mixing and associated turbulence was caused by the passage of the bubbles.

The introduction of a continuous supply of air caused total disruption of the bed and violent particle and liquid mixing. The formation of gas slugs was observed (as with < 0.2 cm. ballotini). Similar behaviour was observed with suspensions of yeast and A.Niger.

In the absence of detailed quantitative results the author will not attempt a complex discussion of three-phase systems, especially with regard to the microbial situation. Tests using 0.2 & 0.6cm. ballotini in air/water fluidisation performed by the author were in general agreement with the observations discussed in the literature review. Qualitative observations with seed and microbial suspensions can be summarised as follows:

- i. Low density suspensions and ,to a lesser extent, small sized ballotini behaved as homogeneous systems. Thus, the concept of a suspension viscosity had reality. This is not the case with large, heavy particles.
- ii. The high "viscosity" led to bubble coalescence and bubble formation. In turn this caused either bed contraction or total disruption.
- iii. The distinction between contraction and disruption can be related to the energy input required to disrupt the bed. Microbial or seed suspensions have a much lower net weight per unit bed volume than that of ballotini. Consequently, a relatively low gas throughput or power input per unit volume is required to move the bed. This is why single bubbles produced bed contraction, whereas a continuous stream of bubbles led to bed disruption when using seed systems.

7.2.3 The behaviour and effects of the gas phase in fermentation

As the aerobic operation of a fermenter requires considerable quantities of air the bed in this situation may be regarded as fully mixed and not fluidised in the conventional sense. Where small amounts of gas are being evolved, as in anaerobic fermentation, the degree of disruption will depend solely on the amount of gas being evolved.

Basically, four fermentation situations are possible, viz.,

- i. anaerobic batch
- ii. anaerobic continuous
- iii. aerobic batch
- iv. aerobic continuous

The information obtained concerning the hold-up of microbial aggregates in static or flowing suspensions may be applied directly to situations i. & ii. Case iv. requires that the rate of washout of aggregates from the mixed suspension should equal the rate of replication of the species. Case iii has been studied in some detail for A. Niger biomass production.

In this instance, the important effect is not that of the gas on the solid-liquid behaviour, but that of the solid on the gas-liquid behaviour. Initial observations on static A. Niger suspensions in the two-dimensional bed indicated that the presence of the solids caused a decrease in the gas holdup due to bubble coalescence (see Table 7.1).

Table 7.1 Effect of A. Niger on gas-liquid behaviour

Mould-free liquid		With 180g. wet weight of 0.2cm mould pellets	
U_G , cm/s,	e_g	U_G , cm/s.	e_g
2	0.090	2	0.046
3	0.156	3	0.074
4	0.220	4	0.100
5	0.265	5	0.122
6	0.300	6	0.146
7	0.315	7	0.170
10	0.260		

7.2.3 The behavior and effects of the gas phase in fermentation

As the aerobic operation of a fermenter requires considerable quantities of air the bed in this situation may be regarded as fully mixed and not fluidized in the conventional sense. Where small amounts of gas are evolved, as in anaerobic fermentation, the degree of dispersion will depend solely on the amount of gas being evolved. Naturally, four fermentation situations are possible, viz.,

- anaerobic batch
- anaerobic continuous
- aerobic batch
- aerobic continuous

The information obtained concerning the hold-up of microbial aggregates in static or flowing suspensions may be applied directly to situations in which the rate of washout of aggregates from the fermenter is equal to the rate of replication of the species. Case (i) requires that the rate of washout of aggregates from the fermenter should equal the rate of replication of the species. Case (ii) requires that the rate of washout of aggregates from the fermenter should equal the rate of replication of the species. Case (iii) requires that the rate of washout of aggregates from the fermenter should equal the rate of replication of the species. Case (iv) requires that the rate of washout of aggregates from the fermenter should equal the rate of replication of the species.

In this instance, the important effect is not that of the gas on the solid-liquid behavior, but that of the solid on the gas-liquid behavior. Initial observations on static *A. Niger* suspensions in the two-dimensional bed indicated that the presence of the solids caused a decrease in the gas holdup due to bubble coalescence (see Table 7.1).

Table 7.1 Effect of *A. Niger* on gas-liquid behavior

Free liquid		With 180g wet weight of 0.2cm mould pellets	
U_g , cm/s	ϵ	U_g , cm/s	ϵ
0.000	2	0.046	2
0.126	3	0.074	3
0.220	4	0.100	4
0.265	5	0.122	5
0.300	6	0.146	6
0.312	7	0.170	7
0.360	8		

FIG. 7.3 GAS HOLDUP IN BATCH *A. NIGER* FERMENTATION

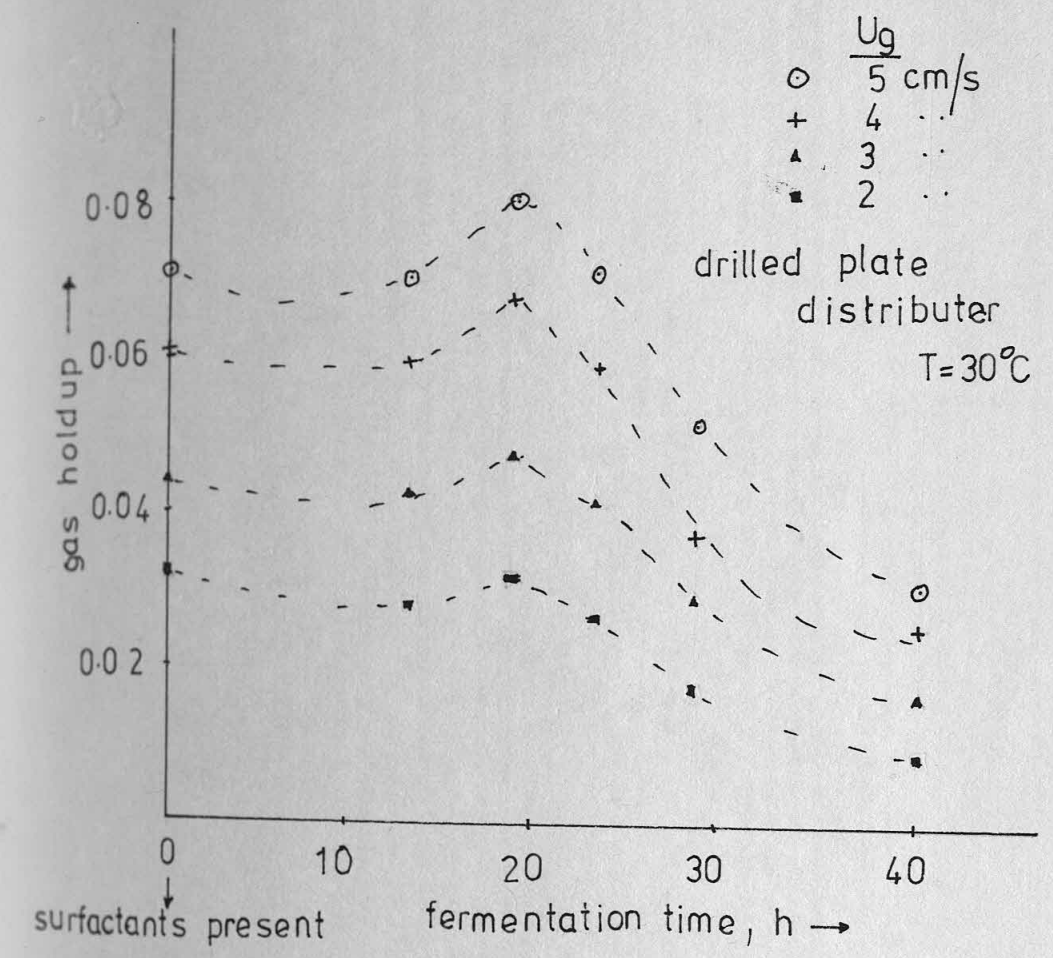
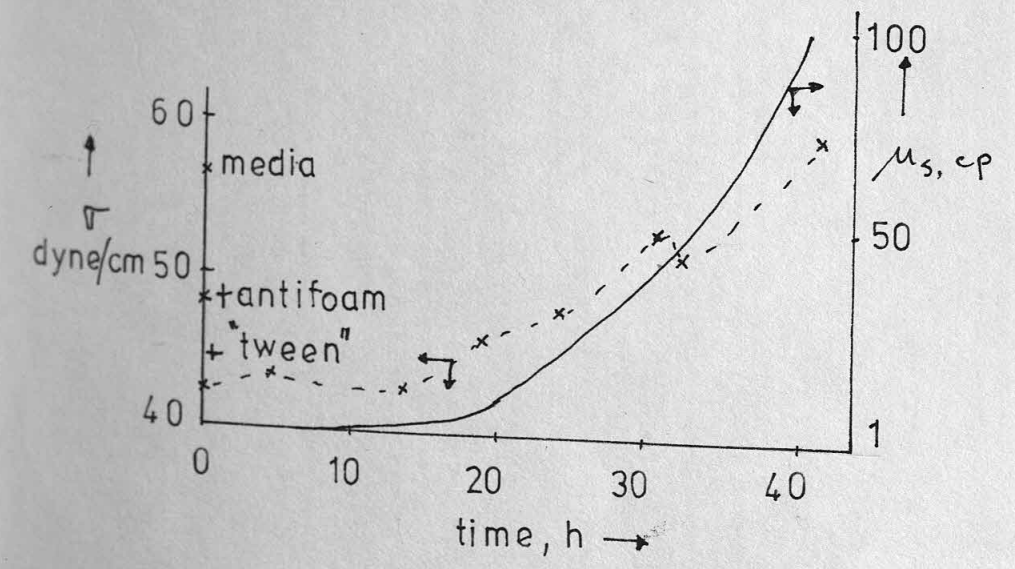


FIG. 7.4 SURFACE TENSION VARIATIONS



This effect was also observed during the aerobic batch production of A.Niger in a 50 litre tower when working in conjunction with Morris (1972). At various time intervals the following measurements were made:

i. surface tension, γ , of the mycelial-free liquid. This was measured using a Cambridge surface tension meter at 23°C. The results were in general agreement with those of Deindoerfer & Gaden, 1955.

ii. Suspension viscosity, μ , and mycelial dry weight concentration (see Table 6.6).

iii. Gas hold-up, e_g , at various superficial gas velocities, U_g . The hold-up results are shown in Fig.7.3. The surface tension and suspension viscosity variations with time are shown in Fig.7.4. These were for a fermenter operating at 30°C, containing a beet-molasses medium which also contained some antifoam and spore dispersing agent, "Tween".

It was noted that between 0 to 19 hours the holdup at a given U_g increased slightly with time. The onset of rapid growth from 19h. onwards led to a rapid increase in dry weight and hence viscosity. This latter factor increasingly controlled the coalescence and holdup of the gas phase until after 23h. the holdup was less than the initial value. This trend continued until the holdup was about 50% of the initial value. As expected gas holdup increased with gas velocity; however, the highest U_g tested was only 5 cm/s. Clearly, the organisms did not receive very much oxygen in the later stages of the fermentation as was discussed in Chapter 6.

7.3 The effect of a fermenting liquid on a fluidised bed of microorganisms

For the fluidisation tests performed on microorganisms (and discussed in Chapter 5) a liquid phase of constant density and temperature was used. However, in a tower system used for a continuous anaerobic fermentation, the liquid composition may change continuously up the tower. Such changes in composition may lead to :

- i. changes in density with axial position,
- ii. changes in the floc-liquid density difference, with position,
- iii. deflocculation and
- iv. changes in microbial concentration.

To examine these effects more fully reference will be made to the best documented tower fermentation process, viz. continuous brewing.

Fluidised yeast flocs

The work of Ault et alia (1969) indicates that the wort (i.e. sugar-containing media used in beer fermentation) gravity falls very rapidly once in contact with yeast, especially at low liquid flowrates. Most of the sugar is fermented in the bottom sixth of the tower length.

Now, the volume concentration of yeast at a point will depend on the superficial velocity of wort, U , and the floc terminal velocity, U_t , amongst others. Hence, the behaviour of the bed may be discussed in terms of the effects of the fermentation upon the U_t value for individual flocs. The results of Chapter 5 indicated that Stokes Law was not strictly applicable to flocs: hence, the Allen equation (1900) will be used

$$U_t = \frac{0.153 d^{1.15} (g (\rho_p - \rho))^{0.715}}{\rho^{0.29} \mu^{0.43}} \dots\dots\dots 7.1$$

(a) The effect of liquid phase density on floc density

Where a fermenting liquid is present some assumption must be made about the density of the liquid within the floc. The extreme cases are

- i. when the density of the interstitial liquid equals the density of the external liquid, and
- ii. the density of the interstitial liquid equals that of water or the final product.

The utilisation of sugars by the floc will require diffusion into the floc. Where diffusion is rate-controlling, case (ii), would be appropriate: where reactions within the cell are rate-controlling, case (i), may hold.

Now, floc density is given by

$$\rho_p = X\rho + (1-X)\rho_y \dots\dots\dots 7.2$$

where X = floc voidage, and ρ_y is assumed constant.

Floc voidage is likely to vary with floc size in the absence of deforming forces. However, under most operating conditions in tower systems some compaction of flocs is unavoidable and it would seem reasonable to assume that X is constant with a value of 0.5.

(b) The possibility of bed stratification

Particles of different sizes and similar densities in a fluidised bed will stratify. Hence, it is not possible, in this system, for small particles to be below larger ones, due to terminal velocity gradients in the bed. However, observations in actual tower fermenters have suggested that points of high yeast concentration may exist other than at the bottom. The mechanism of this phenomena will now be examined using some simple calculations.

The following assumptions will be made for purposes of illustrative calculations.

$\rho_y = 1.07 \text{ g/cm}^3$ (see 3.4.2) ; Initial liquid density = 1.035 g/cm^3 ; Final liquid density = 1.005 g/cm^3 ; Floc size range is from 0.5 to 0.1 cm. diameter.

Example 1

Considering case (i) for floc density; with the floc diameter varying from 0.5 cm at the bottom of the tower to 0.1 cm at the top.

At the bottom of the bed

$$d_1 = 0.5 \text{ cm} ; X = 0.5 ; \rho_1 = 1.035 \text{ g/cm}^3 ; \rho_{p1} = 1.052 \text{ g/cm}^3.$$

At the top of the bed

$$d_2 = 0.1 \text{ cm} ; X = 0.5 ; \rho_2 = 1.005 \text{ g/cm}^3 ; \rho_{p2} = 1.037 \text{ g/cm}^3.$$

Now, high concentration regions surrounded by regions of lower concentration can only occur when at some point in the bed the terminal velocity of large particles is less than or equal to those of smaller particles. Whilst the Allen equation (7.1) should be used for high accuracy, use of the relationship $U_t \propto \frac{d^2 (\rho_p - \rho)}{\rho \mu}$ permits terminal velocity comparisons to be more easily made.

Thus, in example 1, where the floc interstitial liquid has the same density as the external liquid, then

$$U_{t1}/U_{t2} = 28.2 \quad (\text{using the Allen eqn.})$$

$$= 20 \quad (\text{using the above relationship})$$

This indicates that stratification is uniform and therefore no unusual concentration regions will occur.

Example 2

In this case the same conditions as above apply, except that the floc voidage changes from 0.9 at the bottom to 0.5 at the top.

Thus, $U_{t1}/U_{t2} = 4.85$; and therefore, stratification occurs as before. It would therefore seem that where the floc density changes in response to liquid density changes, then it is unlikely that these unusual concentration regions will occur.

Example 3

Now, when the floc density remains constant with position, as it would where the density of the interstitial liquid remains constant, then situations may arise where $(\rho_p - \rho) \leq 0$. e.g. $X = 0.5$ for all flocs; hence, $\rho_p = 1.035$ and therefore at the bottom of the bed $(\rho_p - \rho) = 0$.

When these situations occur then the flocs will rise through the wort until such a position where $(\rho_p - \rho) > 0$, due to the fermentation of the wort. In regions of steep wort density gradients (i.e. at the bottom of the bed), it is possible for flocs of different sizes to have the same terminal velocities, thus leading to regions of unusual concentration.

Fermenting liquids can, therefore, have a marked effect on microbial fluidisation behaviour, and are the cause of the regions of unusually high concentration observed by some in actual tower fermenters.

7.4 A Mathematical Model of a fermentation in a Tower

In collaboration with a colleague, M. Figgett, the author has attempted to use the information discussed in Chapters 3 to 6 to develop a mathematical model of a simple fermentation process in a tower. The model was constructed to allow for a computer evaluation to assist tower design studies. The process considered was :

A continuous, anaerobic fermentation, with no microbial growth

The example chosen for discussion was the continuous production of beer from brewers wort in a tower fermenter.

The Model

This was constructed in the following manner.

A. Preliminaries

The following assumptions were made .

1. The dimensions of the tower were fixed based on current industrial practise (Length = L; circular base area = A; Volume = V).
2. The wort feed rate and specific gravity at the inlet were based on industrial practise. Hence, the superficial velocity, U , could be determined.
3. A normal distribution was assumed to apply to the floc sizes and a mean diameter and variance were chosen to characterise the yeast in the tower; ($d = 0.2\text{cm}$; variance = 0.05 , say).
4. A particular strain or representative strain can be chosen, together with an average floc voidage, X . For simplicity, the floc voidage was assumed to be constant up the tower. An alternative approach would be to vary X with position.
5. An average pseudo-terminal, U_t' , for the yeast in the tower was chosen

based on the results discussed in 5.4.7. Similarly, an average fluidisation index was chosen.

6. The volume of yeast in the tower was divided into 20 equal portions. Hence, each segment of the tower contained $1/20$ of the total yeast volume. Similarly, the floc size distribution was divided into 20 equal portions, and complete stratification was assumed up the tower.

7. The floc density was calculated initially using the relationship discussed in section 7.3, i.e. $\rho_p = X\rho + (1-X)\rho_y$ 7.2
The alternative concept of the floc density being constant could be used.

8. The Michaelis-Menten rate equations were used to describe sugar utilisation.

B. The Calculations

9. The overall yeast voidage in the tower was calculated using

$$e = (U/U_t')^{1/n'} \quad \dots\dots\dots 7.3$$

10. The volume of yeast in the tower was found using

$$\text{yeast volume} = V_y = eV \quad \dots\dots\dots 7.4$$

11. The calculations began at the bottom of the tower, in the 1st. segment.

1st. Segment: 1st. Guess

12. The liquid density in the 1st. segment was considered to equal the inlet wort gravity, and hence, the floc density in this segment was calculated using equation 7.2.

13. For the size of floc in this segment, d_1 , the mean floc terminal velocity was calculated using the Allen equation,
i.e. $U_{t1} = \frac{0.153 d_1^{1.5} (g(\rho_p - \rho))^{0.715}}{\rho_i^{0.29} \mu_i^{0.43}} \quad \dots\dots\dots 7.1$

14. The voidage of this segment was calculated using

$$e_1 = (U/U_{t1})^{1/m}$$

where m is the fluidisation index for the specific conditions of pH, and temperature in the 1st. segment, based on the information in 5.4.7. In some cases m may equal n^{\dagger} .

15. The volume of this first segment was then found using

$$V_1 = e_1 V_y / 20 \dots\dots\dots 7.5$$

Hence, the segment height was found from

$$h_1 = V_1 / A \dots\dots\dots 7.6$$

16. The wort residence time, t_1 , was then found from

$$t_1 = h_1 e_1 / U \dots\dots\dots 7.7$$

Using t_1 , the output sugar concentration from this segment was found by making use of the Michaelis-Menten model.

Second Guess

17. The density of the liquid with the sugar concentration calculated above was then determined (ρ'_1). This served as the basis for a fresh evaluation of ρ_p , U_{t1} , & Re_{t1} . If the two values of U_{t1} were close, then the calculation ceased and then the second segment was considered. If this was not the case, an iteration was performed until the values were approximately equal.

Second Segment :

18. Using the final value of ρ'_1 from above, the second segment was evaluated based on a new mean floc size taken from the next smallest portion of the distribution. Procedures 12 to 18 were followed until the iteration was satisfactory. This was continued up the tower until the final (20th.) segment was evaluated.

19. Twentieth Segment

At the end of the procedure the segment heights were summed and compared to the original chosen height, L . If the two values were in good agreement, the calculation was terminated. If not, the whole procedure was repeated using different initial assumptions, i.e. different U_t' , X , n' , etc.

This method, whilst lengthy, does permit a detailed study of tower operation to be carried out. It illustrates how use has been made of the experimental studies carried out by the author in modelling.

7.5 Operational Characteristics of a Tower Fermenter

7.5.1 The prediction of biomass yield

A fermenter of fixed volume has an upper limit on the amount of a given organism that it can contain. This upper limit represents the maximum biomass yield of the fermenter under given operating conditions. This maximum biomass may not be attained due to limitations of substrate to biomass conversion. However, predictions based on microbial suspension concentration provide very useful indications of the yield that may be achieved.

The fungi, Aspergillus Niger, will be considered with the fermenter operating batchwise and continuously.

1. Batch fermentation using molasses medium

Predictions of the maximum biomass yield are based on the maximum concentration of pellets in suspension. Investigations into the liquid content of pellets (Chapter 3), indicated that total liquid content, A , ranged from 79% by volume for mycelia to 98.5% for isolated pellets with immobile liquid. Now, the amount of immobile liquid will depend on the compression to which the pellet is subjected. Clearly, the least amount of liquid in a pellet will be $A = 79\%$, i.e. all immobile liquid has been squeezed out. Observations with A. Niger suspensions, section 5.6, indicated that the lowest voidage, e , for a suspension of mature pellets was $e = 0.82$. Consequently, the largest dry mycelial volume fraction in suspension will be

$$DMVF = (1 - e)(1 - A) = 0.18 \times 0.21 = 0.0378$$

$$\text{hence, Dry mycelial weight fraction} = (1 - A)(1 - e)\rho_s = 0.047 \dots 7.8$$

$$\text{i.e. } 4.7 \text{ gram } \%, \text{ as } \rho_s = 1.24 \text{ g/cm}^3 \text{ for mature mycelium.}$$

The figure of 4.7 g% represents the upper limit. Using eqn. 7.8 the biomass yields under other conditions can be readily computed and some results are shown in Fig. 7.5. The A. Niger fermentations performed by the author in conjunction with Morris (1972) indicated a maximum

yield of 2 g%. This corresponds to a total liquid content of 91 %, indicating that 40% of the immobile liquid has been removed. In stirred tanks, where conditions of voidage and mycelial structure are different, the maximum observed yield was 2.5 g%.

2. Continuous fermentation with molasses medium

Similar principles may be used to predict the behaviour of a continuous culture of A.Niger; a system that biological researchers have only just begun to examine. In this instance, the variation of biomass with flowrate and morphology is considered. Whilst, the information in section 5.6 is not directly applicable to such a fermentation (due to neglect of the gas phase), it may be used as a guide to likely biomass yields.

For each flowrate, ($U, \text{cm/s}$), the suspension voidage observed experimentally for different pellet morphologies (which may be characterised by pellet size, d_o) was found from Appendix A. Additional structural information could then be used to build up a picture of the fermentation.

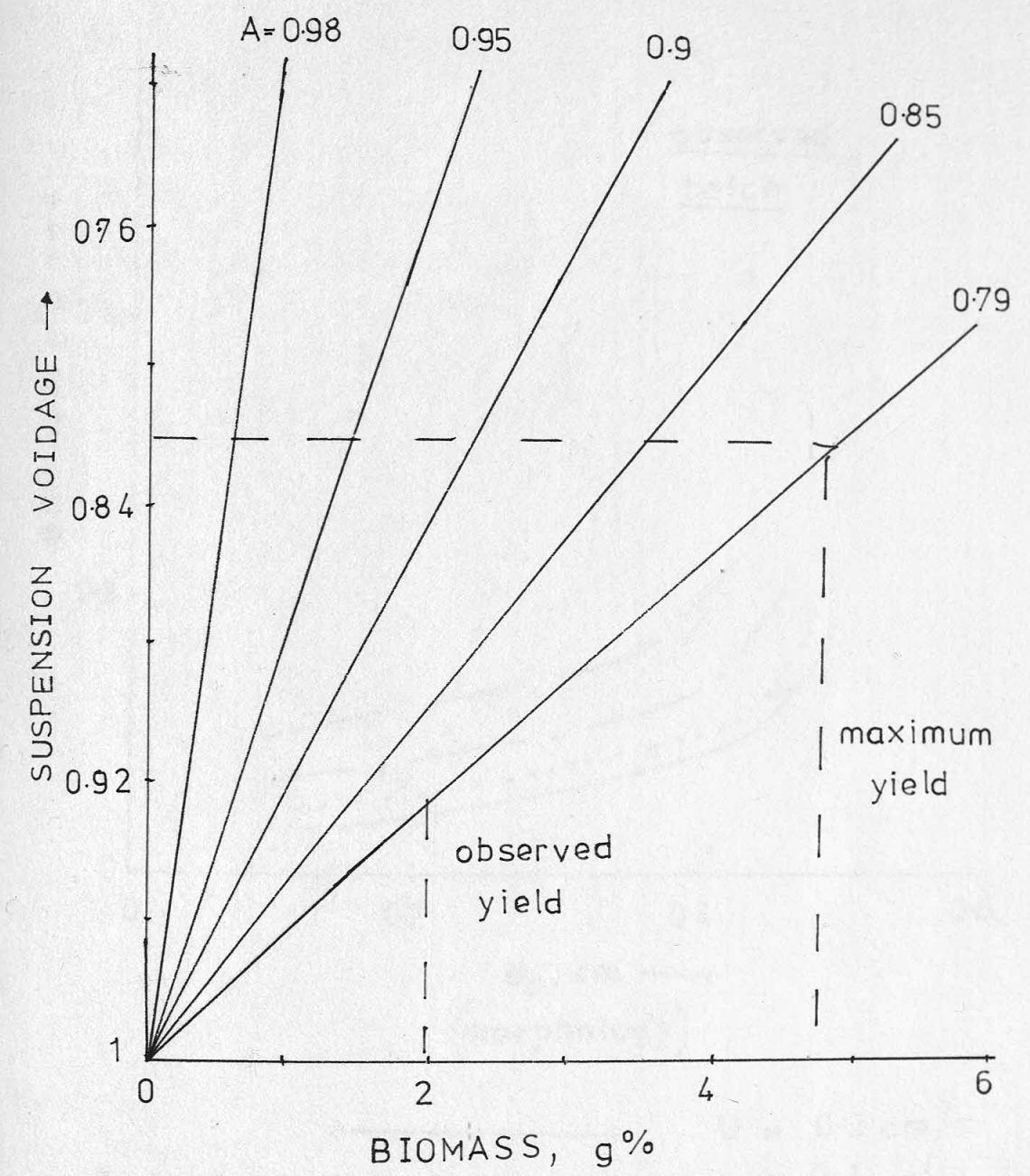
Table 7.2 illustrates the results obtained from such a procedure; these include an estimation of the broth viscosity (based on Fig. 6.1b) and an estimated dry weight concentration. The biomass yield was found using equation 7.8.

Table 7.2 Biomass yield at $U = 0.1 \text{ cm/s}$ for A.Niger

$d_o, \text{cm.}$	A	$\rho_s, \text{g/cm}^3$	e	DWF	Biomass, g%	$\mu_s, \text{cp.}$
0.21	0.984	1.38	0.975	0.00055	0.055	2.30
0.32	0.989	1.28	0.945	0.00080	0.080	1.95
0.41	0.991	1.24	0.900	0.00111	0.111	1.90
0.45	0.991	1.24	0.870	0.00145	0.145	2.20
0.47	0.991	1.24	0.830	0.00189	0.189	2.80

Similar calculations were performed at other flowrates.

FIG. 7.5 BATCH BIOMASS PREDICTIONS
FOR MOLASSES A. NIGER



yield of 2 g. This corresponds to a total liquid content of 21 g. indicating that 40% of the insoluble liquid has been removed. In stirred tanks, where conditions of voidage and rheological structure are different, the maximum observed yield was 2.5 g.

Table 7.2 Biomass yield at $U = 0.1$ cm/s for A. niger

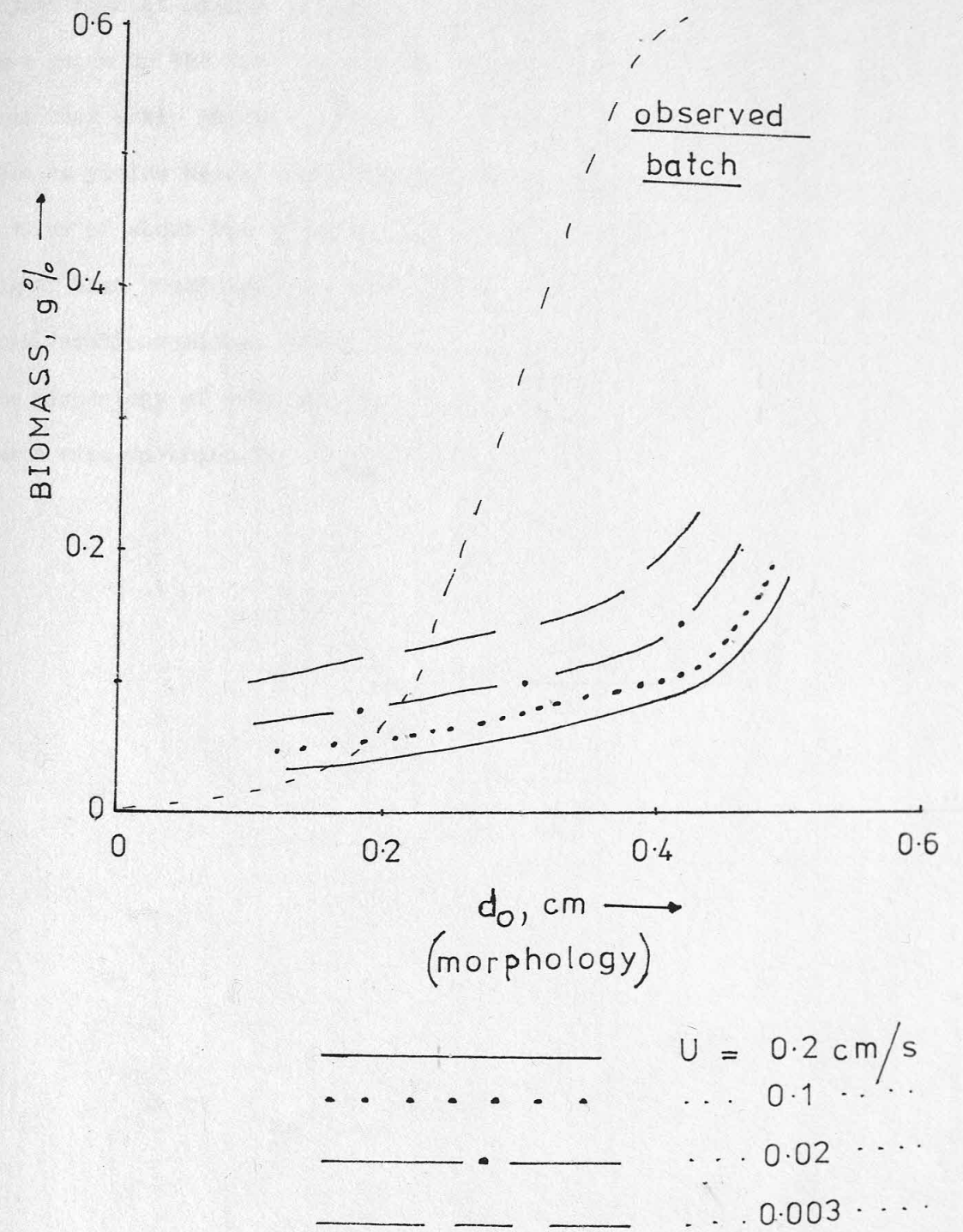
d_o , cm.	A	U , g/cm ³	UW	Biomass, g	Δ , g
0.21	0.984	1.38	0.975	0.0095	0.23
0.32	0.982	1.28	0.945	0.0080	1.95
0.41	0.951	1.24	0.900	0.0011	1.90
0.55	0.921	1.24	0.870	0.0045	2.20
0.71	0.921	1.24	0.830	0.0089	2.80

Table 7.2 illustrates the results obtained from such a procedure; these include an estimation of the broth viscosity (based on η , 6.1b) and an estimated dry weight concentration. The biomass yield was found using equation 7.5. Similar calculations were performed at other flowrates.

For each flowrate (U , cm/s), the suspension voidage observed experimentally for different pellet morphologies (which may be characterized by pellet size, d_p) was found from Appendix A. Additional structural information could then be used to build up a picture of the formation.

Similar principles may be used to predict the behaviour of a continuous culture of A. niger; a system that biological researchers have only just begun to examine. In this instance, the variation of biomass with flowrate and morphology is considered. Whilst, the information in section 7.6 is not directly applicable to such a fermentation (due to neglect of the gas phase), it may be used as a guide to likely biomass yields.

FIG 7.6 BIOMASS PREDICTION FOR
CONTINUOUS A.NIGER PRODUCTION



The results are shown in Fig. 7.6 and may be compared to the experimentally derived batch results which were taken from Table 6.7. The effect of the liquid flow was to considerably reduce the biomass yield. Even very small flows had this effect, although the yield was higher than at higher flowrates. These predictions are only intended to be a guide to the likely biomass yields. However, it was interesting to note that early investigations into continuous A.Niger cultivation gave biomass yields which increased gradually with changing morphology upto a value of about 0.4 g% at a flow of 0.0034 cm/s. This value, whilst higher than predicted, was reasonably close to that predicted by voidage considerations alone. This discrepancy was probably due to the fact that the morphology of continuous culture pellets was slightly different from batch ones, on which the analysis was based.

27.5	0.400	2.6	3.85	0.101
25.7	0.354	2.0	2.96	0.101
25.3	0.348	1.4	2.07	0.071
25.1	0.342	0	0	0

2. 0.3 cm. pellets

Water temperature = 12°C ; Weight of beads = 300 g, $\rho_s = 36.1 \text{ cm}^3$

Bed Ht., cm.	ϵ	Flow, lit/min.	$U, \text{cm/s.}$	ϕ/U_s
26.2	0.577	5.0	7.4	0.255
24.8	0.554	4.4	6.8	0.185
24.2	0.542	4.0	6.2	0.180
23.0	0.519	3.6	5.5	0.163
21.6	0.487	3.4	5.0	0.140
20.3	0.455	3.0	4.4	0.122
19.2	0.424	2.6	3.9	0.107
18.4	0.397	2.3	3.4	0.094
17.3	0.382	1.0	1.48	0.041
17.3	0.382	0.1	0.14	0.020

APPENDIX A

Fluidisation and Sedimentation Results

(a) Ballotini Results

(fluidisation in $1\frac{1}{2}$ " column)

1. 0.2 cm. ballotini

Water temperature = 17°C ; Weight of beads = 500 g.; $U_t = 29.4\text{cm/s}$

Bed Ht., cm.	e	Flow, lit/min.	U, cm/s	U/U_t
38.2	0.568	5.0	7.4	0.252
36.1	0.543	4.6	6.8	0.232
34.3	0.518	4.2	6.2	0.211
31.7	0.479	3.6	5.3	0.181
30.1	0.452	3.2	4.73	0.161
27.5	0.400	2.6	3.85	0.131
25.7	0.358	2.0	2.96	0.101
25.3	0.348	1.4	2.07	0.071
25.1	0.342	0	0	0

2. 0.3 cm. ballotini

Water temperature = 19°C ; Weight of beads = 300 g., $U_t = 36.1\text{ cm/s}$

Bed Ht., cm.	e	Flow, lit/min.	U, cm/s.	U/U_t
26.2	0.577	5.0	7.4	0.205
24.8	0.554	4.6	6.8	0.188
24.2	0.542	4.4	6.5	0.180
23.0	0.518	4.0	5.9	0.163
21.6	0.487	3.4	5.03	0.140
20.3	0.455	3.0	4.44	0.122
19.2	0.424	2.6	3.85	0.107
18.4	0.397	2.3	3.4	0.094
17.9	0.382	1.0	1.48	0.041
17.9	0.382	0.5	0.74	0.020

3. 0.6 cm. ballotini

Water temperature = 19°C; Weight = 320 g; $U_t = 51.8$ cm/s.

Bed Ht., cm.	e	Flow, lit/min.	U, cm/s.	U/U_t
24	0.518	5.4	8.0	0.155
22.3	0.482	5.0	7.4	0.143
21.8	0.469	4.81	7.1	0.137
21.1	0.451	4.6	6.8	0.131
20.9	0.446	4.4	6.52	0.126
20.7	0.441	4.1	6.05	0.117
20.3	0.430	0.6	0.9	0.017
20	0.421	0	0	0

(b) Diakon Results

1. 0.055 cm. diakon fluidised in 3" column

Water temperature = 18°C; Weight = 515 g; $U_t = 1.52$ cm/s.

Bed Ht., cm.	e	Flow, lit/min.	U, cm/s.	U/U_t
79.5	0.877	2.33	0.850	0.559
69.5	0.860	2.16	0.788	0.518
62.0	0.843	2.0	0.730	0.480
55.7	0.825	1.9	0.694	0.457
43.2	0.774	1.55	0.566	0.372
36.7	0.734	1.30	0.476	0.313
31.0	0.685	1.10	0.402	0.265
27.5	0.645	0.80	0.292	0.192
25.0	0.610	0.65	0.237	0.156
20.2	0.517	0.37	0.135	0.089
17.7	0.450	0.21	0.077	0.051
17.1	0.429	0.16	0.058	0.038
16.5	0.409	0.08	0.029	0.019

APPENDIX A

Fluidisation and Sedimentation Results

(a) Ballotini Results (fluidisation in 1 1/2" column)

Water temperature = 17°C; Weight of beads = 500 g; $U_t = 52.4$ cm/s

Bed Ht., cm.	e	Flow, lit/min.	U, cm/s.	U/U_t
38.2	0.568	5.0	7.4	0.141
35.1	0.543	4.6	6.8	0.130
34.8	0.518	4.2	6.2	0.118
31.7	0.479	3.6	5.2	0.099
30.1	0.452	3.2	4.73	0.090
27.5	0.400	2.6	3.82	0.073
25.7	0.358	2.0	2.96	0.056
25.3	0.348	1.4	2.07	0.039
25.1	0.342	0	0	0

(b) Diakon Results

Water temperature = 18°C; Weight of beads = 300 g; $U_t = 36.1$ cm/s

Bed Ht., cm.	e	Flow, lit/min.	U, cm/s.	U/U_t
36.2	0.777	2.0	7.4	0.205
34.8	0.754	1.6	6.8	0.188
34.2	0.742	1.4	5.2	0.144
33.0	0.718	1.0	5.2	0.144
31.2	0.687	0.6	3.03	0.084
30.3	0.652	0.6	4.44	0.123
29.2	0.624	0.6	3.82	0.106
28.1	0.597	0.6	3.4	0.094
27.1	0.582	1.0	1.48	0.041
27.2	0.582	0.2	0.74	0.020

2. 0.055cm. diakon fluidised in two-dimensional bed

Water temperature = 20°C; Weight = 400g; $U_t = 1.6$ cm/s.

Bed Ht., cm,	e	Flow, lit/min.	U, cm/s.	U/U_t	ΔP_b , grams
113.0	0.847	1.0	0.834	0.521	61.78
95.0	0.818	0.91	0.759	0.474	61.78
77.3	0.776	0.77	0.642	0.401	61.78
71.0	0.756	0.70	0.583	0.365	61.78
52.0	0.667	0.49	0.409	0.256	60.59
44.0	0.607	0.36	0.300	0.188	60.59
37.0	0.532	0.23	0.192	0.120	60.59
31.2	0.446	0.10	0.083	0.052	58.21
30.5	0.433	0.07	0.058	0.036	57.02
29.8	0.419	0.053	0.044	0.028	47.52
29.6	0.416	0.042	0.035	0.022	36.83
29.6	0.416	0.034	0.028	0.018	30.89
29.6	0.416	0.032	0.027	0.017	28.51
29.6	0.416	0.046	0.038	0.024	42.77
29.7	0.417	0.067	0.056	0.035	61.78
30.5	0.433	0.080	0.067	0.042	55.84
31.6	0.453	0.114	0.095	0.059	55.84
43.7	0.604	0.360	0.300	0.188	60.59
57.6	0.700	0.590	0.492	0.308	61.78
76.8	0.775	0.760	0.634	0.396	61.78
131.0	0.868	1.080	0.901	0.563	62.96

3. 0.055cm. diakon fluidised in 3.2 cm. tube

Water temperature = 20°C; Weight = 105g; $U_t = 1.6$ cm/s.

Bed Ht., cm.	e	Flow, lit/min.	U, cm/s.	U/U_t
26.4	0.586	0.103	0.224	0.140
24.4	0.564	0.082	0.178	0.111
22.5	0.521	0.061	0.132	0.083
21.0	0.488	0.041	0.088	0.055
18.6	0.430	0.020	0.043	0.027
17.8	0.404	0.010	0.022	0.014

3. 0.055 cm. diakon

Water temperature = 19°C; Weight = 320g; $U_t = 1.6$ cm/s.

Bed Ht., cm.	e	Flow, lit/min.	U, cm/s.	U/U_t
22.3	0.482	0.2	0.4	0.25
21.8	0.482	0.2	0.4	0.25
21.1	0.471	0.2	0.4	0.25
20.9	0.446	0.2	0.4	0.25
20.7	0.441	0.2	0.4	0.25
20.3	0.430	0.2	0.4	0.25
20.0	0.421	0	0	0

(p) Diakon Results

1. 0.055 cm. diakon fluidised in 3" column

Water temperature = 18°C; Weight = 212g; $U_t = 1.52$ cm/s.

Bed Ht., cm.	e	Flow, lit/min.	U, cm/s.	U/U_t
19.2	0.877	2.33	0.850	0.559
18.9	0.860	2.16	0.788	0.518
18.2	0.843	2.0	0.730	0.480
17.7	0.825	1.9	0.694	0.457
17.4	0.774	1.75	0.565	0.372
17.0	0.734	1.30	0.476	0.313
16.8	0.685	1.10	0.402	0.265
16.5	0.645	0.80	0.399	0.262
16.0	0.610	0.65	0.537	0.352
15.5	0.571	0.71	0.512	0.337
15.1	0.524	0.65	0.470	0.310
14.8	0.481	0.61	0.438	0.288
14.5	0.404	0.08	0.059	0.039

4. 0.055cm. diakon sedimenting in two-dimensional bed after fluidisation

Water temperature = 12.5°C; Weight = 400g; $U_t = 1.42$ cm/s.

Initial bed ht., cm.	e	Settling rate, U, cm/s.	U/U_t
130	0.867	0.790	0.556
100	0.827	0.700	0.493
70	0.752	0.500	0.352
60	0.711	0.410	0.289
50	0.653	0.310	0.218
48	0.638	0.272	0.192
43.5	0.600	0.210	0.148
38	0.544	0.144	0.101
35	0.504	0.103	0.073

5. 0.0655 cm. diakon fluidised in 3" column

Water temperature = 19°C; Weight = 720g; $U_t = 1.58$ cm/s.

Bed Ht., cm.	e	Flow, lit/min;	U, cm/s.	U/U_t
82.0	0.828	1.9	0.694	0.439
75.5	0.813	1.82	0.664	0.420
69.5	0.797	1.73	0.631	0.399
56.6	0.751	1.43	0.522	0.330
51.0	0.724	1.25	0.456	0.289
46.7	0.698	1.11	0.405	0.256
40.0	0.648	0.87	0.318	0.201
33.0	0.573	0.55	0.201	0.127
27.7	0.492	0.31	0.113	0.072
26.1	0.460	0.25	0.091	0.058
24.8	0.432	0.16	0.058	0.037
24.0	0.413	0.11	0.039	0.025
23.8	0.408	0.08	0.027	0.017
23.7	0.406	0.05	0.020	0.013

3. 0.055cm. diakon fluidised in two-dimensional bed

Water temperature = 20°C; Weight = 400g; $U_t = 1.42$ cm/s.

Bed Ht., cm.	e	Flow, lit/min.	U, cm/s.	U/U_t
113.0	0.847	1.0	0.724	0.510
92.0	0.818	0.91	0.722	0.508
81.7	0.770	0.77	0.642	0.452
71.0	0.726	0.70	0.583	0.410
52.0	0.667	0.49	0.409	0.288
44.0	0.607	0.36	0.300	0.211
37.0	0.532	0.23	0.192	0.135
31.2	0.440	0.10	0.083	0.058
20.2	0.433	0.07	0.050	0.035
19.8	0.419	0.053	0.044	0.031
18.9	0.416	0.042	0.030	0.021
18.2	0.416	0.034	0.028	0.019
17.0	0.416	0.032	0.027	0.019
16.0	0.416	0.030	0.026	0.018
15.0	0.416	0.028	0.025	0.017
14.0	0.416	0.026	0.024	0.016
13.0	0.416	0.024	0.022	0.015
12.0	0.416	0.022	0.020	0.014
11.0	0.416	0.020	0.018	0.012
10.0	0.416	0.018	0.016	0.011
9.0	0.416	0.016	0.014	0.009
8.0	0.416	0.014	0.012	0.008
7.0	0.416	0.012	0.010	0.007
6.0	0.416	0.010	0.008	0.005
5.0	0.416	0.008	0.006	0.004
4.0	0.416	0.006	0.004	0.003
3.0	0.416	0.004	0.002	0.001
2.0	0.416	0.002	0.001	0.000
1.0	0.416	0.001	0.000	0.000

3. 0.055cm. diakon fluidised in 3.5 cm. tube

Water temperature = 20°C; Weight = 102g; $U_t = 1.42$ cm/s.

Bed Ht., cm.	e	Flow, lit/min.	U, cm/s.	U/U_t
26.4	0.586	0.103	0.072	0.051
24.1	0.562	0.092	0.065	0.046
22.2	0.521	0.080	0.057	0.040
21.0	0.488	0.071	0.050	0.035
18.8	0.430	0.050	0.035	0.025
17.8	0.404	0.040	0.028	0.020

(c) Mustard Seed Results

1. Uncoated, uniformly sized seeds fluidised in two-dimensional bed

Water temperature = 14°C; Dry weight = 245g; $U_t = 4.14$ cm/s.

(The dry weight is the weight before soaking ; the terminal velocity refers to the theoretically calculated value .)

Bed Ht., cm.	e	Flow, lit/min;	U, cm/s.	U/U_t	ΔP_b , grams
130	0.805	1.60	1.330	0.321	33.32
103	0.754	1.24	1.030	0.249	33.32
94	0.731	1.09	0.910	0.220	33.32
74	0.658	0.63	0.525	0.127	34.51
62.5	0.595	0.40	0.334	0.081	33.32
54.7	0.537	0.25	0.209	0.050	32.13
53.8	0.529	0.20	0.167	0.040	29.75
52.1	0.514	0.16	0.133	0.032	28.56
50.5	0.497	0.123	0.103	0.025	26.18
48.5	0.478	0.084	0.070	0.017	23.80
47.3	0.465	0.068	0.057	0.014	20.23
46.5	0.455	0.052	0.043	0.010	17.85
45.0	0.437	0.032	0.027	0.007	13.09
43.8	0.422	0.035	0.029	0.007	13.09
44.0	0.425	0.045	0.033	0.008	16.66
44.5	0.431	0.060	0.050	0.012	21.42
48.0	0.473	0.113	0.094	0.023	27.37
52.0	0.513	0.190	0.158	0.038	32.13
53.2	0.524	0.216	0.180	0.043	32.13
55.0	0.540	0.280	0.233	0.056	34.51
65.0	0.610	0.500	0.417	0.101	32.13
74.5	0.659	0.700	0.585	0.142	34.51
90.0	0.719	1.000	0.834	0.201	35.70
99.0	0.744	1.270	1.060	0.256	36.89
113	0.776	1.560	1.301	0.314	36.89

refluidising
from
compaction

Uncoated, uniformly sized seeds fluidised in two-dimensional bed

Water temperature = 12.5°C; Dry weight = 245g; $U_t = 4.14$ cm/s.

Bed Ht., cm.	e	Flow, lit/min;	U, cm/s.	U/U_t
130	0.805	1.60	1.330	0.321
103	0.754	1.24	1.030	0.249
94	0.731	1.09	0.910	0.220
74	0.658	0.63	0.525	0.127
62.5	0.595	0.40	0.334	0.081
54.7	0.537	0.25	0.209	0.050
53.8	0.529	0.20	0.167	0.040
52.1	0.514	0.16	0.133	0.032
50.5	0.497	0.123	0.103	0.025
48.5	0.478	0.084	0.070	0.017
47.3	0.465	0.068	0.057	0.014
46.5	0.455	0.052	0.043	0.010
45.0	0.437	0.032	0.027	0.007

Water temperature = 12.5°C; Dry weight = 245g; $U_t = 4.14$ cm/s.

Bed Ht., cm.	e	Flow, lit/min;	U, cm/s.	U/U_t
43.8	0.422	0.035	0.029	0.007
44.0	0.425	0.045	0.033	0.008
44.5	0.431	0.060	0.050	0.012
48.0	0.473	0.113	0.094	0.023
52.0	0.513	0.190	0.158	0.038
53.2	0.524	0.216	0.180	0.043
55.0	0.540	0.280	0.233	0.056
65.0	0.610	0.500	0.417	0.101
74.5	0.659	0.700	0.585	0.142
90.0	0.719	1.000	0.834	0.201
99.0	0.744	1.270	1.060	0.256
113	0.776	1.560	1.301	0.314

2. Uncoated, uniformly sized seeds sedimenting in two-dimensional bed

(Bed condition as previously)

Initial bed ht., cm.	e	Settling velocity, U, cm/s.	U/U _t
128	0.802	1.56	0.377
121	0.790	1.54	0.372
113	0.775	1.29	0.312
85	0.701	0.825	0.200
83	0.694	0.800	0.190
75	0.661	0.620	0.147
66.5	0.618	0.450	0.109
58.0	0.562	0.243	0.058

3. Uncoated, multisized seeds fluidised in 3" column

Water temperature = 22°C; Dry weight = 400g.

Theoretical terminal velocity = 4.8 cm/s., Regression U_t = 3.92 cm/s.

Bed Ht., cm.	e	Flow, lit/min.	U, cm/s.	U/U _t
93.0	0.810	3.23	1.179	0.301
87.0	0.797	3.05	1.113	0.284
80.0	0.780	2.70	0.986	0.252
73.0	0.760	2.35	0.858	0.219
67.0	0.737	2.00	0.730	0.186
62.0	0.716	1.68	0.613	0.156
54.5	0.677	1.20	0.438	0.112
49.5	0.644	0.90	0.329	0.084
44.0	0.599	0.70	0.256	0.065
40.5	0.565	0.50	0.183	0.047
37.3	0.527	0.30	0.110	0.028
33.5	0.474	0.05	0.018	0.005

The terminal velocity used was 3.92 cm/s.

4. Coated , uniformly sized seeds fluidised in two-dimensional bed

Water temperature = 16.5°C; Dry weight = 300g;

Theoretical U_t = 4.04 cm/s., regression U_t = 2.95 cm/s (which was the value used in the analysis .)

1. Uncoated, uniformly sized seeds fluidised in two-dimensional bed

Water temperature = 14°C; Dry weight = 245g; U_t = 4.14 cm/s.

(The dry weight is the weight before soaking; the terminal velocity refers to the theoretically calculated value .)

Bed Ht., cm.	e	Flow, lit/min.	U, cm/s.	U/U _t	ΔP, g/cm ²
130	0.805	1.80	1.330	0.321	33.35
103	0.754	1.24	1.030	0.249	33.35
94	0.731	1.09	0.910	0.220	33.35
84	0.658	0.83	0.755	0.182	34.18
62.5	0.595	0.40	0.334	0.081	33.35
54.7	0.537	0.25	0.209	0.050	35.13
53.8	0.529	0.20	0.181	0.040	35.13
52.1	0.514	0.16	0.133	0.032	36.56
50.5	0.497	0.13	0.103	0.025	36.18
48.4	0.478	0.084	0.070	0.017	33.80
47.3	0.465	0.068	0.057	0.014	50.53
46.5	0.455	0.052	0.043	0.010	17.85
45.0	0.437	0.035	0.027	0.007	13.09
43.8	0.425	0.035	0.029	0.007	13.09
44.4	0.425	0.040	0.033	0.008	16.66
44.5	0.431	0.060	0.050	0.012	54.15
48.4	0.473	0.113	0.094	0.023	17.35
52.5	0.512	0.190	0.158	0.038	35.13
53.5	0.524	0.216	0.180	0.043	35.13
55.0	0.540	0.280	0.233	0.056	34.18
65.0	0.610	0.500	0.417	0.101	35.13
74.5	0.689	0.700	0.585	0.142	34.51
80.0	0.719	1.000	0.834	0.201	35.70
89.0	0.744	1.250	1.060	0.256	36.89
111	0.770	1.580	1.201	0.291	36.89

Bed Ht.,cm.	e	Flow,lit/min.	U,cm/s.	U/U _t	ΔP _b ,grams
114	0.728	0.670	0.560	0.211	45.2
95.0	0.674	0.430	0.358	0.135	45.2
82.5	0.624	0.300	0.250	0.094	44.0
745.	0.584	0.205	0.171	0.065	42.8
70.5	0.560	0.150	0.125	0.047	41.7
68.2	0.545	0.120	0.100	0.038	41.7
65.0	0.523	0.090	0.075	0.028	39.3
63.5	0.512	0.084	0.070	0.026	36.9
62.5	0.504	0.060	0.050	0.019	35.7
60.5	0.488	0.045	0.038	0.014	32.1
59.0	0.476	0.036	0.030	0.011	27.4
58.5	0.470	0.032	0.027	0.010	25.0

5. Coated,multisized seeds fluidised in 3" column

Water temperature = 21°C; Dry weight = 280g; Theoretical U_t = 4.8 cm/s., regression U_t = 3.0 cm/s.

Bed Ht.,cm.	e	Flow,lit/min.	U,cm/s.	U/U _{t,theory}	U/U _t actual
116	0.898	4.45	1.620	0.337	0.540
100	0.882	4.00	1.460	0.304	0.490
82.0	0.856	3.50	1.275	0.265	0.430
70.0	0.831	3.00	1.095	0.228	0.365
60.5	0.805	2.50	0.913	0.190	0.304
53.5	0.779	2.00	0.730	0.152	0.243
47.5	0.752	1.75	0.640	0.133	0.213
45.0	0.738	1.50	0.548	0.114	0.183
42.0	0.719	1.25	0.456	0.095	0.152
40.0	0.705	1.10	0.402	0.084	0.134
37.8	0.688	1.00	0.365	0.076	0.122
34.3	0.292	0.80	0.292	0.061	0.097
32.0	0.631	0.60	0.219	0.046	0.073
30.0	0.607	0.40	0.146	0.030	0.049
27.6	0.572	0.20	0.073	0.015	0.024
26.5	0.555	0.10	0.037	0.008	0.012

3. Uncoated,multisized seeds fluidised in 3" column

Bed Ht.,cm.	e	Flow,lit/min.	U,cm/s.	U/U _t
128	0.802	1.26	0.377	0.377
121	0.790	1.24	0.372	0.372
113	0.772	1.22	0.372	0.372
82	0.701	0.822	0.200	0.200
83	0.694	0.800	0.190	0.190
72	0.661	0.620	0.147	0.147
66.2	0.619	0.450	0.102	0.102
58.0	0.562	0.243	0.058	0.058

Water temperature = 22°C; Dry weight = 400g.
Theoretical terminal velocity = 4.8 cm/s., Regression U_t = 3.92 cm/s.

Bed Ht.,cm.	e	Flow,lit/min.	U,cm/s.	U/U _t
93.0	0.810	3.23	1.172	0.301
87.0	0.797	3.02	1.113	0.284
80.0	0.780	2.70	0.986	0.252
73.0	0.760	2.32	0.628	0.212
67.0	0.737	2.00	0.730	0.186
62.0	0.716	1.86	0.612	0.156
54.2	0.677	1.20	0.438	0.112
48.2	0.644	0.90	0.322	0.084
44.0	0.592	0.70	0.326	0.082
40.2	0.562	0.50	0.183	0.047
37.2	0.527	0.30	0.110	0.028
32.2	0.474	0.02	0.018	0.002

Coated, uniformly sized seeds fluidised in two-dimensional bed
Water temperature = 16.2°C; Dry weight = 300g;
Theoretical U_t = 4.04 cm/s., regression U_t = 2.92 cm/s (which was the value used in the analysis).

(d) Aspergillus Niger Results

1. Fluidisation of 40h. molasses pellets in two-dimensional bed

Water temperature = 20.8°C ; Dry weight of mycelium = 3.5 g.

Terminal velocity from data regression = 1.1 cm/s; Sample values obtained experimentally were as follows;

The times to fall 9.7 cm in water in the measuring cylinder were (in sec)
13, 12, 9.3, 13.5, 13.2, 14.3, 10.8, 13.5, 17.8, 18.8, 11.8, 15.8, 12.7.

This gave an average time = 13.59 seconds and hence, $U_t = 0.71$ cm/s.

Bed Ht., cm	e	Flow, lit/hour	U, cm/s	U/U_t reg.	U/U_t measured
91.0	0.896	6.05	0.0848	0.077	0.120
87.5	0.892	4.85	0.0680	0.062	0.096
79.0	0.880	3.63	0.0510	0.046	0.072
69.5	0.864	2.40	0.0340	0.031	0.048
58.7	0.839	1.20	0.0168	0.015	0.024
55.0	0.828	0.90	0.0126	0.011	0.018
51.0	0.815	0.28	0.0039	0.004	0.006
49.5	0.804	0	0	0	0

2. Fluidisation of Czapek pellets in 3.2 cm. tube

Water temperature = 20°C ; Dry weight of mycelium = 0.73g.

Data regression gave $U_t = 0.13$ cm/s

Bed Ht., cm	Bed Vol., cm ³	e	Flow, lit/hour	U, cm/s.	U/U_t reg.
40.5	330	0.941	1.83	0.066	0.493
38.0	310	0.937	1.52	0.055	0.410
32.0	264	0.926	1.22	0.044	0.328
26.0	217	0.910	0.90	0.032	0.239
17.0	146	0.866	0.60	0.022	0.164
9.6	89	0.780	0.28	0.010	0.075
6.7	69	0.716	0	0	0

Bed Ht., cm	e	Flow, lit/min.	U, cm/s.	U/U_t	$\Delta P, \text{cm H}_2\text{O}$
111	0.788	0.670	0.050	0.119	45.5
92.0	0.874	0.430	0.030	0.137	45.5
82.5	0.824	0.300	0.020	0.094	44.0
74.5	0.804	0.205	0.017	0.050	45.8
70.5	0.860	0.150	0.012	0.047	41.7
68.5	0.845	0.150	0.010	0.030	41.7
65.0	0.852	0.090	0.007	0.050	39.3
63.5	0.812	0.084	0.007	0.050	38.9
62.5	0.805	0.080	0.007	0.070	37.7
60.5	0.884	0.045	0.003	0.010	32.1
59.0	0.870	0.030	0.002	0.011	27.4
58.5	0.870	0.032	0.002	0.010	25.0

Water temperature = 21°C; Dry weight = 280g; Theoretical $U_t = 0.8$ cm/s; regression $U_t = 0.8$ cm/s.

Bed Ht., cm	e	Flow, lit/min.	U, cm/s.	U/U_t theory	U/U_t actual
111	0.889	4.45	1.620	0.337	0.240
100	0.885	4.00	1.460	0.304	0.450
82.0	0.850	3.50	1.275	0.265	0.430
70.0	0.831	3.00	1.095	0.258	0.365
60.5	0.805	2.50	0.913	0.190	0.304
55.5	0.777	2.00	0.730	0.152	0.245
47.5	0.827	1.75	0.640	0.133	0.213
45.0	0.738	1.500	0.540	0.114	0.183
45.0	0.719	1.5	0.54	0.095	0.152
40.0	0.705	1.10	0.405	0.084	0.134
37.8	0.888	1.00	0.365	0.076	0.125
34.3	0.895	0.80	0.295	0.080	0.097
32.0	0.831	0.60	0.219	0.046	0.073
30.0	0.805	0.40	0.145	0.030	0.049
27.5	0.825	0.20	0.073	0.075	0.024
26.5	0.855	0.10	0.037	0.008	0.015

Water temperature = 20°C ; dry weight of mycelium = 0.85g ; Data regression gave $U_t = 0.11$ cm/s.

Bed Ht., cm.	Bed Vol., cm ³	e	Flow, lit/hour	U, cm/s.	U/U _t reg.
42.0	342	0.924	1.83	0.066	0.600
35.0	288	0.897	1.52	0.055	0.500
28.0	232	0.856	1.22	0.044	0.400
18.5	158	0.757	0.90	0.032	0.291
10.0	92	0.534	0.60	0.022	0.200
8.7	83	0.478	0.28	0.010	0.092
7.8	77	0.429	0.13	0.005	0.043

3. Sedimentation of Czapek pellets in 250 cm³ measuring cylinder

The following data was obtained using 0.73 g dry mycelial weight of pellets in water at 20°C .

Time, min.	Suspension ht., cm.	Volume, cm ³	voidage, e
0	15.0	163	0.897
0.25	14.7	159	0.894
1.0	14.0	151	0.889
2.0	13.1	141	0.881
4.0	11.3	121	0.861
6.0	9.95	105	0.840
8.0	9.1	95	0.823
10.0	8.5	89	0.811
20.0	7.6	78	0.784
90	7.2	73	0.770
0	21.9	240	0.930
0.33	21.3	233	0.928
1.0	19.7	217	0.922
2.0	17.5	191	0.912
4.0	13.4	144	0.883
6.0	10.4	110	0.847
8.0	9.1	95	0.823
20.0	7.6	78	0.784

Typical analysis of the above gave $e = 0.930$, $U = 0.034$ cm/s, $U/U_t = 0.17$ and $e = 0.889$, $U = 0.015$ cm/s, $U/U_t = 0.075$

(5) *Aspergillus Niger* floccula

1. Fluidization of 40g. *Aspergillus Niger* floccula in two-dimensional bed
Water temperature = 20.8°C ; dry weight of mycelium = 3.5 g.
Terminal velocity from data regression = 1.1 cm/s; Sample values obtained experimentally were as follows:
The times to fall 9.7 cm in water in the measuring cylinder were (in sec)
13.12, 9.3, 13.2, 13.2, 14.3, 10.0, 13.2, 17.8, 19.8, 11.8, 12.7.
This gave an average time = 13.29 seconds and hence, $U_t = 0.71$ cm/s.

Bed Ht., cm.	e	Flow, lit/hour	U, cm/s	U/U _t reg.	U/U _t measured
42.0	0.804	0	0	0	0.120
35.0	0.815	0.28	0.0039	0.004	0.006
28.0	0.828	0.30	0.0126	0.011	0.018
18.5	0.839	1.20	0.0169	0.015	0.024
10.0	0.864	2.40	0.0340	0.031	0.048
7.8	0.880	3.63	0.0510	0.046	0.072
7.5	0.892	4.85	0.0680	0.062	0.096
7.0	0.896	6.07	0.0848	0.077	0.120

2. Fluidization of Czapek pellets in 3.2 cm. tube
Water temperature = 20°C ; dry weight of mycelium = 0.73g.
Data regression gave $U_t = 0.13$ cm/s

Bed Ht., cm.	Bed Vol., cm ³	e	Flow, lit/hour	U, cm/s	U/U _t reg.
40.5	330	0.941	1.83	0.066	0.493
38.0	310	0.937	1.52	0.055	0.410
32.0	264	0.926	1.22	0.044	0.338
26.0	217	0.910	0.90	0.035	0.239
17.0	141	0.866	0.60	0.022	0.164
9.6	89	0.780	0.28	0.010	0.075
7.2	73	0.716	0	0	0

4. Sedimentation of molasses pellets in 250 cm³ measuring cylinder

(A) Autolysed pellets

Water temperature = 25.5°C ; 2.26 g of dry mycelium used;

The average measured value of U_t was 1.42 cm/s

The basic data was as follows,

Time, s	0	5	15	25	35	45	55	90	final
Height, cm.	22.3	20.5	18.9	17.5	15.8	15.2	15.0	14.8	11.7
Vol., cm ³	250	230	212	196	177	170	168	166	131

The following analysis was then performed,

U, cm/s.	U/U_t	e
0.296	0.212	0.856
0.180	0.129	0.844
0.106	0.076	0.831
0.091	0.065	0.813
0.054	0.039	0.805

(B) 18 hour pellets

Analysis of some sample results gave

U, cm/s.	U/U_t	e
0.039	0.260	0.960
0.029	0.192	0.951
0.014	0.095	0.940
0.006	0.043	0.934
0.011	0.077	0.940
0.020	0.143	0.952
0.035	0.250	0.961

The raw data came from tests performed in water at 25.5°C using 0.42 g of dry mycelium.

Time, min.	0	2	4	7	10	13	20	53
Height, cm.	23.2	20.8	19.0	17.3	16.5	16.0	15.7	15.4
Volume, cm ³	250	223	202	183	174	168	165	161

Bed Ht., cm.	Bed Vol., cm ³	e	Flow, lit/hour	U, cm/s.	U/U_t
18.0	177	0.856	0.13	0.005	0.043
16.5	158	0.831	0.00	0.005	0.043
15.8	152	0.844	0.00	0.005	0.043
15.2	148	0.813	0.00	0.005	0.043
14.8	144	0.805	0.00	0.005	0.043
14.0	131	0.856	0.00	0.005	0.043
12.5	100	0.856	0.00	0.005	0.043
11.7	83	0.856	0.00	0.005	0.043
10.0	72	0.856	0.00	0.005	0.043
8.0	54	0.856	0.00	0.005	0.043

5. Sedimentation of Oospora pellets in 250 cm³ measuring cylinder

The following data was obtained using 0.73 g dry mycelium weight of

pellets in water at 20°C.

Time, min.	Suspension ht., cm.	Volume, cm ³	voidage, e
0	15.0	163	0.897
0.25	14.7	159	0.894
1.0	14.0	151	0.889
2.0	13.7	147	0.887
4.0	11.3	121	0.861
6.0	9.92	105	0.840
8.0	9.1	95	0.823
10.0	8.5	89	0.811
20.0	7.6	78	0.784
30	7.2	73	0.770
0	21.2	245	0.930
2.0	21.3	233	0.928
4.0	19.7	217	0.925
6.0	17.5	191	0.915
8.0	16.4	174	0.887
10.0	16.4	170	0.874
20.0	15.7	165	0.853
30.0	15.4	161	0.784

Typical analysis of the above gave $e = 0.930$, $U = 0.034$ cm/s, $U/U_t = 0.11$

and $e = 0.889$, $U = 0.015$ cm/s, $U/U_t = 0.075$

(e) Yeasts

1. CFCC 34 Results

i. Fluidisation

A. The first set of data refers to the tests analysed in detail in 5.4.7. (i.e. $T = 20^{\circ}\text{C}$, $\text{pH} = 4.75$). The centrifuged wet weight = 26g. Data regression based on 50 % floc voidage gave $U_t' = 4.27 \text{ cm/s}$, which was used to compare the data to the Richardson-Zaki equation.

Bed Ht., cm.	Bed Vol., cm^3	e	Flow, l./h.	U, cm/s.	U/U_t'	$C_m, \text{g\%}$
19.5	166	0.803	6.20	0.224	0.052	2.65
16.5	142	0.770	4.93	0.178	0.042	3.11
15.0	130	0.748	3.67	0.132	0.031	3.39
14.0	122	0.732	2.43	0.088	0.021	3.61
12.2	108	0.697	1.18	0.043	0.010	4.08
11.2	100	0.673	0.60	0.022	0.005	4.41
10.2	93	0.648	0.28	0.010	0.002	4.74
9.8	90	0.637	0.13	0.005	0.001	4.89
2.2 (17h)	39	0.161	0	0	0	11.3

The bed was allowed to settle for 17h. against zero flow. The quoted voidage value was based on a retained floc structure of 50% liquid in the interstices. In reality, this would be squeezed out to give a higher bed voidage than quoted, this being based on the 50 % floc voidage criterion.

B. $T = 30^{\circ}\text{C}$, $\text{pH} = 4.85$, Weight = 26 g.

Bed Vol., cm^3	e	Flow, l/h.	U, cm/s.	$C_m, \text{g\%}$
107	0.694	6.20	0.224	4.12
103	0.683	4.93	0.178	4.28
99	0.670	3.67	0.132	4.45
78	0.581	1.18	0.043	5.65
73	0.552	0.60	0.022	6.04

Reduction of molasses pellets in 50 cm measuring cylinder

(A) Anticolligand pellets

Water temperature = 22.5°C ; 2.26 g of dry molasses used;

The average measured value of U_t was 1.42 cm/s

The basic data was as follows:

Time, s	0	5	15	25	35	45	55	90	Final
Height, cm.	22.5	20.5	18.5	17.5	15.8	15.5	15.0	14.8	11.7
Vol., cm^3	250	230	215	196	177	170	168	166	131

The following analysis was then performed:

U/U_t'	e	$U, \text{cm/s.}$
0.224	0.803	0.224
0.178	0.770	0.178
0.132	0.748	0.132
0.088	0.732	0.088
0.043	0.697	0.043
0.022	0.673	0.022
0.010	0.648	0.010
0.005	0.637	0.005
0.001	0.637	0.001
0.000	0.161	0.000

(B) 18 hour pellets

Analysis of some sample results gave:

U/U_t'	e	$U, \text{cm/s.}$
0.224	0.803	0.224
0.178	0.770	0.178
0.132	0.748	0.132
0.088	0.732	0.088
0.043	0.697	0.043
0.022	0.673	0.022
0.010	0.648	0.010
0.005	0.637	0.005
0.001	0.637	0.001
0.000	0.161	0.000

The raw data from tests performed in water at 22.5°C using 0.42 g of

dry molasses:

Time, min.	0	5	4	7	10	13	20	23
Height, cm.	23.5	20.8	19.0	17.3	16.5	16.0	15.7	12.4
Volume, cm^3	250	233	205	183	174	168	165	161

C. $T = 20^{\circ}\text{C}$, $\text{pH} = 4.05$, Centrifuged wet weight = 36.1 g.

Bed Vol., cm^3	e	Flow, l/h.	U, cm/s.	C_m , %
232	0.805	6.20	0.224	2.64
209	0.783	4.93	0.178	2.93
196	0.769	3.67	0.132	3.12
186	0.756	2.43	0.088	3.29
152	0.702	0.60	0.022	4.03

D. $T = 20^{\circ}\text{C}$, $\text{pH} = 5.0$, Weight = 25.6 g.

Bed Vol., cm^3	e	Flow, l/h.	U, cm/s.	C_m , %
190	0.831	6.20	0.224	2.28
179	0.820	4.93	0.178	2.42
157	0.795	3.67	0.132	2.76
142	0.774	2.43	0.088	3.06
124	0.741	1.18	0.043	3.50
46	0.301	0	0	9.43

E. $T = 20^{\circ}\text{C}$, $\text{pH} = 5.4$, Weight = 34.2 g.

Bed Vol., cm^3	e	Flow, l/h.	U, cm/s.	C_m , %
234	0.817	6.20	0.224	2.47
221	0.806	4.93	0.178	2.62
208	0.794	3.67	0.132	2.79
184	0.766	2.43	0.088	3.15
158	0.728	1.18	0.043	3.66
124	0.654	0.28	0.010	4.67
76 ($1\frac{1}{2}\text{h}$)	0.436	0	0	7.62
52 (21h)	0.175	0	0	11.1

ii. Sedimentation

$T = 16^{\circ}\text{C}$, $\text{pH} = 5.3$, Weight = 20.4 g.

U, cm/s.	0.059	0.012	0.330	0.107
e	0.895	0.874	0.937	0.916

Suspension Ht., cm	23.8	21.5	14.5	11.3	9.6	8.7	8.1	6.8	6.4
Time, s.	0	10	30	40	50	60	70	130	150

(e) Results

1. Fluidization

The first set of data refers to the tests analyzed in detail in 2.4.7. (i.e. $T = 20^{\circ}\text{C}$, $\text{pH} = 4.75$). The centrifuged wet weight = 26g. Data regression based on 50% flow voidage gave $U' = 4.27$ cm/s, which was used to compare the data to the Richardson-Zaki equation.

Bed Ht., cm	Bed Vol., cm^3	e	Flow, l/h.	U, cm/s.	U/U'	C_m , %
19.5	188	0.803	6.20	0.224	0.052	2.62
16.5	143	0.770	4.93	0.178	0.042	3.11
15.0	130	0.748	3.67	0.132	0.031	3.39
14.0	122	0.732	2.43	0.088	0.021	3.61
12.5	108	0.697	1.18	0.043	0.010	4.08
11.5	100	0.673	0.60	0.022	0.005	4.41
10.1	93	0.648	0.28	0.010	0.002	4.74
8.8	80	0.637	0.13	0.005	0.001	4.89
5.5 (17h)	38	0.411	0	0	0	11.3

The bed was allowed to settle for 17h. against zero flow. The quoted voidage value was based on a retained fine structure of 50% liquid in the interstices. In reality, this would be expected out to give a higher bed voidage than quoted, this being based on the 50% flow voidage criterion.

2. $T = 30^{\circ}\text{C}$, $\text{pH} = 4.85$, Weight = 26 g.

Bed Vol., cm^3	e	Flow, l/h.	U, cm/s.	C_m , %
107	0.694	6.20	0.224	4.12
103	0.683	4.93	0.178	4.28
92	0.670	3.67	0.132	4.42
78	0.581	1.18	0.043	5.62
57	0.552	0.60	0.022	6.04

2. CFCC 83 Results

i. Fluidisation

A. $T = 20^{\circ}\text{C}$, $\text{pH} = 4.75$, Centrifuged wet weight = 49g.

Bed Vol., cm^3	e	Flow, l/h.	U, cm/s.	C_m , g%
412	0.828	3.05	0.110	2.20
374	0.810	2.43	0.088	2.43
320	0.778	1.17	0.042	2.83
270	0.737	0.60	0.022	3.36
256	0.723	0.43	0.016	3.78

B. $T = 30^{\circ}\text{C}$, $\text{pH} = 4.85$, Weight = 49g.

Bed Vol., cm^3	e	Flow, l/h.	U, cm/s	C_m , g%
376	0.811	3.05	0.110	2.41
326	0.782	1.80	0.065	2.78
308	0.769	1.17	0.042	2.94
302	0.765	0.86	0.031	3.00
258	0.725	0.28	0.010	3.52

C. $T = 20^{\circ}\text{C}$, $\text{pH} = 5.2$, Weight = 49g.

Bed Vol., cm^3	e	Flow, l/h.	U, cm/s.	C_m , g%
412	0.830	3.05	0.110	2.20
388	0.820	2.43	0.088	2.34
348	0.799	1.80	0.065	2.61
210	0.667	0.86	0.031	4.32
150	0.533	0.28	0.010	6.05

D. $T = 20^{\circ}\text{C}$, $\text{pH} = 4.2$, Weight = 37.7g.

Bed Vol., cm^3	e	Flow, l/h.	U, cm/s.	C_m , g%
396	0.862	1.06	0.038	1.76
378	0.856	0.90	0.032	1.85
364	0.850	0.75	0.027	1.92
334	0.837	0.43	0.015	2.09
232	0.765	0.28	0.010	3.01
173	0.684	0.13	0.005	4.03

T = 20°C, pH = 4.05, Centrifuged wet weight = 36.1 g.

Bed Vol., cm^3	e	Flow, l/h.	U, cm/s.	C_m , g%
335	0.805	0.50	0.024	2.54
309	0.783	0.93	0.078	2.93
288	0.759	2.67	0.132	3.12
186	0.726	2.43	0.088	2.92
125	0.705	0.60	0.022	3.03

T = 20°C, pH = 5.0, Weight = 25.6 g.

Bed Vol., cm^3	e	Flow, l/h.	U, cm/s.	C_m , g%
190	0.837	0.50	0.024	2.58
179	0.820	0.93	0.078	2.45
157	0.792	2.67	0.132	2.76
142	0.774	2.43	0.088	3.06
124	0.747	1.18	0.043	3.20
46	0.301	0	0	3.43

T = 20°C, pH = 5.4, Weight = 34.2 g.

Bed Vol., cm^3	e	Flow, l/h.	U, cm/s.	C_m , g%
234	0.817	0.50	0.024	2.47
221	0.806	0.93	0.078	2.65
208	0.794	2.67	0.132	2.79
184	0.766	2.43	0.088	3.12
158	0.728	1.18	0.043	3.66
124	0.654	0.58	0.010	4.67
76 (18h)	0.436	0	0	7.65
25 (24h)	0.172	0	0	11.1

ii. Sedimentation

T = 16°C, pH = 5.3, Weight = 20.4 g.

U, cm/s.	e	Flow, l/h.	Bed Vol., cm^3
0.052	0.042	0.030	101.0
0.022	0.034	0.016	212.0

Time, s.	0	10	20	30	40	50	60	70	80	90	100
Sedimentation Ht., cm	53.8	51.2	48.7	46.1	43.5	40.9	38.3	35.7	33.1	30.5	27.9

E. $T = 20^{\circ}\text{C}$, $\text{pH} = 3.75$, $\text{Weight} = 30.7\text{g}$.

Bed Vol., cm^3	e	Flow, l/h.	U , cm/s.	C_m , g%
385	0.884	1.68	0.061	1.48
330	0.865	1.22	0.044	1.72
295	0.849	0.90	0.032	1.93
264	0.831	0.60	0.022	2.16
220	0.798	0.28	0.010	2.59
162	0.725	0.13	0.005	3.51

3. CFCC 8 Results

i. Fluidisation

A. $T = 20^{\circ}\text{C}$, $\text{pH} = 4.6$, $\text{Weight} = 26\text{g}$.

Bed Vol., cm^3	e	Flow, l/h.	U , cm/s.	C_m , g%
334	0.872	4.30	0.155	1.72
280	0.848	3.67	0.132	2.06
252	0.831	3.04	0.109	2.29
195	0.781	1.80	0.065	2.96
124	0.656	0.60	0.022	4.66

B. $T = 30^{\circ}\text{C}$, $\text{pH} = 4.7$, $\text{Weight} = 26\text{g}$.

Bed Vol., cm^3	e	Flow, l/h.	U , cm/s.	C_m , g%
372	0.885	4.93	0.178	1.55
262	0.837	3.67	0.132	2.21
212	0.799	2.43	0.088	2.73
188	0.773	1.80	0.065	3.07
147	0.710	1.18	0.043	3.93

C. $T = 20^{\circ}\text{C}$, $\text{pH} = 4.1$, $\text{Weight} = 40\text{g}$.

Bed Vol., cm^3	e	Flow, l/h.	U , cm/s.	C_m , g%
370	0.822	2.43	0.088	2.40
332	0.802	1.80	0.065	2.68
280	0.765	1.18	0.043	3.18
154	0.573	0.60	0.022	5.77
130	0.495	0.28	0.010	6.84

i. Fluidisation

A. $T = 20^{\circ}\text{C}$, $\text{pH} = 4.75$, $\text{Weight} = 49\text{g}$.

Bed Vol., cm^3	e	Flow, l/h.	U , cm/s.	C_m , g%
412	0.828	3.02	0.110	2.52
374	0.810	2.43	0.088	2.43
320	0.778	1.17	0.042	2.83
270	0.737	0.60	0.022	3.36
226	0.723	0.43	0.016	3.78

B. $T = 30^{\circ}\text{C}$, $\text{pH} = 4.85$, $\text{Weight} = 49\text{g}$.

Bed Vol., cm^3	e	Flow, l/h.	U , cm/s.	C_m , g%
376	0.811	3.02	0.110	2.41
326	0.782	1.80	0.065	2.78
308	0.769	1.17	0.042	2.94
302	0.762	0.86	0.031	3.00
258	0.722	0.58	0.010	3.22

C. $T = 20^{\circ}\text{C}$, $\text{pH} = 5.2$, $\text{Weight} = 49\text{g}$.

Bed Vol., cm^3	e	Flow, l/h.	U , cm/s.	C_m , g%
412	0.830	3.02	0.110	2.50
388	0.820	2.43	0.088	2.34
348	0.799	1.80	0.065	2.61
270	0.667	0.86	0.031	4.32
120	0.523	0.28	0.010	6.02

D. $T = 20^{\circ}\text{C}$, $\text{pH} = 4.2$, $\text{Weight} = 37.7\text{g}$.

Bed Vol., cm^3	e	Flow, l/h.	U , cm/s.	C_m , g%
396	0.862	1.06	0.038	1.76
378	0.856	0.90	0.032	1.89
364	0.850	0.75	0.027	1.92
334	0.837	0.43	0.015	2.09
232	0.762	0.28	0.010	3.01
172	0.684	0.13	0.002	4.03

ii. Sedimentation

$T = 20^{\circ}\text{C}$, $\text{pH} = 4.1$, $\text{Weight} = 14.7\text{g}$.

$U, \text{cm/s.}$	0.013	0.032	0.058
e	0.880	0.915	0.940

Suspension Ht, cm	23.5	23.2	21.9	20.0	16.5	13.6	10.4	7.25
Time, s.	10	10	30	160	120	180	300	600

4. CFCC 3 Results

i. Fluidisation

A. $T = 20^{\circ}\text{C}$, $\text{pH} = 5.3$, $\text{Weight} = 25.4\text{g}$.

Bed Vol., cm^3	e	Flow, l/h.	$U, \text{cm/s.}$	$C_m, \text{g\%}$
117	0.727	6.20	0.224	3.95
110	0.710	4.93	0.178	4.20
105	0.696	3.67	0.132	4.40
100	0.681	2.43	0.088	4.62
93	0.656	1.18	0.043	4.97

B. $T = 20^{\circ}\text{C}$, $\text{pH} = 4.7$, $\text{Weight} = 19.7\text{g}$.

Bed Vol., cm^3	e	Flow, l/h.	$U, \text{cm/s.}$	$C_m, \text{g\%}$
104	0.744	6.20	0.224	3.44
100	0.734	4.93	0.178	3.58
94	0.716	3.67	0.132	3.81
87	0.694	2.43	0.088	4.11
76	0.649	0.60	0.022	4.70

C. $T = 30^{\circ}\text{C}$, $\text{pH} = 4.8$, $\text{Weight} = 19.7\text{g}$.

Bed Vol., cm^3	e	Flow, l/h.	$U, \text{cm/s.}$	$C_m, \text{g\%}$
98	0.728	6.20	0.224	3.65
94	0.716	4.93	0.178	3.81
89	0.701	3.67	0.132	4.02
81	0.671	2.43	0.088	4.42

5. CFCC 54 Results

Sedimentation

$T = 25^{\circ}\text{C}$, $\text{pH} = 4.9$, $\text{Weight} = 30.3\text{g}$.

$U, \text{cm/s.}$	0.20	0.08	0.35	0.10	0.58	0.72	0.04
e	0.78	0.69	0.85	0.74	0.89	0.91	0.57

$T = 20^{\circ}\text{C}$, $\text{pH} = 4.1$, $\text{Weight} = 30.1\text{g}$.

Bed Vol., cm^3	e	Flow, l/h.	$U, \text{cm/s.}$	$C_m, \text{g\%}$
385	0.884	1.68	0.061	1.48
330	0.865	1.35	0.044	1.75
295	0.845	0.90	0.030	1.93
264	0.831	0.60	0.022	2.16
220	0.798	0.38	0.010	2.52
165	0.755	0.13	0.002	3.21

i. Fluidisation

$T = 20^{\circ}\text{C}$, $\text{pH} = 4.6$, $\text{Weight} = 26\text{g}$.

Bed Vol., cm^3	e	Flow, l/h.	$U, \text{cm/s.}$	$C_m, \text{g\%}$
334	0.875	4.30	0.155	1.75
280	0.846	3.67	0.135	2.06
255	0.831	3.04	0.109	2.52
195	0.781	1.80	0.065	2.96
124	0.656	0.60	0.025	4.66

$T = 30^{\circ}\text{C}$, $\text{pH} = 4.7$, $\text{Weight} = 26\text{g}$.

Bed Vol., cm^3	e	Flow, l/h.	$U, \text{cm/s.}$	$C_m, \text{g\%}$
375	0.885	4.93	0.178	1.55
325	0.837	3.67	0.135	2.21
215	0.795	2.43	0.088	2.73
168	0.773	1.80	0.065	3.07
147	0.710	1.18	0.043	3.93

$T = 20^{\circ}\text{C}$, $\text{pH} = 4.1$, $\text{Weight} = 40\text{g}$.

Bed Vol., cm^3	e	Flow, l/h.	$U, \text{cm/s.}$	$C_m, \text{g\%}$
370	0.855	5.43	0.088	2.40
332	0.805	1.80	0.065	2.68
290	0.765	1.18	0.040	3.18
154	0.573	0.60	0.025	5.77
130	0.455	0.38	0.010	6.84

NOMENCLATURE

- A = volume fraction of total liquid in pellet/floc; surface area of sphere
 a_w = water activity of solution = vapour pressure ratio of solution to solvent
 a = major axis of microbial cell; number of clusters in aggregate
 b = minor axis of microbial cell
 c = volume fraction of cells in suspension
 C_m = dry weight concentration, w/v %
 C_d = drag coefficient = $2R'$
 d = diameter, cms.; may refer to pellet/floc/solid particle
 dv/dy = shear rate, s^{-1}
 D = cluster diameter ; column diameter, cms.
 D_e = equivalent bubble size
 e = suspension voidage ; overall floc voidage in floc model; voidage
 $e', e'', \text{etc.}$ = cluster voidages
 F = average density for mycelial shell; drag force on sphere; Vand constant
 f = hyphal branch to stem length ratio; velocity through a porous sphere / velocity of the approaching fluid
 g = gravity constant
 h_1 = segment of bed height in tower fermenter model
 j = diameter of uncoated spheres of total volume $J \text{ cm}^3$, cm.
 j_0 = diameter of spheres that are coated with microorganism, cm.
 K = viscosity power law constant
 k = fraction of hyphal core surface occupied by protruding hyphal bases
 L = bed length, cm.
 M = "corrected" weight of filtered mycelium; volume fraction of liquid in cell
 M' = tower scale-up factor.
 n = number of particles in a floc ; number of hyphae protruding from core ; Richardson-Zaki equation index; Power Law index
 p_a = pressure at the surface of a sphere

1.1. Sedimentation

T = 20°C, $\eta = 4.1$, Weight = 14.7g.

U, cm/s.	e	0.013	0.032	0.058
0.040	0.012	0.080	0.012	0.040

Suspension Ht, cm	23.2	23.2	21.2	20.0	16.2	13.2	10.4	7.2
Time, s.	10	10	10	10	180	180	300	600

1.1.1. Results

1.1.1.1. Sedimentation

T = 20°C, $\eta = 2.3$, Weight = 25.4g.

Bed Vol., cm^3	e	Flow, l/h.	U, cm/s.	C_m , %
117	0.727	6.20	0.224	3.92
110	0.710	4.93	0.178	4.20
102	0.696	3.61	0.132	4.40
100	0.681	2.43	0.088	4.62
93	0.656	1.18	0.043	4.91

T = 20°C, $\eta = 4.1$, Weight = 19.7g.

Bed Vol., cm^3	e	Flow, l/h.	U, cm/s.	C_m , %
104	0.744	6.20	0.224	3.44
100	0.734	4.93	0.178	3.58
94	0.716	3.61	0.132	3.81
87	0.694	2.43	0.088	4.11
76	0.649	0.60	0.022	4.40

T = 20°C, $\eta = 4.8$, Weight = 19.7g.

Bed Vol., cm^3	e	Flow, l/h.	U, cm/s.	C_m , %
98	0.728	6.20	0.224	3.62
94	0.716	4.93	0.178	3.81
89	0.701	3.61	0.132	4.02
81	0.671	2.43	0.088	4.42

1.1.1.1. Results

T = 25°C, $\eta = 4.9$, Weight = 30.2g.

U, cm/s.	0.20	0.09	0.32	0.10	0.28	0.72	0.04
e	0.78	0.68	0.62	0.74	0.69	0.91	0.21

ΔP_b = pressure drop through a bed of solids ,grams

SVI = settled volume index , cm^3 / g

S = surface area / unit solids volume , $\text{cm}^2 / \text{cm}^3$

T = temperature , $^{\circ}\text{C}$

t = residence time

U_i = sphere to liquid relative velocity , cm/s

U = superficial liquid velocity , cm/s

U' = terminal velocity corrected for wall-effect

V = volume of immobile liquid in pellet ; tower volume , cm^3

V_{∞} = particle terminal velocity , cm/s

V_r = liquid velocity at a sphere's surface

W = mycelial liquid weight ; weight of wet material in suspension, g.

X = weight fraction of liquid in hyphae ; floc voidage

x = dry weight of material in suspension, g .

Y = volume fraction of liquid in hyphae

Z = volume fraction of cavity inside autolysed pellet

z = seed swelling ratio = final / initial diameters

Greek Letters

ρ = density , g/cm^3 (ρ_y = weight of dry mycelium / unit pellet volume)

μ = viscosity , g/cm.s (μ_o = liquid phase viscosity)

σ = surface tension , dyne/cm.

λ, ω = dry weight concentration criteria

τ = shear stress , dyne/cm^2 (τ_o = yield stress, dyne/cm^2)

θ = direction angle of flow through a porous sphere

$\delta = x/d$, where x = distance between spheres in suspension

ψ = friction factor

ϕ = volume fraction of solids in suspension

Dimensionless Groups

Re = Reynolds Number = $dU\rho/\mu$; Fr = Froude Number = U_{mf}^2 / gd

$Re' = \text{Blake Number} = U\rho/S\mu(1-e)$; $Ga = \text{Galileo Number} = l(\rho_s - \rho)gd^3/\mu^2$;
 $\psi = \text{Friction Factor} = e^3(\rho_s - \rho)g / S\rho U^2$

Subscripts

agg. = aggregate B = bulk property
 c = suspension i = refers to inner hyphal core
 m = medium liquid mf = minimum fluidisation velocity condition
 o = outer condition of pellet p = pellet property
 g = gas phase property r = relative property
 s = solid phase or dry mycelial property
 t = terminal velocity condition ("pt" when referring to a particle)
 y = cellular property

$\Delta P = \text{pressure drop through a bed of solids, grams}$

$\epsilon_{VI} = \text{settled volume index, cm}^3/\text{g}$

$\epsilon = \text{surface area / unit solid volume, cm}^2/\text{cm}^3$

$T = \text{temperature, } ^\circ\text{C}$

$t = \text{residence time}$

$U_1 = \text{space to liquid relative velocity, cm/s}$

$U = \text{superficial liquid velocity, cm/s}$

$U' = \text{terminal velocity corrected for wall-effect}$

$V = \text{volume of immobile liquid in pellet; lower volume, cm}^3$

$V_{\infty} = \text{particle terminal velocity, cm/s}$

$V_T = \text{liquid velocity at a sphere's surface}$

$W = \text{mycelial liquid weight; weight of wet material in suspension, g}$

$X = \text{weight fraction of liquid in hyphae; free volume}$

$x = \text{dry weight of material in suspension, g}$

$Y = \text{volume fraction of liquid in hyphae}$

$Z = \text{volume fraction of cavity inside autolyzed pellet}$

$z = \text{seed swelling ratio} = \text{final / initial diameter}$

Greek Letters

$\rho = \text{density, g/cm}^3$; $\rho' = \text{weight of dry mycelium / unit pellet volume}$

$\mu = \text{viscosity, g/cm.s}$; $\mu_0 = \text{liquid phase viscosity}$

$\nu = \text{surface tension, dyne/cm}$

$\omega = U / U_T$; $\omega = \text{dry weight concentration criteria}$

$\tau = \text{shear stress, dyne/cm}^2$; $\tau_0 = \text{yield stress, dyne/cm}^2$

$\Theta = \text{direction angle of flow through a porous sphere}$

$\delta = x/5$; where $x = \text{distance between spheres in suspension}$

$\psi = \text{friction factor}$

$\phi = \text{volume fraction of solids in suspension}$

Dimensionless Groups

$Re = \text{Reynolds Number} = U\rho/\mu$; $Fr = \text{Froude Number} = U^2/g$

BIBLIOGRAPHY

(For Chapters 1 to 6)

1. Akin, C. & Lagomarcino, S. Z., Proc. A. M. Amer. Soc. Brew. Chem., 135, 1965.
2. Aiba, S. & Nagatani, M., "Advances in Biochemical Engineering", I, 31, Springer-Verlag, 1971.
3. Aiba, S., Kitai, S., Ishida, N., J. Gen. Appl. Microbiology, 8, 103, 1962.
4. Aiba, S., Kitai, S., Heima, H., J. Gen. Appl. Microbiology, 10, 3, 1964.
5. Allen, H. S., Phil. Mag., 1, 323, 1900.
6. Allen, B. G., & Smith, J. W., Can. J. Chem. Eng., 49, 430, 1971.
7. Atkinson, B. & Davies, I. J., Trans. Inst. Chem. Engr., 50, 208, 1972.
8. Ault, R. G., Hampton, A. N., Newton, R., Roberts, R. H., J. Inst. Brew., 75, 260, 1969.
9. Bond, A. W., J. Inst. Water Engrs., 20, 477, 1966.
10. Bongenaar, J. J. T. M., Kossen, N. W. F., Metz, B., Meijboom, F. W., Biotech. & Bioeng., 15, 201, 1973.
11. Brinkman, H. C., Appl. Sci. Res., A1, 27, 1947.
12. Burkholder, P. R. & Sinnott, E. W., Am. J. Botany, 32, 424, 1945.
13. Burns, J. A., J. Inst. Brew., 43, 31, 1937.
14. Carpenter, P., "Microbiology", Saunders, 1967.
15. Coe, H. S. & Clevenger, G. H., Trans. Am. Inst. Min. Engrs., 55, 356, 1916.
16. Coulson, J. M. & Richardson, J. F., "Chemical Engineering", 2, Pergamon, 1966.
17. Davidson, J. F. & Harrison, D., "Fluidised Particles", Cambridge, 1963.
18. Deindoerfer, F. H. & West, J. M., Adv. in Appl. Microbiology, 2, 265, 1960.
19. Deindoerfer, F. H. & Gaden, E. L., Appl. Microbiology, 3, 253, 1955.
20. Doudoroff, M., Stanier, R. Y., Adelburg, E. A., "Microbial World", Prentice-Hall, 1970.
21. Downie, J. M., Ph. D. Thesis, The University of Aston in Birmingham, 1972.
22. Edeline, F., Tesarik, I., Vostreil, J., "Advances in Water Pollution Research", p. 523, Prague, 1969.
23. Eirich, F. R., & Mark, H., Papier Fabrikant, 27, 251, 1937.
24. Eirich, F. R., Kolloid Z., 74, 276, 1936.

25. Eirich, F.R., (ed.), "Rheology", 4, 204, Academic, 1967.
26. Einstein, A., Ann. Physik, 34, 591, 1911.
27. Ergun, S., Chem. Eng. Prog., 48, 89, 1952.
28. Erickson, L.E., Lee, S.S., Fan, L.T., J. Appl. Chem. & BioTechnol., 22, 199, 1972.
29. Falch, E.A. & Gaden, E.L., BioTech. & BioEng., 11, 927, 1969.
30. 12, 465, 1970.
31. Galbraith, J. & Smith, J.E., J. Gen. Microbiology, 59, 31, 1969.
32. Ganser, L.L. & Wang, D.I.C., BioTech. & BioEng., 12, 873, 1972.
33. Gaudin, A.M. & Fuerstenau, M., Mining Eng., 11, 613, 1958.
34. Geys, K., J. Inst. Brew., 28, 479, 1922.
35. Gilliland, R.B., Pro. Cong. Europ. Brew. Conv., Brighton, 1951.
36. Godard, K.E. & Richardson, J.F., Chem. Eng. Sci., 24, 363, 1969.
37. Goldstein, S., Proc. Roy. Soc., A123, 225, 1929.
38. Greenshields, R.N. & Smith, E.L., Chem. Engr., 182, 249, 1971.
39. Gunn, D.J. & Malik, A.A., Trans. Inst. Chem. Engrs., 44, 260, 1966.
40. Gunn, D.J. & Malik, A.A., Int. Symp. Fluidisation, Eindhoven, p. 52, 1967.
41. Guth, E. & Simha, R., Kolloid Z., 74, 266, 1936.
42. Haddad, S.A. & Lindegren, C.C., Appl. Microbiology, 1, 153, 1953.
43. Hanratty, T.J. & Bandukwala, A., A.I.Ch.E.J., 3, 293, 1957.
44. Handley, D., Doraisamy, A., Butcher, K.L., Franklin, N.L., Trans. Inst. Chem. Engrs., 44, 260, 1966.
45. Happel, J., A.I.Ch.E.J., 4, 197, 1958.
46. Happel, J., J. Appl. Phys. 28, 1288, 1957.
47. Happel, J., & Brenner, H., A.I.Ch.E.J., 3, 506, 1957.
48. Happel, J. & Epstein, N., Ind. Eng. Chem., 46, 1187, 1954.
49. Harrison, D., Davidson, J.F., DeKock, J.W., Trans. Inst. Chem. Engrs., 39, 202, 1961.
50. Harris, C.C., Nature, 183, 530, 1959.
51. Harris, C.C., Nature, 184, 716, 1959.
52. Hawkey, P.G.W., Inst. Phys. Symp., 114, 1950.
53. Henzelmann, F., Szucs, F., Borlai, O., Blikle, T., Symp. Fluidisation, Eindhoven, 66, 1967.

BIBLIOGRAPHY

(For Chapters 1 to 6)

1. Allen, B. & Leamon, S., Proc. A.M. Soc. Brew. Chem., 135, 1965.
2. Alpa, S. & Nagaoka, M., "Advances in Biochemical Engineering", 1, 31, Springer-Verlag, 1971.
3. Alpa, S., Kital, S., Ishida, M., J. Gen. Appl. Microbiology, 8, 103, 1962.
4. Alpa, S., Kital, S., Heima, H., J. Gen. Appl. Microbiology, 10, 3, 1964.
5. Allen, H.S., Phil. Mag., 1, 323, 1900.
6. Allen, B.G. & Smith, J.W., Can. J. Chem. Eng., 49, 430, 1971.
7. Atkinson, B. & Davies, I.J., Trans. Inst. Chem. Engrs., 50, 208, 1970.
8. Ault, R.G., Hampton, A.H., Newton, R., Roberts, R.H., J. Inst. Brew., 12, 260, 1966.
9. Bond, A.W., J. Inst. Water Engrs., 20, 477, 1966.
10. Bongenaar, J.J.T.M., Kossen, N.W.F., Mata, P., Malfroid, F.W., BioTech. & BioEng., 12, 201, 1972.
11. Brinman, H.C., Appl. Sci. Res., A1, 27, 1947.
12. Burkholder, R.R. & Stumpe, F.W., Am. J. Botany, 33, 424, 1945.
13. Burns, J.A., J. Inst. Brew., 33, 31, 1937.
14. Carpenter, R., "Microbiology", Saunders, 1967.
15. Gee, H.S. & Givenger, G.H., Trans. Am. Inst. Min. Engrs., 22, 356, 1916.
16. Coulson, J.M. & Richardson, J.T., "Chemical Engineering", 2, Pergamon, 1966.
17. Davidson, J.F. & Harrison, D., "Fluidised Particles", Cambridge, 1963.
18. Deindoerfer, F.H. & West, J.M., Adv. in Appl. Microbiology, 2, 265, 1960.
19. Deindoerfer, F.H. & Gaden, E.L., Appl. Microbiology, 3, 253, 1955.
20. Deindoerfer, F.H., Stenier, E.Y., Adelburg, E.A., "Microbial World", Prentice-Hall, 1970.
21. Downie, J.M., Ph.D. Thesis, The University of Aston in Birmingham, 1972.
22. Edeline, P., Tenzik, I., Vestrol, J., "Advances in Water Pollution Research", p. 523, Prague, 1969.
23. Eirich, F.R. & Hart, H., Papier Fabrikant, 21, 251, 1937.
24. Eirich, F.R., Kolloid Z., 1A, 276, 1936.

54. Heywood, H., J. Imp. Coll. Chem. Eng. Soc., 4, 17, 1948.
55. Hummel, R.L. & Popovich, A.T., Chem. Eng. Sci., 22, 21, 1967.
56. James, D.F. & Gupta, O.P., Chem. Eng. Prog. Symp., 67, 111, 62, 1971.
57. James, D.F. & Acosta, A.J., J. Fluid Mech., 42, 269, 1970.
58. Jottrand, R., Chem. Eng. Sci., 3, 12, 1954.
59. Jottrand, R., J. Appl. Chem., 2, Supp. 1, 317, 1952.
60. Karow, E.O., J. Agr. Food Chem., 1, 302, 1953.
61. Kennedy, S.G. & Breton, R.H., A.I.Ch.E.J., 13, 24, 1966.
62. Kermack, W.O., Proc. Roy. Soc. Edinburgh, 49, 1929.
63. Kitai, A., Tone, H., Ozaki, A., BioTech. & BioEng., 11, 911, 1969.
64. Kitai, A. & Yamagita, T., Process Biochem., 52, Nov., 1970.
65. Kloppe, W.J., Roberts, R.H., Royston, M.G., Ault, R.G., Proc. 10th Congress, Stockholm, Eurp. Brew. Convn., p. 238, Elsevier, 1965.
66. Koga, S., J. Gen. Appl. Microbiology, 5, 35, 1959.
67. Kynch, G.J., Trans. Faraday Soc., 48, 1966, 1952.
68. Ladenburg, R., Ann. Phys., 23, 447, 1907.
69. Laine, B., Can. J. Chem. Eng., 50, 2, 153, 1972.
70. Latif, B.A.J. & Richardson, J.F., Chem. Eng. Sci., 27, 1933, 1972.
71. Lawson, A. & Hassett, N.J., Int. Symp. Fluidisation, Eindhoven, 1967.
72. Lewis, E.W. & Bowermann, F.W., Chem. Eng. Prog., 48, 603, 1952.
73. Lewis, W. & Gilliland, E.R., Ind. Eng. Chem., 41, 1104, 1949.
74. Liaw, G.C., Zakin, J.L., Patterson, G.K., A.I.Ch.E.J., 17, 391, 1971.
75. Loeffler, A.L. & Ruth, B.F., A.I.Ch.E.J., 5, 310, 1959.
76. Lyons, T.P. & Hough, J.S., J. Inst. Brew., 76, 574, 1970.
77. Malkow, A., Zentr. Bakt. Parasitenk., 90, 212, 1934.
78. Martin, J., McCabe, W.L., Monrad, C.C., Chem. Eng. Prog., 47, 91, 1951.
79. Mateles, R.I. & Tannenbaum, S.R., (eds.), "Single Cell Protein", M.I.T. Press, Massachusetts, 1968.
80. McGregor, W.C. & Finn, R.K., BioTech. & BioEng., 11, 127, 1969.
81. McMillan, M.L., Chem. Eng. Prog. Symp., 67, 27, 1971.
82. Means, C.W., Savage, G.M., Reusser, F., BioTech. & BioEng., 4, 5, 1962.

83. Meyer, J., B'ham. Univ. Chem. Engr., 24, 10, 1973.
84. Miam, I., M.Sc. Thesis, The University of Aston in Birmingham, 1969.
85. Michaels, A.S. & Bolger, J.C., Ind. Eng. Chem. Fund., 1, 24, 1962.
86. Mill, P.S., J. Gen. Microbiology, 35, 53, 1964.
87., 35, 61, 1964.
88., 44, 329, 1966.
89. Morris, G.G., Ph.D. Thesis, The University of Aston in Birmingham, 1972.
90. Mohlmann, F.W., Sewage Works Jnl., 6, 119, 1934.
91. Moulik, S.P., J. Phys. Chem., 72, 4682, 1968.
92. Mueller, J.A., Voelkel, K.G., Boyle, W.C., J. San. Eng. Div., Proc. A.S.C.E., 92, 1966.
93. Mueller, J.A., Morand, J., Boyle, W.C., Appl. Microbiology, 15, 125, 1967.
94. Oliver, D.R., Chem. Eng. Sci., 15, 230, 1961.
95. Patterson, G.K., Zakin, J.L., Rodriguez, J.M., Ind. Eng. Chem., 61, 22, 1969.
96. Pelczar, M. & Reid, R., "Microbiology", McGraw-Hill, 1972.
97. Pipes, W.O., Adv. Appl. Microbiology, 9, 185, 1967.
98. U.S. President's Science Advisory Committee, "The World Food Problem",
1, 2, 3, Washington, 1967.
99. Prokop, A., Erickson, L.E., Fernandez, J., Humprhey, A.E., BioTech. & BioEng.,
11, 945, 1969.
100. Pruden, B. & Epstein, N., Chem. Eng. Sci., 19, 696, 1964.
101. Rakmann-Zade, Y.A., Rizaev, N.V., Yusipov, M.M., Int. Chem. Eng., 11, 677, 1971.
102. Reuter, H., Chem. Eng. Sci. Symp., 62, 1966.
103. Richardson, J.F. & Zaki, W.N., Trans. Inst. Chem. Engrs., 32, 35, 1954.
104. Richardson, J.F. & Mielke, R.A., Trans. Inst. Chem. Engrs., 39, 348, 1961.
105. Richardson, J.F. & Carlos, Chem. Eng. Sci., 23, 813, 1968.
106. Robson, J.E., Radioisotopes Sci. Res. Proc. Int. Conf., Paris, 4, 29, 1957.
107. Rowe, P.N., Trans. Inst. Chem. Engrs., 39, 175, 1961.
108. Rowe, P.N. & Henwood, G.A., Trans. Inst. Chem. Engrs., 39, 43, 1961.
109. Royston, M.G., Process Biochem., 1, 215, 1966.
110. Rubey, W.W., Am. J. Sci., 25, 325, 1933.

81. ... , 25, 325, 1933.
82. ... , 25, 325, 1933.
83. ... , 25, 325, 1933.
84. ... , 25, 325, 1933.
85. ... , 25, 325, 1933.
86. ... , 25, 325, 1933.
87. ... , 25, 325, 1933.
88. ... , 25, 325, 1933.
89. ... , 25, 325, 1933.
90. ... , 25, 325, 1933.
91. ... , 25, 325, 1933.
92. ... , 25, 325, 1933.
93. ... , 25, 325, 1933.
94. ... , 25, 325, 1933.
95. ... , 25, 325, 1933.
96. ... , 25, 325, 1933.
97. ... , 25, 325, 1933.
98. ... , 25, 325, 1933.
99. ... , 25, 325, 1933.
100. ... , 25, 325, 1933.
101. ... , 25, 325, 1933.
102. ... , 25, 325, 1933.
103. ... , 25, 325, 1933.
104. ... , 25, 325, 1933.
105. ... , 25, 325, 1933.
106. ... , 25, 325, 1933.
107. ... , 25, 325, 1933.
108. ... , 25, 325, 1933.
109. ... , 25, 325, 1933.
110. ... , 25, 325, 1933.

111. Ryan, E.J. & Smith, J.W. & Hummel, S.R., Int. Symp. Fluidisation, Eindhoven, 74, 1967.
112. Schiller, L. & Naumann, A., Z. Ver. Deut. Ing., 77, 318, 1933.
113. Schofield, R.K. & Samson, H.R., Discussions of Faraday Soc., 18, 135, 1954.
114. Schroepfer, G.J., Johnson, A.S., Ziemke, N.R., San. Eng. Report, 101S, Univ. of Minnesota, 1955.
115. Schoenfeld, A., Wochschr. Brau., 35, 342, 1918.
116. Sentandreu, R. & Northcote, D.H., J. Gen. Microbiology, 55, 393, 1969.
117. Shayegan, J.S., M.Sc. Thesis, The University of Aston in Birmingham, 1970.
118. Shore, D.T. & Royston, M.G., Chem. Engr., 218, CE99, 1968.
119. Simpson, H.C. & Rodger, B.W., Chem. Eng. Sci., 16, 153, 1961.
120. Snyder, H.E., Advances in Food Research, 18, 85, 1970.
121. Solomons, G.L. & Perkin, M.P., J. Appl. Chem., 8, 251, 1958.
122. Solomons, G.L., "Continuous Culture of Microorganisms" (Malek, ed.), Czech. Acad. Sci., Prague, 1962.
123. Smith, T.N., Trans. Inst. Chem. Engrs., 43, 69, 1965.
124. Smoluchowski, M.V., Z. Physik Chem., 92, 129, 1917.
125. Steinour, H.H., Ind. Eng. Chem., 36, 618, 1944; 36, 840, 1944; 36, 901, 1944.
126. Sterbacek, Z., Folia Microbiologica, 17, 117, 1972.
127. Stevens, N.J., Chem. Eng. Prog. Symp., 62, 69, 1966.
128. Steel, R., Lentz, C.P., Martin, S.M., Can. J. Microbiology, 1, 150, 1954.
129., 11, 299, 1955.
130. Stokes, G.G., Trans. Camb. Phil. Soc., 2, 8, 1851.
131. Sutherland, D.N., J. Colloid Interface Sci., 25, 373, 1967.
132. Sutherland, D.N. & Tan, C.T., Chem. Eng. Sci., 25, 1948, 1970.
133. Sutherland, D.N. & Goodarz-nia, I., Chem. Eng. Sci., 26, 2071, 1971.
134. Taguchi, H., "Advances in Biochemical Engineering", Springer-Verlag, 1, 1971.
135. Takahashi, J., "Fermentation Advances" (Perlman, ed.), p. 512, Academic, 1969.
136. Tambo, N. & Watanabe, Y., J. Water Works Assn. (Japan), No. 397, 1967.
137. Thomas, D.G., Ind. Eng. Chem., 55, 11, 1963.

138. Thomas, D.G., A.I.Ch.E.J., 2, 310, 1963.
139. Thorne, R.S.W., Wallerstein Labs. Commun., 15, 201, 1952.
140. Thorne, R.S.W., J.Inst.Brew., 60, 227, 1954.
141. Toms, B.A., Proc. 1st. Int. Cong. on Rheology, 2, 135, 1948.
142. Trinci, A.P.J., Trans.Br.Mycol.Soc., 55, 17, 1970.
143. Trupp, A.C., Fluidisation Symp., Montreal, I.Ch.E. Series, 30, 1968.
144. U.N. Economic & Social Council, "Increasing the Production & Use of ,
Edible Protein", E4343, New York, 1967.
145. Vand, V., J.Phys.Colloid Chem., 52, 277, 1948.
146. Van Vlack, L.H., "Elements of Materials Science", p.380, Addison-Wesley, 1964.
147. Vanecek, V. & Hummel, R.L., Fluidisation Symp., Montreal, I.Ch.E. Series,
30, 1968.
148. Volpicelli, G., Massimilla, L., Zenz, F.A., Chem.Eng.Prog.Symp., 62, 67, 1966.
149. Vold, M.J., J.Phys.Chem., 63, 1608, 1959.
150., 64, 1616, 1960.
151. Vold, M.J., J.Colloid Sci., 18, 684, 1963.
152. Wallis, G.B., "One Dimensional Two Phase Flow", McGraw-Hill, 1969.
153. Wadsworth, M.E. & Citler, I.B., Mining Eng., 8, 830, 1956.
154. Wen, C.Y. & Yu, Y.H., Chem.Eng.Prog.Symp., 62, 100, 1966.
155. Wetherell, D.F. & Pollack, J.D., J.Bacteriol., 84, 191, 1962.
156. Wilhelm, R.H. & Kwauk, M., Chem.Eng.Prog., 44, 201, 1948.
157. Yanagita, T., J.Gen.Appl.Microbiology, 9, 179, 1963.
158. Yano, T., Kodama, T., Yamada, K., Agr.Biol.Chem., 25, 580, 1961.
159. Yosida, T., Shimizu, T., Taguchi, H., Teramoto, S., J.Fermt.Technol., 45, 1119, 1967.
160. Zakin, J.L. & Chiang, J.L., Nature(physical), 239, 26, 1972.
161. Zamorvera, T.A., Izv.VVZSSSR, Khimya i Khim Teknologiya, 1, 148, 1964.
162. Zamorvera, T.A. & Slavyanov, Y.N., Meditsinskaya Prom., 10, 31, 1961.

BIBLIOGRAPHY

(For Chapter 7)

163. Efremov, G.I. & Vakhrushev, I.A., *Int. Chem. Eng.*, 10, 37, 1970.
164. Kato, Y., *Kagaku Kogaku*, 1, 3, 1963.
165. Kolbel, H., Hammer, H., Henne, H.J., Maenning, H.G., *Dechema Monograph*, 49, 277, 1964.
166. Østergaard, K., *Chem. Eng. Sci.*, 20, 165, 1965.
167. Østergaard, K. & Thiessen, P.I., *Chem. Eng. Sci.*, 21, 413, 1966.
168. Østergaard, K., "Advances in Chemical Engineering", 7, 71, 1968.
169. Østergaard, K. & Michelson, M.L., *Chem. Eng. Jnl.*, 1, 37, 1970.
170. Østergaard, K. & Fosbøl, P., *Chem. Eng. Jnl.*, 3, 105, 1972.
171. Rigby, G.R. & Capes, C.E., *Can. J. Chem. Eng.*, 48, 343, 1970.
172. Roy, N.K., Guha, D.K., Rao, M.N., *Chem. Eng. Sci.*, 19, 215, 1964.
173. Stewart, P.S.B., & Davidson, J.F., *Chem. Eng. Sci.*, 19, 319, 1964.
174. Vail, Y.K., Manakov, N.K., Manshilin, V.V., *Int. Chem. Eng.*, 10, 244, 1970.
175. Viswanathan, S., Kakav, A.S., Murli, P.S., *Chem. Eng. Sci.*, 20, 903, 1965.